THE SURFACE AND THROUGH CRACK PROBLEMS IN LAYERED ORTHOTROPIC PLATES

by

Fazil Erdogan and Binghua Wu

Lehigh University
Bethlehem, Pennsylvania

May, 1991

FINAL TECHNICAL REPORT
NATIONAL AERONAUTICS AND SPACE ADMINISTRATION
GRANT NAG-1-713

THE SURFACE AND THROUGH CRACK PROBLEMS IN LAYERED ORTHOTROPIC PLATES

by

Fazil Erdogan and Binghua Wu

Lehigh University
Bethlehem, Pennsylvania
May, 1991

FINAL TECHNICAL REPORT
NATIONAL AERONAUTICS AND SPACE ADMINISTRATION
GRANT NAG-1-713

Acknowledgements

This report describes the research carried out under the most recent grant we received from NASA-Langley. The program started in 1964 and dealt with some experimental but mostly theoretical and computational aspects of a rather wide ranging topics related to the fatigue and fracture of aerospace structures. Some of the topics studied were fatigue crack propagation and fracture stability in plates and shells, delamination problems in layered materials, crack penetration problems in bonded dissimilar materials, stress intensity factors under thermal stresses and dynamic loading conditions, the interface crack in fiber reinforced materials, crack problems in bonded isotropic and orthotropic layers with periodic structure, the free end effect in layered materials, effect of various stiffeners and reinforcements on the stress intensity factors in plates and shells containing through or part-through cracks, plasticity effects on the crack opening displacements in plates and shells, multiple site surface and through cracks in plates and shells, modeling of interfacial zones in bonded materials, circumferential and axial surface crack problems in thick-walled cylinders, modeling and analysis of adhesively bonded joints, the effect of material nonhomogeneity on the stress intensity factors in debonding and fracture penetration problems, the effect of various end conditions on the stress intensity factors in cylindrical shells containing a through or part-through crack, toughening mechanisms in ceramics, surface and through crack problems in layered orthotropic plates, surface and through crack problems in plates and shells under mixed-mode loading conditions, development of function-theoretic methods to analyze mixed boundary value problems and to determine the nature of stress singularities, and development of computational techniques for solving singular integral equations arising from various kinds of crack problems. We would like to take this opportunity to thank the following individuals at the Materials Division, NASA-Langley who monitored the work and provided encouragement during the course of the research program: H. Hardrath, W. Illg, J. Davidson, J.H. Crews, Jr., W.B. Fichter, R.A. Everett, Jr., W. Elber, J.C. Newman, Jr., S. Johnson, C.C. Poe, Jr., C.A. Bigelow and C.E. Harris.

Table of Contents

List of Tables

Table 4.18 Normalized stress intensity factor at the center of a semi-elliptical surface crack in a two-layer plate subjected to bending. In 18a the normalization factor k_{ob}^{∞} is calculated from the corresponding crack depth $L=L_0$. The results in 18b are normalized with respect to $k_{0b} = \sigma_b\sqrt{h_1}$, $\sigma_b=6M/h^2$.

(Material Pair B, $h_2/h_1=1.$)

Table 4.19 Normalized stress intensity factor at the center of a semi-elliptical surface crack in a two-layer plate subjected to tension. In 19a the normalization factor k_{ot}^{∞} is calculated from the corresponding crack depth $L=L_0$. The results in 19b are normalized with respect to $k_{0t} = \sigma_t\sqrt{h_1}$ $\sigma_t= N/h$.

(Material Pair B, $h_2/h_1=10.$)

Table 4.20 Normalized stress intensity factor at the center of a semi-elliptical surface crack in a two-layer plate subjected to bending. In 20a the normalization factor k_{ob}^{∞} is calculated from the corresponding crack depth $L=L_0$. The results in 20b are normalized with respect to $k_{0b} = \sigma_b\sqrt{h_1}$, $\sigma_b=6M/h^2$.

(Material Pair B, $h_2/h_1=10.$)

Table 4.21 Normalized stress intensity factor at the center of a semi-elliptical surface crack in a two-layer plate subjected to tension. In 21a the normalization factor k_{ot}^{∞} is calculated from the corresponding crack depth $L=L_0$. The results in 21b are normalized with respect to $k_{0t} = \sigma_t\sqrt{h_1}$ $\sigma_t= N/h$.

(Material Pair B, $h_2/h_1=0.1$)

Table 4.22 Normalized stress intensity factor at the center of a semi-elliptical surface crack in a two-layer plate subjected to bending. In 22a the normalization factor k_{ob}^{∞} is calculated from the corresponding crack depth $L=L_0$. The results in 22b are normalized with respect to $k_{0b} = \sigma_b\sqrt{h_1}$, $\sigma_b=6M/h^2$.

(Material Pair B, $h_2/h_1=0.1$)

Table 4.23 Normalized stress intensity factor at the center of a semi-elliptical surface crack in a two-layer plate subjected to tension. In 23 the normalization factor k_{ot}^{∞} is calculated from the corresponding crack depth $L=L_0$. The results in 23b are normalized with respect to $k_{0t} = \sigma_t\sqrt{h_1}$ $\sigma_t = N/h$.

(Material Pair C, $h_2/h_1=1.$)

Table 4.24 Normalized stress intensity factor at the center of a semi-elliptical surface crack in a two-layer plate subjected to bending. In 24a the normalization factor k_{ob}^{∞} is calculated from the corresponding crack depth $L=L_0$. The results in 24b are normalized with respect to $k_{0b} = \sigma_b\sqrt{h_1}$, $\sigma_b=6M/h^2$.

(Material Pair C, $h_2/h_1=1.$)

Table 4.25 Normalized stress intensity factor at the center of a semi-elliptical surface crack in a two-layer plate subjected to tension. In 25a the normalization factor k_{ot}^{∞} is calculated from the corresponding crack depth $L=L_0$. The results in 25b are normalized with respect to $k_{0t} = \sigma_t\sqrt{h_1}$ $\sigma_t = N/h$.

(Material Pair C, $h_2/h_1=5.$)

Table 4.26 Normalized stress intensity factor at the center of a semi-elliptical surface crack in a two-layer plate subjected to bending. In 26a the normalization factor k_{ob}^{∞} is calculated from the corresponding crack depth $L=L_0$. The results in 26b are normalized with respect to $k_{0b} = \sigma_b\sqrt{h_1}$, $\sigma_b=6M/h^2$.

(Material Pair C, $h_2/h_1=5.$)

Table 4.27 Normalized stress intensity factor at the center of a semi-elliptical surface crack in a two-layer plate subjected to tension. In 27a the normalization factor k_{ot}^{∞} is calculated from the corresponding crack depth $L=L_0$. The results in 27b are normalized with respect to $k_{0t} = \sigma_t\sqrt{h_1}$ $\sigma_t = N/h$.

(Material Pair D, $h_2/h_1=1.$)

Table 4.28 Normalized stress intensity factor at the center of a semi-elliptical surface crack in a two-layer plate subjected to bending. In 28a the normalization factor k_{ob}^{∞} is calculated from the corresponding crack depth $L=L_0$. The results in 28b are normalized with respect to $k_{0b} = \sigma_b\sqrt{h_1}$, $\sigma_b=6M/h^2$.

(Material Pair D, $h_2/h_1=1.$)

Table 4.29 Normalized stress intensity factor at the center of a semi-elliptical surface crack in a two-layer plate subjected to tension. In 29a the normalization factor k_{ot}^{∞} is calculated from the corresponding crack depth $L=L_0$. The results in 29b are normalized with respect to $k_{0t} = \sigma_t\sqrt{h_1}$ $\sigma_t = N/h$.

(Material Pair D, $h_2/h_1=5.$)

Table 4.30 Normalized stress intensity factor at the center of a semi-elliptical surface crack in a two-layer plate subjected to bending. In 30a the normalization factor k_{ob}^{∞} is calculated from the corresponding crack depth $L=L_0$. The results in 30b are normalized with respect to $k_{0b} = \sigma_b\sqrt{h_1}$, $\sigma_b=6M/h^2$.

(Material Pair D, $h_2/h_1=5.$)

Table 4.31 Normalized stress intensity factor at the center of a semi-elliptical surface crack in a two-layer plate subjected to tension. In 31a the normalization factor k_{ot}^{∞} is calculated from the corresponding crack depth $L=L_0$. The results in 31b are normalized with respect to $k_{0t} = \sigma_t\sqrt{h_1}$ $\sigma_t = N/h$.

(Material Pair D, $h_2/h_1=0.2$)

Table 4.32 Normalized stress intensity factor at the center of a semi-elliptical surface crack in a two-layer plate subjected to bending. In 32a the normalization factor k_{ob}^{∞} is calculated from the corresponding crack depth $L=L_0$. The results in 32b are normalized with respect to $k_{0b} = \sigma_b\sqrt{h_1}$, $\sigma_b=6M/h^2$.

(Material Pair D, $h_2/h_1=0.2$)

Table 4.33 Normalized stress intensity factor at the center of a semi-elliptical surface crack in a two-layer plate subjected to tension. In 33a the normalization factor k_{ot}^{∞} is calculated from the corresponding crack depth $L=L_0$. The results in 33b are normalized with respect to $k_{0t} = \sigma_t\sqrt{h_1}$ $\sigma_t = N/h$.

(Material Pair E, $h_2/h_1=1.$)

Table 4.34 Normalized stress intensity factor at the center of a semi-elliptical surface crack in a two-layer plate subjected to bending. In 34a the normalization factor k_{ob}^{∞} is calculated from the corresponding crack depth $L=L_0$. The results in 34b are normalized with respect to $k_{0b} = \sigma_b\sqrt{h_1}$, $\sigma_b=6M/h^2$.

(Material Pair E, $h_2/h_1=1.$)

Table 4.35 Normalized stress intensity factor at the center of a semi-elliptical surface crack in a two-layer plate subjected to tension. In 35a the normalization factor k_{ot}^{∞} is calculated from the corresponding crack depth $L=L_0$. The results in 35b are normalized with respect to $k_{0t} = \sigma_t\sqrt{h_1}$ $\sigma_t = N/h$.

(Material Pair E, $h_2/h_1=5.$)

Table 4.36 Normalized stress intensity factor at the center of a semi-elliptical surface crack in a two-layer plate subjected to bending. In 36a the normalization factor k_{ob}^{∞} is calculated from the corresponding crack depth $L=L_0$. The results in 36b are normalized with respect to $k_{0b} = \sigma_b\sqrt{h_1}$, $\sigma_b=6M/h^2$.

(Material Pair E, $h_2/h_1=5.$)

Table 4.37 Normalized stress intensity factor at the center of a semi-elliptical surface crack in a two-layer plate subjected to tension. In 37a the normalization factor k_{ot}^{∞} is calculated from the corresponding crack depth $L=L_0$. The results in 37b are normalized with respect to $k_{0t} = \sigma_t\sqrt{h_1}$ $\sigma_t= N/h$.

(Material Pair E, $h_2/h_1=0.2$)

Table 4.38 Normalized stress intensity factor at the center of a semi-elliptical surface crack in a two-layer plate subjected to bending. In 38a the normalization factor k_{ob}^{∞} is calculated from the corresponding crack depth $L=L_0$. The results in 38b are normalized with respect to $k_{0b} = \sigma_b\sqrt{h_1}$, $\sigma_b=6M/h^2$.

(Material Pair E, $h_2/h_1=0.2$)

Table 4.39 Normalized stress intensity factor at the crack front for a semi-elliptical surface crack in a two-layer plate subjected to tension. The normalization factor k_{ot}^{∞} is the corresponding value for an edge-cracked strip under plane strain conditions with the same crack depth $L=L_0$.

(Material Pair B, $a/h = 1$, $h_2/h_1=1.$)

Table 4.40 Normalized stress intensity factor at the crack front for a semi-elliptical surface crack in a two-layer plate subjected to bending. The normalization factor k_{ob}^{∞} is the corresponding value for an edge-cracked strip under plane strain conditions with the same crack depth $L=L_0$.

(Material Pair B, $a/h = 1$, $h_2/h_1=1.$)

Table 4.41 Normalized stress intensity factor at the crack front for a rectangular surface crack in a two-layer plate subjected to tension. The normalization factor k_{ot}^{∞} is the corresponding value for an edge-cracked strip under plane strain conditions with the same crack depth $L=L_0$.

(Material Pair B, $a/h = 1$, $h_2/h_1=1.$)

Table 4.42 Normalized stress intensity factor at the crack front for a rectangular surface crack in a two-layer plate subjected to bending. The normalization factor k_{ob}^{∞} is the corresponding value for an edge-cracked strip under plane strain conditions with the same crack depth $L=L_0$.

(Material Pair B, $a/h = 1$, $h_2/h_1=1.$)

List of Figures

Figure 2.6 Normalized stress intensity factor in a 3-symmetrically-layered plate containing a through crack of length 2a. (see Figure 2.2 a)
(both Material I and Material II are isotropic materials with $\nu_1 = \nu_2 = 0.3$ and different E_2/E_1 ratios)
($k_0 = \sigma_b \sqrt{a}$, $\sigma_b = 6\, M^{\infty}/h^2$, $h_1 = h_2 = h/2.$)

Figure 2.7 Normalized stress intensity factor in a 3-symmetrically-layered plate containing a through crack of length 2a. (see Figure 2.2 a)
(both Material I and Material II are isotropic materials with $\nu_1 = \nu_2 = 0.3$ and different E_2/E_1 ratios)
($k_0 = \sigma_b \sqrt{a}$, $\sigma_b = 6\, M^{\infty}/h^2$, $h_1/h_2 = 0.1$)

Figure 2.8 Normalized stress intensity factor in a 3-symmetrically-layered plate containing a through crack of length 2a. (see Figure 2.2 a)
(both Material I and Material II are isotropic materials with $\nu_1 = \nu_2 = 0.3$ and different E_2/E_1 ratios)
($k_0 = \sigma_b \sqrt{a}$, $\sigma_b = 6\, M^{\infty}/h^2$, $h_1/h_2 = 10$)

Figure 2.9 Normalized stress intensity factor in a 3-symmetrically-layered "honeycomb structure" plate containing a through crack of length 2a.
(Material I is isotropic material and being fixed ,

for Material II $TT = \frac{G_{xz}}{G_{xy}} = \frac{G_{yz}}{G_{xy}}$)

($k_0 = \sigma_b \sqrt{a}$, $\sigma_b = 6\, M^{\infty}/h^2$, $h_1/h_2 = 5$, $E_2/E_1 = 5$)

Figure 2.10 Normalized stress intensity factor in a 3-symmetrically-layered "honeycomb structure" plate containing a through crack of length 2a.
(Material I is isotropic material and being fixed ,

for Material II $TT = \frac{G_{xz}}{G_{xy}} = \frac{G_{yz}}{G_{xy}}$)

($k_0 = \sigma_b \sqrt{a}$, $\sigma_b = 6\, M^{\infty}/h^2$, $h_1/h_2 = 5$, $a/h = 1$)

Figure 2.11 Normalized stress intensity factor in a 3-symmetrically-layered "honeycomb structure" plate containing a through crack of length 2a.
(Material I is isotropic material and being fixed ,

for Material II $TT = \frac{G_{xz}}{G_{xy}} = \frac{G_{yz}}{G_{xy}}$)

($k_0 = \sigma_b \sqrt{a}$, $\sigma_b = 6\ M^{\infty}/h^2$, $h_1/h_2 = 5$; $a/h = 1$)

Figure 2.12 Normalized stress intensity factor in a 3-symmetrically-layered "honeycomb structure" plate containing a through crack of length 2a.
(Material I is isotropic material and being fixed ,

for Material II $TT = \frac{G_{xz}}{G_{xy}} = \frac{G_{yz}}{G_{xy}}$)

($k_0 = \sigma_b \sqrt{a}$, $\sigma_b = 6\ M^{\infty}/h^2$, $E_2/E_1 = 10$, $a/h = 1$)

Figure 2.13 Normalized stress intensity factor in a 3-symmetrically-layered "honeycomb structure" plate containing a through crack of length 2a.
(Material I is isotropic material and being fixed ,

for Material II $TT = \frac{G_{xz}}{G_{xy}} = \frac{G_{yz}}{G_{xy}}$)

($k_0 = \sigma_b \sqrt{a}$, $\sigma_b = 6\ M^{\infty}/h^2$, $E_2/E_1 = 10$, $a/h = 10$)

Figure 2.14 Normalized stress intensity factor in a two - layer isotropic plate containing a through crack of length 2a under bending. (see Figure 2.2 b)
(both Material I and Material II are isotropic materials
with $\nu_1 = \nu_2 = 0.3$ and different E_2/E_1 ratios)
($k_2 = k(h\text{-}c_0)$, $k_0 = \sigma_b \sqrt{a}$, $\sigma_b = 6\ M^{\infty}/h^2$, $h_2/h_1 = 0.1$)

Figure 2.15 Normalized stress intensity factor in a two - layer isotropic plate containing a through crack of length 2a under bending. (see Figure 2.2 b)
(both Material I and Material II are isotropic materials with $\nu_1 = 0.3$ and different ν_2/ν_1 ratios)
($k_2 = k(h\text{-}c_0)$, $k_0 = \sigma_b \sqrt{a}$, $\sigma_b = 6\, M^{\infty}/h^2$, $h_2/h_1 = 1$)

Figure 2.16 Normalized stress intensity factor in a two - layer isotropic plate containing a through crack of length 2a under tension. (see Figure 2.2 b)
(both Material I and Material II are isotropic materials with $\nu_1 = 0.3$ and different ν_2/ν_1 ratios)
($k_2 = k(h\text{-}c_0)$, $k_0 = \sigma_t \sqrt{a}$, $\sigma_t = N^{\infty}/h$, $h_2/h_1 = 1$)

Figure 2.17 Normalized stress intensity factor in a two - layer isotropic plate containing a through crack of length 2a under bending. (see Figure 2.2 b)
(both Material I and Material II are isotropic materials with $\nu_1 = \nu_2 = 0.3$ and different E_2/E_1 ratios)
($k_2 = k(h\text{-}c_0)$, $k_0 = \sigma_b \sqrt{a}$, $\sigma_b = 6\, M^{\infty}/h^2$, $h_2/h_1 = 0.1$)

Figure 2.18 Normalized stress intensity factor in a two - layer orthotropic plate containing a through crack of length 2a under bending. (see Figure 2.2 b)
(both Material I and Material II are orthotropic materials with Material I being Material A and Material II being Material B)
($k_2 = k(h\text{-}c_0)$, $k_0 = \sigma_b \sqrt{a}$, $\sigma_b = 6\, M^{\infty}/h^2$)

Figure 2.19 Normalized stress intensity factor in a two - layer orthotropic plate containing a through crack of length 2a under bending. (see Figure 2.2 b)
(both Material I and Material II are orthotropic materials with Material I being Material C and Material II being Material D)
($k_2 = k(h\text{-}c_0)$, $k_0 = \sigma_b \sqrt{a}$, $\sigma_b = 6\, M^{\infty}/h^2$)

Figure 2.20 The effect of individual material constants on the normalized stress intensity factor in a two - layer plate containing a through crack of length 2a under bending moment M^{∞}. (see Figure 2.2 b)
(Material I is isotropic materials and it is fixed; Material II is assumed to be "isotropic" expect one constant varies)
($k_2 = k(h\text{-}c_0)$, $k_0 = \sigma_b \sqrt{a}$, $\sigma_b = 6\, M^{\infty}/h^2$)
($a/h = 1$, $h_1/h_2 = 1$)

Figure 2.21 The effect of individual material constants on the normalized stress intensity factor in a two - layer plate containing a through crack of length 2a under bending moment M^{∞}. (see Figure 2.2 b)
(Material I is Material D, an orthotropic material, Material II is assumed to be "isotropic", with E = 5.86 (GPA), expect one constant varies)
($k_2 = k(h\text{-}c_0)$, $k_0 = \sigma_b \sqrt{a}$, $\sigma_b = 6\, M^{\infty}/h^2$)
($a/h = 1$, $h_2/h_1 = 1$)

Figure 2.22 The effect of individual material constants on the normalized stress intensity factor in a two - layer plate containing a through crack of length 2a under bending moment M^{∞}. (see Figure 2.2 b)
(Material I is Material A, an orthotropic material, Material II is assumed to be "isotropic", with E = 39.0 (GPA), expect one constant varies)
($k_2 = k(h\text{-}c_0)$, $k_0 = \sigma_b \sqrt{a}$, $\sigma_b = 6\, M^{\infty}/h^2$)

Figure 2.23 Normalized stress intensity factor distribution in a two - layer orthotropic plate containing a through crack of length 2a under tension. (see Figure 2.2 b)
(both Material I and Material II are orthotropic materials with Material I being Material A and Material II being Material B)
($\bar{z} = z + c_0$, $k_0 = \sigma_t \sqrt{a}$, $\sigma_t = N^{\infty}/h$)
($a/h = 1$, $h_2/h_1 = 1$)

Figure 2.24 Normalized stress intensity factor distribution in a two - layer orthotropic plate containing a through crack of length 2a under bending. (see Figure 2.2 b)
(both Material I and Material II are orthotropic materials
with Material I being Material A and Material II being Material B)
($\bar{z} = z + c_0$, $k_0 = \sigma_b \sqrt{a}$, $\sigma_b = 6\, M^{\infty}/h^2$)
($a/h = 1$, $h_2/h_1 = 1$)

Figure 2.25 Normalized stress intensity factor distribution in a two - layer orthotropic plate containing a through crack of length 2a under tension. (see Figure 2.2 b)
(both Material I and Material II are orthotropic materials
with Material I being Material A and Material II being Material B)
($\bar{z} = z + c_0$, $k_0 = \sigma_t \sqrt{a}$, $\sigma_t = N^{\infty}/h$)
($a/h = 1$, $h_2/h_1 = 10$)

Figure 2.26 Normalized stress intensity factor distribution in a two - layer orthotropic plate containing a through crack of length 2a under bending. (see Figure 2.2 b)
(both Material I and Material II are orthotropic materials
with Material I being Material A and Material II being Material B)
($\bar{z} = z + c_0$, $k_0 = \sigma_b \sqrt{a}$, $\sigma_b = 6\, M^{\infty}/h^2$)
($a/h = 1$, $h_2/h_1 = 10$)

Figure 2.27 Normalized stress intensity factor distribution in a 3-unsymmetrically -layered plate containing a through crack under tension. (see Figure 2.2 c)
(Materials I and III are isotropic, with $\nu_1 = \nu_3 = 0.3$,
and $E_1/E_2 = 3.0$, $E_3/E_2 = 10.$;
Material II is "as if" isotropic, with E_2 and $\nu_2 = 0.3$,
and $G_{xz} = G_{yz} = 3\, G_{xy}$)
($\bar{z} = z + c_0$, $k_0 = \sigma_t \sqrt{a}$, $\sigma_t = N^{\infty}/h$)
($a/h = 0.5$, $h_3/h_2 = 0.2$, $h_1/h_2 = 0.2$)

Figure 2.28 Normalized stress intensity factor distribution in a 3-unsymmetrically -layered plate containing a through crack under bending. (see Figure 2.2 c)
(Materials I and III are isotropic, with $\nu_1 = \nu_3 = 0.3$,
and $E_1/E_2 = 3.0$, $E_3/E_2 = 10.$;
Material II is "as if" isotropic, with E_2 and $\nu_2 = 0.3$,
and $G_{xz} = G_{yz} = 3\ G_{xy}$)
($\bar{z} = z + c_0$, $k_0 = \sigma_b \sqrt{a}$, $\sigma_b = 6\ M^{\infty}/h^2$)
($a/h = 0.5$, $h_3/h_2 = 0.2$, $h_1/h_2 = 0.2$)

Figure 2.29 Normalized stress intensity factor distribution in a 3-unsymmetrically -layered plate containing a through crack under tension. (see Figure 2.2 c)
(Materials I and III are isotropic, with $\nu_1 = 0.5$ and $\nu_3 = 0.2$,
and $E_1/E_2 = 3.0$, $E_3/E_2 = 10.$;
Material II is "as if" isotropic, with E_2 and $\nu_2 = 0.$,
and $G_{xz} = G_{yz} = 3\ G_{xy}$)
($\bar{z} = z + c_0$, $k_0 = \sigma_t \sqrt{a}$, $\sigma_t = N^{\infty}/h$)
($a/h = 0.5$, $h_3/h_2 = 0.2$, $h_1/h_2 = 0.2$)

Figure 2.30 Normalized stress intensity factor distribution in a 3-unsymmetrically -layered plate containing a through crack under bending. (see Figure 2.2 c)
(Materials I and III are isotropic, with $\nu_1 = 0.5$ and $\nu_3 = 0.2$,
and $E_1/E_2 = 3.0$, $E_3/E_2 = 10.$;
Material II is "as if" isotropic, with E_2 and $\nu_2 = 0.$,
and $G_{xz} = G_{yz} = 3\ G_{xy}$)
($\bar{z} = z + c_0$, $k_0 = \sigma_b \sqrt{a}$, $\sigma_b = 6\ M^{\infty}/h^2$)
($a/h = 0.5$, $h_3/h_2 = 0.2$, $h_1/h_2 = 0.2$)

Abstract

The main objective of this study is to develop an analytical method for a relatively accurate calculation of Stress Intensity Factors in a laminated orthotropic plate containing a through or a part-through crack. The laminated plate is assumed to be under bending or membrane loading and the mode I problem is considered.

First three transverse shear deformation plate theories (Mindlin's displacement based first-order theory, Reissner's stress-based first-order theory and a simple-higher order theory due to Reddy) are reviewed and examined for homogeneous, laminated and heterogeneous orthotropic plates. Then based on a general linear laminated plate theory, a method by which the stress intensity factors can be obtained in orthotropic laminated and heterogeneous plates with a through crack is developed. Examples are given for both symmetrically and unsymmetrically laminated plates and the effect of various material properties on the stress intensity factors are studied.

In order to implement the line-spring model which is used later to study the surface crack problem, the corresponding plane elasticity problem of a two-bonded orthotropic plate containing a crack perpendicular to the interface is also considered. Three different crack profiles: an internal crack, an edge crack and a crack terminating at the interface are considered. The effect of the different material combinations, geometries and material orthotropy on the stress intensity factors and on the power of stress singularity for a crack terminating at the interface is fully examined.

The Line Spring model of Rice and Levy is used for the part-through crack problem. The surface crack is assumed to lie in one of the two-layered laminated orthotropic plates due to the limitation of the available plane strain results. Rather extensive numerical results are given for both laminated composite and bonded metal-ceramic structural materials with various geometrical configurations. These results will be useful in brittle fracture analysis and more importantly, in subcritical crack growth studies.

All problems considered in this study are of the mixed boundary value type and are reduced to Cauchy type of singular integral equations which are then solved numerically.

Chapter 1. Transverse Shear Deformation Theories

1.1 INTRODUCTION

In recent years the potential of laminated composite materials for use as structural members has inspired considerable research activity in the study of the response of anisotropic laminated media. Because of the complicated internal structure of composites the stress field in the system is truly three-dimensional in character. One possible means of simplifying the three-dimensional equations of elasticity is to use the concept adopted in the formulation of plate theories. By following this approach various theories have been developed to treat the mechanical response of composite laminates. For example, classical laminated plate theory, which is an extension of the classical plate theory to laminated plates, was discussed by Lekhnitskii [1] by employing the Kirchhoff hypothesis in the analysis of symmetrical laminates. However, the classical laminate theory is inadequate for laminated plates made of advanced filamentary composite materials because most of these advanced composites have a low ratio of the transverse shear modulus to the in-plane modulus. Moreover, when we study the problem of a cracked plate under general loading conditions, the classical theory gives the following asymptotic results for the stress resultant distributions around the crack tip

$$N_{ij} \simeq \frac{1}{\sqrt{2r}} [\, k_1{}^t f_{ij}{}^1(\theta) + k_2{}^t f_{ij}{}^2(\theta)] \,,$$

$$M_{ij} = \frac{1}{\sqrt{2r}} [\, k_1{}^b g_{ij}{}^1(\theta,\nu) + k_2{}^b g_{ij}{}^2(\theta,\nu)] \,,$$

$$V_i \simeq \frac{1}{r^{3/2}}\ k_3 h_{3i}(\theta,\nu), \qquad (i,j=1,2), \tag{1.1a}$$

whereas an appropriate transverse shear deformation theory (such as that of Reissner's or Mindlin's) provides the corresponding fields as follows:

$$N_{ij} \simeq \frac{1}{\sqrt{2r}} [\, k_1{}^t f_{ij}{}^1(\theta) + k_2{}^t f_{ij}{}^2(\theta)] \,,$$

$$M_{ij} \simeq \frac{1}{\sqrt{2r}} [\, k_1{}^b f_{ij}{}^1(\theta) + k_2{}^b f_{ij}{}^2(\theta)] \,,$$

$$V_i \simeq \frac{1}{\sqrt{2r}} k_3 f_i{}^3(\theta), \qquad (\, i,j = 1,2 \,), \qquad (1.1b)$$

where N_{ij}, M_{ij} and V_i are respectively membrane, bending and transverse shear components of the stress resultants, k_1, k_2 and k_3 are respectively the modes I, II, and III stress intensity factors, r and θ are the local polar coordinats in x_1x_2 plane, and the angular expressions $f_{ij}{}^1$, $f_{ij}{}^2$ and $f_i{}^3$ are identical to the results given by the continuum elasticity solutions of crack problems [2] and [3].

Expressions (1.1a) clearly show that the solutions regarding the bending and transverse shear stress states at the crack tip given by classical theory do not conform to the standard results obtained from the elasticity solutions. That is, the angular distributions for M_{ij} and V_i differ from the expected elasticity results and are dependent on the Poisson's ratio, and the 3/2 singularity given for V_i is physically unacceptable. Furthermore, because of these discrepencies, the critical fracture mechanics parameters $k_1{}^b$, $k_2{}^b$ and k_3 obtained from the classical theory are bound to be inaccurate. These inconsistencies are perhaps due to the fact that the classical theory can accommodate only two boundary conditions on the crack surface, namely the normal component of the bending moment and the Kirchhoff's effective transverse shear resultant combining the twisting moment and the transverse shear resultant, and it is likely to be inaccurate in the region of primary interest near the crack tip. All these shortcomings are seem to be removed when a transverse shear deformation theory is used.

Currently two groups of shear deformation plate theories are known in the literature: (1) stress-based theories and (2) displacement-based theories. The first stress-based shear deformation plate theory is due to Reissner [4], [5] and is based on a linear distribution of the in-plane normal and shear stresses through the thickness. The origin of displacement-based theories is attributed to Basset [6], and Hildebrand & Reissner & Thomas [7]. These first-order shear deformation theories assumed the following displacement field

$$u_1 (x, y, z) = u (x, y) + z \psi_x (x, y) ,$$

$$u_2 (x, y, z) = v (x, y) + z \psi_y (x, y) ,$$

$$u_3 (x, y, z) = \omega (x, y) . \qquad (1.2)$$

The shear deformation theory based on equation (1.2) for plate is often referred to as the Mindlin plate theory [8]. Analogous to the approaches, which are based on introducing a priori plausible assumptions regarding the variation of displacement, strain and/ or stresses in the thickness direction, Yang, Norris and Stavsky [9] presented a generalization of Mindlin's first order shear deformation plate theories for anisotropic plates. In Mindlin type of first-order theory a correction factor has to be introduced to account for the fact that it predicts a uniform shear stress through the thickness of the plate, which is obviously incorrect for most of cases.

For a more realistic evaluation of the stress fields and the shear stresses, high-order shear deformation theories have been proposed [10]. These high-order theories are cumbersome and computationally more demanding, because with each additional power of the thickness coordinate, an additional dependent unknowns is introduced into the theory. Recently Reddy [11] has extended the Levinson simple-high-order [12] approach of homogeneous isotropic plates to the laminated anisotropic composite plates. This simple-high-order laminated plate theory not only accounts for the parabolic variation of the transverse shear strains through the thickness, but also contains the same 5 dependent unknowns as in the first order theories.

These three above mentioned transverse shear deformation theories (Reissner's, Mindlin's and Reddy's) are reviewed and examined in this chapter. For each approach the basic assumptions, strain and stress fields, the plate constitutive equations and governing equations are examined. In addition, the controversies that definitely exist in the plate theory approach are explored. Homogeneous plate theories are studied first, then follows the extension to the laminated plate theories. Here, the laminated plate theories are the so-called single-layer laminate theories which are based on replacing the laminated plate by an equivalent single-layer anisotropic plate and introducing global displacement, strain and/or stress approximations in the thickness direction. It has been shown that these single-layer laminate theories, even the first-order theory, are adequate in representing global behavior, such as deflections

and stresses, of thin composites. If the local effects, such as interlaminar stress distributions, delaminations on fiber/matrix interface, etc, are to be studied one then has to consider the so-called multi-layer laminate theories, which are based on piecewise stress/ displacement approximations in the thickness direction. Here only single-layer laminate theories are studied.

1.2 TRANSVERSE SHEAR DEFORMATION PLATE THEORIES ----------HOMOGENEOUS ISOTROPIC PLATE

In this section the plate under consideration is assumed to be a thin elastic homogeneous isotropic plate of thickness h. The origin of a Cartesian coordinate system is located within the midplane (x, y) with the z axis being normal to this plane. As in the standard plate theory, it is also assumed that the plate surfaces $z = \pm h/2$ are subjected to surface traction defined by

$$\sigma_{xz} (x, y, \pm h/2) = 0,$$
$$\sigma_{yz} (x, y, \pm h/2) = 0, \qquad (1.3\ a)$$

and

$$\sigma_z (x, y, + h/2) = - q_1,$$
$$\sigma_z (x, y, - h/2) = - q_2, \qquad (1.3\ b)$$

where q_1 and q_2 can be arbitrary functions of x and y.

The stress and moment resultants, each per unit length, are defined in the usual way, i.e.

$$(Q_x, Q_y) = \int_{-h/2}^{+h/2} (\sigma_{xz}, \sigma_{yz}) \, dz,$$

$$(M_x, M_y, M_{xy}) = \int_{-h/2}^{+h/2} (\sigma_x, \sigma_y, \sigma_{xy}) \, z \, dz. \qquad (1.4)$$

Because linear homogeneous plate bending theory is used, the in-plane stress resultants N_x, N_y and N_{xy}, which are uncoupled with the bending resultant components, are not presented here.

Based on the above general assumptions, three different plate bending theories are discussed in detail in the following subsections.

1.2.1 Mindlin's Displacement Based First-order Plate Theory

1.2.1.1 The Assumed Displacement Field

In Mindlin's plate theory, the primary assumptions are based on the displacement fields [8], which, in the absence of the time parameter t, are described as follows:

$$u(x, y, z) = z\,\psi_x(x, y),$$
$$v(x, y, z) = z\,\psi_y(x, y),$$
$$\omega(x, y, z) = \omega(x, y). \qquad (1.5)$$

Notice u and v are linear functions of z and ω is independent of z. Here the three plate displacement components ψ_x, ψ_y and ω are the unknown functions. Because of the linear features of u and v, this theory is referred to as the first order theory.

1.2.1.2 The Strain Field

Using standard linear elasticity approach, the strain field can be obtained from (1.5) as

$$\epsilon_x = \frac{\partial u}{\partial x} = z\,\frac{\partial \psi_x}{\partial x},$$
$$\epsilon_y = \frac{\partial v}{\partial y} = z\,\frac{\partial \psi_y}{\partial y},$$
$$\gamma_{xy} = \frac{\partial u}{\partial y} + \frac{\partial v}{\partial x} = z\left(\frac{\partial \psi_x}{\partial y} + \frac{\partial \psi_y}{\partial x}\right), \qquad (1.6)$$
$$\gamma_{xz} = \frac{\partial u}{\partial z} + \frac{\partial \omega}{\partial x} = \psi_x + \frac{\partial \omega}{\partial x},$$
$$\gamma_{yz} = \frac{\partial v}{\partial z} + \frac{\partial \omega}{\partial y} = \psi_y + \frac{\partial \omega}{\partial y},$$
$$\epsilon_z = 0 \qquad (1.7)$$

We can see that by using assumption (1.5) the in-plane strains are linear functions of z while the out-of-plane strains are constants through the thickness of the plate. Normal strain ϵ_z is neglected.

1.2.1.3 Constitutive Equations

For the thin plate, we assume the transverse normal stress may be neglected in comparison with the other stress components. Then the constitutive equations for the homogeneous isotropic plate can be obtained as follows:

$$\epsilon_x = \frac{1}{E} (\sigma_x - \nu \sigma_y) ,$$

$$\epsilon_y = \frac{1}{E} (- \nu \sigma_x + \sigma_y) ,$$

$$\gamma_{yz} = \frac{1}{G} \sigma_{yz} , \quad \gamma_{xz} = \frac{1}{G} \sigma_{xz} , \quad \gamma_{xy} = \frac{1}{G} \sigma_{xy} , \qquad (1.8)$$

$$\sigma_x = \frac{E}{1 - \nu^2} (\epsilon_x + \nu \epsilon_y) ,$$

$$\sigma_y = \frac{E}{1 - \nu^2} (\epsilon_y + \nu \epsilon_x) ,$$

$$\sigma_{yz} = G \gamma_{yz} , \quad \sigma_{xz} = G \gamma_{xz} , \quad \sigma_{xy} = G \gamma_{xy} . \qquad (1.9)$$

1.2.1.4 The Stress Field

(a) Obtaining the stress fields from the constitutive equations

The general constitutive equations assume the linear strain-stress relationship. Considering expressions (1.6), (1.7) and (1.9) the stress field in the plate may be expressed as

$$\sigma_x = z \left(\frac{E}{1 - \nu^2} \right) \left(\frac{\partial \psi_x}{\partial x} + \nu \frac{\partial \psi_y}{\partial y} \right) = c_1 (x, y) z$$

$$\sigma_y = z \left(\frac{E}{1 - \nu^2} \right) \left(\frac{\partial \psi_y}{\partial y} + \nu \frac{\partial \psi_x}{\partial x} \right) = c_2 (x, y) z$$

$$\sigma_{xy} = z G \left(\frac{\partial \psi_x}{\partial y} + \frac{\partial \psi_y}{\partial x} \right) = c_3 (x, y) z \qquad (1.10)$$

$$\sigma_{xz} = G \left(\psi_x + \frac{\partial \omega}{\partial x} \right) = c_4 (x, y)$$

$$\sigma_{yz} = G \left(\psi_y + \frac{\partial \omega}{\partial y} \right) = c_5 (x, y) \qquad (1.11)$$

where c_i ($i = 1, 5$) are functions of x and y only.

Again, the in-plane stresses are linear functions of z and the out-of-plane stresses are constant through the thickness direction. Expressions (1.11) obviously violate the boundary conditions (1.3 a).

(b) Obtaining stress field from the equilibrium equations :

Here the in-plane normal and shear stresses are the same as expressed in (1.10) but, we use a different approach, an equilibrium equation approach, to express the out-of-plane shear stresses. From the standard equilibrium equations in elasticity

$$\frac{\partial \sigma_x}{\partial x} + \frac{\partial \sigma_{xy}}{\partial y} + \frac{\partial \sigma_{xz}}{\partial z} = 0 \ , \qquad (1.12)$$

we have

$$\frac{\partial \sigma_{xz}}{\partial z} = -\left(\frac{\partial \sigma_x}{\partial x} + \frac{\partial \sigma_{xy}}{\partial y} \right) . \qquad (1.13)$$

Integrating (1.12) and using the expressions (1.10) we find

$$\sigma_{xz}(x, y) = \int_{-h/2}^{z} \frac{\partial \sigma_{xz}}{\partial z}\, dz = \int_{-h/2}^{z} - \left(\frac{\partial \sigma_x}{\partial x} + \frac{\partial \sigma_{xy}}{\partial y} \right) dz$$

$$= \int_{-h/2}^{z} - \left(\frac{\partial c_1}{\partial x} + \frac{\partial c_3}{\partial y} \right) z\, dz \,. \qquad (1.14)$$

It can easily be seen that σ_{xz} has the term of z^2 , i. e.

$$\sigma_{xz} \propto z^2 + \ldots\ldots \qquad (1.15\ a)$$

In the same manner, it can be shown that

$$\sigma_{yz} \propto z^2 + \ldots\ldots \qquad (1.15\ b)$$

Comparing (1.11) with (1.15), it is clear that in Mindlin's plate theory there is an inherent inconsistency regarding the stress field.

1.2.1.5 Plate Constitutive Equations

Substituting (1.6) and (1.7) into equations (1.9) and performing the integration from (- h/2) to (+ h/2), the following equations are obtained between the moment resultants to the plate-displacement components:

$$\begin{bmatrix} M_x \\ M_y \\ M_{xy} \end{bmatrix} = D \begin{bmatrix} 1 & \nu & 0 \\ \nu & 1 & 0 \\ 0 & 0 & (1-\nu)/2 \end{bmatrix} \begin{bmatrix} k_x \\ k_y \\ k_{xy} \end{bmatrix}, \qquad (1.16)$$

where

$$D = \frac{E\, h^3}{12\,(1 - \nu^2)}\,, \qquad (1.17)$$

and

$$k_x = \frac{\partial\, \psi_x}{\partial\, x}\,,\quad k_y = \frac{\partial\, \psi_y}{\partial\, y}\,,\quad k_{xy} = \frac{\partial\, \psi_x}{\partial\, y} + \frac{\partial\, \psi_y}{\partial\, x}\,,$$

and

$$Q_x = K\,G\,h\,(\ \psi_x + \frac{\partial \omega}{\partial x}\ ),$$

$$Q_y = K\,G\,h\,(\ \psi_y + \frac{\partial \omega}{\partial y}\ ). \qquad (1.18)$$

Notice that a parameter K has been introduced into the expressions for the transverse shear resultants. Here the constant, K, commonly known as a correction factor, is used to account for the fact that the transverse shear stresses are constant through the thickness of the plate. By comparing to the exact theory various values of K has been used for homogeneous isotropic plates. For example Reissner [4], Mindlin [13], and Uflyand [14] used values of 5/6, $\pi^2/12$, and 3/2 respectively. The evaluation of K in a specific problem depends on either the exact elasticity solution of the problem or experimental evidence.

1.2.1.6 Governing Equations:

As in the standard plate theory, the stress resultants must satisfy the equilibrium equations:

$$\frac{\partial M_x}{\partial x} + \frac{\partial M_{xy}}{\partial y} - Q_x = 0\ ,$$

$$\frac{\partial M_y}{\partial y} + \frac{\partial M_{xy}}{\partial x} - Q_y = 0\ ,$$

$$\frac{\partial Q_x}{\partial x} + \frac{\partial Q_y}{\partial y} = 0\ . \qquad (1.19)$$

Substituting (1.16), (1. 18) into (1. 19) the governing equations can be obtained as

$$L_i (\omega_{,kk};\ \omega_{,k};\ \psi_{x,kk};\ \psi_{x,k};\ \psi_{y,kk};\ \psi_{y,k};\ \psi_x ;\ \psi_y) = 0 ,$$

$$i = (1, 2, 3) , \quad k = (x, y) . \qquad (1.20)$$

Under proper boundary conditions, the unknown functions ω, ψ_x and ψ_y could be solved for various specific problems.

1.2.2 Reissner's Stress Based First-order Plate Theory

1.2.2.1 The Assumed Stress Field

Reissner's plate theory is based on a linear distribution of the in-plane normal and shear stresses through the thickness:

$$\sigma_x = \frac{M_x}{h^2/6} \frac{z}{h/2} ,$$

$$\sigma_y = \frac{M_y}{h^2/6} \frac{z}{h/2} ,$$

$$\sigma_{xy} = \frac{M_{xy}}{h^2/6} \frac{z}{h/2} . \qquad (1.21)$$

The distribution of the transverse normal and shear stresses is determined from the equilibrium equations of the elasticity theory:

$$\frac{\partial \sigma_x}{\partial x} + \frac{\partial \sigma_{xy}}{\partial y} + \frac{\partial \sigma_{xz}}{\partial z} = 0 ,$$

$$\frac{\partial \sigma_{xy}}{\partial x} + \frac{\partial \sigma_y}{\partial y} + \frac{\partial \sigma_{yz}}{\partial z} = 0 ,$$

$$\frac{\partial \sigma_{xz}}{\partial x} + \frac{\partial \sigma_{yz}}{\partial y} + \frac{\partial \sigma_z}{\partial z} = 0 . \qquad (1.22)$$

Integrating equations (1.22) and using the boundary conditions, following (1.21) and the plate equilibrium equations (1.19) we can derive the expressions σ_{xz} as follows:

$$\sigma_{xz} = - \int_{-h/2}^{z} \frac{\partial \sigma_{xz}}{\partial z} \, dz = - \int_{-h/2}^{z} \left(\frac{\partial \sigma_x}{\partial x} + \frac{\partial \sigma_{xy}}{\partial y} \right) dz$$

$$= - \int_{-h/2}^{z} \left(\frac{\partial M_x}{\partial x} + \frac{\partial M_{xy}}{\partial y} \right) \frac{z}{h^3/12} \, dz$$

$$= - Q_x \int_{-h/2}^{z} \frac{z}{h^3/12} \, dz \, ,$$

$$\sigma_{xz} = \frac{3 \, Q_x}{2 \, h} \left[1 - \left(\frac{2z}{h} \right)^2 \right] . \qquad (1.23 \text{ a})$$

Similarly the transverse stress σ_{yz} and the normal stress σ_z can be obtained in term of their resultants and the coordinate z

$$\sigma_{yz} = \frac{3 \, Q_y}{2 \, h} \left[1 - \left(\frac{2z}{h} \right)^2 \right] , \qquad (1.23 \text{ b})$$

and

$$\sigma_z = - \frac{3 \, q}{4} \left[\frac{2}{3} - \frac{2 \, z}{h} + \frac{1}{3} \left(\frac{2 \, z}{h} \right)^3 \right] ,$$

where $q = q_1 - q_2$. (1.24 a, b)

From expressions (1.21), it can be seen that in-plane normal and shear stress are linearly distributed through the thickness, which is the same as in Mindlin's theory (see expressions (1.10)). Because of this in literature both of these theories are often called Mindlin-Ressiner's first-order plate theory. On the other hand, in Reissner's theory the transverse shear stresses, obtained from the equilibrium equations, are parabolicly distributed through the thickness. Therefore the boundary conditions at top and bottom of the plate [see (1.3 a)] are satisfied.

1.2.2.2 The Strain Field

Assuming an isotropic material and the displacements u, v and ω of any point in the plate to be small as compared with its thickness h, we use the following general stress-strain relations:

$$\epsilon_x = \frac{\partial u}{\partial x} = \frac{1}{E} [\sigma_x - \nu (\sigma_y + \sigma_z)] ,$$

$$\epsilon_y = \frac{\partial v}{\partial y} = \frac{1}{E} [\sigma_y - \nu (\sigma_x + \sigma_z)] ,$$

$$\gamma_{xy} = \frac{\partial u}{\partial y} + \frac{\partial v}{\partial x} = \frac{1}{G} \sigma_{xy} , \qquad (1.25)$$

$$\gamma_{xz} = \frac{\partial u}{\partial z} + \frac{\partial \omega}{\partial x} = \frac{1}{G} \sigma_{xz} ,$$

$$\gamma_{yz} = \frac{\partial v}{\partial z} + \frac{\partial \omega}{\partial y} = \frac{1}{G} \sigma_{yz} , \qquad (1.26)$$

$$\epsilon_z = \frac{\partial \omega}{\partial z} = \frac{1}{E} [\sigma_z - \nu (\sigma_x + \sigma_y)] . \qquad (1.27)$$

Notice that, for the case q = 0, the in-plane normal and shear stress are linear function of z, which is again the same as those in Mindlin's theory. However, as expressed in (1.26) and following (1.23) the transverse shear strains have the form of $az^2 + b$.

1.2.2.3 The Displacement Field

Substituting (1.21) into (1.25), letting q = 0 and performing the integrations we can easily see that the in-plane displacements u and v are linearly distributed through the thickness, which again are same as the expressions in Mindlin's theory. Unlike the assumption that the plate deflection ω is constant throughout the thickness of the plate in Mindlin's theory, the expression for ω in Reissner's theory has an inconsistency. Using the sixth relationship in the stress-strain relation

$$\frac{\partial \omega}{\partial z} = \frac{1}{E} [\, \sigma_z - \nu (\sigma_x + \sigma_y) \,] \qquad (1.27)$$

for q = 0, and the linear law for the distribution of the stresses σ_x and σ_y, ω will have the term of z^2. Note that the same conclusion can be drawn from the expression (1.26). However in Reissner's original article [4], he stated that to be consistent with the assumption of linear bending stress distribution it is assumed that the displacement u and v vary linearly over the thickness of the plate and that ω does not vary over the thickness of the plate. To overcome this inconsistency, some authors later (for example [15]) have introduced some average value $\bar{\omega}$ of the transverse displacement, taken over the thickness of the plate, and then arrived at the governing equations in terms of this average value of $\bar{\omega}$. In this way instead of finding the actual distribution of ω (x, y, z), somehow the average value ω as a function of x and y is sought.

1.2.2.4 Plate Constitutive Equations

Following [15], introducing some average value ω of the transverse displacement, taken over the thickness of the plate, as well as some average values ψ_x and ψ_y of the rotation of the sections x = constant and y = constant respectively, and defining these quantities by equating the work of the resultant couples on the average rotations and the work of resultant forces on the average displacement to the work of the corresponding stresses on the actual displacements u_0 (x, y, z), v_0 (x, y, z) and ω_0 (x, y, z) in the same section, we find

$$\int_{-h/2}^{+h/2} \sigma_x \; u_0 \, dz = M_x \, \psi_x \,, \qquad \int_{-h/2}^{+h/2} \sigma_y \; v_0 \, dz = M_y \, \psi_y \,,$$

$$\int_{-h/2}^{+h/2} \sigma_{xy} \, v_0 \, dz = M_{xy} \, \psi_y \,, \qquad \int_{-h/2}^{+h/2} \sigma_{xy} \, u_0 \, dz = M_{xy} \, \psi_x \,,$$

$$\int_{-h/2}^{+h/2} \sigma_{xz} \, \omega_0 \, dz = Q_x \, \omega \,, \qquad \int_{-h/2}^{+h/2} \sigma_{yz} \, \omega_0 \, dz = Q_y \, \omega \,.$$

(1.28)

Now substituting expressions (1.21) for the stresses into equations (1.28) the following relations between the average and actual displacement can be obtained

$$\omega = \frac{3}{2\,h} \int_{-h/2}^{+h/2} \omega_0 \left[1 - \left(\frac{2z}{h} \right)^2 \right] dz \,,$$

$$\psi_x = \frac{12}{h^2} \int_{-h/2}^{+h/2} \frac{u_0}{h}\, z\, dz \,,$$

$$\psi_y = \frac{12}{h^2} \int_{-h/2}^{+h/2} \frac{v_0}{h}\, z\, dz \,. \qquad (1.29)$$

Using the stress-strain relations (1.25), for q = 0, we can express the in-plane stresses components σ_x, σ_y and σ_{xy} in terms of the actual displacements as follows:

$$\sigma_x = \frac{E}{1 - \nu^2} \left(\frac{\partial u_0}{\partial x} + \nu \frac{\partial v_0}{\partial y} \right),$$

$$\sigma_y = \frac{E}{1 - \nu^2} \left(\frac{\partial v_0}{\partial y} + \nu \frac{\partial u_0}{\partial x} \right),$$

$$\sigma_{xy} = G \left(\frac{\partial u_0}{\partial y} + \frac{\partial v_0}{\partial x} \right) = \frac{E}{2\,(1 + \nu)} \left(\frac{\partial u_0}{\partial y} + \frac{\partial v_0}{\partial x} \right). \qquad (1.30)$$

Substituting (1.30) into (1.21), multiplying by $\frac{12}{h^3}\, z\, dz$, integrating between $z = -h/2$ and $z = h/2$, and observing relations (1.29), we arrive at the expressions

$$\begin{bmatrix} M_x \\ M_y \\ M_{xy} \end{bmatrix} = D \begin{bmatrix} 1 & \nu & 0 \\ \nu & 1 & 0 \\ 0 & 0 & (1-\nu)/2 \end{bmatrix} \begin{bmatrix} k_x \\ k_y \\ k_{xy} \end{bmatrix},$$

where

$$D = \frac{E\,h^3}{12\,(1 - \nu^2)} \,,$$

and

$$k_x = \frac{\partial \psi_x}{\partial x} , \qquad k_x = \frac{\partial \psi_y}{\partial y} , \qquad k_{xy} = \frac{\partial \psi_x}{\partial y} + \frac{\partial \psi_y}{\partial x} .$$

(1.31)

In like manner, substituting expressions (1.23) into (1.26), multiplying the result by $\frac{3}{2h} \left[1 - \left(\frac{2z}{h} \right)^2 \right] dz$, and integrating between the limits $z = \pm h/2$, we obtain:

$$\begin{bmatrix} Q_x \\ Q_y \end{bmatrix} = \frac{5}{12} \frac{Eh}{1+\nu} \begin{bmatrix} \psi_x + \frac{\partial \omega}{\partial x} \\ \psi_y + \frac{\partial \omega}{\partial y} \end{bmatrix} = \frac{5}{6} G h \begin{bmatrix} \psi_x + \frac{\partial \omega}{\partial x} \\ \psi_y + \frac{\partial \omega}{\partial y} \end{bmatrix}$$

(1.32)

Reissner, in his treatment of this subject, makes use of Castigliano's principle of least work to obtain the above expressions (1.31) and (1.32).

Comparing the plate constitutive equations (1.31) and (1.32) from Reissner's theory with (1.16) and (1.18) from Mindlin's theory we can see that for the bending moments' expressions, the two theories are exactly the same, whereas for the transverse shear resultants, if we let $K = 5/6$ in Mindlin's expressions, we arrive at the identical expressions of Reissner's expressions.

1.2.2.5 Governing Equations

Using the same equilibrium equations for stress resultants, for $q = 0$, we have

$$\frac{\partial M_x}{\partial x} + \frac{\partial M_{xy}}{\partial y} - Q_x = 0 ,$$

$$\frac{\partial M_y}{\partial y} + \frac{\partial M_{xy}}{\partial x} - Q_y = 0 ,$$

$$\frac{\partial Q_x}{\partial x} + \frac{\partial Q_y}{\partial y} = 0 . \qquad (1.33)$$

Now substituting (1.32) into (1.31), eliminating the quantities ψ_x and ψ_y from these equations, and taking into account the last equation of (1.33), we obtain

$$M_x = - D \left(\frac{\partial^2 \omega}{\partial x^2} + \nu \frac{\partial^2 \omega}{\partial y^2} \right) + \frac{h^2}{5} \frac{\partial Q_x}{\partial x} ,$$

$$M_y = - D \left(\frac{\partial^2 \omega}{\partial y^2} + \nu \frac{\partial^2 \omega}{\partial x^2} \right) + \frac{h^2}{5} \frac{\partial Q_y}{\partial y} ,$$

$$M_{xy} = (1 - \nu) D \frac{\partial^2 \omega}{\partial x \partial y} - \frac{h^2}{10} \left(\frac{\partial Q_x}{\partial y} + \frac{\partial Q_y}{\partial x} \right) . \qquad (1.34)$$

Substituting these expressions in (1.34) into the first two equations of (1.33), the following results can be obtained

$$Q_x - \frac{h^2}{10} \nabla^2 Q_x = - D \frac{\partial (\nabla \omega)}{\partial x} ,$$

$$Q_y - \frac{h^2}{10} \nabla^2 Q_y = - D \frac{\partial (\nabla \omega)}{\partial y} . \qquad (1.35)$$

Observing the expressions (1.34) and (1.35), for the particular case of $h \rightarrow 0$, that is, of infinitely thin plates, the foregoing set of five equations gives the corresponding expressions in classical bending theory.

Introducing a new stress function Φ, after some manipulations (see [15] for details) the more convenient form for the governing equations can be obtained as follows

$$\nabla^4 \omega = 0 ,$$

$$\nabla^2 \Phi - \frac{10}{h^2} \Phi = 0 , \qquad (1.36)$$

where

$$Q_x = - D \frac{\partial (\nabla \omega)}{\partial x} + \frac{\partial \Phi}{\partial x} ,$$

$$Q_y = - D \frac{\partial (\nabla \omega)}{\partial y} + \frac{\partial \Phi}{\partial y} . \qquad (1.37)$$

From equations (1.34) the expressions for M_x, M_y and M_{xy} can be obtained. For given boundary conditions, the plate bending problem can be solved for various specific case.

1.2.3 A Simple Higher-order plate theory

1.2.3.1 The Assumed Displacement Field

In this simple higher-order plate theory, the primary assumptions based on the displacement field [11] in absence of the time parameter t, are the following:

$$u (x, y, z) = z \psi_x (x, y) + z^2 \phi_x (x, y),$$

$$v (x, y, z) = z \psi_y (x, y) + z^2 \phi_y (x, y),$$

$$\omega (x, y, z) = \omega (x, y) . \qquad (1.38)$$

As we can see in the sequel, these assumptions allow for the nonuniform shear stresses in the thickness direction of the plate, as well as the possibility of satisfying shear-free boundary conditions (1.3 a) on the surface of the plate at $z = \pm h/2$.

Observing the boundary conditions

$$\sigma_{xz} (x, y, \pm h/2) = 0 ,$$

$$\sigma_{yz} (x, y, \pm h/2) = 0 . \qquad (1.3 a)$$

for an isotropic plate and possibly for an orthotropic plate, these conditions are equivalent to the requirement that the corresponding strains are zero on these surfaces. Then, we have

$$\gamma_{xz}\,(\,x,\,y,\,\pm\,h/2\,) = 0\,,$$

$$\gamma_{yz}\,(\,x,\,y,\,\pm\,h/2\,) = 0\,. \qquad (\,1.39\,)$$

From the strain-displacement relations and expressions (1.38) we find

$$\gamma_{xz} = \frac{\partial u}{\partial z} + \frac{\partial \omega}{\partial x} = \psi_x + 3\,z^2\,\phi_x + \frac{\partial \omega}{\partial x}\,,$$

$$\gamma_{yz} = \frac{\partial v}{\partial z} + \frac{\partial \omega}{\partial y} = \psi_x + 3\,z^2\,\phi_y + \frac{\partial \omega}{\partial x}\,. \qquad (\,1.40\,)$$

Thus using (1.2) or (1.39), we obtain

$$\phi_x = -\frac{4}{3\,h^2}\,(\,\psi_x + \frac{\partial \omega}{\partial x}\,)\,,$$

$$\phi_y = -\frac{4}{3\,h^2}\,(\,\psi_y + \frac{\partial \omega}{\partial y}\,)\,. \qquad (\,1.41\,)$$

Then, the displacements in equation (1.38) become

$$u = z\,[\,\psi_x - \frac{4}{3}\,\frac{z^2}{h^2}\,(\,\psi_x + \frac{\partial \omega}{\partial x}\,)\,]\,,$$

$$v = z\,[\,\psi_y - \frac{4}{3}\,\frac{z^2}{h^2}\,(\,\psi_y + \frac{\partial \omega}{\partial y}\,)\,]\,,$$

$$\omega = \omega\,(\,x,\,y\,)\,. \qquad (\,1.42\,)$$

These are the lowest order expressions antisymmetric in z which can be made to satisfy the shear-free conditions on $z = \pm\,h/2$. Also notice that there are still three unknown functions, ψ_x, ψ_y and ω.

1.2.3.2 The Strain Field

Introducing the following notation for convenience

$$k_x = \frac{\partial \psi_x}{\partial x}\,, \qquad k_x^{(2)} = -\frac{4}{3\,h^2}\left(\frac{\partial \psi_x}{\partial x} + \frac{\partial^2 \omega}{\partial x^2}\right),$$

$$k_y = \frac{\partial \psi_y}{\partial y}\,, \qquad k_y^{(2)} = -\frac{4}{3\,h^2}\left(\frac{\partial \psi_y}{\partial y} + \frac{\partial^2 \omega}{\partial y^2}\right),$$

$$k_{xy} = \frac{\partial \psi_x}{\partial y} + \frac{\partial \psi_y}{\partial x}\,, \qquad k_{xy}^{(2)} = -\frac{4}{3\,h^2}\left(\frac{\partial \psi_y}{\partial x} + \frac{\partial \psi_x}{\partial y} + 2\,\frac{\partial^2 \omega}{\partial y \partial x}\right),$$

$$k_{xz} = \psi_x + \frac{\partial \omega}{\partial x}\,, \qquad k_{xz}^{(2)} = -\frac{4}{h^2}\left(\psi_x + \frac{\partial \omega}{\partial x}\right),$$

$$k_{yz} = \psi_y + \frac{\partial \omega}{\partial y}\,, \qquad k_{yz}^{(2)} = -\frac{4}{h^2}\left(\psi_y + \frac{\partial \omega}{\partial y}\right).$$

(1.43)

The stain field associated with the displacement given by equations (1.42) is found to be

$$\epsilon_x = z\left(k_x + z^2\, k_x^{(2)}\right),$$

$$\epsilon_y = z\left(k_y + z^2\, k_y^{(2)}\right),$$

$$\epsilon_z = 0\,,$$

$$\gamma_{xy} = z\left(k_{xy} + z^2\, k_{xy}^{(2)}\right); \qquad (1.44)$$

$$\gamma_{xz} = k_{xz} + z^2\, k_{xz}^{(2)}\,,$$

$$\gamma_{yz} = k_{yz} + z^2\, k_{yz}^{(2)}\,. \qquad (1.45)$$

From the above expressions we can see that the in-plane strain will have the term of z^3 while the out-of plane strains will have the term of z^2.

1.2.3.3 The Stress Field

As in Mindlin's theory, there are also inherent contradictions in the transverse stress expressions in this displacement based theory. If we use constitutive equation (1.9) to obtain the stress field, the transverse stresses σ_{xz} and σ_{yz} will have the term of z^3, the same order as γ_{xz} and γ_{yz}. On the other hand, if we use equilibrium equation from elasticity in deriving the σ_{xz} and σ_{yz}, observing that the in-plane stresses have the term of z^3, we would have a quadratic expressions of σ_{xz} and σ_{yz}.

1.2.3.4 Plate Constitutive Equations

Substituting expressions (1.44) into equation (1.9) and performing the integration from z = -h/2 to z = + h/2, the following equations are obtained between the moment resultants and the plate - displacement components:

$$\{ C_m \} = [CD] \{ C_k \} , \qquad (1.46)$$

where

$$CD = \begin{bmatrix} D & \nu D & 0 & D_1 & \nu D_1 & 0 \\ \nu D & D & 0 & \nu D_1 & D_1 & 0 \\ 0 & 0 & D\,(1-\nu)/2 & 0 & 0 & D_1(1-\nu)/2 \end{bmatrix},$$

$$C_m = \begin{bmatrix} M_x \\ M_y \\ M_{xy} \end{bmatrix}, \qquad C_k = \begin{bmatrix} k_x \\ k_y \\ k_{xy} \\ k_x^{(2)} \\ k_y^{(2)} \\ k_{xy}^{(2)} \end{bmatrix},$$

$$D = \frac{E\,h^3}{12\,(1-\nu^2)}, \qquad D_1 = \frac{E\,h^5}{80\,(1-\nu^2)}. \qquad (1.47)$$

In like manner, substituting expressions (1.45) into equations (1.9) performing the same integration, we arrive at the expressions:

$$\begin{bmatrix} Q_x \\ Q_y \end{bmatrix} = G\,h \begin{bmatrix} 1 & 0 & h^2/12 & 0 \\ 0 & 1 & 0 & h^2/12 \end{bmatrix} \begin{bmatrix} k_{xz} \\ k_{yz} \\ k_{xz}^{(2)} \\ k_{yz}^{(2)} \end{bmatrix} \qquad (1.48)$$

Notice that, due to the high - order terms introduced in the displacement field, as expected there are more terms involved in this plate constitutive equation, which differs greatly from the first-order theory.

1.2.3.5 Governing Equations

Using the standard plate theory approach, the stress resultants must satisfy the equilibrium equations as expressed before

$$\frac{\partial M_x}{\partial x} + \frac{\partial M_{xy}}{\partial y} - Q_x = 0,$$

$$\frac{\partial M_y}{\partial y} + \frac{\partial M_{xy}}{\partial x} - Q_y = 0,$$

$$\frac{\partial Q_x}{\partial x} + \frac{\partial Q_y}{\partial y} = 0. \qquad (1.49)$$

Substituting (1.47) and (1.48) into the above equations, the governing equations can be obtained for ω, ψ_x and ψ_y.

1.3 TRANSVERSE SHEAR DEFORMATION PLATE THEORIES
----- LAMINATED OR HETEROGENEOUS ORTHOTROPIC PLATE

In the last section, three transverse shear deformation plate theories are studied for homogeneous isotropic plates. In this section these theories will be extended to deal with plates that are non-homogeneous in the thickness direction. The non-homogeneity of the plate may be of two types

(a) the elastic moduli vary continuously in the thickness direction of the so called " heterogeneous plate";

(b) thin homogeneous layers of different elastic properties are assembled to form a "laminated plate" in which the moduli are piecewise constant.

It will be shown that these two types of nonhomogeneous plate problems could be solved in basically the same manner as the so called "single layer laminated plate theory". In the case of a nonhomogeneous plate, the stiffness matrix is derived by continuous integration through the thickness for a heterogeneous plate and by stepwise integration for a laminated plate. In this study only laminated plates will be considered. The technique could easily be extended to heterogenous plates.

The laminated plate under consideration consists of an arbitrary number of thin bonded orthotropic layers, with a total thickness h. In the "single-layer" laminated plate theory we assume the individual lamina is elastic and the laminae are perfectly bonded along interfaces. Cartesian coordinate system is used with the $z = 0$ and $z = h$ referred to lower and upper surfaces of the plate and cylindrical boundaries $f_b(x,y) = 0$ are defined by plane curves parallel to the x-y plane. As before, the top and bottom surfaces of the plate are assumed to be free of shear stresses but subjected to transverse normal stress, as follows:

$$\sigma_{xz} (x, y, 0) = 0 , \qquad \sigma_{xz} (x, y, h) = 0 ,$$
$$\sigma_{yz} (x, y, 0) = 0 , \qquad \sigma_{yz} (x, y, h) = 0 ; \qquad (1.50)$$

$$\sigma_z (x, y, 0) = 0, \qquad \sigma_z (x, y, z) = p_z . \qquad (1.51)$$

Note that the lower surface of the plate is chosen as $z = 0$ plane which is call "reference plane". For a symmetrical laminated plate, for convenience, we usually choose the symmetry plane, the midplane, as the reference plane. However, for unsymmetrical laminated plate any plane parallel to the plate can be chosen as the reference plane (in practice the lower surface, the upper surface or the neutral plane of the plate). we choose $z = 0$ as reference plane because it is a general form for both laminated plate and heterogeneous plate.

It will also be shown in this section that the asymmetry in composition and geometry will introduce a coupling phenomenon between bending and stretching which was studied by Reissner and Stavsky [16] and [17] in conjunction with the classical bending theory. By assuming the symmetrical laminates the bending and stretching problem can be decoupled whereas the problem of unsymmetrical laminates are inherently coupled. In this section only two displacement based transverse shear deformation theories are studied for the laminated orthotropic plate. Because of the inconsistency in the displacement field, the Reissner's stress based plate theory will not be considered.

1.3.1 A General Linear Laminated or Heterogeneous Plate Theory

---------- An Extended Mindlin's Approach

1.3.1.1 The Assumed Displacement Field

The general linear laminated plate theory is attributed to Yang, Norris and Stavsky [9] who extended Mindlin's theory for homogeneous plate [8] to laminates consisting of an arbitrary number of bonded anisotropic layers and to heterogeneous plates. The assumed displacement field is:

$$u (x, y, z) = u_0 (x, y) + z \psi_x (x, y) ,$$

$$v (x, y, z) = v_0 (x, y) + z \psi_y (x, y) ,$$

$$\omega (x, y, z) = \omega (x, y), \qquad (0 < z < h) , \tag{1.52}$$

where u, v, and ω are the displacement components in the x, y and z directions, respectively, and u_0 and v_0 are the displacement components in x and y directions of reference plane (i.e. z = 0 plane). Note that these relations involve combined action of bending and extension which characterizes the general behavior of laminated and heterogeneous plates shown by Reissner and Stavsky [16], [17]. Comparing to the corresponding equations for a homogeneous plate, we can see that instead of three plate - displacement components here we have all five components u_0, v_0, ψ_x, ψ_y and ω as the unknown functions.

1.3.1.2 The Strain Field

Again, using the standard linear elasticity approach, the strain field can be obtained from (1.52) as follows:

$$\epsilon_x = \frac{\partial u}{\partial x} = \frac{\partial u_0}{\partial x} + z \frac{\partial \psi_x}{\partial x} = \epsilon_{x0} + z\, k_x ,$$

$$\epsilon_y = \frac{\partial v}{\partial y} = \frac{\partial v_0}{\partial y} + z \frac{\partial \psi_y}{\partial y} = \epsilon_{y0} + z\, k_y ,$$

$$\gamma_{xy} = \frac{\partial u}{\partial y} + \frac{\partial v}{\partial x} = \frac{\partial u_0}{\partial y} + \frac{\partial v_0}{\partial x} + z \left(\frac{\partial \psi_x}{\partial y} + \frac{\partial \psi_y}{\partial x} \right) = \gamma_{xy0} + z\, k_{xy} ,$$

(1.53)

$$\gamma_{xz} = \frac{\partial u}{\partial z} + \frac{\partial \omega}{\partial x} = \psi_x + \frac{\partial \omega}{\partial x} = \gamma_{xz0} ,$$

$$\gamma_{yz} = \frac{\partial v}{\partial z} + \frac{\partial \omega}{\partial y} = \psi_y + \frac{\partial \omega}{\partial y} = \gamma_{yz0} ,$$

$$\epsilon_z = 0 , \qquad (1.54)$$

where

$$\epsilon_{x0} = \frac{\partial u_0}{\partial x} , \qquad \epsilon_{y0} = \frac{\partial v_0}{\partial y} , \qquad \gamma_{xy0} = \frac{\partial u_0}{\partial y} + \frac{\partial v_0}{\partial x} , \qquad (1.55)$$

$$k_x = \frac{\partial \psi_x}{\partial x}, \qquad k_y = \frac{\partial \psi}{\partial y}, \qquad k_{xy} = \frac{\partial \psi_x}{\partial y} + \frac{\partial \psi_y}{\partial x} \qquad (1.56)$$

Besides the coupling characteristics the strain field has the same features as in the homogenous case.

1.3.1.3 Constitutive Equations for Any Layer

Assuming the generalized Hooke's law for the stress - strain relations, the constitutive relations of orthotropic materials for any layer are given by:

$$\{ \Sigma \} = [CE] \{ \Omega \}, \qquad (1.57\ a)$$

where

$$CE = \begin{bmatrix} C_{11} & C_{12} & C_{13} & 0 & 0 & 0 \\ C_{21} & C_{22} & C_{23} & 0 & 0 & 0 \\ C_{31} & C_{32} & C_{33} & 0 & 0 & 0 \\ 0 & 0 & 0 & C_{44} & 0 & 0 \\ 0 & 0 & 0 & 0 & C_{55} & 0 \\ 0 & 0 & 0 & 0 & 0 & C_{66} \end{bmatrix}$$

$$\Sigma = \begin{bmatrix} \sigma_x \\ \sigma_y \\ \sigma_z \\ \sigma_{yz} \\ \sigma_{xz} \\ \sigma_{xy} \end{bmatrix}, \qquad \Omega = \begin{bmatrix} \epsilon_x \\ \epsilon_y \\ \epsilon_z \\ \gamma_{yz} \\ \gamma_{xz} \\ \gamma_{xy} \end{bmatrix},$$

(1.57 b)

Observing that $C_{ij} = C_{ji}$, there are only 9 independent constants. For a heterogeneous plate, these 9 elastic coefficients c_{ij} could be specified as functions of z but do not vary in the x, y directions. Following [18], for future convenience, we now employ a contracted notation to put the constitutive equation (1.57) into the form:

$$\sigma_i = C_{ij}\,\epsilon_j \ , \qquad (i, j = 1, 2, 3) \ , \qquad (1.58)$$

where

$$\sigma_1 = \sigma_x \ , \qquad \sigma_2 = \sigma_y \ , \qquad \sigma_3 = \sigma_z \ ,$$

and the engineering strain ϵ_j are defined in an analogous manner. For the equation corresponding to i = 3 we then solve for ϵ_3 and resubstitute it into equation (1.58), the results will be

$$\sigma_i = Q_{i\alpha}\,\epsilon_\alpha + \frac{C_{i3}}{C_{33}}\,\sigma_3 \ , \quad (i = 1, 2, 3) \ , \ (\alpha = 1, 2) \ , \qquad (1.59)$$

where

$$Q_{i\alpha} = C_{i\alpha} - \frac{C_{i3}}{C_{33}}\,C_{3\alpha} \ . \qquad (1.60)$$

The form of the constitutive relations given by equations (1.59) will be used in subsequent work. Integrals involving σ_3 will be dropped because for the thin plate in comparison with the other stress components σ_z may be neglected.

Again as addressed in the subsection (2.1.4) the inconsistency for transverse shear stresses is still there.

1.3.1.4 Plate Constitutive Equations

The plate stress resultants and stress couples are defined as follows:

$$(N_x, N_y, N_{xy}) = \int_0^h (\sigma_x, \sigma_y, \sigma_{xy})\,dz \ , \qquad (1.61)$$

$$(Q_x, Q_y) = \int_0^h (\sigma_{xz}, \sigma_{yz})\,dz \ , \qquad (1.62)$$

$$(M_x, M_y, M_{xy}) = \int_0^h (\sigma_x, \sigma_y, \sigma_{xy}) \; z \, dz \, . \qquad (1.63)$$

Substituting (1.53) and (1.54) into (1.57) and (1.59) , and integrating, according to the definition (1.61 - 1.63) we obtain the plate constitutive equations as follows:

$$\{ C_m \} = [CC] \{ C_\epsilon \} , \qquad (1.64 \; a)$$

where

$$CC = \begin{bmatrix} A_{11} & A_{12} & 0 & B_{11} & B_{12} & 0 \\ A_{21} & A_{22} & 0 & B_{21} & B_{22} & 0 \\ 0 & 0 & A_{66} & 0 & 0 & B_{66} \\ B_{11} & B_{12} & 0 & D_{11} & D_{12} & 0 \\ B_{21} & B_{22} & 0 & D_{21} & D_{22} & 0 \\ 0 & 0 & B_{66} & 0 & 0 & D_{66} \end{bmatrix}$$

$$C_m = \begin{bmatrix} N_x \\ N_y \\ N_{xy} \\ M_x \\ M_y \\ M_{xy} \end{bmatrix} , \qquad C_\epsilon = \begin{bmatrix} \epsilon_{x0} \\ \epsilon_{yo} \\ \gamma_{xy0} \\ k_x \\ k_y \\ k_{xy} \end{bmatrix} , \qquad (1.64 \; b)$$

and

$$\begin{bmatrix} Q_x \\ Q_y \end{bmatrix} = \begin{bmatrix} A_{44} & 0 \\ 0 & A_{55} \end{bmatrix} \begin{bmatrix} \gamma_{yz0} \\ \gamma_{xz0} \end{bmatrix} , \qquad (1.65)$$

where the reference plane strains ϵ_{x0} , ϵ_{y0} , and γ_{xy0}, reference bending curvatures k_x, k_y and k_{xy} and transverse shear strains γ_{xz0} , γ_{yz0} are defined in expressions (1.55) ,

(1.56) and (1.54) respectively, and for laminated plate

$$(A_{ij}, B_{ij}, D_{ij}) = \sum_{k=1}^{n} \int_{h_{k-1}}^{h_k} Q_{ij}^{(k)} (1, z, z^2) \, dz , \qquad (1.66)$$

$$(i, j = 1, 2) ,$$

$$(A_{66}, B_{66}, D_{66}) = \sum_{k=1}^{n} \int_{h_{k-1}}^{h_k} C_{66}^{(k)} (1, z, z^2) \, dz , \qquad (1.67)$$

$$(A_{44}, A_{55}) = \sum_{k=1}^{n} \int_{h_{k-1}}^{h_k} (C_{44}^{(k)}, C_{55}^{(k)}) \, dz . \qquad (1.68)$$

where $Q_{ij}^{(k)}$ and $C_{mm}^{(k)}$ ($m = 4, 5, 6$) are the material constants defined in (1.60) and (1.57) for the kth layer of the n-layer laminated plate.

1.3.1.5 Governing Equations

The stress and moment resultants must satisfy the following equilibrium equations:

$$\frac{\partial N_x}{\partial x} + \frac{\partial N_{xy}}{\partial y} = 0 ,$$

$$\frac{\partial N_{xy}}{\partial x} + \frac{\partial N_y}{\partial y} = 0 ,$$

$$\frac{\partial M_x}{\partial x} + \frac{\partial M_{xy}}{\partial y} - Q_x = 0 ,$$

$$\frac{\partial M_y}{\partial y} + \frac{\partial M_{xy}}{\partial x} - Q_y = 0 ,$$

$$\frac{\partial Q_x}{\partial x} + \frac{\partial Q_y}{\partial y} = 0 , \qquad (1.69)$$

where it is assumed that q = 0.
Substituting equations (1.63) and (1.64) into (1.69) the governing equations can then be obtained for the five unknown functions u_0, v_0, ψ_x, ψ_y and ω.

1.3.2 A Simple-higher-order Theory

--------- Reddy's Approach

1.3.2.1 The assumed Displacement Field

This simple-higher order laminated plate theory is due to Reddy [11] which is based on the displacement field:

$$u(x, y, z) = u_0(x, y) + z\left[\psi_x - \frac{4}{3}\left(\frac{z}{h}\right)^2\left(\psi_x + \frac{\partial \omega}{\partial x}\right)\right],$$

$$v(x, y, z) = v_0(x, y) + z\left[\psi_y - \frac{4}{3}\left(\frac{z}{h}\right)^2\left(\psi_y + \frac{\partial \omega}{\partial y}\right)\right],$$

$$\omega(x, y, z) = \omega(x, y). \qquad (1.70)$$

Comparing to (1.42) for the homogeneous case, besides the reference plane displacement u_0 and v_0 which is due to the bending and stretching coupling, the two assumed displacement fields have the same z dependence. Here we have chosen the midplane of the plate as the reference plane for convenience. Again these are the lowest order expressions which can be made to satisfy the shear-free conditions on the lower and upper surfaces $z = \pm h/2$ with the same five unknown functions u_0, v_0, ψ_x, ψ_y and ω.

1.3.2.2 The Strain Field and Constitutive Equations

Introducing the same notations as in the expressions (1.43) and the reference plane (here the midplane) strains as defined in (1.55), the strain field associated with the displacement given by equations (1.70) are

$$\epsilon_x = \epsilon_{x0} + z\,(k_x + z^2\, k_x^{(2)})\,,$$

$$\epsilon_y = \epsilon_{y0} + z\,(k_y + z^2\, k_y^{(2)})\,,$$

$$\epsilon_z = 0\,; \qquad (1.71)$$

$$\gamma_{xy} = \gamma_{xy0} + z\,(k_{xy} + z^2\, k_{xy}^{(2)})\,,$$

$$\gamma_{xz} = k_{xz} + z^2\, k_{xz}^{(2)} = \gamma_{xz0}\,,$$

$$\gamma_{yz} = k_{yz} + z^2\, k_{yz}^{(2)} = \gamma_{yz0}\,. \qquad (1.72)$$

Besides the coupling phenomenon these strains have the same feature as discussed for the homogeneous case.

The constitutive equations for each layer will be the same as expressed in equations (1.57) and (1.59) because the physical properties of the laminated plate will remain the same regardless of what plate theory is used.

1.3.2.3 Equilibrium Equations and Plate Constitutive Equations

In this subsection we consider the plate constitutive equations and the equilibrium equations at the same time. Because two approaches are used to obtain the plate equilibrium equations which require different plate stress and moment resultants.

(a) Standard Plate Equilibrium Equations

As generally used for the plate problem, the standard equilibrium equations [15] are

$$\frac{\partial N_x}{\partial x} + \frac{\partial N_{xy}}{\partial y} = 0\,,$$

$$\frac{\partial N_{xy}}{\partial x} + \frac{\partial N_y}{\partial y} = 0 ,$$

$$\frac{\partial M_x}{\partial x} + \frac{\partial M_{xy}}{\partial y} - Q_x = 0 ,$$

$$\frac{\partial M_y}{\partial y} + \frac{\partial M_{xy}}{\partial x} - Q_y = 0 ,$$

$$\frac{\partial Q_x}{\partial x} + \frac{\partial Q_y}{\partial y} = 0 . \qquad (1.73)$$

These equations have been used by Levinson [12] for a homogeneous plate. Corresponding to the set of equilibrium equations (1.73) , defining the stress resultants and stress couples N_x, N_y, N_{xy}, Q_x, Q_y and M_x, M_y, M_{xy} as in the expressions (1.61), (1.62) and (1.63), we could arrive at the same type of plate constitutive equations as expressed in (1.64) and (1.65), where the coefficients A_{ij}, B_{ij} and C_{ij} are defined exactly the same as in the expressions (1.66) - (1.68). Of course, the correction factor K is not needed any more.

(b) Using the Principle of Virtual Displacement to Derive the Plate Equilibrium Equations:

As could be seen later, the equilibrium equations (1.73) are variationally inconsistent with those derived from the principle of virtual displacements for the displacement field used in (1.70), because (1.73) is the equilibrium equations corresponding to the first-order plate theories. By using the equilibrium equations (1.73), the higher-order terms of the displacement field are accounted for only in the calculation of the strains but not in the governing differential equations. Reddy [11] corrected these equilibrium equations by deriving the plate equilibrium equations by means of the virtual work principle.

The principle of virtual displacement can be stated in analytical form as

$$0 = \int_{-h/2}^{+h/2} \int_{\Omega} [\, \sigma_x \, \delta\epsilon_x + \sigma_y \, \delta\epsilon_y + \sigma_{xy} \, \delta\gamma_{xy} + \sigma_{yz} \, \delta\gamma_{yz} + \sigma_{xz} \, \delta\gamma_{xz} \,] \, dA \, dz$$

$$+ \int_{\Omega} q \, \delta\omega \, dx \, dy , \qquad (1.74)$$

where h Ω is the volume of the laminated plate and δ denotes the variational symbol.Substituting the strains from (1.71) and (1. 72) into (1.74), for example, we have for the first term:

$$\int_{-h/2}^{+h/2} \int_{\Omega} \sigma_x \, \delta\epsilon_x \, dA \, dz = \int_{\Omega} \int_{-h/2}^{+h/2} \sigma_x \, \delta\epsilon_x \, dz \, dA$$

$$= \int_{\Omega} \int_{-h/2}^{+h/2} \sigma_x \, \delta \left[\epsilon_{x0} + z \left(k_x + z^2 \, k_x^{(2)} \right) \right] dz \, dA$$

$$= \int_{\Omega} \{ \, \delta\epsilon_{x0} \left[\int_{-h/2}^{+h/2} \sigma_x \, dz \, \right] + \delta k_x \left[\int_{-h/2}^{+h/2} \sigma_x \, z \, dz \right]$$

$$+ \delta k_x^{(2)} \left[\int_{-h/2}^{+h/2} \sigma_x \, z^3 \, dz \right] \} \, dA$$

$$= \int_{\Omega} \frac{\partial \, \delta u_0}{\partial x} N_x \, dA + \int_{\Omega} \frac{\partial \, \delta\psi_x}{\partial x} M_x \, dA$$

$$+ \int_{\Omega} \left[-\frac{4}{3 \, h^2} \left(\frac{\partial \, \delta\psi_x}{\partial x} + \frac{\partial^2 \, \delta\omega}{\partial x^2} \right) \right] P_x \, dA \, , \qquad (1.75)$$

where

$$(N_x, M_x, P_{xy}) = \int_{-h/2}^{+h/2} \sigma_x \, (1, z, z^3) \, dz \, . \qquad (1.76)$$

Thus, defining the following stress resultants

$$(N_x, N_y, N_{xy}) = \int_{-h/2}^{+h/2} (\sigma_x , \sigma_y , \sigma_{xy}) \, dz$$

$$(M_x, M_y, M_{xy}) = \int_{-h/2}^{+h/2} (\sigma_x , \sigma_y , \sigma_{xy}) \, z \, dz$$

$$(P_x, P_y, P_{xy}) = \int_{-h/2}^{+h/2} (\sigma_x , \sigma_y , \sigma_{xy}) \, z^3 \, dz$$

$$(Q_x, Q_y) = \int_{-h/2}^{+h/2} (\sigma_{xz} , \sigma_{yz}) \, dz$$

$$(R_x, R_y) = \int_{-h/2}^{+h/2} (\sigma_{xz} , \sigma_{yz}) \, z^2 \, dz \qquad (1.77 \text{ a - e })$$

equation (1.74) can be written as

$$0 = \int_{\Omega} N_x \frac{\partial \delta u_0}{\partial x} + M_x \frac{\partial \delta \psi_x}{\partial x} + P_x \left[- \frac{4}{3 h^2} \left(\frac{\partial \delta \psi_x}{\partial x} + \frac{\partial^2 \delta \omega}{\partial x^2} \right) \right]$$

$$+ N_y \frac{\partial \delta v_0}{\partial y} + M_y \frac{\partial \delta \psi_y}{\partial y} + P_y \left[- \frac{4}{3 h^2} \left(\frac{\partial \delta \psi_y}{\partial y} + \frac{\partial^2 \delta \omega}{\partial y^2} \right) \right]$$

$$+ N_{xy} \left(\frac{\partial \delta u_0}{\partial y} + \frac{\partial \delta v_0}{\partial x} \right) + M_{xy} \left(\frac{\partial \delta \psi_x}{\partial y} + \frac{\partial \delta \psi_y}{\partial x} \right)$$

$$+ P_{xy} \left[- \frac{4}{3 h^2} \left(\frac{\partial \delta \psi_x}{\partial y} + \frac{\partial \delta \psi_y}{\partial x} + 2 \frac{\partial^2 \delta \omega}{\partial y \, \partial x} \right) \right]$$

$$+ Q_y \left(\delta \psi_y + \frac{\partial \delta \omega}{\partial y} \right) + R_y \left[- \frac{4}{h^2} \left(\delta \psi_y + \frac{\partial \delta \omega}{\partial y} \right) \right]$$

$$+ Q_x \left(\delta \psi_x + \frac{\partial \delta \omega}{\partial x} \right) + R_x \left[- \frac{4}{h^2} \left(\delta \psi_x + \frac{\partial \delta \omega}{\partial x} \right) \right] + q \, \delta \omega \Big\} \, dx \, dy \, .$$

(1. 78)

Integrating the expressions in equation (1.78) by parts, and collecting the coefficients of δu, δv, $\delta \omega$, $\delta \psi_x$ and $\delta \psi_y$, for q =0 we obtain the following equilibrium in the domain Ω:

$$\delta u : \qquad \frac{\partial N_x}{\partial x} + \frac{\partial N_{xy}}{\partial y} = 0 \, ,$$

$$\delta v : \qquad \frac{\partial N_{xy}}{\partial x} + \frac{\partial N_y}{\partial y} = 0 \, ,$$

$$\delta\omega : \qquad \frac{\partial Q_x}{\partial x} + \frac{\partial Q_y}{\partial y} - \frac{4}{h^2}\left(\frac{\partial R_x}{\partial x} + \frac{\partial R_y}{\partial y} \right)$$

$$+ \frac{4}{3\,h^2}\left(\frac{\partial^2 P_x}{\partial x^2} + 2\,\frac{\partial^2 P_{xy}}{\partial y \partial x} + \frac{\partial^2 P_y}{\partial y^2} \right) = 0 \,.$$

$$\delta\psi_x : \qquad \frac{\partial M_x}{\partial x} + \frac{\partial M_{xy}}{\partial y} - Q_x + \frac{4}{h^2} R_x - \frac{4}{3\,h^2}\left(\frac{\partial P_x}{\partial x} + \frac{\partial P_{xy}}{\partial y} \right) = 0 \,,$$

$$\delta\psi_y : \qquad \frac{\partial M_{xy}}{\partial x} + \frac{\partial M_x}{\partial y} - Q_y + \frac{4}{h^2} R_y - \frac{4}{3\,h^2}\left(\frac{\partial P_{xy}}{\partial x} + \frac{\partial P_y}{\partial y} \right) = 0 \,.$$

(1.79 a - e)

Comparing to equations (1.73), the underlined terms are the consequence of the higher-order terms in the displacement expressions (1.70).

Corresponding to the equilibrium equations (1.79) the plate constitutive equations will have the following form:

$$\{ CM \} = [CC] \{ CE \} \,, \qquad (1.80 \text{ a})$$

where

$$CC = \begin{bmatrix}
A_{11} & A_{12} & 0 & B_{11} & B_{12} & 0 & E_{11} & E_{12} & 0 \\
A_{21} & A_{22} & 0 & B_{21} & B_{22} & 0 & E_{21} & E_{22} & 0 \\
0 & 0 & A_{66} & 0 & 0 & B_{66} & 0 & 0 & E_{66} \\
B_{11} & B_{12} & 0 & D_{11} & D_{12} & 0 & F_{11} & F_{12} & 0 \\
B_{21} & B_{22} & 0 & D_{21} & D_{22} & 0 & F_{21} & F_{22} & 0 \\
0 & 0 & B_{66} & 0 & 0 & D_{66} & 0 & 0 & F_{66} \\
E_{11} & E_{12} & 0 & F_{11} & F_{12} & 0 & H_{11} & H_{12} & 0 \\
E_{21} & E_{22} & 0 & F_{21} & F_{22} & 0 & H_{21} & H_{22} & 0 \\
0 & 0 & E_{66} & 0 & 0 & F_{66} & 0 & 0 & H_{66}
\end{bmatrix}$$

$$CM = \left[\begin{array}{cccccccccc} N_x & N_y & N_{xy} & M_x & M_y & M_{xy} & P_x & P_y & P_{xy} \end{array} \right]^T,$$

$$CE = \left[\begin{array}{cccccccccc} \epsilon_{x0} & \epsilon_{y0} & \gamma_{xy0} & k_x & k_y & k_{xy} & k_x^{(2)} & k_y^{(2)} & k_{xy}^{(2)} \end{array} \right]^T,$$

(1.80 b)

and

$$\{ CQ \} = [CCR] \{ CK \} , \qquad (1.81 \ a)$$

where

$$CCR = \left[\begin{array}{cccc} A_{44} & 0 & D_{44} & 0 \\ 0 & A_{55} & 0 & D_{55} \\ D_{44} & 0 & F_{44} & 0 \\ 0 & D_{55} & 0 & F_{55} \end{array} \right],$$

$$CQ = \left[\begin{array}{c} Q_x \\ Q_y \\ R_x \\ R_y \end{array} \right], \qquad CK = \left[\begin{array}{c} \gamma_{yz0} \\ \gamma_{xz0} \\ k_{yz}^{(2)} \\ k_{xz}^{(2)} \end{array} \right],$$

(1.81 b)

where A_{ij} , B_{ij} , etc. , are the plate stiffnesses, defined by

$$(A_{ij} , B_{ij} , D_{ij} , E_{ij} , F_{ij} , H_{ij}) = \int_{-h/2}^{+h/2} Q_{ij} (1 , z , z^2 , z^3 , z^4 , z^6) \, dz , \quad (i , j = 1, 2),$$

$$(A_{44} , D_{44} , F_{44}) = \int_{-h/2}^{+h/2} C_{44} (1 , z^2 , z^4) \, dz ,$$

$$(A_{55} , D_{55} , F_{55}) = \int_{-h/2}^{+h/2} C_{55} (1 , z^2 , z^4) \, dz ,$$

$$(A_{66} , B_{66} , D_{66} , E_{66} , F_{66} , H_{66}) = \int_{-h/2}^{+h/2} C_{66} (1 , z , z^2 , z^3 , z^4 , z^6) \, dz .$$

(1.82 a - e)

1.3.2.4 Governing Equations:

For each set of equilibrium equations (1.73) and (1.79), substituting the corresponding plate constitutive equations, the governing partial differential equations in terms of the unknown functions u_0, v_0, ω, ψ_x and ψ_y can be derived. It must be emphasized that in solving the governing equations derived from (1.79), the corresponding boundary conditions, which are also derived from the principle of virtual displacements, must be used. Upon solving the governing equations the five unknown functions u_0, v_0, ω, ψ_x and ψ_y can be obtained and the corresponding elasticity problem can be solved.

Chapter 2. Laminated Plates with a Through Crack

2.1 INTRODUCTION

In chapter 1, prior to treating the more complicated problem of a laminated plate containing imperfections or cracks, a brief review of several commonly used transverse shear deformation plate theories were presented. In this chapter, the focus is on the laminated and heterogeneous plates containing a through thickness crack.

As we know the primary purpose of the stress analysis in structures is to study their strength and failure. In many cases the failure is attributed to the growth of cracks or crack-like flaws that exist in the structure. This requires, in addition to the application of standard failure theories specified by the traditional strength of material, the treatment of the problem of acceptance and safety from the viewpoint of fracture mechanics. Presently no complete solution of the plates failure problem in non-homogeneous or anisotropic plates is available because of the inherent difficulties in stress analysis and material characterization of such laminated structures. During the past two decades many investigators have studied the stress state in the immediate neighborhood of the crack tip in a homogeneous isotropic medium since the local fracture of the structure appears to be governed mainly by this stress field. The stress intensity factor, which represents the singular behavior of the stress state near the crack tip, has been used quite effectively as the primary load factor in the fracture analysis. Moreover, the knowledge of the stress intensity factors is a prerequisite for the fracture control, the residual strength, and subcritical crack growth analysis. The main interest in this chapter is in obtaining the stress intensity factors in laminated or heterogeneous plates containing a through thickness crack.

The orthotropic laminated plate, which could represent laminated composites or bonded materials, is composed of thin homogeneous layers of different orthotropic elastic properties. The heterogeneous plate may have continuously varying properties through the thickness. By using the so called "single-layer laminated plate theories" discussed in Chapter 1, we will assume that the individual lamina are elastic and are perfectly bonded along interfaces. Global laminated properties are obtained by integrating lamina properties through the thickness. The general linear laminated and

heterogeneous plate theory developed by Yang, Norris and Stavsky [7] and examined in Chapter 1 is used here, because it is believed that this theory is the best compromise between simplicity and accuracy. Some observations in this regard are given later in this chapter. The governing equations which are a set of partial differential equations will be solved by using Fourier Transformation technique. Finally a pair of singular integral equations will be derived to solve the related mixed boundary value problem. Then the stress intensity factors can be obtained for various geometries and bending or membrane loading conditions. Only the mode I crack problem will be considered.

2.2 FORMULATION OF THE PROBLEM

The problem of interest is shown in Figure 2.1. The "infinite" laminated plate consisting of an arbitrary number of bonded orthotropic layers contains a through crack of length 2a. The total thickness of the plate is h. The system of coordinates and the definition of the variables are defined in the same way as in Chapter 1, particularly as in the general linear first order plate theory described in subsection (1.3.1) of Chapter 1. We also assume that the coordinates x, y, and z axes correspond to the princople orthotropy axes of each layer.

2.2.1 Fourier Integral Transformation

Following the general linear laminated plate theory reviewed in (1.3.1) of Chapter 1 the assumed displacement field is :

$$
\begin{aligned}
&u(x,y,z) = u_0(x,y) + z\,\psi_x(x,y),\\
&v(x,y,z) = v_0(x,y) + z\,\psi_y(x,y),\\
&\omega(x,y,z) = \omega(x,y), \qquad\qquad (0 < z < h),
\end{aligned}
\tag{2.1}
$$

where u, v, and ω are the displacement components in the x, y and z directions respectively, u_0 and v_0 are the displacement components in x and y directions of reference plane (i.e. z = 0 plane) and ψ_x and ψ_y are the rotations of the sections of x=constant and y=constant.

By defining the reference plane strains ϵ_{x0} , ϵ_{y0} , and γ_{xy0}, reference bending curvatures k_x, k_y and k_{xy} and transverse shear strains γ_{xz0} , γ_{yz0} as follows:

$$
\begin{aligned}
&\epsilon_{x0} = \frac{\partial u_0}{\partial x}, \qquad \epsilon_{y0} = \frac{\partial v_0}{\partial y}, \qquad \gamma_{xy0} = \frac{\partial u_0}{\partial y} + \frac{\partial v_0}{\partial x},\\
&k_x = \frac{\partial \psi_x}{\partial x}, \qquad k_y = \frac{\partial \psi}{\partial y}, \qquad k_{xy} = \frac{\partial \psi_x}{\partial y} + \frac{\partial \psi_y}{\partial x},\\
&\gamma_{xz0} = \psi_x + \frac{\partial \omega}{\partial x}, \quad \gamma_{yz0} = \psi_y + \frac{\partial \omega}{\partial y},
\end{aligned}
\tag{2.2}
$$

the plate constitutive equations can be written in the following form (see 1.64)

$$\{ C_m \} = [CC] \{ C_\epsilon \} , \qquad (2.3 \text{ a})$$

where

$$CC = \begin{bmatrix} A_{11} & A_{12} & 0 & B_{11} & B_{12} & 0 \\ A_{21} & A_{22} & 0 & B_{21} & B_{22} & 0 \\ 0 & 0 & A_{66} & 0 & 0 & B_{66} \\ B_{11} & B_{12} & 0 & D_{11} & D_{12} & 0 \\ B_{21} & B_{22} & 0 & D_{21} & D_{22} & 0 \\ 0 & 0 & B_{66} & 0 & 0 & D_{66} \end{bmatrix}$$

$$C_m = \begin{bmatrix} N_x \\ N_y \\ N_{xy} \\ M_x \\ M_y \\ M_{xy} \end{bmatrix}, \qquad C_\epsilon = \begin{bmatrix} \epsilon_{x0} \\ \epsilon_{yo} \\ \gamma_{xy0} \\ k_x \\ k_y \\ k_{xy} \end{bmatrix}, \qquad (2.3 \text{ b})$$

and

$$\begin{bmatrix} Q_x \\ Q_y \end{bmatrix} = \begin{bmatrix} A_{44} & 0 \\ 0 & A_{55} \end{bmatrix} \begin{bmatrix} \gamma_{yz0} \\ \gamma_{xz0} \end{bmatrix}, \qquad (2.3 \text{ c})$$

where the stiffness constants A_{ij}, B_{ij} and D_{ij} (i, j = 1, 2) are defined in (1.66) and A_{ij} (i = 4, 5, 6) in (1.68) and (1.67). For example

$$B_{ij} = \sum_{k=1}^{n} \int_{h_{k-1}}^{h_k} Q_{ij}^{(k)} \, z \, dz, \qquad (i, j = 1, 2), \qquad (2.4)$$

for a laminated plate of n layers and Q_{ij} of each layer are defined in (1.60).

Note that the bending - membrane coupling phenomenon, which was first studied by Reissner and Stavsky with classical bending theory, can be seen easily in the expressions (2.1) and (2. 3). Unless B_{ij} (i, j = 1, 2) are all zero, the problem will remain coupled. If the plate is symmetrically layered, and taking the plane of symmetry (i. e. the midplane) as the reference plane it may be shown that the B_{ij}'s (see expression (2. 4)) are all zero, and consequently the problem becomes uncoupled.

For convenience, for this general linear laminated plate theory the five unknown functions, u_0, v_0, ω , ψ_x and ψ_y, are defined as the "displacement" vector [U] as follows

$$[\,U\,] = \left[\begin{array}{ccccc} u_1 & u_2 & u_3 & u_4 & u_5 \end{array}\right]^T = \left[\begin{array}{ccccc} u_0 & v_0 & \psi_x & \psi_y & \omega \end{array}\right]^T . \qquad (2.5)$$

Substituting (2.3) into plate equilibrium equations (1.69) and considering (2.5), the governing partial differential equations in terms of the unknown functions u_i are found to be

$$A_{11}u_{1,xx} + (A_{12} + A_{66})\, u_{2,yx} + A_{66}\, u_{1,yy} + B_{11}\, u_{3,xx} + (B_{12} + B_{66})\, u_{4,xy} + B_{66}\, u_{3,yy} = 0,$$

$$A_{66}u_{2,xx} + (A_{12} + A_{66})\, u_{1,xy} + A_{22}\, u_{2,yy} + B_{66}\, u_{4,xx} + (B_{12} + B_{66})\, u_{3,xy} + B_{22}\, u_{4,yy} = 0,$$

$$B_{11}u_{1,xx} + (B_{12} + B_{66})\, u_{2,yx} + B_{66}\, u_{1,yy} + D_{11}\, u_{3,xx} + (D_{12} + D_{66})\, u_{4,xy} + D_{66}\, u_{3,yy} - A_{55}\, u_3 - A_{55}\, u_{5,x} = 0,$$

$$B_{66}u_{2,xx} + (B_{12} + B_{66}) u_{1,xy} + B_{22} u_{2,yy}$$

$$+ D_{66} u_{4,xx} + (D_{12} + D_{66}) u_{3,xy} + D_{22} u_{4,yy} - A_{44} u_4 - A_{44} u_{5,y} = 0,$$

$$A_{44} u_{4,y} + A_{44}\omega_{5,yy} + A_{55} u_{3,x} + A_{55} u_{5,xx} = 0.$$

(2.6 a - e)

Taking the Fourier Transforms of equations (2.6) and defining

$$u_i = \frac{1}{2\pi} \int_{-\infty}^{\infty} \phi_i (x, \alpha) e^{-i\alpha y} d\alpha,$$

(2.7 a)

$$\phi_i = \int_{-\infty}^{\infty} u_i (x, y) e^{i\alpha y} dy,$$

$$i = 1, ... 5,$$

(2.7 b)

we arrive at the following ordinary differential equations:

$$CA\ \ddot{\Phi} + CB\ \dot{\Phi} + CD\Phi = 0,$$

(2.8)

where

$$[\Phi] = \begin{bmatrix} \phi_1 & \phi_2 & \phi_3 & \phi_4 & \phi_5 \end{bmatrix}^T,$$

(2.9)

$$\ddot{\Phi} = \Phi_{,xx}\ , \qquad \dot{\Phi} = \Phi_{,x}\ ,$$

$$CA = \begin{bmatrix} A_{11} & 0 & B_{11} & 0 & 0 \\ 0 & A_{66} & 0 & B_{66} & 0 \\ B_{11} & 0 & D_{11} & 0 & 0 \\ 0 & B_{66} & 0 & D_{66} & 0 \\ 0 & 0 & 0 & 0 & -A_{55} \end{bmatrix}$$

$$CB=(-i\alpha)\begin{bmatrix} 0 & A_{11}+A_{66} & 0 & B_{12}+B_{66} & 0 \\ A_{12}+A_{66} & 0 & B_{12}+B_{66} & 0 & 0 \\ 0 & B_{12}+B_{66} & 0 & D_{12}+D_{66} & -A_{55}\frac{i}{\alpha} \\ B_{12}+B_{66} & 0 & D_{12}+D_{66} & 0 & 0 \\ 0 & 0 & -A_{55}\frac{i}{\alpha} & 0 & 0 \end{bmatrix}$$

$$CD = \begin{bmatrix} -\alpha^2 A_{66} & 0 & -\alpha^2 B_{66} & 0 & 0 \\ 0 & -\alpha^2 A_{22} & 0 & -\alpha^2 B_{22} & 0 \\ -\alpha^2 B_{66} & 0 & -(\alpha^2 D_{66}+A_{44}) & 0 & 0 \\ 0 & -\alpha^2 B_{22} & 0 & -(\alpha^2 D_{22}+A_{44}) & i\alpha A_{44} \\ 0 & 0 & 0 & i\alpha A_{44} & \alpha^2 A_{44} \end{bmatrix}$$

(2.11 a-c)

Upon determining the eigenvalues s_i and the eigenfunctions C_{ij} of equations of (2.8), observing that ϕ_i (i = 1,.... 5) must be finite when $x \rightarrow \infty$, and thus taking the coefficients of the terms having $e^{s_i x}$ with $Re(s_i)>0$ to be zero, we finally obtain the solutions of equation (2.8) as:

$$\phi_i = \sum_{j=1}^{5} C_{ij} A_j(\alpha)\ e^{s_j x}, \qquad Re(s_j)<0, \quad (i,j) = 1,...5.$$

(2.13)

Thus, the unknown displacement components u_i can be expressed as

$$u_i = \frac{1}{2\pi} \int_{-\infty}^{\infty} \phi_i(x, \alpha)\, e^{-i\alpha y}\, d\alpha$$

$$= \frac{1}{2\pi} \int_{-\infty}^{\infty} \sum_{j=1}^{5} C_{ij} A_j(\alpha)\, e^{s_j x}\, e^{-i\alpha y}\, d\alpha, \qquad (i, j) = 1,\ldots. 5, \qquad (2.14)$$

where A_j, ($j = 1,\ldots, 5$) are the unknown functions which can be obtained by applying the boundary conditions. Substituting (2.13) into expressions (1.53 - 1.56) we obtain the strain components. Furthermore, substituting these into plate constitutive equation (2.3), the relevant expressions of stresses, moments, and transverse shear resultants can be obtained.

2.2.2 Boundary Conditions

Assuming that $x = 0$ and $y = 0$ are planes of symmetry with respect to loading and geometry and that the problem has been reduced to a perturbation problem in which the crack surface stress and moment resultants are the only nonzero external loads, the boundary conditions may be expressed as (Figure 2.1):

$$N_{xy}(0^+, y) = 0,$$
$$M_{xy}(0^+, y) = 0,$$
$$Q_x(0^+, y) = 0, \qquad (-\infty < y < \infty), \qquad (2.14\ a\text{-}c)$$

$$N_x(0^+, y) = f_1(y), \qquad |y| < a,$$
$$u_0(0^+, y) = 0, \qquad |y| > a,$$

$$M_x(0^+, y) = f_2(y), \qquad |y| < a,$$
$$\psi_x(0^+, y) = 0, \qquad |y| > a. \qquad (2.14\ d,e)$$

Three of the unknown functions $A_1,\ldots,A_5$ maybe eliminated by using the homogeneous conditions (2.14 a-c). The remaining two are then obtained from the mixed boundary conditions (2.14 d,e).

2.2.3 Singular Integral Equations

To solve this mixed boundary value problem, we define the new unknown functions as follows:

$$\frac{\partial}{\partial y}\,\psi_x\,(0,y) = G_2\,(y), \qquad (-\infty < y < \infty), \tag{2.15}$$

$$\frac{\partial}{\partial y}\,u_0\,(0,y) = G_1\,(y), \qquad (-\infty < y < \infty). \tag{2.16}$$

By using (2.4) and (2.13), it can be shown that

$$G_2\,(y) = \frac{\partial}{\partial y}\,\psi_x\,(0,y) = \frac{\partial}{\partial y}\,u_3$$

$$= \lim_{x\to 0}\ \frac{1}{2\pi}\int_{-\infty}^{\infty}\ \sum_{j=1}^{5} C_{3j}\,A_j(\alpha)\,e^{s_j x}\,(-i\alpha)\,e^{-i\alpha y}\,d\alpha,$$

$$\sum_{j=1}^{5} C_{3j}\,A_j(\alpha)\,(-i\alpha) = \int_{-\infty}^{\infty} G_2\,(y)\,e^{i\alpha y}\,dy$$

$$= \int_{-a}^{a} G_2\,(t)\,e^{i\alpha t}\,dt = g_2\,(\alpha)\,, \tag{2.17}$$

$$G_1(y) = \frac{\partial}{\partial y} u_0(0, y) = \frac{\partial}{\partial y} u_1$$

$$= \lim_{x \to 0} \frac{1}{2\pi} \int_{-\infty}^{\infty} \sum_{j=1}^{5} C_{1j} A_j(\alpha) e^{s_i x} (-i\alpha) e^{-i\alpha y} d\alpha,$$

$$\sum_{j=1}^{5} C_{1j} A_j(\alpha) (-i\alpha) = \int_{-\infty}^{\infty} G_1(y) e^{i\alpha y} dy$$

$$= \int_{-a}^{a} G_1(t) e^{i\alpha t} dt = g_1(\alpha).$$

(2.18)

To obtain the unknown functions $A_i(\alpha)$, ($i = 1, \ldots 5$), in terms of g_1 and g_2, the homogeneous boundary conditions (2.9 a-c) are applied first. Starting with

$$N_{xy}(0^+, y) = 0,$$

and by substituting (2.13) into (2.3), we obtain

$$N_{xy} = A_{66} u_{1,y} + A_{66} u_{2,x} + B_{66} u_{3,y} + B_{66} u_{4,x}$$

$$= \frac{1}{2\pi} \int_{-\infty}^{\infty} [A_{66} \sum_{j=1}^{5} C_{1j} A_j(\alpha) e^{s_j x} (-i\alpha)$$

$$+ B_{66} \sum_{j=1}^{5} C_{3j} A_j(\alpha) e^{s_j x} (-i\alpha) + A_{66} \sum_{j=1}^{5} C_{2j} A_j(\alpha) e^{s_j x} (s_j)$$

$$+ B_{66} \sum_{j=1}^{5} C_{4j} A_j(\alpha) e^{s_i x} (s_j)] e^{-i\alpha y} d\alpha .$$

(2.19)

By inverting the Fourier integral, we find

$$\sum_{j=1}^{5} [\, C_{1j}\, A_{66}\, (-i\alpha) + C_{3j}\, B_{66}\, (-i\alpha) + C_{2j}\, A_{66}\, s_j + C_{4j}\, B_{66}\, s_j \,]\, A_j(\alpha) = 0. \qquad (2.20)$$

Similarly, from

$$M_{xy}(0^+, y) = 0 \quad \text{and} \quad Q_x(0^+, y) = 0,$$

it can be shown that

$$\sum_{j=1}^{5} [\, C_{1j}\, B_{66}\, (-i\alpha) + C_{3j}\, D_{66}\, (-i\alpha) + C_{2j}\, B_{66}\, s_j + C_{4j}\, D_{66}\, s_j \,]\, A_j(\alpha) = 0. \qquad (2.21)$$

$$\sum_{j=1}^{5} [\, C_{3j}\, A_{55} + C_{5j}\, A_{55}\, s_j \,]\, A_j(\alpha) = 0. \qquad (2.22)$$

Solving the system of linear algebraic equations (2.17 - 2.18) and (2.20 - 2.22) $A_i(\alpha)$ may be expressed as follows

$$A_i(\alpha) = Q_{i1}\, g_1(\alpha) + Q_{i2}\, g_2(\alpha)$$

$$= Q_{i1} \int_{-a}^{a} G_1(t)\, e^{i\alpha t}\, dt + Q_{i2} \int_{-a}^{a} G_2(t)\, e^{i\alpha t}\, dt ,$$

$$(i = 1, \ldots\ldots 5) ,$$

$$(2.23)$$

where Q_{i1} and Q_{i2} are the algebraic expressions from the solution of the equations (2.17-2.18) and (2.20-2.22) .

Substituting (2.23) and (2.13) into the strain field (1.53) - (1.56), and using (2.31), the resultants N_x and M_x may be expressed as:

$$M_x = B_{11}\, u_{1,x} + B_{12}\, u_{2,y} + D_{11}\, u_{3,x} + D_{12}\, u_{4,y} ,$$

$$(2.24)$$

$$M_x = \frac{1}{2\pi} \int_{-\infty}^{\infty} \Big[B_{12} \sum_{j=1}^{5} C_{2j} A_j(\alpha)\, e^{s_j x} (-i\alpha) + D_{12} \sum_{j=1}^{5} C_{4j} A_j(\alpha)\, e^{s_j x} (-i\alpha) + B_{11} \sum_{j=1}^{5} C_{1j} A_j(\alpha)\, e^{s_j x} (s_j) + D_{11} \sum_{j=1}^{5} C_{3j} A_j(\alpha)\, e^{s_j x} (s_j) \Big]\, e^{-i\alpha y}\, d\alpha$$

$$= \frac{1}{2\pi} \int_{-a}^{a} G_1(t)\, dt \int_{-\infty}^{\infty} H_{21}(\alpha, x)\, e^{i\alpha (t-y)}\, d\alpha + \frac{1}{2\pi} \int_{-a}^{a} G_2(t)\, dt \int_{-\infty}^{\infty} H_{22}(\alpha, x)\, e^{i\alpha (t-y)}\, d\alpha ,$$

$$(2.25)$$

$$H_{2k} = \sum_{j=1}^{5} \{ [B_{11}C_{1j} s_j + B_{12} C_{2j} (- i \alpha) + D_{11}C_{3j} s_j + D_{12} C_{4j} (- i \alpha)] Q_{jk} e^{s_j x}, \quad (k = 1, 2),$$

(2.26)

$$N_x = A_{11} u_{1,x} + A_{12} u_{2,y} + B_{11} u_{3,x} + B_{12} u_{4,y},$$

(2.27)

$$N_x = \frac{1}{2\pi} \int_{-a}^{a} G_1 (t) dt \int_{-\infty}^{\infty} H_{11} (\alpha, x) e^{i \alpha (t-y)} d\alpha + \frac{1}{2\pi} \int_{-a}^{a} G_2 (t) dt \int_{-\infty}^{\infty} H_{12} (\alpha, x) e^{i \alpha (t-y)} d\alpha ,$$

(2.28)

$$H_{1k} = \sum_{j=1}^{5} \{ [A_{11}C_{1j} s_j + A_{12} C_{2j} (- i \alpha) + B_{11}C_{3j} s_j + B_{12} C_{4j} (- i \alpha)] Q_{jk} e^{s_j x} , \quad (k = 1, 2) .$$

(2.29)

Observing expressions (2.25) and (2.26) and applying the mixed boundary conditions (2.14 d, e), we finally obtain two integral equations to determine the new unknown functions G_1 and G_2 in the following form:

$$\lim_{x \to 0} \int_{-a}^{a} \sum_{j=1}^{2} G_j(t) \int_{-\infty}^{\infty} H_{ij}(\alpha, x)\, e^{i\alpha(t-y)}\, d\alpha = f_i(y),$$

$$(i = 1, 2), \qquad |y| < a.$$

(2.30)

By further examining the functions H_{ij}, it can be shown that they are bounded everywhere for finite α. Therefore any possible singularity of the kernels in (2.30) at $y=t$ must be due to the behavior of $H_{ij}(\alpha,x)$ as $\alpha \to \mp\infty$. Note that H_{ij} contains exponential damping terms of the form $e^{s_j x}$, where $Re(s_j)<0$. However, since in the limit x will go to zero, for $y=t$ this damping does not insure the convergence of the inner integrals in (2.30). The major difficulty in this problem, of course, is that the functions $s_j(x)$ are not known explicitly in terms of α. For the purpose of examining the singular behavior of the kernels in (2.30) and extracting the singular parts, all one needs, however, is the asymptotic behavior of s_j as $|\alpha| \to \infty$. Thus, from (2.8) - (2.11) it can be shown that for large values of $|\alpha|$ we have

$$\frac{s_j(\alpha)}{|\alpha|} = -\left(s_0 + \frac{s_{j1}}{\alpha} + \frac{s_{j2}}{\alpha^2} + \ldots\ldots\right),$$

(2.31)

where s_0 is a constant.

Now using the relations (2.31) and separating the asymptotic values of H_{ij} for large $|a|$, the kernels in (2.30) may be expressed as :

$$\int_{-\infty}^{\infty} H_{ij}(\alpha, x)\, e^{i\alpha(t-y)}\, d\alpha = \int_{-\infty}^{\infty} H_{ij}^{\infty}(\alpha, x)\, e^{i\alpha(t-y)}\, d\alpha$$

$$+ \int_{-\infty}^{\infty} \left[H_{ij}(\alpha, x) - H_{ij}^{\infty}(\alpha, x) \right] e^{i\alpha(t-y)}\, d\alpha,$$

where H_{ij}^{∞} is the asymptotic value of H_{ij} for $|\alpha| \to \infty$.

The first term on the right- hand gives Cauchy-type kernels $\frac{1}{t - y}$, and the second integral is uniformly convergent for all t and y (in which the limit x=0 can be therefore be put under the integral sign). After the asymptotic analysis and some lengthy but straightforward manipulations the integral equations and the kernels may then be expressed as follows:

$$\sum_{j=1}^{2} \frac{\mu_{1j}}{\pi} \int_{-a}^{a} \frac{G_j(t)}{t - y}\, dt + \sum_{j=1}^{2} \int_{-a}^{a} k_{1j}(y, t)\, G_j(t)\, dt = f_1(y),$$

$$\sum_{j=1}^{2} \frac{\mu_{2j}}{\pi} \int_{-a}^{a} \frac{G_j(t)}{t - y}\, dt + \sum_{j=1}^{2} \int_{-a}^{a} k_{2j}(y, t)\, G_j(t)\, dt = f_2(y),$$

(2.33 a, b)

where μ_{ij} (i,j = 1, 2) are material constants obtained from the asymptotic analysis, f_i (y), (i = 1, 2) are defined by (2.14 d, e) and the Fredholm kernels K_{ij} are obtained from

$$k_{ij}(y, t) = \frac{1}{2\pi} \int_{-\infty}^{\infty} [\, H_{ij}(\alpha, 0) - H_{ij}^{\infty}(\alpha, 0)\,]\, e^{i\alpha(t-y)}\, d\alpha,$$

(i, j = 1, 2).

(2.34)

From the definitions of G_1 and G_2 given by (2.15) and (2.16) it follows that (2.33) must be solved under the following single - valuedness conditions

$$\int_{-a}^{a} G_j(y)\, dy = 0, \quad (i = 1, 2).$$

(2.35)

Note that, when the plate is symmetrically layered about the z = 0 plane, by taking the plane of symmetry as the reference plane we find $H_{12} = H_{21} = 0$, and consequently $\mu_{12} = \mu_{21} = 0$ and $k_{12} = k_{21} = 0$. Thus, the bending and in - plane stretching problems would be decoupled.

2.3 STRESS INTENSITY FACTORS

2.3.1 Solution of the Singular Integral Equations

The two unknown density functions G_1 and G_2 can be obtained by solving the singular integral equations (2.33 a, b) numerically. The two most commonly known numerical methods for solving such singular integral equations are Quadrature method [19] and Collocation method [20], [21]. In this chapter, the singular integral equations are solved by collocation method (also called expansion method). To solved the integral equations:

$$\sum_{j=1}^{2} \frac{\mu_{1j}}{\pi} \int_{-a}^{a} \frac{G_j(t)}{t-y}\,dt + \sum_{j=1}^{2} \int_{-a}^{a} k_{1j}(y,t)\,G_j(t)\,dt = f_1(y),$$

$$\sum_{j=1}^{2} \frac{\mu_{2j}}{\pi} \int_{-a}^{a} \frac{G_j(t)}{t-y}\,dt + \sum_{j=1}^{2} \int_{-a}^{a} k_{2j}(y,t)\,G_j(t)\,dt = f_2(y),$$

$$|y| < a,$$

(2.33 a, b)

we first express the unknown functions in terms of their weight functions

$$G_i(t) = \frac{\overline{g_i}(t)}{(a^2 - t^2)^{1/2}},$$

(2.36)

and then normalize the interval (- a, a) by defining

$$t = ar, \qquad (-a \le t \le a, \quad -1 \le r \le 1),$$

$$y = as, \qquad (-a \le y \le a, \quad -1 \le s \le 1),$$

$$f_i (y) = \overline{f}_i (s),$$

$$G_i (t) = \frac{g_i (r)}{(1 - r^2)^{1/2}}, \qquad \overline{g}_i (t) = a\, g_i (r),$$

$$L_{ij} (r, s) = a\, k_{ij} (y, t).$$

(2.37)

By substituting (2.36) and (2.37) into (2.33), we obtain:

$$\sum_{j=1}^{2} \frac{\mu_{1j}}{\pi} \int_{-a}^{a} \frac{g_j (r)}{(1 - r^2)^{1/2} (r - s)}\, dr + \sum_{j=1}^{2} \int_{-a}^{a} L_{1j} (r, s)\, g_j (r)\, dr = \overline{f}_1 (s),$$

$$\sum_{j=1}^{2} \frac{\mu_{2j}}{\pi} \int_{-a}^{a} \frac{g_j (r)}{(1 - r^2)^{1/2} (r - s)}\, dr + \sum_{j=1}^{2} \int_{-a}^{a} L_{2j} (r, s)\, g_j (r)\, dr = \overline{f}_2 (s),$$

$$| s | < 1.$$

(2.38)

In applying the collocation method, we choose

$$g_1 (r) = \sum_{j=1}^{N} a_j\, h_{j-1} (r),$$

$$g_2 (r) = \sum_{j=1}^{N} b_j \, h_{j-1} (r),$$

(2.39)

where $h_j (r)$ are linearly independent coordinate functions chosen to "fit the curve" and the a_j and b_j are coefficients to be determined. It is believed that the best choice of $h_j (r)$ are orthoganol polynomials, because the coefficients show convergence as N is increased (see [21]).

Here, we let

$$h_{j-i} (r) = T_{j-i} (r) ,$$

(2.40)

where $T_{j-1} (r)$ are the Chebychev polynomial of the first kind corresponding to the weight function of expression (2.36). Note that these equations must be solved under the following single-valueness conditions:

$$\int_{-a}^{a} G_1 (t) \, dt = 0, \quad \text{or} \quad \int_{-1}^{1} \frac{g_1 (r)}{(1 - r^2)^{1/2}} \, dr = 0,$$

$$\int_{-a}^{a} G_2 (t) \, dt = 0, \quad \text{or} \quad \int_{-1}^{1} \frac{g_2 (r)}{(1 - r^2)^{1/2}} \, dr = 0,$$

(2.41)

From (2.39) and (2.40) it can be seen that these extra conditions are:

$$\sum_{j=1}^{N} a_j \int_{-1}^{1} \frac{T_{j-1} (r)}{(1 - r^2)^{1/2}} \, dr = 0 ,$$

$$\sum_{j=1}^{N} b_j \int_{-1}^{1} \frac{T_{j-1}(r)}{(1-r^2)^{1/2}}\, dr = 0 .$$

(2.42)

Using the orthogonal conditions:

$$\int_{-1}^{1} \frac{T_n(r)\, T_0(r)}{(1-r^2)^{1/2}}\, dr = \begin{cases} 0, & n \neq 0, \\ \pi, & n = 0, \end{cases}$$

(2.43)

and observing that $T_0(r) \equiv 1$, we obtain

$$a_1 \equiv 0,$$
$$b_1 \equiv 0,$$

(2.44)

Considering (2.44) for further convenience, we rewrite the unknown functions as follows:

$$g_1(r) = \sum_{k=1}^{M} a_k T_k(r),$$
$$g_2(r) = \sum_{k=M+1}^{2M} a_k T_{k-M}(r).$$

(2.45)

Substituting (2.45) into (2.38) the singular integral equations can then be expressed as follows:

$$\sum_{k=1}^{M} \frac{\mu_{11}}{\pi} a_k \int_{-1}^{1} \frac{T_k(r)}{(1-r^2)^{1/2}(r-s)}\,dr + \sum_{k=M+1}^{2M} \frac{\mu_{12}}{\pi} a_k \int_{-1}^{1} \frac{T_{k-M}(r)}{(1-r^2)^{1/2}(r-s)}\,dr + \sum_{k=1}^{M} a_k \int_{-1}^{1} L_{11}(r,s)\,\frac{T_k(r)}{(1-r^2)^{1/2}}\,dr + \sum_{k=M+1}^{2M} a_k \int_{-1}^{1} L_{12}(r,s)\,\frac{T_{k-M}(r)}{(1-r^2)^{1/2}}\,dr = \overline{f_1}(s),$$

$$\sum_{k=1}^{M} \frac{\mu_{21}}{\pi} a_k \int_{-1}^{1} \frac{T_k(r)}{(1-r^2)^{1/2}(r-s)}\,dr + \sum_{k=M+1}^{2M} \frac{\mu_{22}}{\pi} a_k \int_{-1}^{1} \frac{T_{k-M}(r)}{(1-r^2)^{1/2}(r-s)}\,dr + \sum_{k=1}^{M} a_k \int_{-1}^{1} L_{21}(r,s)\,\frac{T_k(r)}{(1-r^2)^{1/2}}\,dr + \sum_{k=M+1}^{2M} a_k \int_{-1}^{1} L_{22}(r,s)\,\frac{T_{k-M}(r)}{(1-r^2)^{1/2}}\,dr = \overline{f_2}(s),$$

$$|s| < 1,$$

(2.46 a, b)

where the unknowns are a_k (k= 1, ... 2M).

In the collocation method there is no restriction on the choice of s. In this study we choose $T_M (s_i) = 0$ or

$$s_i = \cos \left(\frac{2i - 1}{2M} \pi \right), \qquad (i = 1,.... M).$$

(2.47)

In (2.46) for a given value of s there are two integrations to be evaluated. Any standard technique can be used, for example, Gauss - Chebychev quadrature which takes advantage of the weight

$$\int_{-1}^{1} \frac{h(r)}{(1 - r^2)^{1/2}} \, dr = \sum_{j=1}^{N} W_j \, h (r_j),$$

(2.48)

where

$$r_j = \cos \left(\frac{j - 1}{N - 1} \pi \right),$$

$$\omega_1 = \frac{1}{2} \frac{\pi}{N - 1},$$

$$\omega_j = \frac{\pi}{N - 1}, \qquad j = 2,..... N-1 ,$$

$$\omega_N = \frac{1}{2} \frac{\pi}{N - 1}.$$

(2.49)

For the singular integrals, such expansion function T_j (r) give the closed form expressions:

$$\int_{-1}^{1} \frac{T_j(r)}{(1-r^2)^{1/2}(r-s)}\, dr = \pi\, U_{j-1}(s), \qquad (2.50)$$

where U_j (r) are the Chebychev polynomials of the second kind.
Using (2.49) and (2.50) with the collocation points s_j as in the equation (2.47), the singular integral equations (2.46 a, b) can be evaluated at M different points giving 2M linear algebraic equations for a_1 ... a_{2M}. The unknown functions G_1 (t) and G_2 (t) can then be obtained from (2.45) and (2.37).

2.3.2 Displacement Components along the Crack

From the previous subsection and (2.15) and (2.16) we could express the unknown functions as follows

$$G_1(y) = \frac{\partial}{\partial y} u_0(0, y) = \sum_{k=1}^{M} a_k \frac{T_k(y/a)}{(a^2 - y^2)^{1/2}}\, a,$$

$$G_2(y) = \frac{\partial}{\partial y} \psi_x(0, y) = \sum_{k=M+1}^{2M} a_k \frac{T_{k-M}(y/a)}{(a^2 - y^2)^{1/2}}\, a,$$

$$|y| < a, \qquad (2.51)$$

where T_k are the Chebychev polynomial of first kind, a_k (k = 1,...., 2M) are the coefficients determined by solving the singular integral equations (2.46 a, b) numerically, and a is the half crack length.

From the definition it is clear that for $| y | \geq a$

$$G_1 (y) \equiv 0, \quad G_2 (y) \equiv 0.$$

(2.52)

From (2.15) , (2.16) and (2.52) we could then easily obtain the displacement components along the crack as follows

$$u_0 (0, y) = \int_{-a}^{y} G_1 (y) \, dy$$

$$= a \sum_{k=1}^{M} a_k \int_{-a}^{y} \frac{T_k(y/a)}{(a^2 - y^2)^{1/2}} \, dy ,$$

(2.53)

$$\psi_x (0, y) = \int_{-a}^{y} G_2 (y) \, dy$$

$$= a \sum_{k=M+1}^{2M} a_k \int_{-a}^{y} \frac{T_{k-M} (y/a)}{(a^2 - y^2)^{1/2}} \, dy ,$$

(2.54)

Note that physically u_0 is the displacement in x direction in a given reference plane z = 0, and ψ_x is the rotation of x = constant plane in the plate. From the basic assumptions of the displacement-based plate theory (1.52) we obtain the displacement of the plate in x-direction as follows (see figure 2.1 and expressions (2.1)):

$$u (x, y, z) = u_0 (x, y) + z \, \psi_x (x, y).$$

(2.55)

We also observe that due to the first oder theory used the value of u_0 (x, y) depends on the choice of the reference plane whereas the value of u (x, y, z) and ψ_x (x, y) will not do so. In this study for further convenience, and without any loss in generality, we choose the neutral plane of the laminated plate as reference plane. From (2.53), (2.54) and (2.55), the u (0, y, z) which is the displacement in x-direction along the y - z plane (i. e. the crack plane) can then be obtained as

$$u (0, y, z) = u_0 (0, y) + z \psi_x (0, y)$$

$$= \int_{-a}^{y} [G_1 (y) + z G_2 (y)] \, dy ,$$

$$| y | < a. \qquad (2.56)$$

Since the laminated plate consists of layers with different material properties, the displacement component u (0, y, z) or u_0 (0, y) and ψ_x (0, y) , which are essential to describe the behavior of the through - thickness crack, will depend on the stacking order of the layers. In this work the nature of u (0, y, z) will be studied for the following combinations:

i) symmetrically laminated plate;

ii) unsymmetrically laminated plate;

under uniform tension or bending.

I. Symmetrically Laminated Plate

For a symmetrically laminated plate the neutral plane corresponds to the plane of symmetry of the plate. For such a plate by taking the symmetry plane as the reference plane, the bending and in-plane stretching problems may be decoupled. Therefore, the singular integral equations (2.33) become:

$$\frac{\mu_{11}}{\pi} \int_{-a}^{a} \frac{G_1 (t)}{t - y} \, dt = f_1 (y), \qquad (2.57)$$

for in-plane stretching problem,

$$\frac{\mu_{22}}{\pi} \int_{-a}^{a} \frac{G_2(t)}{t-y}\,dt + \int_{-a}^{a} k_{22}(y,t)\,G_2(t)\,dt = f_2(y), \qquad |y| < a. \tag{2.58}$$

for bending problem. Here $f_1(y)$ and $f_2(y)$ are defined by equations (2.14).

From (2.57) and (2.58) we can easily see that the in-plane stretching problem and the bending problem are reduced to , respectively, a homogeneous single-layer plane stress problem and a bending problem for a plate with a central crack. This is expected because we have used the so-called single-layer laminated plate theory which is based on replacing the laminated plate by an equivalent single-layer anisotropic plate. Note that $G_1(y)$, $G_2(y)$ and $u(0, y, z)$ are the global quantities introduced by this type of plate theory. After solving for the unknown functions $G_1(y)$ and $G_2(y)$, the displacement component along the crack $u(0, y, z,)$ can be obtained

$$u(0, y, z) \equiv u_0(0, y), \tag{2.59}$$

for the in-plane stretching problem, and

$$u(0, y, z) \equiv z\,\psi_x(0, y), \tag{2.60}$$

for the bending problem.

II. Unsymmetrically Laminated Plate

Unlike the symmetrically laminated plate problem, the unsymmetrical plate problem is inherently coupled. It is expected that for such a plate even if is under uniform tension applied in its neutral plane, there exist both the in-plane displacement $u_0(0, y)$ and the rotation $\psi_x(0, y)$. The singular integral equations in this case are

$$\sum_{j=1}^{2} \frac{\mu_{1j}}{\pi} \int_{-a}^{a} \frac{G_j(t)}{t-y}\,dt + \sum_{j=1}^{2} \int_{-a}^{a} k_{1j}(y,t)\,G_j(t)\,dt = f_1(y),$$

$$\sum_{j=1}^{2} \frac{\mu_{2j}}{\pi} \int_{-a}^{a} \frac{G_j(t)}{t-y}\,dt + \sum_{j=1}^{2} \int_{-a}^{a} k_{2j}(y,t)\,G_j(t)\,dt = f_2(y),$$

$$|y| < a.$$

(2.33 a, b)

The problem will be solved separately under uniform tension and uniform bending defined by

$$f_1(y) = N^{\infty},$$
$$f_2(y) = 0,$$

(2.61)

and

$$f_1(y) = 0,$$
$$f_2(y) = M^{\infty},$$

(2.62)

respectively.

Again using the numerical procedure described in subsection (2.3.1), after obtaining the unknown function $G_1(y)$ and $G_2(y)$, the displacement component along the crack plane can be determined by the equation

$$u(0,y,z) = \int_{-a}^{y} [G_1(y) + z\,G_2(y)]\,dy,$$

$$|y| < a.$$

(2.56)

2.3.3 Stress Intensity Factor

It is well known that from the linear elastic theory of crack problem, the mode I stress intensity factor at the embedded crack tip can be obtained by one of the two alternate definitions

$$k_I(z) = \lim_{y \to a^+} \sqrt{2(y-a)}\ \sigma_x(0, y, z), \tag{2.63}$$

$$k_I(z) = \lim_{y \to a^-} \overline{\mu}\ \sqrt{2(a-y)}\ \frac{\partial}{\partial y} u(0, y, z), \tag{2.64}$$

where $\overline{\mu}$ is a material constants defined by

$$\overline{\mu} = \frac{4\mu}{1+\kappa}, \quad \text{for isotropic material, where } \kappa = 3 - 4\nu \text{ for plane strain,}$$

$$\text{and } \kappa = \frac{3-\nu}{1+\nu} \text{ for plane strain,}$$

$$\overline{\mu} = \frac{E}{2}, \quad \text{for plane stress,}$$

$$\overline{\mu} = \frac{E}{2(1-\nu^2)}, \quad \text{for plane strain,}$$

and

$$\overline{\mu} = \frac{1}{2}\left(\frac{d_{11}d_{12}}{2}\right)^{-1/2}\left[\left(\frac{d_{11}}{d_{22}}\right)^{1/2} + \frac{2d_{12}+d_{66}}{2d_{22}}\right]^{-1/2}, \tag{2.65}$$

for orthotropic material when crack is located in yz plane and d_{ij} is defined in Appendix I.

Note that definition (2.63) is based on the stress distribution outside the crack, whereas definition (2.64) is based on the displacement component along the crack plane u (0, y, z) inside the crack. Naturally, for this displacement based plate

theory we use definition (2.64) to get the stress intensity factor at the crack tip as follows

$$k_I (z) = \lim_{y \to a^-} \overline{\mu_m} \sqrt{2 (a - y)} \frac{\partial}{\partial y} u (0, y, z), \qquad (2.66)$$

where $\overline{\mu_m}$ is a material constants defined by (2.65) for the mth layer of the laminated plate and the displacement component u (0, y, z) has been discussed in detail in the previous subsection (2.3.2).

2.4 RESULTS AND DISCUSSION

Two types of plate problems, a homogeneous plate and a laminated plate with a central crack, are studied in this chapter. The mode I stress intensity factors are obtained for each case. For homogeneous materials, we are interested in cracked plates subjected to bending only. Although in this chapter only the general linear laminated plate theory is implemented to solve the crack problem, in a similar manner, the other three transverse shear deformation plate theories reviewed and discussed in chapter 1 have been used to solve the crack problem in an isotropic homogeneous plate. This is done to investigate how different plate theories affect the description of crack tip stress behavior and to give an assessment to the plate theory used in solving the laminated plate problem. For a laminated plate the results given are by using the general linear laminated plate theory. As will be seen later, this approach can be justified from the homogeneous plate results. In this case the problem is solved under both tension and bending loads. It should be emphasized that when we say the plate is under bending it is always assumed that the plate is under membrane as well as bending loads so that there is no interference of the crack surfaces on the compressive side of the plate. This can be achieved by linear superposition.

The elastic constants of orthotropic materials used in the numerical examples are given in Table 2.1. These materials are all fiber reinforced graphite-epoxy composite laminates. Note that material B is the same as material A, except that the axes are rotated 90° about z, which is true also for materials D and C. For isotropic materials, E_i and ν_i (i = 1, 2, 3) represent the Young's modulus and Poisson's ratio of the ith layer in the plate. To study the effect of the material properties on the stress intensity factor, some hypothetical material constants are also used to solve the problem.

2.4.1 Homogeneous Plate

The elastic problem for the symmetric bending of a cracked homogeneous plate has been considered before. For example, with Reissner's stress-based first order plate theory, the problem was solved for an isotropic plate in [21] and for an orthotropic plate in [22]. In this study some additional results are given in conjunction with the displacement-based plate theories, namely, Mindlin's first-order

plate theory and a simple higher - order plate theory described in Chapter 1. Table 2.2 shows the effect of the thickness ratio a/h on the stress intensity factor, which are obtained by different plate theories. Classical bending theory's results are included for the purpose of comparison. Because of the Kirchhoff assumption the classical theory gives rather inaccurate results near the boundaries. In a crack problem the crack surfaces are plate boundaries and the important part of the solution is its behavior very near the crack tip. Therefore, classical plate theory is somewhat inaccurate in solving the crack problem. This can be seen in Table 2.2, since it gives the same normalized stress intensity factors regardless of the value of a/h. Moreover, from Table 2.2, it can be seen that the other three transverse shear deformation theories give much the same values regarding the normalized stress intensity factor, with the variation of only about 1%. Later on, based on this observation, for computational convenience, a generalized Mindlin's displacement based first-order plate theory will be used for laminated plate problems. In the meantime, the effect of the transverse shear correction factor K in Mindlin's theory [see (1.18)] on the stress intensity factor is also studied. The results are given in Table 2.3. As stated before, by taking K as 1 and 5/6, we could obtain Mindlin's and Reissner's theories (which are first order theories). In Table 2.3 some extreme values of K are also considered in order to observe the trends.

2.4.2 Laminated Plates

In this part of the study, the results are given for both symmetric and unsymmetric bending as well as the membrane loading (i.e., for the neutral - plane tension). For convenience, we take the neutral plane of the laminated plate as the reference plane. In this case the corresponding boundary conditions are

$$f_1 (y) = N^{\infty},$$
$$f_2 (y) = 0, \qquad (2.67)$$

for the membrane loading and

$$f_1(y) = 0,$$

$$f_2(y) = M^{\infty}, \qquad (2.68)$$

for the bending case.

First a three-layer symmetric laminated plate is considered. This is a simplified model for a sandwich plate and a "honeycomb" structure. The notation of the plate is shown in Figure 2.2a.

Because of the nature of the plate theory used, the displacement components u, v, the stress components σ_x,σ_y, τ_{xy} as well as the stress intensity factor will be piecewise linear functions of z. As expected, while the displacement components are continuous functions, the stress and stress intensity factor will have a discontinuity at $z = \pm h_1/2$, [see (2.66)] due to the nonhomogeneity of the laminated plate. Figures 2.3 and 2.4 show the effect of the thickness ratio a/h on the stress intensity factors at $z = h_1/2$ of Material I and $z = h/2$, respectively. The results are given for different material combinations with material I fixed as Material A and Material II being Material A, Material B and other hypothetical isotropic material (having a Young's modulus of 0.39, 3.9 and 390 GPA). Figure 2.5 and 2.6 show the effect of the thickness ratio a/h and ratio E_2/E_1 on the stress intensity factor. Here both materials are isotropic. Similar results are shown in Figures 2.7 and 2.8 with different h_1/h_2 ratios. From Figure 2.7 it may be observed that the variation in the stress intensity factors for different ratios E_2/E_1 is relatively insignificant. This is expected because with $h_1 = 0.1\ h_2$, the core material near the symmetry plane have very little influence on the behavior of the plate when it is under bending only. On the other hand as shown in Figure 2.8, the thin layers on the outside will have a much more significant effect on the stress intensity factor.

A material of some considerable practical interest is a "honeycomb structure" which can be modeled as a 3-layer symmetric plate with the following features: (referring to Figure 2.2 a)

a. $h_1 \gg h_2$,

b. $E_2 \gg E_1$,

c. for Material I the out-of-plane shear stiffnesses G_{xz} and G_{yz} are much

greater than the in-plane shear stiffness G_{xy}.

Figures 2.9 - 2.13 show the results for such a structure. Here, Material II is isotropic having the elastic constants E_2 and $\nu_2 = 0.3$, and Material I is assumed to have the properties E_1, $G_{xy} = \frac{E_1}{2(1+\nu_1)}$, $\nu_1 = 0.3$ and $G_{xz} = G_{yz} = TT\ G_{xy}$. The results given in these figures are rather self-explanatory. While Figure 2.9 shows the effect of the thickness ratio a/h and TT on the stress intensity factors, Figures 2.10 and 2.11 show such effects due to the variation of E_2/E_1 and TT. The effect of h_1/h_2 for various values of TT and E_2/E_1 is shown in Figures 2.12 and 2.13. It may be seen that for $h_1/h_2 \rightarrow 0$ the isotropic result $k/k_0 = 0.74$ is recovered.

As second example the bending and membrane loading of a two-layer unsymmetric plate problem is considered. The notation used is shown in Figure 2.2 b. Note that we choose the neutral plane of the plate as the reference plane, with c_0 being the vertical distance between the lower surface of the plate and the neutral plane.

Figures 2.14 - 2.18 are results obtained for such two - layer plate, which are all plotted as k_2/k_0 v.s. a/h. Here a/h is the crack length and plate thickness ratio, $k_0 = \sigma_b \sqrt{a}$ with $\sigma_b = \frac{M^{\infty}}{h^2/6}$ when the plate is subjected to uniform bending moment M at the infinity and $k_0 = \sigma_t \sqrt{a}$ with $\sigma_t = \frac{N^{\infty}}{h}$ when the plate is under the membrane load $N_x = N^{\infty}$ only, and k_2 is mode I stress intensity factor at the upper surface of the plate with $z = h - c_0$. Figure 2.14 gives the results obtained for different E_2/E_1 values where both materials are isotropic and ν_1 is equal to ν_2. The results given are for uniform bending moment. It is interesting to note that in this problem even though the singular integral equations are coupled, we obtain $\psi_x \equiv 0$ when the plate is under the in-plane tension and $u_0 \equiv 0$ when it is under bending. These are quite similar to the uncoupled case. Figure 2.15 and 2.16 show the effect of ν_2/ν_1 ratio on the stress intensity factor in a composite plate under bending and membrane loading respectively. It must be emphasized that for the membrane loading due to the coupling the stress intensity factor is still a linear function of z despite the factor the external force N^{∞} is applied in the neutral plane of the plate. These results are quite significant because if we use a plane elasticity approach to solve this kind of problem it might give misleading results. Figures 2.17, 2.18 and 2.19 give the results for plates consisting of two bonded orthotropic layers.

In an attempt to determine the effect of the individual material constants on the stress intensity factors for the two-layer plate, the bending stress intensity factors for $a/h = 1$ and $h_2/h_1 = 1$ are calculated. In these examples, Material I is fixed as being an isotropic material in figure 2.20 or an orthotropic materials in Figures 2.21 and 2.22 and Material II is assumed to be a series of fictitious orthotropic materials where in each case only one or two material constants are varied. Here Material II with the exception of the particular material constant that is varied, is assumed to be "isotropic". For example, in Figure 2.20 for the curve of $R = G_{13}/ G_{12}$ Material I is assumed to be isotropic with constants $E^{(1)}$ and $\nu_1 = 0.3$, whereas for the Material II we assumed that

$$E^{(2)} = E^{(1)},$$

and

$$G_{12} = G_{23} = \frac{E^{(1)}}{2(1 + 0.3)},$$

and only G_{13} is varied relative to the remaining constants. It should be pointed out that in all cases, the stress intensity factor k_2 is a monotonically increasing or decreasing function of R except for varying G_{12} for which it seems to have a maximum for some value of $R > 1$. Similar results were observed in homogeneous orthotropic plates [22].

Figures 2.23 - 2.26 show the results regarding the distributions of the stress intensity factor along the plate thickness direction in the two-layer orthotropic plate, where Material I is Material A and Material II being Material B. For convenience the results given are $k(\overline{z})/k_0$ v.s. $\overline{z}/h$, where

$$\overline{z} = z + c_0,$$

so that $\overline{z}/h = 1$ and $\overline{z}/h = 0$ correspond the upper and lower surfaces of the plate.

Figures 2.23 and 2.24 are results when the plate is subjected to uniform tension and pure bending respectively with the thickness ratio $h_2/h_1 = 1$. Notice that in Figure 2.24 the negative value of stress intensity factor, k, is due to the pure bending moment loading. Figures 2.25 and 2.26 show similar results with $h_2/h_1 = 10$. It is

clearly shown that due to the nature of the plate theory used, the stress intensity factors are linearly distributed along the thickness of the plate. In Figure 2.24 because the Material A in layer I is "stiffer" than Material B in layer II, it is expected that $|k(0)| = 0.833$ is larger than $|k(1)| = 0.792$. Similar trends may be find in other three figures too.

Finally we consider two examples concerning unsymmetric plates that consist of three layers subjected to both tension and bending. The geometry and the notation used are shown in figure 2.2c. We use the same convention as in the two-layer case, namely

$$k_0 = \sigma_b \sqrt{a} \ , \quad \sigma_b = \frac{M^{\infty}}{h^2/6} \ ,$$

for the bending case, and

$$k_0 = \sigma_t \sqrt{a} \ , \quad \sigma_t = \frac{N^{\infty}}{h} \ ,$$

for the tension case.

Figures 2.27 and 2.28 are the stress intensity factor distributions in materials having the same Poisson's ratio $\nu = 0.3$ and Figures 2.29 and 2.30 are the results for materials similar to that considered in Figure 2.27 and 2.28 with different ν_1, ν_2 and ν_3. The same uncoupling features are observed as in the two - layer case. That is when all ν's are same in isotropic materials, $\psi_x \equiv 0$ for the membrane loading and $u_0 \equiv 0$ for bending. This uncoupling phenomenon disappears when the ν's are different. It is expected that the coupling becomes more significant when all the materials are orthotropic. In such cases it would be more appropriate to use a plate theory instead of plane elasticity theory to solve the crack problem under membrane loading.

Chapter 3. Stress Intensity Factor in Two-bonded Orthotropic Layers Containing a Crack Perpendicular to and on the Interface

3.1 INTRODUCTION

In modern engineering layered multimaterial systems have been widely used, ranging from laminated composites to microelectronic devices. In structural analysis and design of such systems, one of the most important considerations is the fracture of individual layers. It would be very attractive to develop special types of designs that improve the structural resistance to fracture failure. As one example of such design practice one may mention the process of manufacturing laminated composites in order to improve the structural resistance to unstable crack propagation by strengthening the material in certain directions, choosing the laminates with different material properties, and stacking the laminates in different sequences. All these increasing use of modern technologies have generated new problems for the structural design and failure analysis. Among the multitude of problems in this study we are mainly interested in the fracture analysis of a mutilayered medium and specifically in the influence of material properties on the fracture behavior of the system.

If one examines the evolution of typical fracture failure in layered structural components, one may invariably trace the initial cause to a localized imperfection. One of the common forms of such imperfections is the surface flaw which may have the potential for growing into macroscopic cracks. Under cyclic loading and/or adverse environmental effects a surface flaw may grow into a part-through surface crack. Upon further application of the loads the surface crack may propagate subcritically through the thickness of the first layer which, in some cases, may cause the total failure of the system. In analyzing the subcritical growth of these surface cracks as well as the cracks imbedded into individual homogeneous layers, it is now generally accepted that the stress intensity factor can be used quite effectively as the primary correlation parameter. In studying the fracture of multilayered materials the basic mechanics problems is then the calculation of stress intensity factors along the crack front for physically relevant external loads and crack geometries. To do this, a mathematical model which may realistically take into account the geometrical and

C-2

physical properties of the medium and the real mechanism of fracture is needed. Because of mathematical difficulties, in recent studies the geometry and the material properties have been considerably simplified by introducing certain two-dimensional or axisymmetric approximations along with the material isotropy. In the early solutions the medium was generally assumed to be infinite consisting of either semi-infinite spaces with or without a layer in between, or periodically stacked laminates. For example, the plane and axisymmetric problems for a medium which consists of two or three different materials and which contains a crack perpendicular to the interfaces may be found in [23-26]. The layered composite which consists of periodically arranged two dissimilar orthotropic bonded layers was considered in [27]. The effect of the elastic properties and the thickness of the adhesive in bonded layered materials was studied in [28]. Later, the plane problem, which is somewhat closer to the actual problem, of two bonded layers containing cracks of various orientations and sizes was studied in [29] and [30]. In that study the individual layers were considered as being isotropic. Particularly in studying composites, the assumption clearly is not very realistic.

In this study the plane elasticity problem of two-bonded orthotropic layers containing a crack perpendicular to the interface is considered. It is assumed that the crack is located in one of the two layers and in a principal plane of orthotropy. The crack problem of a multi-layered medium can be treated as a two layer problem which consists of the layer that contains the crack and a homogenized composite layer representing the remaining part of the medium. Three different problems are studied: the internal or embedded crack problem, the edge crack problem and the problem of a crack terminating at the interface. A general formulation of the problems is given for plane strain case with the material type I. The singular behavior of the stress around crack tip and at the bimaterial interface is studied. The resulting singular integral equations are solved numerically and the stress intensity factors are calculated for various crack geometries and various material combinations. The effect of different material combinations and material orthotropy on the power of stress singularity for a crack terminating at the interface is fully examined.

3.2 THE FORMULATION OF THE PROBLEM

Consider a two-dimensional medium which is formed of two orthotropic infinite layers having thicknesses h_1 and h_2 as shown in Figure 3.1. Assume the layers are perfectly bonded along $y=h_1$ plane and contain a crack on the $x=0$ plane in the first layer. Further assume that by proper superposition the problem is reduced to a perturbation problem in which the crack surface tractions are the only external loads.

3.2.1 Solution of Differential Equations

Let the coordinate systems be selected as in Figure 3.1 and let $u^{(i)}$, $v^{(i)}$, $(i=1,2)$ be the x and y components of the displacement vector in the layers. The following differential equations which result from the plane theory of elasticity must be solved for each layer under appropriate boundary and continuity conditions:

$$\beta_1 \frac{\partial^2 u}{\partial x^2} + \frac{\partial^2 u}{\partial y^2} + \beta_3 \frac{\partial^2 v}{\partial x \partial y} = 0 , \qquad (3.1a)$$

$$\frac{\partial^2 v}{\partial x^2} + \beta_2 \frac{\partial^2 v}{\partial y^2} + \beta_3 \frac{\partial^2 u}{\partial x \partial y} = 0 , \qquad (3.1b)$$

where

$$\beta_1 = \frac{b_{11}}{G_{xy}} , \qquad \beta_2 = \frac{b_{22}}{G_{xy}} ,$$

$$\beta_3 = 1 + \frac{b_{12}}{G_{xy}} , \qquad (3.2a)$$

and $$[B] = [C]^{-1} \qquad (3.2b)$$

and

$$c_{11} = \frac{1- \nu_{xz}\, \nu_{zx}}{E_x} \quad , \qquad c_{22} = \frac{1- \nu_{yz}\, \nu_{zy}}{E_y} \quad ,$$

$$c_{12} = c_{21} = - \frac{\nu_{yx} + \nu_{zx}\, \nu_{yz}}{E_y} = - \frac{\nu_{xy} + \nu_{zy}\, \nu_{xz}}{E_x} \quad ,$$

(3.3a)

for plane strain, and

$$c_{11} = \frac{1}{E_x}, \qquad c_{22} = \frac{1}{E_y},$$

$$c_{12} = c_{21} = - \frac{\nu_{yx}}{E_y} = - \frac{\nu_{xy}}{E_x} \quad ,$$

(3.3b)

for plane stress.

Because of symmetry, the problem will be considered for $0 > x > \infty$ only.

Let the solution of (3.1) be expressed in terms of the following Fourier integrals:

$$u^{(i)}(x,y) = \frac{2}{\pi} \int_0^\infty f_1^{(i)}(y,\alpha)\sin\alpha\, x\, d\alpha + \frac{2}{\pi} \int_0^\infty g_1^{(i)}(x,\gamma)\cos\gamma\, y\, d\gamma$$

$$= u_1^{(i)} + u_2^{(i)} ,$$

$$v^{(i)}(x,y) = \frac{2}{\pi} \int_0^\infty f_2^{(i)}(y,\alpha)\cos\alpha\, x\, d\alpha + \frac{2}{\pi} \int_0^\infty g_2^{(i)}(x,\gamma)\sin\gamma\, y\, d\gamma$$

$$= v_1^{(i)} + v_2^{(i)} .$$

(3.4 a,b)

For simplicity at the beginning we will ignore the index (i). Note that f_i and g_i (i=1,2) are also functions of the material properties in each layer. By substituting from

$$u_1(x,y) = \frac{2}{\pi} \int_0^{\infty} f_1(y,\alpha)\sin\alpha\, x\, d\alpha ,$$

$$v_1(x,y) = \frac{2}{\pi} \int_0^{\infty} f_2(y,\alpha)\cos\alpha\, x\, d\alpha, \qquad 0<x<\infty, \qquad 0<y<h, \tag{3.5}$$

into the equilibrium (3.1), we obtain

$$\beta_1 (- \alpha^2) f_1 + f_1'' + \beta_3 f_2' (- \alpha) = 0 ,$$

$$f_2 (- \alpha^2) + \beta_2 f_2'' + \beta_3 f_1' (+ \alpha) = 0 . \tag{3.6}$$

Assuming the solution of (3.6) in the form

$$f_1 (y,\alpha) = A(\alpha)\, e^{sy\alpha} ,$$

$$f_2 (y,\alpha) = B(\alpha)\, e^{sy\alpha} , \tag{3.7}$$

we obtain the following characteristic equation:

$$s^4 + \beta_4 s^2 + \beta_5 = 0 , \tag{3.8}$$

where β_4 and β_5 are defined as:

$$\beta_4 = \frac{\beta_3^2 - \beta_1 \beta_2 - 1}{\beta_2} , \qquad \beta_5 = \frac{\beta_1}{\beta_2} . \tag{3.9}$$

The roots of (3.8) are

$$s^2 = \frac{-\beta_4 \pm \sqrt{\beta_4{}^2 - 4\,\beta_5}}{2} \,. \qquad (3.10)$$

Defining

$$\beta_6 = \sqrt{\beta_4{}^2 - 4\,\beta_5} \quad , \qquad (3.11)$$

we find

$$s_1 = \omega_1 + i\,\omega_2 = \sqrt{(-\beta_4 + \beta_6)/2} \quad , \qquad s_3 = -s_1 \quad ,$$

$$s_2 = \omega_3 + i\,\omega_4 = \sqrt{(-\beta_4 - \beta_6)/2} \quad , \qquad s_4 = -s_2 \quad , \qquad (3.12)$$

where ω_1 and ω_3 are assumed to be positive.

Thus, from (3.6), (3.7) and (3.12) it can be shown that

$$f_1(y,\alpha) = A_1(\alpha)\, e^{s_1 y\alpha} + A_2(\alpha)\, e^{-s_1 y\alpha} + A_3(\alpha)\, e^{s_2 y\alpha} + A_4(\alpha)\, e^{-s_2 y\alpha} \,,$$

$$f_2(y,\alpha) = \beta_7 \left[A_1(\alpha)\, e^{s_1 y\alpha} - A_2(\alpha)\, e^{-s_1 y\alpha} \right]$$

$$+ \beta_8 \left[A_3(\alpha)\, e^{s_2 y\alpha} - A_4(\alpha)\, e^{-s_2 y\alpha} \right],$$

(3.13 a, b)

where $$\beta_7 = \frac{\beta_3 s_1}{1 - \beta_2 s_1^2}, \qquad \beta_8 = \frac{\beta_3 s_2}{1 - \beta_2 s_2^2}. \qquad (3.14)$$

Similarly, substituting from

$$u_2(x,y) = \frac{2}{\pi} \int_0^\infty g_1(x,\gamma)\cos\gamma y \, d\gamma ,$$

$$v_2(x,y) = \frac{2}{\pi} \int_0^\infty g_2(x,\gamma)\sin\gamma y \, d\gamma , \qquad 0<x<\infty , \qquad 0<y<h ,$$

(3.15)

into equilibrium equations (3.1) it maybe shown that

$$\beta_1 g_1'' - \gamma^2 g_1 + \beta_3 \gamma g_2' = 0 ,$$

$$g_2'' - \gamma^2 \beta_2 g_2 + \beta_3 g_1'(-\gamma) = 0 . \qquad (3.16)$$

If we now let

$$g_1(x,\gamma) = C(\gamma) e^{mx\gamma} ,$$

$$g_2(x,\gamma) = D(\gamma) e^{mx\gamma} , \qquad (3.17)$$

the characteristic equation becomes

$$m^4 + \frac{\beta_4}{\beta_5} m^2 + \frac{1}{\beta_5} = 0 . \qquad (3.18)$$

From (3.18) it may be shown that

$$m_1 = \frac{1}{\sqrt{\beta_5}} \sqrt{(-\beta_4+\beta_6)/2} \quad , \qquad m_3 = -m_1 \ ,$$

$$m_2 = \frac{1}{\sqrt{\beta_5}} \sqrt{(-\beta_4-\beta_6)/2} \quad , \quad m_4 = -m_2 \ , \quad (\mathrm{Re}\,(m_1, m_2) > 0\,).$$

(3.19)

Considering now the regularity conditions at $x = \infty$, from (3.16), (3.17) and (3.19) it may be seen that

$$g_1(x,\gamma) = C_1(\gamma)\, e^{-m_1 x\gamma} + C_2(\gamma)\, e^{-m_2 x\gamma},$$

$$g_2(x,\gamma) = -\beta_9\, C_1(\gamma)\, e^{-m_1 x\gamma} - \beta_{10}\, C_2(\gamma)\, e^{-m_2 x\gamma}, \qquad (3.20\ a, b)$$

where

$$\beta_9 = -\frac{1}{\beta_3}\left[\frac{\beta_1 s_1}{\sqrt{\beta_5}} - \frac{\sqrt{\beta_5}}{s_1}\right],$$

$$\beta_{10} = -\frac{1}{\beta_3}\left[\frac{\beta_1 s_2}{\sqrt{\beta_5}} - \frac{\sqrt{\beta_5}}{s_2}\right]. \qquad (3.21)$$

3.2.2 Displacements u(x,y) and v(x,y) for Material type I :

Examining the following roots of the characteristic equation (3.6)

$$s_1 = \sqrt{\beta_5}\ m_1 = \omega_1 + i\,\omega_2 = \sqrt{(-\beta_4+\beta_6)/2} \quad ,$$

$$s_2 = \sqrt{\beta_5}\ m_2 = \omega_3 + i\,\omega_4 = \sqrt{(-\beta_4-\beta_6)/2} \quad , \qquad (3.22)$$

it can be shown that s_1 and s_2 are either real or complex conjugates. We define Materials type I and II as follows:

Material type I :

$$s_1 = \sqrt{\beta_5}\ m_1 = \omega_1 , \qquad \omega_2 = 0 ,$$

$$s_2 = \sqrt{\beta_5}\ m_2 = \omega_3 , \qquad \omega_4 = 0 , \qquad (3.23)$$

Material type II :

$$s_1 = \sqrt{\beta_5}\ m_1 = \omega_1 + i\,\omega_2 ,$$

$$s_2 = \sqrt{\beta_5}\ m_2 = \omega_3 + i\,\omega_4 . \qquad (3.24)$$

In this study we will assume that the material is of type I. The results for type II materials may be obtained with slight modification in the analysis. Note that s_1 and s_2 are the roots with positive real part and $\beta_5 > 0$. Defining now

$$\beta_{11} = \frac{\omega_1}{\sqrt{\beta_5}} , \qquad \beta_{12} = \frac{\omega_3}{\sqrt{\beta_5}} , \qquad (3.25)$$

$$K_1 = (A_1 - A_2) , \qquad K_2 = (A_1 + A_2) ,$$

$$K_3 = (A_3 - A_4) , \qquad K_4 = (A_3 + A_4) , \qquad (3.26)$$

from (3.4), (3.13) and (3.20) it may be shown that

$$u(x,y) = \frac{2}{\pi}\int_0^\infty [\, K_1(\alpha)\sinh(\omega_1\alpha y) + K_2(\alpha)\cosh(\omega_1\alpha y) + K_3(\alpha)\sinh(\omega_3\alpha y)$$

$$+ K_4(\alpha)\cosh(\omega_3\alpha y)]\, \sin\alpha x\, d\alpha$$

$$+ \frac{2}{\pi} \int_0^\infty [C_1(\gamma)\exp(-\omega_1 \cdot \gamma \cdot x/\sqrt{\beta_5}) + C_2(\gamma) \exp(-\omega_1 \cdot \gamma \cdot x/\sqrt{\beta_5}) \cos\gamma\, y\, d\gamma \ ,$$

$$v(x,y) = \frac{2}{\pi} \int_0^\infty [\beta_7 K_2(\alpha) \sinh(\omega_1 \alpha y) + \beta_7 K_1(\alpha)\cosh(\omega_1 \alpha y) + \beta_8 K_4(\alpha)\sinh(\omega_3 \alpha y)$$

$$+\beta_8 K_3(\alpha)\cosh(\omega_3 \alpha y)] \cos\alpha x d\alpha$$

$$- \frac{2}{\pi} \int_0^\infty \beta_9\, C_1(\gamma)\exp(-\omega_1 \cdot \gamma \cdot x/\sqrt{\beta_5}) + \beta_{10} C_2(\gamma)\exp(-\omega_3 \cdot \gamma \cdot x/\sqrt{\beta_5}\ )]\sin\gamma y\, d\gamma \ ,$$

(3. 27 a, b)

where $K_1(\alpha)$, $K_2(\alpha)$, $K_3(\alpha)$, $K_4(\alpha)$, $C_1(\gamma)$ and $C_2(\gamma)$ are the unknown functions to be determined from the boundary conditions.

3.2.3 Stress Field:

Using the following stress-strain and stress-displacement relations:

$$\sigma_{xx} = b_{11}\, \epsilon_x + b_{12}\, \epsilon_y \ , \qquad (3.28)$$

$$\frac{\sigma_{xx}}{b_{11}} = \epsilon_x + \frac{b_{12}}{b_{11}} \epsilon_y$$

$$= \frac{\partial u}{\partial x} + \frac{b_{12}}{b_{11}} \frac{\partial v}{\partial y} \ ; \qquad (3.29)$$

$$\sigma_{yy} = b_{12}\, \epsilon_x + b_{22}\, \epsilon_y \ , \qquad (3.30)$$

$$\frac{\sigma_{yy}}{b_{22}} = \frac{b_{12}}{b_{22}} \epsilon_x + \epsilon_y$$

$$= \frac{b_{12}}{b_{22}} \frac{\partial u}{\partial x} + \frac{\partial v}{\partial y} \ ; \qquad (3.31)$$

$$\sigma_{xy} = G_{xy}\,\gamma_{xy} = G_{xy}\left(\frac{\partial u}{\partial x} + \frac{\partial v}{\partial y}\right) \qquad (3.32)$$

$$\frac{1}{G_{xy}}\,\sigma_{xy} = \frac{\partial u}{\partial x} + \frac{\partial v}{\partial y}\ ; \qquad (3.33)$$

where

$$[B] = [C]^{-1} \qquad (3.34)$$

and c_{ij} are defined in (3.3),

from (3.17) we obtain the stress as follows:

$$\frac{1}{b_{11}}\,\sigma_{xx} = \frac{2}{\pi}\int_0^\infty [\,\lambda_1 K_1(\alpha)\sinh(\omega_1\alpha y) + \lambda_1 K_2(\alpha)\cosh(\omega_1\alpha y) + \lambda_2 K_3(\alpha)\sinh(\omega_3\alpha y) + \lambda_2 K_4(\alpha)\cosh(\omega_3\alpha y)]\,\alpha\cos\alpha x\,d\alpha$$

$$-\frac{2}{\pi}\int_0^\infty [\lambda_3 C_1\,\gamma\exp(-\omega_1\cdot\gamma\cdot x/\sqrt{\beta_5}) + \lambda_4 C_2\gamma\exp(-\omega_1\cdot\gamma\cdot x/\sqrt{\beta_5})\cos\gamma y\,d\gamma\ , \qquad (3.35)$$

$$\frac{1}{b_{22}}\,\sigma_{yy} = \frac{2}{\pi}\int_0^\infty [\,\lambda_5 K_1(\alpha)\sinh(\omega_1\alpha y) + \lambda_5 K_2(\alpha)\cosh(\omega_1\alpha y) + \lambda_6 K_3(\alpha)\sinh(\omega_3\alpha y) + \lambda_6 K_4(\alpha)\cosh(\omega_3\alpha y)]\,\alpha\cos\alpha x\,d\alpha$$

$$-\frac{2}{\pi}\int_0^\infty [\lambda_7 C_1\,\gamma\exp(-\omega_1\cdot\gamma\cdot x/\sqrt{\beta_5}) + \lambda_8 C_2\gamma\exp(-\omega_1\cdot\gamma\cdot x/\sqrt{\beta_5})\cos\gamma y\,d\gamma\ , \qquad (3.36)$$

$$\frac{1}{G_{xy}}\,\sigma_{xy} = \frac{2}{\pi}\int_0^{\infty} [\,\lambda_9\, K_1(\alpha)\cosh(\omega_1\alpha y) + \lambda_9\, K_2(\alpha)\sinh(\omega_1\alpha y)$$

$$+ \lambda_{10}\, K_3(\alpha)\cosh(\omega_3\alpha y) + \lambda_{10}\, K_4(\alpha)\sinh(\omega_3\alpha y)]\;\alpha\,\sin\alpha\, x\, d\alpha$$

$$- \frac{2}{\pi}\int_0^{\infty} [\lambda_{11}\, C_1\exp(-\omega_1\cdot\gamma\cdot x/\sqrt{\beta_5}) + \lambda_{12}\, C_2\,\exp(-\omega_1\cdot\gamma\cdot x/\sqrt{\beta_5})\;\gamma\,\sin\gamma\, y\, d\gamma\ ,$$

(3.37)

where

$$\lambda_1 = 1 + \beta_7\,\omega_1\,\frac{b_{12}}{b_{11}}\ ,\quad \lambda_2 = 1 + \beta_8\,\omega_3\,\frac{b_{12}}{b_{11}}\ ,$$

$$\lambda_3 = \beta_{11} + \beta_9\,\frac{b_{12}}{b_{11}}\ ,\quad \lambda_4 = \beta_{12} + \beta_{10}\,\frac{b_{12}}{b_{11}}\ ,$$

$$\lambda_5 = \frac{b_{12}}{b_{22}} + \beta_7\,\omega_1\ ,\qquad \lambda_6 = \frac{b_{12}}{b_{22}} + \beta_8\,\omega_3\ ,$$

$$\lambda_7 = \frac{b_{12}}{b_{22}}\,\beta_{11} + \beta_9\ ,\qquad \lambda_8 = \frac{b_{12}}{b_{22}}\,\beta_{12} + \beta_{10}\ ,$$

$$\lambda_9 = \omega_1 - \beta_7\ ,\qquad \lambda_{10} = \omega_3 - \beta_8\ ,$$

$$\lambda_{11} = 1 - \beta_9\,\beta_{11}\ ,\qquad \lambda_{12} = 1 - \beta_{10}\,\beta_{12}\ .$$

(3.38)

3.3 THE INTEGRAL EQUATION

Using the condition that σ_{xy} must vanish for x = 0, which follows from the assumed symmetry, from (3.37) we obtain

$$C_1 = - \frac{\lambda_{12}}{\lambda_{11}} C_2 \ . \qquad (3.39)$$

Defining the new unknown function

$$\frac{\partial u}{\partial y}(0, y) = \phi_1(y), \qquad y \in L,$$

$$= 0, \qquad y \in L', \qquad (3.40)$$

where $(L + L') = (0, h_1)$, L refers to the crack,
from (3.27a) for layer 1, we find

$$\frac{2}{\pi} \int_0^\infty (C_1 + C_2)(-\gamma) \sin\gamma y \, d\gamma = \phi_1(y) \ . \qquad (3.41)$$

Inverting the Fourier integral, from (3.39) - (3.41) it follows that

$$C_1 = \lambda_{14} \frac{1}{\gamma} \int_0^\infty \phi_1(t) \sin\gamma t \, dt = \lambda_{14} \frac{1}{\gamma} \int_0^b \phi_1(t) \sin\gamma t dt \ ,$$

$$C_2 = \lambda_{13} \frac{1}{\gamma} \int_0^\infty \phi_1(t) \sin\gamma t \, dt = \lambda_{13} \frac{1}{\gamma} \int_0^b \phi_1(t) \sin\gamma t dt \ ,$$

(3.42)

where

$$\lambda_{13} = \frac{\lambda_{11}}{\lambda_{12} - \lambda_{11}}, \qquad \lambda_{14} = - \frac{\lambda_{12}}{\lambda_{11}} \lambda_{13} \ . \qquad (3.43)$$

We now use u, v, σ_{xx}, σ_{yy} and σ_{xy} to express the displacement and stress components in the first layer (that contains the cracks) and u^*, v^*, σ_{xx}^*, σ_{yy}^* and σ_{xy}^* in the second layer. Then, referring to Figure 1, We have the following boundary and continuity conditions:

$$\sigma_{yy}(0,x)=0 \ , \qquad \sigma_{xy}(0,x) = 0 \ ,$$

$$\sigma_{yy}^*(h_2,x) = 0 \ , \qquad \sigma_{xy}^*(h_2, x) = 0 \ ; \qquad (3.44\ a - d)$$

$$u(h_1,x) = u^*(0,x) \ , \qquad v(h_1,x) = v^*(0,x) \ ,$$

$$\sigma_{yy}(h_1,x) = \sigma_{yy}^*(0,x) \ , \qquad \sigma_{xy}(h_1,x) = \sigma_{xy}^*(0,x) \ . \qquad (3.45\ a - d)$$

We observe that the displacement and stress expressions for layers 1 and 2 contain nine unknowns, K_1, K_2, K_3, K_4, K_1^*, K_2^*, K_3^*, K_4^* and $\phi_1(t)$. Using the eight boundary and continuity conditions (3.44) and (3.45) we can obtain K_i and K_i^* (i=1,4) in terms of the unknown ϕ_1. The function $\phi_1(t)$ can then be obtained from the following mixed boundary condition:

$$\sigma_{xx}(0,y) = -\,p(y), \qquad y \in L$$

$$u(0,y) = 0, \qquad y \in L' \ . \qquad (3.46\ a,b)$$

By substituting from (3.36) into (3.44 a) and by inverting the Fourier integral, we find

$$[\lambda_5 K_2 + \lambda_6 K_4]\,\alpha = \frac{2}{\pi}\int_0^\infty \int_0^\infty [\,\lambda_7 C_1 e^{-\beta_{11}\gamma x} + \lambda_8 C_2 e^{-\beta_{12}\gamma x}]\gamma \cos\gamma y \cos\gamma x \, d\gamma \, dx. \qquad (3.47)$$

After evaluating the integrals from (3.47) and (3.42) it may be shown that

$$[\rho_3 K_2 + \rho_4 K_4]\,\alpha = [-2 B_5 e^{-\alpha/\beta_{11}t} - 2 B_6 e^{-\alpha/\beta_{12}t}]\ \bar{F}\,, \qquad (3.48)$$

where $\bar{F} = \int_L \phi_1(t)\, dt\,,$ (3.49)

and see Appendix II for ρ_3 and ρ_4 and B_5 and B_6.
Similarly, from (3.44b) and (3.37) we obtain

$$[\rho_5 K_1 + \rho_6 K_3]\,\alpha = 0. \qquad (3.50)$$

By using again the general expressions (3.36) and (3.37), for layer 2 from the boundary conditions (3.44 c) and (3.44 d) we find

$$[\,\rho_3^* \sinh(\omega_1^* \alpha h_2) K_1^* + \rho_3^* \cosh(\omega_1^* \alpha h_2) K_2^* + \rho_4^* \sinh(\omega_3^* \alpha h_2) K_3^* + \rho_4^* \cosh(\omega_3^* \alpha h_2) K_4^*]\,\alpha = 0\,,$$

$$[\,\rho_5^* \cosh(\omega_1^* \alpha h_2) K_1^* + \rho_5^* \sinh(\omega_1^* \alpha h_2) K_2^* + \rho_6^* \cosh(\omega_3^* \alpha h_2) K_3^* + \rho_6^* \sinh(\omega_3^* \alpha h_2) K_4^*]\,\alpha = 0\,. \qquad (3.51\ a, b)$$

where the quantities with the superscript * are those in layer II having the same expressions with the quantities without * in layer I. For example, ω_1^* is the characteristic root for the material in layer II with the same expression as in (3.12).

In a similar way, by substituting from the general displacement expressions (3.27) into the continuity conditions (3.45) and by evaluating the related integrals we obtain

$$K_1 \sinh(\omega_1\alpha\, h_1) + K_2 \cosh(\omega_1\alpha\, h_1) + K_3 \sinh(\omega_3\alpha\, h_1) + K_4\cosh(\omega_3\alpha\, h_1)$$

$$- K_2^* - K_4^* = \left(- \frac{1}{\alpha} \right) [\, B_1[\, \exp(- (h_1\text{-}t)\, \alpha/\beta_{11}) - \exp (- (h_1 + t)\, \alpha/\beta_{11})]$$

$$+ B_2[\, \exp(- (h_1\text{-}t)\, \alpha/\beta_{12}) - \exp (- (h_1 + t)\, \alpha/\beta_{12})]\,]\, \bar{F} \ ,$$

$$[\, \rho_1 K_1 \cosh(\omega_1\alpha\, h_1) + \rho_1 K_2 \sinh(\omega_1\alpha\, h_1) + \rho_2 K_3 \cosh(\omega_3\alpha\, h_1)$$

$$+ \rho_2 K_4 \sinh(\omega_3\alpha\, h_1) - \rho_1^* K_1^* - \rho_2^* K_4^*$$

$$= \left(- \frac{1}{\alpha} \right) [\, B_3[\, \exp(- (h_1\text{-}t)\, \alpha/\beta_{11}) - \exp (- (h_1 + t)\, \alpha/\beta_{11})]$$

$$+ B_4[\, \exp(- (h_1\text{-}t)\, \alpha/\beta_{12}) - \exp (- (h_1 + t)\, \alpha/\beta_{12})]\,]\, \bar{F} \ ,$$

$$[\rho_3 K_1 \sinh(\omega_1\alpha\, h_1) + \rho_3 K_2 \cosh(\omega_1\alpha\, h_1) + \rho_4 K_3 \sinh(\omega_3\alpha\, h_1)$$

$$+ \rho_4 K_4 \cosh(\omega_3\alpha\, h_1) - \rho_{01}\rho_3^* K_2^* - \rho_{01}\rho_4^* K_4^*$$

$$= \left(- \frac{1}{\alpha} \right) [\, B_5[\, \exp(- (h_1\text{-}t)\, \alpha/\beta_{11}) - \exp (- (h_1 + t)\, \alpha/\beta_{11})]$$

$$+ B_6[\, \exp(- (h_1\text{-}t)\, \alpha/\beta_{12}) - \exp (- (h_1 + t)\, \alpha/\beta_{12})]\,]\, \bar{F} \ ,$$

$$[\, \rho_5 K_1 \cosh(w_1\alpha\, h_1) + \rho_5 K_2 \sinh(w_1\alpha\, h_1) + \rho_6 K_3 \cosh(w_3\alpha\, h_1)$$

$$+ \rho_6 K_4 \sinh(w_3\alpha\, h_1) - \rho_{02}\rho_5^* K_1^* - \rho_{02}\rho_6^* K_3^*$$

$$= \left(\frac{1}{\alpha} \right) [\, B_7[\, \exp(-(h_1-t)\, \alpha/\beta_{11}) - \exp(-(h_1 + t)\, \alpha/\beta_{11})]$$

$$+ B_8[\, \exp(-(h_1-t)\, \alpha/\beta_{12}) - \exp(-(h_1 + t)\, \alpha/\beta_{12})]\,]\, \bar{F}\,, \qquad (3.52\ a - d)$$

where

$$\rho_{01} = \frac{b_{22}}{b_{22}^*}\,, \qquad \rho_{02} = \frac{G_{xy}}{G_{xy}^*}\,. \qquad (3.53)$$

and see Appendix II for expressions ρ_i (i = 1, 6) and B_i (i = 1, 8).

In summary, the system of equations for the unknowns $K_i(\alpha)$ and $K_i^*(\alpha)$, (i = 1,.. ,4) may be expressed as follows:

$$\alpha\, P\, K = \bar{F}\, f\,, \qquad (3.54)$$

$$P = (\, P_{ij}\,),$$

$$K = [\, K_1\ K_2\ K_3\ K_4\ K_1^*\ K_2^*\ k_3^*\ K_4^*\,]^{\top}\,,$$

$$f = f_1 \exp[\, -(\, \alpha/\, \beta_{11})\, t\,] + f_2 \exp[\, -(\, \alpha/\, \beta_{12})\, t\,]$$

$$+ f_3 \exp[-(\alpha/\, \beta_{11})\, (h_1 - t\,)\,] + f_4 \exp[-(\alpha/\, \beta_{12})\, (h_1 - t\,)\,]$$

$$+ f_5 \exp[-(\alpha/\, \beta_{11})\, (h_1 + t\,)\,] + f_6 \exp[-(\alpha/\, \beta_{12})\, (h_1 + t\,)\,]\,, \qquad (3.55)$$

$$
P = \begin{bmatrix}
0 & \rho_3 & 0 & \rho_4 & 0 & 0 & 0 & 0 \\
\rho_5 & 0 & \rho_6 & 0 & 0 & 0 & 0 & 0 \\
0 & 0 & 0 & 0 & P_{35} & P_{36} & P_{37} & P_{38} \\
0 & 0 & 0 & 0 & P_{45} & P_{46} & P_{47} & P_{48} \\
P_{51} & P_{52} & P_{53} & P_{54} & 0 & -1 & 0 & -1 \\
P_{61} & P_{62} & P_{63} & P_{64} & -\rho_1^* & 0 & -\rho_2^* & 0 \\
P_{71} & P_{72} & P_{73} & P_{74} & 0 & P_{76} & 0 & P_{78} \\
P_{81} & P_{82} & P_{83} & P_{84} & P_{85} & 0 & P_{87} & 0
\end{bmatrix}
$$

where

$$P_{35} = \rho_3^* \sinh (\omega_1^* \alpha h_2), \quad P_{36} = \rho_3^* \cosh (\omega_1^* \alpha h_2),$$

$$P_{37} = \rho_4^* \sinh (\omega_3^* \alpha h_2), \quad P_{38} = \rho_4^* \cosh (\omega_3^* \alpha h_2),$$

$$P_{45} = \rho_5^* \cosh (\omega_1^* \alpha h_2), \quad P_{46} = \rho_5^* \sinh (\omega_1^* \alpha h_2),$$

$$P_{47} = \rho_6^* \cosh (\omega_3^* \alpha h_2), \quad P_{48} = \rho_6^* \sinh (\omega_3^* \alpha h_2),$$

$$P_{51} = \sinh (\omega_1 \alpha h_1), \quad P_{52} = \cosh (\omega_1 \alpha h_1),$$

$$P_{53} = \sinh (\omega_3 \alpha h_1), \quad P_{54} = \cosh (\omega_3 \alpha h_1),$$

$$P_{61} = \rho_1 \cosh (\omega_1 \alpha h_1), \quad P_{62} = \rho_1 \sinh (\omega_1 \alpha h_1),$$

$$P_{63} = \rho_2 \cosh (\omega_3 \alpha h_1), \quad P_{64} = \rho_2 \sinh (\omega_3 \alpha h_1),$$

$$P_{71} = \rho_3 \sinh (\omega_1 \alpha h_1), \quad P_{72} = \rho_3 \cosh (\omega_1 \alpha h_1),$$

$$P_{73} = \rho_4 \sinh (\omega_3 \alpha h_1), \quad P_{74} = \rho_4 \cosh (\omega_3 \alpha h_1),$$

$$P_{81} = \rho_5 \cosh (\omega_1 \alpha h_1) P_{82} = \rho_5 \sinh (\omega_1 \alpha h_1),$$

$$P_{83} = \rho_6 \cosh (\omega_3 \alpha h_1) P_{84} = \rho_6 \sinh (\omega_3 \alpha h_1),$$

$$P_{76} = - \rho_{01} \rho_3^*, \qquad P_{78} = -\rho_{01} \rho_4^*,$$

$$P_{85} = - \rho_{02} \rho_5^*, \qquad P_{87} = -\rho_{02} \rho_6^*, \qquad (3.56)$$

$$f_1 = [\, 2B_5 \;\; 0 \;\; 0 \;\; 0 \;\; 0 \;\; 0 \;\; 0 \;\; 0 \,]^T,$$

$$f_2 = [\, 2B_6 \;\; 0 \;\; 0 \;\; 0 \;\; 0 \;\; 0 \;\; 0 \;\; 0 \,]^T,$$

$$f_3 = [\, 0 \;\; 0 \;\; 0 \;\; 0 \;\; -B_1 \;\; -B_3 \;\; B_5 \;\; -B_7 \,]^T,$$

$$f_4 = [\, 0 \;\; 0 \;\; 0 \;\; 0 \;\; -B_2 \;\; -B_4 \;\; B_6 \;\; -B_8 \,]^T,$$

$$f_5 = [\, 0 \;\; 0 \;\; 0 \;\; 0 \;\; B_1 \;\; B_3 \;\; -B_5 \;\; B_7 \,]^T,$$

$$f_6 = [\, 0 \;\; 0 \;\; 0 \;\; 0 \;\; B_2 \;\; B_4 \;\; -B_6 \;\; B_8 \,]^T. \qquad (3.57)$$

After determining K_i and K_i^*, (i = 1,..,4) by solving (3.54) in terms of ϕ_1 (y), this remaining unknown function may be obtained from the mixed boundary conditions (3.46). By substituting from (3.35) into (3.46 a), using (3.42), and from (3.46 b) by observing that ϕ_1 (y) = 0 on L′ we find

$$\frac{\pi}{2}\frac{1}{b_{11}}\sigma_{xx} = \int_0^\infty [\,\lambda_1 K_1(\alpha)\sinh(\omega_1\alpha y) + \lambda_1 K_2(\alpha)\cosh(\omega_1\alpha y)$$

$$+ \lambda_2 K_3(\alpha)\sinh(\omega_3\alpha y) + \lambda_2 K_4(\alpha)\cos(\omega_3\alpha y)]\,\alpha\cos\alpha x\,d\alpha$$

$$+ B_{11}\int_L \phi_1(t)\,dt\left(\frac{1}{t-y}+\frac{1}{t+y}\right) = -\frac{\pi}{2}\frac{1}{b_{11}}p(y), \qquad y \in L.$$

(3.58)

Finally, assuming that L = (a, b) or the crack is located along x = 0, a< y<b, the integral equation (3.58) may be expressed in the following standard form:

$$\int_a^b \left[\frac{1}{t-y} + k(y,t)\right]\phi_1(t)\,dt = -\frac{\pi}{2B_{11}}\frac{1}{b_{11}}p(y). \qquad a < y < b$$

(3.59)

where the Fredholm kernel, k(y, t), is defined as:

$$k(y,t) = \frac{1}{t+y} + \frac{1}{B_{11}}\int_0^\infty [\,E_1 e^{-\alpha/\beta_{11}t} + E_2 e^{-\alpha/\beta_{12}t}$$

$$+ E_3 e^{-\alpha/\beta_{11}(h_1 - t)} + E_4 e^{-\alpha/\beta_{12}(h_1 - t)}$$

$$+ E_5 e^{-\alpha/\beta_{11}(h_1 + t)} + E_6 e^{-\alpha/\beta_{12}(h_1 + t)}\,]\,d\alpha$$

(3.60)

where the E_i (i = 1, 6) are known functions of K_i, K_i^* (i =1, 4) which may be obtained by solving the equations (3.54) .

From the definition of the function ϕ_1 given by (3.40) it is clear that for an imbedded crack the solution of the integral equation (3.59) must satisfy the following singlevaluedness condition:

$$\int_a^b \phi_1(t)\, dt = 0 . \qquad (3.61)$$

3.4 THE SINGULARITY AT THE CRACK TIP

It is well known that the stress field around a crack tip is proportional to r^{-s}, where r is a small distance from the crack tip at which we measure the stress field, and s is called the power of singularity which should be between zero and one, i.e. $0 < s < 1$. If s is less than zero, the stress is bounded as $r \rightarrow 0$ and there is no singularity at the crack tip. If s is greater than one, the strain energy density is unbounded as $r \rightarrow 0$, which is physically impossible.

The value of singularity s is dependent on the crack configuration as well as material properties. In this work, three crack configurations will be studied, namely: (referring to Figure 3.1)

i) embedded crack, $a > 0$, $b < h_1$,

ii) edge crack, $a = 0$, $b < h_1$,

iii) crack terminating at the interface, $a \geq 0$, $b = h_1$.

For each crack configuration, the singularity of the stress state around the crack tip or the irregular points a and b may be examined by using the function theoretic method described in [31], [32] and [33].

3.4.1 Embedded Crack

For the case of a crack embedded in a homogeneous material, the only singular term in the integral equation (3.32) is the dominant term $\frac{1}{t-y}$ and the remaining kernels are bounded. The singular integral equations can thus be written in the form:

$$\int_a^b \frac{\phi_1(t)}{t-y}\, dt + B.\,T. = -\frac{\pi}{2\,B_{11}}\,\frac{1}{b_{11}}\,p(y)\,, \qquad a > y > b\,. \tag{3.62}$$

where B.T. corresponds to the bounded term.

To examine the behavior of the unknown function $\phi_1(t)$ around the irregular points a and b, following Muskhelishvili [31], we assume that the unknown function ϕ_1 may be expressed as

$$\phi_1(t) = \frac{g_1(t)}{(t-a)^{\alpha}\,(b-t)^{\beta}} = g_1(t)\, W_1(t)\,, \qquad (3.63)$$

where $g_1(t)$ satisfies a Hölder condition in closed interval $a \leq t \leq b$ and $g_1(a) \neq 0$, $g_1(b) \neq 0$. Also α, β are the singularities at the irregular points which should satisfy the condition $0 < \mathrm{Re}\ (\alpha,\beta) < 1$, and $W_1(t)$ is any definite branch which varies continuously on the interval $a<t<b$.

Define the following sectionally holomorphic function

$$F_1(z) = \frac{1}{\pi} \int_a^b \frac{\phi_1(t)}{t-z}\, dt\,, \qquad (3.64)$$

substituting equation (3.63) into equation (3.64) we obtain

$$F_1(z) = \frac{1}{\pi} \int_a^b \frac{g_1(t)\, \exp(i\,\pi\,\beta)}{(t-a)^{\alpha}\,(t-b)^{\beta}\,(t-z)}\, dt\,. \qquad (3.65)$$

Following Muskhelishvili, equation (3.65) can be written

$$F_1(z) = \frac{g_1(a)\, \exp(i\,\pi\,\alpha)}{(b-a)^{\beta}\,(z-a)^{\alpha}\sin(\pi\alpha)} + \frac{g_1(b)}{(b-a)^{\alpha}\,(z-b)^{\beta}\sin(\pi\beta)} + F_{01}(z)\,. \qquad (3.66)$$

$F_{01}(z)$ is bounded everywhere except possibly at the end points a, b, where it has the following behavior

$$|F_{01}(z)| < \frac{C_k}{|z-e_k|^{p_k}}\,, \qquad k=1,2\,, \qquad (3.67)$$

$e_1 = a$, $e_2 = b$, $p_1 < \mathrm{Re}\,(\alpha)$, $p_2 < \mathrm{Re}\,(\beta)$ and e_k, p_k are real constants, that is, $F_{01}(z)$ has singularities weaken than α, β.

Using the Plemelj formula [31]

$$\frac{1}{\pi}\int_a^b \frac{\phi_1(t)}{t-z}\,dt = \frac{i}{2}\,[\,F_1^{+}(y) + F_1^{-}(y)\,], \qquad a<y<b\,, \qquad (3.68)$$

from (3.66) it follows that

$$\frac{1}{\pi}\int_a^b \frac{\phi_1(t)}{t-y}\,dt = \frac{g_1(a)\cot(\pi\alpha)}{(b-a)^{\beta}\,(y-a)^{\alpha}} - \frac{g_1(b)\cot(\pi\beta)}{(b-a)^{\alpha}\,(b-y)^{\beta}} + F_{01}(y)\,. \qquad (3.69)$$

Substituting equation (3.69) into (3.62) we find

$$\frac{g_1(a)\cot(\pi\alpha)}{(b-a)^{\beta}\,(y-a)^{\alpha}} - \frac{g_1(b)\cot(\pi\beta)}{(b-a)^{\alpha}\,(b-y)^{\beta}} = \psi_1(y)\,, \qquad (3.70)$$

where $\psi_1(y)$ contain all the bounded functions.

By multiplying equation (3.70) first by $(y-a)^{\alpha}$ and letting $y \to a$, and then by $(b-y)^{\beta}$ and letting $y \to b$, we obtain the following characteristic equations for α, β,

$$\frac{g_1(a)\cot(\pi\alpha)}{(b-a)^{\beta}} = 0\,, \qquad \text{or} \qquad \cot(\pi\alpha) = 0\,,$$

$$\frac{g_1(b)\cot(\pi\beta)}{(b-a)^{\alpha}} = 0, \qquad \text{or} \qquad \cot(\pi\beta) = 0\,. \qquad (3.71\ a, b)$$

The acceptable roots of these equations are $\alpha = \frac{1}{2}$, $\beta = \frac{1}{2}$, which are the well known results in the crack problems. Hence, the fundamental function of the singular integral equation is

$$W(t) = \frac{1}{(t-a)^{1/2}(b-t)^{1/2}} . \qquad (3.72)$$

Therefore as long as we have internal cracks, the power of singularity will be 1/2.

3.4.2 Edge Crack

This is the case that $a = 0$ and $b<h_1$. Now the crack is an edge crack with one crack tip in the medium and the other crack tip going to the boundary.

For this case the integrand of Fredholm kernel, k(y,t) expressed in (3.60), is no longer bounded as $\alpha \rightarrow \infty$. Therefore the singular part of the kernel must be separated and evaluated in closed form. We can write the kernel k(y, t) in two parts.

$$k(y, t) = k_s(y, t) + k_b(y, t). \qquad (3.73)$$

where k_s is the singular part and k_b is the bounded part of k.

The singular integral equation can then be written as

$$\int_0^b \left[\frac{1}{t-y} + k_s(y, t)\right] \phi_1(t)\, dt + \int_0^b k_b(y, t)\, \phi_1(t)\, dt = -\frac{\pi}{2 B_{11}} \frac{1}{b_{11}} p(y)$$

$$0 < y < b . \qquad (3.74)$$

Following the same function theoretic analysis as in the embedded crack case, the only acceptable roots for the characteristic equation are found to be $\alpha = 0$ and $\beta = 1/2$ (see [34] for details), that is, for the crack going to the free boundary, there is no singularity at the crack tip. Therefor the fundamental function of the singular

integral equation is

$$W(t) = \frac{1}{(b - t)^{1/2}} . \qquad (3.75)$$

3.4.3 Crack Terminating at the Interface

This is the case that $a \geq 0$ and $b = h_1$. The problem of interest here is the singularity at the crack tip $y = h_1$. Thus, without any loss in generality we assume $a > 0$ and $b = h_1$ for the analysis. The similar problem has been studied by Delale in [27].

For this case the integrand of Fredholm kernel, $k(y, t)$, expressed in (3.59), is no longer bounded as $\alpha \rightarrow \infty$ when $y \rightarrow h_1$ and $t \rightarrow h_1$, at the same time. Therefore, to study the singular behavior at the interface and to make the kernel numerically integrable, the singular part of the kernel must be separated and evaluated in the closed form. Again, we express the kernel $k(y, t)$ as

$$k(y, t) = k_s(y, t) + k_b(y, t). \qquad (3.76)$$

where k_s is the singular part and k_b is the bounded part.
To make the manipulations manageable without any loss in accuracy, we obtain the singular part from the symmetric crack problem shown in figure 3.2. In this case, the symmetry about the y axis is maintained and we have

$$u(x, y) = u(x, -y),$$

$$v(x, y) = -v(x, -y). \qquad (3.77)$$

Thus, it is sufficient to consider the problem for $y > 0$ only. Observing the general solution of the displacement $u(x, y)$ as expressed in (3.27), the coefficients of the

nosymmetric terms sine and hyperbolic sine must be zero, i.e. $K_1 = 0$, $K_3 = 0$, $K_1^* = 0$ and $K_3^* = 0$, which makes the analysis considerably simpler and makes it possible to obtain the closed form expression of singular kernel k_s (y, t).

Following the same procedure described in [27], it can be shown that k_s(y, t) can be expressed as follows:

$$k_s = k_{s1} + k_{s2} + k_{s3} + k_{s4}$$

$$= P_{11} \frac{\omega_1 h_1 + (h_1 - t)/\beta_{11}}{(\omega_1 h_1 + (h_1 - t)/\beta_{11})^2 - (\omega_1 y)^2}$$

$$+ P_{12} \frac{\omega_1 h_1 + (h_1 - t)/\beta_{12}}{(\omega_1 h_1 + (h_1 - t)/\beta_{12})^2 - (\omega_1 y)^2}$$

$$+ P_{13} \frac{\omega_3 h_1 + (h_1 - t)/\beta_{11}}{(\omega_3 h_1 + (h_1 - t)/\beta_{11})^2 - (\omega_3 y)^2}$$

$$+ P_{14} \frac{\omega_3 h_1 + (h_1 - t)/\beta_{12}}{(\omega_3 h_1 + (h_1 - t)/\beta_{12})^2 - (\omega_3 y)^2} \qquad (3.78)$$

where P_{1i} (i = 1, 4) are the expressions of material constants which are obtained from the asymptotic analysis.

The governing singular integral equation then becomes:

$$\int_a^b \left[\frac{1}{t-y} + \frac{1}{B_{11}} k_s (y, t) \right] \phi_1(t)\, dt + \int_a^b \frac{1}{B_{11}} k_b (y, t) \ \phi_1(t)\, dt$$

$$= - \frac{\pi}{2 B_{11}} \frac{1}{b_{11}} p(y)$$

$$0 < y < b ,$$

$$k_b (y, t) = k (y, t) - k_s (y, t). \qquad (3.79)$$

We again define

$$\phi_1(t) = \frac{g_1(t)}{(t-a)^{1/2}(h_1-t)^{\beta}} = g_1(t)\, W_1(t) . \qquad (3.80)$$

Here the singularity β will be different from 1/2 because of the additional singular kernel $k_s(y,t)$.

To examine the singularity β, we use the symmetric case as the illustration. Referring to Fig. 3.2 the singular integral equation may be expressed as

$$\frac{1}{\pi}\int_{-h_1}^{h_1}\left[\frac{1}{t-y} + \frac{1}{B_{11}} k_s(y,t)\right]\phi_1(t)\,dt = \text{bounded terms} .$$

$$-h_1 \le y \le h_1 \qquad (3.81)$$

Following Muskhelishvili, the unknown function $\phi_1(t)$ can be written

$$\phi_1(t) = \frac{F_1(t)}{(h_1^2 - t^2)^{\beta}} , \qquad (3.82)$$

where $F_1(t)$ is bounded and Holder - continuous in the interval $|t| < h_1$, and $0 < \mathrm{Re}(\beta) < 1$.

Define the sectionally holomophic function:

$$\Phi(z) = \frac{1}{\pi}\int_{-h_1}^{h_1}\frac{\phi_1(t)}{t-z}\,dt = \frac{1}{\pi}\int_{-h_1}^{h_1}\frac{F_1(t)\exp(i\pi\beta)}{(t-h_1)^{\beta}(t+h_1)^{\beta}(t-z)}\,dt ,$$

$$(3.83\,a)$$

Then, the equation (3.83 a) can be written as [31]

$$\Phi(z) = \frac{F_1(-h_1)\exp(i\pi\gamma)}{(2h_1)^{\beta}\sin(\pi\beta)(z+h_1)^{\beta}} - \frac{F_1(h_1)}{(2h_1)^{\beta}\sin(\pi\beta)(z-h_1)^{\beta}} + \Phi_0(z)$$

$$(3.83\,b)$$

where $\Phi_0(z)$ is bounded everywhere except at the end points $\pm h_1$, where it has the following behavior

$$|\Phi_0(z)| < \frac{F_1(\pm h)}{|z \pm h|^{\beta_0}}, \qquad \mathrm{Re}(\beta_0) < \mathrm{Re}(\beta). \tag{3.84}$$

When $z = y$ is on the cut, using Plemelj formula:

$$\Phi(y) = \frac{F_1(-h_1)\cot(\pi\beta)}{(2h_1)^{\beta}(h_1+y)^{\beta}} - \frac{F_1(h_1)\cot(\pi\beta)}{(2h_1)^{\beta}(h_1-y)^{\beta}} + \Phi^*(y) \qquad |y| < h_1 \tag{3.85}$$

Now consider the following integral

$$\begin{aligned} I_1 &= \frac{1}{\pi}\int_{-h_1}^{h_1} k_{s1}(y,t)\,\phi_1(t)\,dt \\ &= \frac{1}{\pi}\int_{-h_1}^{h_1} P_{11}\,\frac{\omega_1 h_1 + (h_1 - t)/\beta_{11}}{(\omega_1 h_1 + (h_1 - t)/\beta_{11})^2 - (\omega_1 y)^2}\,\phi_1(t)\,dt \\ &= \frac{1}{\pi}\int_{-h_1}^{h_1}\left(-\frac{\beta_{11}P_{11}}{2}\right)\frac{\phi_1(t)}{t - [h_1 + \beta_{11}\omega_1(h_1 - y)]}\,dt \\ &+ \frac{1}{\pi}\int_{-h_1}^{h_1}\left(-\frac{\beta_{11}P_{11}}{2}\right)\frac{\phi_1(t)}{t - [h_1 + \beta_{11}\omega_1(h_1 + y)]}\,dt, \end{aligned} \tag{3.86 a}$$

from (3.83 a)

$$I_1 = \frac{1}{\pi} \int_{-h_1}^{h_1} \left(- \frac{\beta_{11} P_{11}}{2} \right) \frac{F_1(t) \exp (i \pi \beta)}{(t-h_1)^{\beta} (t + h_1)^{\beta} (t - [h_1 + \beta_{11} \omega_1 (h_1 - y)])} \, dt$$

$$+ \frac{1}{\pi} \int_{-h_1}^{h_1} \left(- \frac{\beta_{11} P_{11}}{2} \right) \frac{F_1(t) \exp (i \beta \pi)}{(t-h_1)^{\beta} (t + h_1)^{\beta} (t - [h_1 + \beta_{11} \omega_1 (h_1 + y)])} \, dt ,$$

(3.86 b)

when $z= h_1 + \beta_{11} \omega_1 (h_1 - y)$ and $z= h_1 + \beta_{11} \omega_1 (h_1 + y)$ are outside the branch cut we have

$$I_1 = - \frac{F_1 (- h_1)}{(2 h_1)^{\beta} \sin (\pi \beta) [\beta_{11} \omega_1 (h_1 + y)]^{\beta}} + \Phi_1^* (y)$$

$$- \frac{F_1 (- h_1)}{(2 h_1)^{\beta} \sin (\pi \beta) [\beta_{11} \omega_1 (h_1 - y)]^{\beta}} + \Phi_2^* (y) ,$$

(3.83 c)

where $\Phi_1^* (y)$ and $\Phi_2^* (y)$ are similar to $\Phi_0^* (y)$ in equation (3.83 b).

Observing that $F_1 (y) = - F_1 (- y)$, the integration I_1 can be written as :

$$I_1 = \left(\frac{\beta_{11} P_{11}}{2} \right) \frac{F_1 (h_1)}{(2 h_1)^{\beta} \sin (\pi \beta) (\beta_{11} \omega_1)^{\beta}} \left[\frac{1}{(h_1 - y)^{\beta}} \right.$$

$$+ \frac{1}{(h_1 + y)^{\beta}} \Big] .$$

(3.87 a)

Following the same procedure, we can obtain the following integrations:

$$I_2 = \frac{1}{\pi} \int_{-h_1}^{h_1} k_{s2}(y, t)\, \phi_1(t)\, dt$$

$$= \left(\frac{\beta_{12} P_{12}}{2} \right) \frac{F_1(h_1)}{(2 h_1)^{\beta} \sin(\pi \beta) (\beta_{12} \omega_1)^{\beta}} \left[\frac{1}{(h_1 - y)^{\beta}} \right.$$

$$\left. + \frac{1}{(h_1 + y)^{\beta}} \right] ,$$

(3.87 b)

$$I_3 = \frac{1}{\pi} \int_{-h_1}^{h_1} k_{s3}(y, t)\, \phi_1(t)\, dt$$

$$= \left(\frac{\beta_{11} P_{13}}{2} \right) \frac{F_1(h_1)}{(2 h_1)^{\beta} \sin(\pi \beta) (\beta_{11} \omega_3)^{\beta}} \left[\frac{1}{(h_1 - y)^{\beta}} \right.$$

$$\left. + \frac{1}{(h_1 + y)^{\beta}} \right] ,$$

(3.87 c)

$$I_4 = \frac{1}{\pi} \int_{-h_1}^{h_1} k_{s4}(y, t)\, \phi_1(t)\, dt$$

$$= \left(\frac{\beta_{12} P_{14}}{2} \right) \frac{F_1(h_1)}{(2 h_1)^{\beta} \sin(\pi \beta) (\beta_{12} \omega_3)^{\beta}} \left[\frac{1}{(h_1 - y)^{\beta}} \right.$$

$$+ \frac{1}{(h_1 + y)^{\beta}} \Big] .$$

(3.87 d)

Substituting I_1 , I_2 , I_3 , I_4 and (3.85) into (3.81) and letting $y \rightarrow h_1$ and noting that $F_1 (h_1) \neq 0$, the characteristic equation for β becomes:

$$-2 \cos (\pi \beta) + \beta_{11} P_{11} \frac{1}{(\beta_{11} \omega_1)^{\beta}} + \beta_{12} P_{12} \frac{1}{(\beta_{12} \omega_1)^{\beta}}$$

$$\beta_{11} P_{13} \frac{1}{(\beta_{11} \omega_3)^{\beta}} + \beta_{12} P_{14} \frac{1}{(\beta_{12} \omega_3)^{\beta}} = 0 .$$

(3.88)

This is the same equation found in [27]. Choosing the orthotropic elastic constants close to isotropic constants numerically we find the same singularity power computed in [23] and [30]. The characteristic equation (3.88) can be solved numerically to obtain β. For practical orthotropic materials equation (3.88) has only one root between 0 and 1. If material II is stiffer than material I, the root will be less than 1/2. But if material I is stiffer than material II, then the root will be greater than 1/2.

For the two bonded strip problem, when $a > 0$ and $b = h_1$, the fundamental function is

$$W_1 (t) = \frac{1}{(t - a)^{1/2} (h_1 - t)^{\beta}} , \qquad (3.89)$$

where β is the root of equation (3.88).

3.5 SOLUTION OF THE SINGULAR INTEGRAL EQUATION AND THE STRESS INTENSITY FACTOR

The solution of the problem depends on the unknown density function ϕ_1 which can be obtained by solving the singular integral equation (3.59) numerically using any one of the known techniques [35], [33] . In this work the quadrature method described in [33] is used. To solve the integral equation:

$$\int_a^b \left[\frac{1}{t-y} + k(y,t) \right] \phi_1(t)\, dt = -\frac{\pi}{2 B_{11}} \frac{1}{b_{11}} p(y), \qquad a < y < b, \tag{3.90}$$

we first normalize the interval (a, b) by defining:

$$t = \frac{b-a}{2} r + \frac{b+a}{2}, \qquad (a \le t \le b, \; -1 \le r \le 1)$$

$$y = \frac{b-a}{2} s + \frac{b+a}{2}, \qquad (a \le y \le b, \; -1 \le s \le 1)$$

$$\phi_1(t) = F(r),$$

$$\frac{b-a}{2} k(y,t) = k(r,s),$$

$$-\frac{\pi}{2 B_{11}} \frac{1}{b_{11}} p(y) = p(s). \tag{3.91 a - e}$$

Equation (3.90) may then be expressed as

$$\int_{-1}^{1} \left[\frac{1}{r-s} + k(r,s) \right] F(r)\, dr = p(s) \qquad -1 < s < 1 . \qquad (3.92)$$

The unique solution of the singular integral equation (3.92) can be obtained for given crack configuration. Three typical crack geometries will be investigated separately in the following subsections.

3.5.1 Embedded Crack

In this case the solution of the singular integral equation (3.92) will be obtained under the single - valuedness condition

$$\int_{-1}^{1} F(r)\, dr = 0 . \qquad (3.93)$$

Since F(r) has a power singularity 1/2 at the end points the solution will be sought in the form

$$F(r) = \frac{f(r)}{\sqrt{1-r^2}} \qquad (3.94)$$

where f(r) is Holder continuous in the interval $-1 \le r \le 1$.

Following the procedure described in [33] we get the system as follows

$$\frac{1}{2} K^*(s_k, r_1) f(r_1) + \sum_{i=2}^{n-1} K^*(s_k, r_i) f(r_i) + \frac{1}{2} K^*(s_k, r_n) f(r_n) = \frac{n-1}{\pi} p(s_k) , \quad (k = 1, ..., n-1), \qquad (3.95)$$

and

$$\frac{1}{2} f(r_1) + \sum_{i=2}^{n-1} f(r_i) + \frac{1}{2} f(r_n) = 0 , \qquad (3.96)$$

where

$$K^*(s, r) = \frac{1}{r - s} + k(r, s),$$

$$r_i = \cos\left(\frac{i - 1}{n - 1}\pi\right), \qquad i = 1, \ldots, n$$

$$s_k = \cos\left(\frac{2k - 1}{2n - 1}\pi\right), \quad k = 1, \ldots, n-1. \qquad (3.97\ a - c)$$

From (3.95) and (3.96) n unknowns $f(r_i)$, $i = 1, \ldots n$ can be solved.

3.5.2 Edge Crack

For the case of an edge crack the singular integral equation (3.92) will be the same but the single - valuedness condition (3.93) for the displacement will not be valid anymore. The unknown function F(r) will have a 1/2 power singularity at one end and no singularity at the other.

Considering an edge crack a = 0, F(r) will be singular only for r = 1. Therefore in (3.94) $(1 + r)^{1/2}$ is included with the extra condition that

$$f(-1) = f(r_n) = 0. \qquad (3.98)$$

Given this condition the number of unknown is reduced to n - 1 and using equations (3.95), $f(r_i)$, (i = 1, ..., n - 1) can be easily solved.

3.5.3 Crack Terminating at the Interface

For the case in which a > 0, b = h_1, the singularity at the end points are α = 1/2 and β, where β is obtained from equation (3.88). Therefor the solution will be sought in the form

$$F(r) = \frac{f(r)}{(1+r)^{1/2}(1-r)^{\beta}} . \qquad (3.99)$$

Again, the single - valuedness condition will be

$$\int_{-1}^{1} F(r)\, dr = 0 . \qquad (3.100)$$

Following [33], we obtain:

$$\sum_{i=1}^{n} K^*(s_k, r_i)\, W(r_i)\, f(r_i) = p(s_k), \qquad k = 1,\ldots, n-1 , \qquad (3.101)$$

and

$$\sum_{i=1}^{n} W(r_i)\, f(r_i) = 0 , \qquad (3.102)$$

where

$$P_n^{(-1/2,\ -\beta)}(r_i) = 0, \qquad i = 1,\ldots, n ,$$

$$P_{n-1}^{(1/2,\ 1-\beta)}(s_k) = 0, \qquad k = 1,\ldots, n-1 , \qquad (3.103\ a, b)$$

and $W(r)$ is the weight of the Jacobi polynomials

$$P_n^{(-1/2,\ -\beta)}(r) .$$

Solving the n × n system of linear equations, the n unknowns f (r_i), (i = 1, ... , n), can be obtained.

3.5.4 The Stress Intensity Factors

In this problem we are mostly interested in the computation of the stress intensity factors which may be expressed in terms of the density function F (r).

For the embedded crack where $0 < a < b < h_1$ the stress intensity factors are defined as follows:

$$K(a) = \lim_{y \to a} \sqrt{2(a-y)}\, \sigma_x(0,y) \quad ,$$

$$K(b) = \lim_{y \to b} \sqrt{2(y-b)}\, \sigma_x(0,y) \quad . \qquad (3.104\ a, b)$$

Using the above definition and as described in [34] we obtain:

$$K(a) = 2\, B_{11}\, b_{11} \lim_{y_1 \to a} \sqrt{2(a-y)}\, \sigma_x(0,y)$$

$$= 2\, B_{11}\, b_{11}\, f(-1)\, \sqrt{(b-a)/2} \quad ,$$

$$K(b) = -\,2\, B_{11}\, b_{11} \lim_{y_1 \to b} \sqrt{2(b-y)}\, \sigma_x(0,y)$$

$$= -\,2\, B_{11}\, b_{11}\, f(1)\, \sqrt{(b-a)/2} \quad ,$$

(3.105 a, b)

where

$$B_{11}\, b_{11} = \frac{2\mu}{1+k} \, ,$$

when the material is isotropic.

For the case of an edge crack (a = 0) the stress intensity factor becomes

$$k(b) = -2 B_{11} b_{11} f(1) \sqrt{b} \quad . \qquad (3.106)$$

For a crack terminating at the interface, the stress intensity factor at $b = h_1$ can be obtained from simplified symmetric crack problem (see Figure 3.2), described in subsection 3.4.3, when $a = h_1$, we have

$$\frac{1}{b_{11}^*}\sigma_{xx}^* = \frac{2}{\pi}\int_0^\infty [\lambda_1^* K_2(\alpha)\cosh(\omega_1^*\alpha y_2) + \lambda_2^* K_4^*(\alpha)\cosh(\omega_3^*\alpha y_2)]\,\alpha\cos\alpha x\, d\alpha \ ,$$

$$\lim_{x\to 0}\frac{1}{b_{11}^*}\sigma_{xx}^* = \frac{2}{\pi}\int_0^\infty [\lambda_1^* K_2(\alpha)\cosh(\omega_1^*\alpha y_2) + \lambda_2^* K_4^*(\alpha)\cosh(\omega_3^*\alpha y_2)]\,\alpha\, d\alpha$$

$$= \int_{-h_1}^{h_1} k_s^*(y_2, t)\,\phi_1(t)\,dt \ , \qquad (3.107)$$

where, the quantities with * represent the corresponding quantities in the second layer and k_s^* is as follows (see [27] for details)

$$k_s^* = k_{s1}^* + k_{s2}^* + k_{s3}^* + k_{s4}^*$$

$$= P_{11}^* \frac{\omega_1^* h_1 + (h_1 - t)/\beta_{11}}{(\omega_1^* h_1 + (h_1 - t)/\beta_{11})^2 - (\omega_1^* y_2)^2} + P_{12}^* \frac{\omega_1^* h_1 + (h_1 - t)/\beta_{12}}{(\omega_1^* h_1 + (h_1 - t)/\beta_{12})^2 - (\omega_1^* y_2)^2}$$

$$+ P_{13}^* \frac{\omega_3^* h_1 + (h_1 - t)/\beta_{11}}{(\omega_3^* h_1 + (h_1 - t)/\beta_{11})^2 - (\omega_3^* y_2)^2} + P_{14}^* \frac{\omega_3^* h_1 + (h_1 - t)/\beta_{12}}{(\omega_3^* h_1 + (h_1 - t)/\beta_{12})^2 - (\omega_3^* y_2)^2} \ .$$

(3.108)

Defining

$$k(h_1) = \lim_{y \to -h_2} 2^{\beta} (y_2 + h_2)^{\beta} \sigma_x^*(0,y) , \qquad (3.109\ a)$$

and following a procedure similar to that used in obtaining (3.86), the stress intensity factor at the crack tip h_1 is found to be

$$k(h_1) = B_{11}^* b_{11}^* \frac{f(1)}{h_1^{\beta}} \frac{1}{\sin \pi \beta}$$

$$\times \{ \beta_{11} P_{11}^* \frac{1}{(\beta_{11} \omega_1^*)^{\beta}} + \beta_{12} P_{12}^* \frac{1}{(\beta_{12} \omega_1^*)^{\beta}}$$

$$+ \beta_{11} P_{13}^* \frac{1}{(\beta_{11} \omega_3^*)^{\beta}} + \beta_{12} P_{14}^* \frac{1}{(\beta_{12} \omega_3^*)^{\beta}} \} .$$

(3.109 b)

3.6 RESULTS AND DISCUSSION

The problem is solved numerically for three particular crack configurations which are, referring to Figure 3.1, the embedded crack ($0<a<b<h_1$), the edge crack ($a=0$, $b<h_1$) and the crack terminating at the interface ($a=0$, $b=h_1$). The results refering to the stress intensity factors are shown in Figures 3.3-3.7 and Table 3.3. Generally the results presented in these figures and the table are self-explanatory.

The results given in this study are obtained for self equilibrating crack surface tractions. If the external loads are applied to the layered material at locations sufficiently far from the region of cracks, the crack surface tractions in the perturbation problem would be uniform. For example, if the medium is loaded in tension parallel to the x - axis away from the crack region the crack surface tractions are constant and are related by

$$\frac{1 - \nu_{xz1}\,\nu_{zx1}}{E_{x1}}\,p_1 = \frac{1 - \nu_{xz2}\,\nu_{zx2}}{E_{x2}}\,p_2\,, \qquad (3.110)$$

for plane strain and

$$\frac{p_1}{E_{x1}} = \frac{p_2}{E_{x2}}\,, \qquad (3.111)$$

for plane stress. Here the subscripts 1 stands for the properties in material I and 2 for material II. In this study only plane strain case is considered.

To investigate the effect of orthotropic material properties on stress intensity factor in the cracked plane, we first rewrite the singular integral equation (3.90) in the following form:

$$\frac{1}{\pi}\int_a^b \left[\frac{1}{t-y} + k(y,t) \right] \phi_1(t)\, dt = -\frac{1}{\mu_1^*}\, p(y), \qquad a < y < b, \tag{3.112}$$

here $\mu_1^* = 2\, B_{11}\, b_{11}$, $\quad \phi_1(y) = \frac{\partial u_1}{\partial y}(0, y)$,

and p(y) is the self equilibrating crack surface traction in material I, and the subscript 1 again refers to the material I.

The physical meaning of μ^* in this general form of a crack problem is revealed in the following relationship (see [36])

$$G = \frac{1}{2\,\mu^*}\,\pi\, k_1^2, \tag{3.113}$$

here G is the energy release rate, and k_1 is the stress intensity factor for mode I crack.

For isotropic material μ^* is given as:

$$\mu^* = \frac{4\,\mu}{1+\kappa}, \quad \text{where} \quad \kappa = 3 - 4\nu \text{ for plane strain,}$$
$$\text{and } \kappa = \frac{3-\nu}{1+\nu} \text{ for plane strain,}$$
$$\mu^* = \frac{E}{2}, \quad \text{for plane stress,}$$
$$\mu^* = \frac{E}{2(1-\nu^2)}, \quad \text{for plane strain,} \tag{3.114 a}$$

and for orthotropic materials

$$\mu^* = 2\, B_{11} b_{11}, \tag{3.114 b}$$

where b_{11} is defined in (3.2) and B_{11} in Appendix II. It can be seen that μ^* is

somehow a measurement of material orthotropy in the crack problem. Greater μ^* stands for "stiffer" material.

Table 3.1 shows the different elastic constants used throughout the analysis. Materials 1 and 2 are orthotropic which are fiber- reinforced composite laminates. Note that material 2 is the same as material 1, except that the axes are rotated 90^0 about the z axis. Materials 3, 4 and 5 are isotropic. Generally speaking, material 3 is steel, 4 is zirconia and 5 is Alumina, both 4 and 5 are ceramics. Table 3.2 shows the material pairs A to I for which extensive numerical results are given. Choosing the same materials and letting a, b, h_1 or h_2 go to proper limits we recover all the special cases considered in [23], [30] and [34].

Figure 3.3 shows the stress intensity factors in two-orthotropic bonded layers with an embedded crack of half length $l = \frac{b - a}{2} = \frac{h_1}{4}$. Note that as the crack tip b approaches the interface (i. e., as $c/l \rightarrow 3$) k_b tends to zero for $\mu_2^* > \mu_1^*$ and to infinity for $\mu_2^* < \mu_1^*$. This well - known behavior is due to the fact that for $b = h_1$ the power of the stress singularity β is less than 0.5 for $\mu_2^* > \mu_1^*$ and greater than 0.5 if $\mu_2^* < \mu_1^*$. For these cases, the definition of the stress intensity factors are given by equation (3.104). For the material combinations used in this figure $\beta = 0.520$ for pair A and $\beta = 0.481$ for pair B. Also note that as the crack tip approaches the free boundary as expected K_a tends to infinity.

Stress intensity factors for an edge crack in two-orthotropic layers and two-isotropic layers are shown in Figures 3.4 and 3.5. In these cases too note that as the crack tip b approaches the interface k_b tends to zero for $\mu_2^* > \mu_1^*$ and to infinity for $\mu_2^* < \mu_1^*$. Also note that as the crack length decreases the stress intensity factor approaches 1.1215 for isotropic material in Figure 3.5 and 1.101 for orthotropic material in Figure 3.4 which are the value obtained for the semi-infinite plane having an edge crack of length b. Figure 3.6 shows the effect of thickness ratio on the stress intensity factor in two- orthotopic layers with a pressurized edge crack. The results for the crack terminating at the interface are shown in figure 3.6 (the curve corresponding to $\frac{b}{h_1} = 1$). In all these figures the Stress Intensity Factors are obtained from (3.106) for edge crack and (3.109) for crack terminating at the interface.

Figure 3.7 shows the Stress Intensity factor in two-orthotropic layers

containing an edge crack and subjected to uniform bending away from the crack region. In the uncracked two-layer plate the relevant stress is given by

$$\sigma_{x1}(y_1) = -p_1(y_1) = -p_b(1 - y_1/c_1), \qquad 0 < y_1 < h_1,$$

$$c_1 = \frac{E_{x1}^* h_1^2 + 2E_{x2}^* h_1 h_2 + E_{x2} h_2^2}{2(E_{x1} h_1 + E_{x2} h_2)}, \qquad (3.115\ a, b)$$

$$E_x^* = E_x, \qquad \text{for plane stress}$$

$$= \frac{E_x}{1 - \nu_{xz}\nu_{zx}}, \qquad \text{for plane strain}$$

where $y_1 = c_1$ determines the location of the neutral axis and the constant p_b is the magnitude of the stress at the plate surface which is related to the bending moment M by

$$p_b = \frac{3c_1 M}{c_1^3 + (E_{x2}^*/E_{x1}^* - 1)(c_1 - h_1)^3 + E_{x2}^*/E_{x1}^*(h_1 + h_2 - c_1)^3}. \qquad (3.116)$$

Table 3.3 shows the Stress Intensity Factors for an edge crack under constant pressure and bending conditions for material pair I, that is, for a homogeneous isotropic strip. These results are given here for the purpose of comparison. Tables 3.4-3.7 show the effects of material combinations and properties on the power of stress singularity β which is obtained from equation (3.88) for a crack terminating at the interface. All the results are obtained for plane strain case. Results in Tables 3.4 and 3.5 are given for fixed elastic properties in material I and varying elastic properties in material II. These results are for both isotropic and orthotropic material pairs. To

give some idea about how the material constants in material II effect β for a full range of μ_2^* hypothetical material constants are used. Here μ^* are calculated from (3.114). From these tables note that as the second material becomes "stiffer", i.e. as $\mu_2^*/\ \mu_1^*$ increases, the value β decreases in a certain range of $\mu_2^*/\ \mu_1^*$. Beyond that range, the ratio $\mu_2^*/\ \mu_1^*$ has almost no effect on β. It is also important to note that the value β is heavily dependent on the material parameters in the first layer due to the fact that the crack is in the first layer. For the orthotropic material pairs results in Tables 3.4 and 3.5 correspond to three different orthotropic material pairs with μ_1^* values of 1.35, 12.078 and 61.6 (GPA). It is clearly seen that when the "stiffeness" in the first layer decreases, β becomes smaller.

The effect of individual material constants in the second layer on the power of stress singularity β are examined in Tables 3.6 and 3.7. The results are only done for partial variations of the variable c because materials with the other half variations are material of type II. In Tables 3.6 and 3.7 material I is fixed as an isotropic material and material II is the same as material I except one material constant is changed which is E_y in Table 3.6a and G_{xy} in Table 3.6b. We can see that E_y in the second layer almost have no effect on β because the crack located in the *y-z* plane. In contrast to this G_{xy} in second layer has much large effect on β. Similar effects are studied for the fixed orthotropic materials I. The results are shown in Tables 3.7. As expected $E_{x2}/\ E_{x1}$ has the most significant effect on β. The effect of G_{xy2}/G_{xy1} on β is similar to the isotropic cracked layer.

Finally it should be pointed out that the accuracy of the numerical results for Stress Intensity Factors is not uniform. For Stress Intensity Factors at an imbedded crack the convergence was relatively fast. However, in the calculation of the Stress Intensity Factors for an edge crack, particularly for $\mu_1^* > \mu_2^*$, there were convergence difficulties for $b \rightarrow h_1$ and $b = h_1$.

3.7 RECOMMENDATIONS

In the present work, a general formulation of the fracture problem of layered orthotropic strips with a crack perpendicular to the interface is given. The formulations done only for the case where both materials are of type I. This would have a limitation on the choice of the materials. Following the same procedure, the problem can also be studied for orthotropic materials of type II, or for the combination of type I and type II.

In this study the crack is limited in the first layer only. A further study could be done for the case when the crack crosses the interface, when there is a T shaped crack with the crack going along the interface and when there are cracks in both layers.

In our formulation the thickness of the adhesive bonding the layers has been neglected. The study of the adhesive also can be recommended. Also, the bonded materials with more than two-layers could more realistic for the study of the composite materials, but it requires lengthy algebra.

There are many other problems to be studied in the fracture of bonded materials. We hope that our work will have its contributions in the study of these problems.

Chapter 4. Surface Cracks in a Two-layer Orthotropic Plate

4.1 INTRODUCTION

The surface or part-through crack problem in a structural component which may locally be represented by a "plate" or a "shell" is certainly one of the most important problems in Fracture Mechanics. It is a truly three-dimensional problem in which the stress field perturbed by the crack interacts very strongly with the surfaces of the solid. Because of its complexity generally the problem seems to lend itself only to numerical techniques. At the present, a neat analytical treatment of surface crack problem, even for the linear elastic isotropic solids, appears to be intractable. Consequently, the available solutions of the problem very heavily rely on some kind of numerical technique such as the finite element method [37, 38], the alternating method [39, 40], the boundary integral method [41], the finite element alternating method [42], the method of weight functions [43], and the body force method [44]. For reviews of various methods and solutions see [45, 46]. Also see [21] for the extension of various methods to the shell problem.

The line-spring model, proposed by Rice and Levy [47, 48] and incorporated in a plate theory that allows for transverse shear deformation [2, 3], competes with these methods because of its simplicity and relatively high accuracy. Basically this model transforms the part-through crack problem into a through crack problem by making use of the corresponding plane strain edge crack solution. Figures 4.2-4.5 show the comparisons of Line-Spring model with the finite element method and the effect of transverse shear in a homogeneous plate containing a surface crack and subjected to membrane and bending loads. It may be seen that this model indeed gives very good results.

Because Line-Spring model allows for the solution of the three-dimensional surface crack problem within the two-dimensional plate theory, it reduces the computational effort considerably. Once the verification of this model has been established more extensive parameter studies can be made. Due to the lack of other solutions for the non-homogeneous plate, this verification is done only for the homogeneous plate [21, 49]. Also it is important to point out that for surface cracks

the most important point is the deepest penetration point of the crack front which lie in the center of the more accurate and applicable area of this model. In this study most of the results are given for quantities at the deepest penetration point. We refer to [21] for the behavior of the surface crack around the end points.

In this study the surface crack problems (Figure 4.1) are solved for a two-layer orthotropic plate under uniform tension and bending moment with the surface crack penetrating only through one of the two layers. This restriction is due to the fact that the corresponding two-layer edge-notched orthotropic plane strain results are available only for this geometry and that the line spring model for cracks intersecting the bimaterial interfaces has not yet been formulated. The solution of the plane strain problem needed in this study is given in Chapter 3 where extensive numerical results are provided for various material combinations. Among these material combinations considered the following are of considerable practical interest: (a) fiber reinforced laminated composite materials; (b) ceramic and metal bonded structural components, and (c) the films on elastic substrates used in the microelectronic devices. The results given for all these material combinations are for various geometrical parameters of plates and cracks. Also the effects of material orthotropy on the stress intensity factors are examined.

4.2 THE LINE-SPRING MODEL

4.2.1 The Description of Line - Spring Model

The Line - Spring model was first proposed by Rice and Levy [47] in 1972 and since then many improvements and modifications have been made. We refer to [21] for a literature survey and for various modifications of the model.

Briefly, the model allows one to use a plate theory to formulate the problem by removing the "net ligament", and replacing it by unknown, thickness averaged stress resultants which may then be treated as crack surface loads in a through crack problem. Figure 4.6 illustrates this process for Mode I crack problem. This technique reduces by one dimension the complexity of the analysis. Moreover, it allows both through and part-through crack problems to be solved with the same plate theory formulation.

Recall that in Chapter 2, the two-dimensional formulation of through crack problem in a plate is solved as a mixed boundary value problem with the mixed boundary conditions as follows:

$$N_x(0, y) = -N_x^{\infty}, \qquad |y| < a,$$

$$u_0(0, y) = 0, \qquad |y| > a,$$

and

$$M_x(0, y) = -M_x^{\infty}, \qquad |y| < a,$$

$$\phi_x(0, y) = 0, \qquad |y| > a, \tag{4.1}$$

where the general principle of superposition is used to account for the loading N_x^{∞} and M_x^{∞} applied to the structure at "infinity" or away from the crack region.

In the case of part-through crack problem the net ligament is replaced by appropriate resultants N and M (Figure 4.6) and therefore, the corresponding mixed boundary value problem must be solved under the conditions:

$$N_x (0, y) = - N_x^{\infty} + N , \qquad | y | < a,$$

$$u_0 (0, y) = 0 , \qquad | y | > a,$$

and

$$M_x (0, y) = - M_x^{\infty} + M , \qquad | y | < a,$$

$$\phi_x (0, y) = 0 , \qquad | y | > a.$$

(4.2)

Thus referring to (2.33) for the corresponding through crack formulation, the governing equations for the two-layer plate with a surface crack may be expressed as:

$$\frac{\mu_{11}}{\pi} \int_{-a}^{a} [\frac{1}{t - y} + k_{11} (y, t)] g_1(t) dt + \frac{\mu_{12}}{\pi} \int_{-a}^{a} [\frac{1}{t - y} + k_{12} (y, t)] g_2(t) dt = - N_x^{\infty} + N ,$$

$$\frac{\mu_{12}}{\pi} \int_{-a}^{a} [\frac{1}{t - y} + k_{12} (y, t)] g_1(t) dt + \frac{\mu_{22}}{\pi} \int_{-a}^{a} [\frac{1}{t - y} + k_{22} (y, t)] g_2(t) dt = - M_x^{\infty} + M ,$$

$$| y | < a,$$

(4.3)

where

$$g_1(t) = \frac{\partial u_0 (t)}{\partial t},$$

$$g_2(t) = \frac{\partial \psi_x (t)}{\partial t}.$$

(4.4)

The unknowns in equations (4. 3) are N, M, u_0 and ψ_x, where N and M are net ligament stress resultants illustrated in Figure 4.6, u_0 is the in-plane displacement of the x direction in nuetral plane and ψ_x is the rotation of the section x=constant. Since there are four unknowns and only two equations more information is needed. In the line-spring model, N and M are linearly related to u_0 and ψ_x in the manner of a spring. After substitution of these relationships into equation (4.3), g_1 or g_2 (or u_x or ψ_x) can be numerically determined from which all quantities of interest can be calculated.

4.2.2 The Compliance Functions

The Line-Spring model is based on two assumptions. The first, previously stated and illustrated in Figure 4.6, involves replacing the net ligament (in which the state of stress is two-dimensional) by resultant forces which are functions of y only. The second assumption is that the stress intensity factors along the crack front may be obtained from these resultant forces as though the stress state were one of plane strain. Clearly, very near the end points the assumption would not be valid. Therefore, this model is most accurate in the center of the crack and improves as the crack gets longer for a given crack depth, i.e. as plane strain conditions are approached.

In order to make use of this analogy, the plane strain stress intensity factor solutions for the corresponding two-layer edge-notched strip must be available. Such solutions used in this study are obtained from the results of Chapter 3 and along with a curve fit in the form of:

$$g_t(\xi) = \frac{k_I}{\sigma_t \sqrt{h}} = \sqrt{\pi \xi} \sum_{k=0}^{n} c_{tk} \xi^k,$$

$$g_b(\xi) = \frac{k_I}{\sigma_b \sqrt{h}} = \sqrt{\pi \xi} \sum_{k=0}^{n} c_{bk} \xi^k,$$

$$0 \leq \xi \leq 0.9, \qquad (4.5)$$

where

$\xi = L(y)/h$, (Figure 4.6).

In the literature, g_b and g_t are often referred as shape functions which can be obtained once the edge cracked plane-strain results are given. Then, the stress intensity factor for the strip can be expressed as

$$K_I = \sqrt{h}\ (\sigma_t\, g_t + \sigma_b\, g_b). \qquad (4.6)$$

In these expressions $\sigma_t(y)$ and $\sigma_b(y)$ represents the averaged net ligament stresses as follows:

$$\sigma_t = \frac{N}{h}, \qquad \text{and} \quad \sigma_b = \frac{M}{h^2/6}. \qquad (4.7)$$

The derivation is based on expressing the energy available for fracture along the crack front in two different ways. First, in a plate with an edge crack subjected to a uniform tension N and bending moment M (Figure 4.7 a), if K is the stress intensity factor given by the plane strain solution, from the crack closure energy, the energy (per unit width) available for fracture may be obtained as [50, 51]

$$G = \frac{\partial}{\partial L}(U - V) = \lambda K_I^2, \qquad (4.8)$$

where

$$\lambda = \frac{1-\nu^2}{E}, \qquad \text{for isotropic materials,}$$

or

$$\lambda = \left(\frac{e_{11}\, e_{33}}{2}\right)^{1/2} \left[\left(\frac{e_{11}}{e_{33}}\right)^{1/2} + \frac{2\, e_{13} + e_{55}}{2\, e_{33}}\right]^{1/2},$$

for orthotropic materials. (4.9)

See Appendix I for expressions of e_{ij}. With the assumption of coplanar crack growth, equation (4.6) are substituted into (4.8) to obtain,

$$G = \frac{\partial}{\partial L} (U - V) = h \lambda (\sigma_t^2 g_t^2 + 2 \sigma_b \sigma_t g_t g_b + \sigma_b^2 g_b^2). \qquad (4.10)$$

Next consider the crack to extend from L to L + ΔL under "fixed load" conditions. The resulting changes in U and V are as follows (Figure 4.7 b):

$$\begin{aligned} dU &= N\, d\delta + M\, d\theta, \\ dV &= \frac{1}{2} [N (\delta + d\delta) + M (\theta + d\theta)] - \frac{1}{2} (N \delta + M \theta) \\ &= \frac{1}{2} (N\, d\delta + M\, d\theta). \end{aligned} \qquad (4.11)$$

Equations (4.11) give the energy available for a crack growth dL as follows:

$$d (U - V) = \frac{1}{2} (N\, d\delta + M\, d\theta). \qquad (4.12)$$

Note that N and M are fixed loads, and for a change of dL in the crack length we have

$$d\delta = \frac{\partial \delta}{\partial L} dL, \qquad d\theta = \frac{\partial \theta}{\partial L} dL. \qquad (4.13)$$

Thus, from (4.12) and (4.13) it follows that

$$G = \frac{\partial}{\partial L} (U - V) = \frac{1}{2} (N \frac{\partial \delta}{\partial L} + M \frac{\partial \theta}{\partial L}), \qquad (4.14)$$

and by using (4.9) we find

$$\frac{1}{2} (N \frac{\partial \delta}{\partial L} + M \frac{\partial \delta}{\partial L}) = h \lambda (\sigma_t^2 g_t^2 + 2 \sigma_b \sigma_t g_t g_b + \sigma_b^2 g_b^2), \qquad (4.15)$$

where g_t and g_b are known functions and expressions of σ_t and σ_b are given in (4.7).

Assuming

$$\tau = \begin{bmatrix} \tau_1 \\ \tau_2 \end{bmatrix} = \begin{bmatrix} \sigma_t \\ \sigma_b \end{bmatrix},$$

$$\omega = \begin{bmatrix} \omega_1 \\ \omega_2 \end{bmatrix} = \begin{bmatrix} \delta \\ \frac{h}{6}\theta \end{bmatrix},$$

and

$$G(\xi) = \begin{bmatrix} g_t^2 & g_t g_b \\ g_t g_b & g_b^2 \end{bmatrix}, \qquad (4.16)$$

equation (4.15) may be written as

$$\frac{h}{2}\, \tau^{\top}\, \frac{\partial \omega}{\partial L} = h\, \lambda\, \tau^{\top}\, G\, \tau. \qquad (4.17)$$

From (4.17) it is seen that

$$\frac{\partial \omega}{\partial L} = 2\, \lambda\, G\, \tau. \qquad (4.18)$$

By observing that G is a function of L, τ is independent of L and $\omega = 0$, for $L = 0$, from (4.18) we find :

$$\omega = 2\, \lambda\, h\, \left(\frac{1}{h} \int_0^L G\, dL \right) \tau = 2\, h\, \lambda [\, A\,]\, \tau, \qquad (4.19)$$

where

$$[\,A\,] = \frac{1}{h}\int_0^L G\,dL = [\,a_{ij}\,],$$

$$a_{11} = \frac{1}{h}\int_0^L g_t^{\,2}\,dL\,, \qquad a_{12} = a_{21} = \frac{1}{h}\int_0^L g_t\,g_b\,dL\,,$$

$$a_{22} = \frac{1}{h}\int_0^L g_b^{\,2}\,dL\,. \qquad (4.20)$$

From (4.19) and (4.20) one may write

$$\tau = \begin{bmatrix} \sigma_t \\ \sigma_b \end{bmatrix} = \frac{1}{2\,h\,\lambda}\,\Gamma \begin{bmatrix} \delta \\ \frac{h}{6}\theta \end{bmatrix}$$

where

$$\Gamma = [\,\gamma_{ij}\,] = [\,A\,]^{-1}. \qquad (4.21)$$

Thus, the relationship between (N, M) and (δ, θ) may be expressed as follows:

$$\begin{bmatrix} N \\ M \end{bmatrix} = \begin{bmatrix} \sigma_t \\ \frac{h^2}{6}\sigma_b \end{bmatrix} = \frac{1}{2\,h\,\lambda}\,C \begin{bmatrix} \delta \\ \theta \end{bmatrix}$$

where

$$C = [\,c_{ij}\,],$$

and

$$c_{11} = \gamma_{11}, \qquad c_{12} = c_{21} = \frac{h}{6}\,\gamma_{12},$$

$$c_{22} = \frac{h^2}{36}\,\gamma_{22}.$$

(4.22)

From definition (4.4) and observing that (Figure 4.7)

$$\delta = 2\,u_0\,(0, y),$$

$$\theta = 2\,\psi_x\,(0, y),$$

(4.23)

we obtain

$$\begin{bmatrix} N \\ M \end{bmatrix} = \frac{1}{\lambda} \begin{bmatrix} c_{11} & c_{12} \\ c_{12} & c_{22} \end{bmatrix} \begin{bmatrix} g_{c1} \\ g_{c2} \end{bmatrix},$$

$$g_{c1} = \int_{-a}^{y} g_1(t)\,dt\,,$$

$$g_{c2} = \int_{-a}^{y} g_2(t)\,dt\,.$$

(4.24)

Equation (4.24) gives the information that is needed for substitution into integral equations (4.3). From this the surface crack problem may be solved numerically in a manner similar to the case of the through crack problem.

4.3 SINGULAR INTEGRAL EQUATIONS

4.3.1 The Singular Integral Equations

As mentioned in subsection (4.2), the singular integral equations for part-through crack problems may obtained directly from the corresponding through crack equations combined with the compliance function (4.24). From (4.3) and (4.24), they may be expressed as follows:

$$\frac{\mu_{11}}{\pi}\int_{-a}^{a}\left[\frac{1}{t-y}+k_{11}(y,t)\right]g_1(t)\,dt+\frac{\mu_{12}}{\pi}\int_{-a}^{a}\left[\frac{1}{t-y}+k_{12}(y,t)\right]g_2(t)\,dt-\frac{c_{11}}{\lambda}\int_{-a}^{y}g_1(t)\,dt-\frac{c_{12}}{\lambda}\int_{-a}^{y}g_2(t)\,dt=-N_x^{\infty},$$

$$\frac{\mu_{12}}{\pi}\int_{-a}^{a}\left[\frac{1}{t-y}+k_{12}(y,t)\right]g_1(t)\,dt+\frac{\mu_{22}}{\pi}\int_{-a}^{a}\left[\frac{1}{t-y}+k_{22}(y,t)\right]g_2(t)\,dt-\frac{c_{21}}{\lambda}\int_{-a}^{y}g_1(t)\,dt-\frac{c_{22}}{\lambda}\int_{-a}^{y}g_2(t)\,dt=-M_x^{\infty},$$

$$|y|<a. \qquad (4.25)$$

We refer to (2.33) and (2.34) for the expressions of μ_{ij} and k_{ij}, λ can be obtained from (4.8), and $g_1(t)$ and $g_2(t)$ are the unknown functions defined in (4.4).

Also these singular integral equations must be solved under the following single-valuedness conditions:

$$\int_{-a}^{a} g_1(t)\,dt = 0, \qquad \text{and} \qquad \int_{-a}^{a} g_2(t)\,dt = 0. \tag{4.26}$$

Since the dominant part of the system of integral equations (4.25) has only a Cauchy kernel (which is the same as in the through crack case), the solution is of the following form:

$$g_i(t) = \frac{f_i(t)}{\sqrt{a^2 - t^2}}, \qquad (i = 1, 2), \tag{4.27}$$

where the function f_1 and f_2 are bounded in the closed interval $|t| < a$.

Following similar numerical procedures as in the through crack case, described in subsection (2.3.1) of Chapter 2, by first normalizing the equations from $-a < y < a$ to $-1 < s < 1$, and then using the collocation method, the unknown functions $g_1(y)$ and $g_2(y)$ or $f_1(y)$ and $f_2(y)$ may easily be determined numerically.

4.3.2 The Stress Intensity Factors

After solving the singular integral equations (4.25) under the single-valuedness conditions (4.26), the unknown functions $g_1(y)$ and $g_2(y)$ can be obtained. Then, using the expressions (4.24), the stress intensity factor $K(y)$ along the crack front may be determined as follows:

$$K_I = \sqrt{h}\,(\sigma_t\, g_t + \sigma_b\, g_b), \tag{4.28}$$

where $\sigma_t = \frac{N}{h}$, and $\sigma_b = \frac{M}{h^2/6}$, which are equivalent net-ligament stresses and g_t and g_b are known functions obtained from the corresponding edge-notched plane strain results.

Notice that while the solution of a through crack gives the stress intensity factor at $y = \pm a$, the line-spring model provides stress intensity factors along the front of a surface crack, that is $-a < y < a$.

Since the model is most accurate in the central portion of the crack, it is best applied to problems where failure occurs when the surface crack grows through the thickness leading either to leaking or to the development of a through crack which then grows in length to a critical size. Because of the plane strain assumption, the model becomes less applicable near the ends of the crack. Because of this the results given in these study are mostly at the maximum penetration point and for $a/h \geq 0.5$.

4.4 RESULTS AND DISCUSSION

The main interest of the study in this chapter is in evaluating the stress intensity factors in a two-layer isotropic and orthotropic plates with a surface crack. The similar problems for homogeneous one-layer isotropic and orthotropic plates have been considered before in [21], [49], [22] and elsewhere. Some of those results are shown here for the purpose of comparison.

The elastic constants of the material combinations used in the numerical examples are given in Tables 4.1 and 4.2. The material combinations considered here are of important practical interest: Material Pair A and B are fiber reinforced laminated (graphite-epoxy) composites, which have long been widely used in aerospace industry; Material Pairs C, D and E are ceramic and steel bonded structural components, which have recently been receiving increasing attention in a number of applications of metal/ceramics joints [52, 53]. Material Pair I represents an isotropic homogeneous plate which is included here for the purpose of comparison. Extensive numerical results are given for all these material combinations with various geometrical configurations.

As in previous studies, the stress intensity factors are given in their normalized form. For the Line-Spring model, the stress intensity factors are normalized in two different ways. First, they are normalized with respect to the corresponding plane strain values (corresponding to the limiting values when $a/h \to \infty$), namely

$$\frac{k_t(0)}{k_t^{\infty}}, \qquad \text{and} \qquad \frac{k_b(0)}{k_b^{\infty}},$$

where k_t^{∞} and k_b^{∞} are the corresponding values for an edge-cracked strip under plane strain conditions with the same L_0/h ratio (Figure 4.1). These normalizations show how the constraining effect of the ends affect the crack driving force. For the same a/h value, when

the value L_0/h increases $\frac{k_i(0)}{k_i^{\infty}}$ (i = t, b) may decrease, this is because k_i^{∞} (i = t, b) are relatively more rapidly increasing functions of L_0/h. To give some idea about the absolute values of the stress intensity factors, part of the results are given for a fixed normalizing stress intensity factor, i.e.,

$$\frac{k_t(0)}{\sigma_t^{\infty}\sqrt{h_1}}, \qquad \text{and} \qquad \frac{k_b(0)}{\sigma_b^{\infty}\sqrt{h_1}},$$

where

$$\sigma_t^{\infty} = \frac{N^{\infty}}{h}, \qquad \sigma_b^{\infty} = \frac{6M^{\infty}}{h^2},$$

and h_1 is the thickness of the first layer of the plate.

In this form it is expected that for a given a/h when L_0/h increases (i.e., the surface crack gets deeper) the normalized stress intensity factor $\frac{k_i(0)}{\sigma_i^{\infty}\sqrt{h_1}}$ (i = i, b) would also increase.

In both normalization forms, the stress intensity factor $k_t(0)$ and $k_b(0)$ are the values calculated at the maximum penetration point of the crack under the membrane and bending loads respectively. Here it should be observed that, as in the through crack case, when we say the plate is under the bending load we always assume that the plate is under membrane load of sufficiently high magnitude as well, so that there is no interference of the crack surfaces on the compressive side of the plate. In the case of a part-through crack, as can be seen from the results later, under bending the stress intensity factors change sign as the crack gets deeper. Since a negative stress intensity factor has no meaning, these solutions, similar to the through crack case, require a superposition of a tensile solution to make $k_i > 0$, (i = t,b).

As noted before, for the application of the line-spring model, the contour of the part-through crack can be any reasonable curve. Elliptic cracks are mainly studied here since it is believed that the ellipse is the closest contour for the actual shape of the crack which may be encountered in practical application. One could refer to [21] for results of some different contours and their effects on the convergence of the results. Here for elliptical contour, the crack depth for any cross section is defined by (Figure 4.1)

$$L(y) = L_0\sqrt{1-(y/a)^2}, \qquad |y| < a, \tag{4.29}$$

where L_0 is the crack depth at the midsection (y = 0).

Tables 4.3 - 4.8 show the stress intensity factors in the two - layer strip containing an edge crack under membrane loading N and bending moment M for the material pairs given in Table 4.2. These are the actual values for k_t^{∞} and k_b^{∞} (see the first normalization form) and are calculated from the results of Chapter 3. Based on these plane strain results the coefficients c_{bk} and c_{tk} in the shape function $g_t(\xi)$ and $g_b(\xi)$ of the corresponding material pairs are given in Tables 4.9 - 4.14. To make a better curve fit in all material pairs considered $g_b(\xi)$ has the form of

$$g_b(\xi) = \sqrt{\pi \xi} \sum_{k=1}^{n} c_{bk} \xi^{(k-1)}, \qquad (4.30)$$

while

$$g_t(\xi) = \sqrt{\pi \xi} \sum_{k=1}^{n} c_{tk} \xi^{2(k-1)}, \qquad (4.31a)$$

for $h_2/h_1 = 1., 0.2,$ and

$$g_t(\xi) = \sqrt{\pi \xi} \sum_{k=1}^{n} c_{tk} \xi^{(k-1)}, \qquad (4.31b)$$

for $h_2/h_1 = 10., 5.$

The extensive numerical surface crack results are given in Figures 4.8 - 4.17 and Tables 4.15 - 4.42, which are very much self -- explanatory. Before giving further results about two - layer orthotropic plates, the surface crack results for a homogeneous isotropic plate (Material Pair I) are shown first in Figures 4.8 - 4.11, which correspond to the two normalization forms under bending and tension respectively. The trends discussed before for these two stress intensity factor normalization forms can be clearly observed in these figures. Figures 4.12 - 4.16 are the results for Material Pair B and Figure 4.17 is the comparison of the Material Pair I (i.e. the homogeneous isotropic plate) and Material Pair B (which consist of fiber reinforce composites). As we can see here the material orthotropy does have a

significant effect on the normalized stress intensity factor, especially when L_0/h_1 increases.

Tables 4.15 - 4.38 show the results for all the material pairs given in Table 4.2, which are given again in both normalization forms. Based on all these results the surface crack behavior could be observed and moreover, combining with proper crack propagation model the subcritical crack growth and fatigue crack growth problem, which are very important practical problems, can be studied. Tables 4.39-4.42 give the results regarding the distribution of the normalized stress intensity factor at the crack front for Material B under bending and tension respectively. Tables 4.39 and 4.40 are results for a semi-elliptic surface crack and Tables 4.41 and 4.42 are for a rectangular surface crack. Here the rectangular surface crack contour for any cross section is defined by (Figure 4.1)

$$L(y) \equiv L_0 \qquad | y | < a, \tag{4.30}$$

where L_0 is the crack depth at the midsection ($y = 0$).

Finally it must be noted that, due to the lack of available surface crack results in the layered orthotropic plate, the comparison with other results is made only with homogeneous material, which has been shown to give very good results (figures 4.2 - 4.5). Because of the relative simplicity and high accuracy of the model more extensive parameter studies for wider range of orthotropic and isotropic material combinations can be done whenever it is needed.

Table 2.1 The Material Elastic Constants. (Unit: GPA)

Materials A, B, C and D: Fiber Reinforced Composites

	A	B	C	D
E_x	39.0	30.6	153.07	40.41
E_y	30.6	39.0	40.41	153.07
E_z	6.4	6.4	22.75	22.75
G_{xy}	19.7	19.7	29.30	29.30
G_{yz}	4.5	4.5	1.55	4.08
G_{xz}	4.5	4.5	4.08	1.55
ν_{xy}	0.447	0.351	1.834	0.484
ν_{yz}	0.275	0.275	0.261	0.195
ν_{xz}	0.275	0.275	0.195	0.261

Table 2.2 The effect of the thickness ratio a/h on the stress intensity factor in a cracked plate under uniform bending.

($\sigma_b = 6\ M_o / h^2$)

$k_I (h/2) / \sigma_b \sqrt{a}$

a/h	Classical	Reissner	Mindlin	Reddy
0.05	1.0000	0.9885	0.9868	
0.1	1.0000	0.9677	0.9632	0.9676
0.25	1.0000	0.8992	0.8895	0.8992
0.5	1.0000	0.8193	0.8087	0.8193
1.	1.0000	0.7475	0.7401	0.7477
2.	1.0000	0.6997	0.6982	0.7008

Table 2.3 The effect of the thickness ratio a/h and the transverse shear correction factor K (see 1.18) on the stress intensity factor in a cracked plate under uniform bending.

$$(\sigma_b = 6\, M_o / h^2)$$

$$k_I (h/2) / \sigma_b \sqrt{a}$$

K	0.0001	5/6	1	10	100
a/h					
0.05	1.000	0.9885	0.9868	0.9338	0.8141
0.1	1.000	0.9677	0.9632	0.8634	0.7449
0.25	1.000	0.8992	0.8895	0.7610	0.6898
0.5	0.9997	0.8193	0.8087	0.7090	0.6684
1.0	0.9990	0.7475	0.7401	0.6793	

Table 3.1 The Material Elastic Constants. (Unit: GPA)

Material 1 and Material 2: Fiber Reinforced Composites

Material 1	Material 2
E_x=39.0	E_x=30.6
E_y=30.6	E_y=39.0
E_z=6.4	E_z=6.4
Gxy=19.7	Gxy=19.7
G_{yz}=4.5	G_{yz}=4.5
G_{xz}=4.5	G_{xz}=4.5
ν_{xy}=0.447	ν_{xy}=0.351
ν_{xz}=0.275	νxz=0.275
ν_{yz}=0.275	ν_{yz}=0.275

Material 3: Steel

E=200., ν=0.26

Material 4: Zirconia

E=137.9, ν=0.26

Material 5: Alumina

E=325., ν=0.3

Table 3.2 The Material Pairs. (Figure 3.1)

	Materials	
Material Pair	Layer I	Layer II
A	2	1
B	1	2
C	5	3
D	4	3
E	3	4
I	3	3

Table 3.3 Stress Intensity Factor in a strip containing an edge crack under membrane loading N and bending moment M. (Material Pair I)

($\sigma_t = N/h$, $\sigma_b = 6M/h^2$)

$\frac{L}{(h/2.)}$	$\frac{k_t}{\sigma_t \sqrt{L}}$	$\frac{k_b}{\sigma_b \sqrt{L}}$
0.001	1.1215	1.1215
0.1	1.1399	1.0708
0.2	1.1892	1.0472
0.3	1.2652	1.0432
0.4	1.3673	1.0553
0.5	1.4975	1.0826
0.6	1.6599	1.1241
0.7	1.8612	1.1826
0.8	2.1114	1.2606
0.9	2.4253	1.3630

Table 3.4 Power of singularity, β, for a crack terminating at the interface. (I)
(Fig. 3.1, Eq. 3.88)

isotropic $\nu_1 = \nu_2 = 0.3$		orthotropic $\mu_1^* = 12.078$	
$\frac{\mu_2^*}{\mu_1^*}$	β	$\frac{\mu_2^*}{\mu_1^*}$	β
0.001	0.963	0.045	0.835
0.01	0.915	0.119	0.755
0.045	0.826	0.375	0.650
0.1	0.246	0.659	0.564
0.98	0.502	0.871	0.520
1.0	0.50	1.0	0.50
1.02	0.498	3.642	0.346
10.0	0.333	5.10	0.313
22.22	0.301	13.66	0.242
44.44	0.30	91.06	0.193
100.0	0.294	273.2	0.186
1000.	0.290	546.6	0.184

Table 3.5 Power of singularity, β, for a crack terminating at the interface.(II)
(Fig. 3.1, Eq. 3.88)

orthotropic $\mu_1^* = 1.35$		orthotropic $\mu_1^* = 61.6$	
$\frac{\mu_2^*}{\mu_1^*}$	β	$\frac{\mu_2^*}{\mu_1^*}$	β
$0.41*10^{-5}$	0.998	$0.446*10^{-5}$	0.998
$0.41*10^{-4}$	0.995	$0.446*10^{-4}$	0.995
$0.41*10^{-3}$	0.986	$0.446*10^{-3}$	0.984
0.0041	0.954	0.0089	0.931
0.041	0.863	0.129	0.775
0.4075	0.644	0.196	0.725
0.998	0.520	0.999	0.528
1.00	0.5	1.00	0.5
5.9	0.286	17.86	0.279
7.79	0.277	89.27	0.254
41.0	0.157	892.7	0.248
$4.1*10^3$	0.121	$8.93*10^3$	0.2477
$4.1*10^4$	0.117	$8.93*10^4$	0.2477
$4.1*10^5$	0.117	$8.93*10^5$	0.2477

Table 3.6 The effect of the individual material constants on the power of singularity.
(Material I is isotropic, Material II is assumed to be "isotropic"
with the same material constants as Materials I
except: a. varying E_y, $c_1 = E_y/E_x = E_y/E$;
b. varying G_{xy}, $c_2 = G_{xy}/E_x = G_{xy}/E$)

c_1	μ_2^*/μ_1^*	β
1.0	1.	0.5
10.	1.186	0.48
100.	12.88	0.459

c_2	μ_2^*/μ_1^*	β
1.0	1.	0.5
0.1	0.3667	0.603
0.01	0.1178	0.7385

Table 3.7 The effect of the individual material constants on the power of singularity.
(Material I is othotropic, Material 1, and Material II is assumed to be "othotropic" with the same material constants as Materials I except: a. varying E_{x2}, $c_1 = E_{x2}/E_{x1}$;
b. varying G_{xy2}, $c_2 = G_{xy2}/G_{xy1}$)

c_1	μ_2^*/μ_1^*	β
0.5	0.6363	0.564
1.0	1.	0.5
2.0	1.661	0.427
5.0	5.1	0.283

c_2	μ_2^*/μ_1^*	β
1.0	1.	0.5
0.1	0.369	0.607
0.01	0.1192	0.744

Table 4.1 The Material Elastic Constants. (Unit: GPA)

Material 1 and Material 2: Fiber Reinforced Composites

Material 1	Material 2
E_x=39.0	E_x=30.6
E_y=30.6	E_y=39.0
E_z=6.4	E_z=6.4
Gxy=19.7	Gxy=19.7
G_{yz}=4.5	G_{yz}=4.5
G_{xz}=4.5	G_{xz}=4.5
ν_{xy}=0.447	ν_{xy}=0.351
ν_{xz}=0.275	ν_{xz}=0.275
ν_{yz}=0.275	ν_{yz}=0.275

Material 3: Steel

E=200., ν=0.26

Material 4: Zirconia

E=137.9, ν=0.26

Material 5: Alumina

E=325., ν=0.3

Table 4.2 The Material Pairs. (Figure 4.1)

	Materials	
Material Pair	Layer I	Layer II
A	2	1
B	1	2
C	5	3
D	4	3
E	3	4
I	3	3

Table 4.3 Stress Intensity Factor in a homogeneous isotropic strip containing an edge crack under membrane loading N and bending moment M. (Material Pair I)

($\sigma_t = N/h$, $\sigma_b = 6M/h^2$)

$\frac{L}{(h/2.)}$	$\frac{k_t}{\sigma_t \sqrt{L}}$	$\frac{k_b}{\sigma_b \sqrt{L}}$
0.001	1.1215	1.1215
0.1	1.1399	1.0708
0.2	1.1892	1.0472
0.3	1.2652	1.0432
0.4	1.3673	1.0553
0.5	1.4975	1.0822
0.6	1.6599	1.1241
0.7	1.8612	1.1826
0.8	2.1114	1.2606
0.9	2.4253	1.3630

Table 4.4 Stress Intensity Factor in a two-layer strip containing an edge crack under membrane loading N and bending moment M. (Material Pair A)

($\sigma_t = N/h$, $\sigma_b = 6M/h^2$, $h_2/h_1=1.$)

$\frac{L}{(h_1)}$	$\frac{k_t}{\sigma_t \sqrt{L}}$	$\frac{k_b}{\sigma_b \sqrt{L}}$
0.001	1.106	1.106
0.1	1.115	1.060
0.2	1.160	1.030
0.3	1.237	1.033
0.4	1.334	1.047
0.5	1.455	1.074
0.6	1.602	1.114
0.7	1.780	1.165
0.8	1.990	1.228
0.9	2.226	1.296

Table 4.5 Stress Intensity Factor in a two-layer strip containing an edge crack under membrane loading N and bending moment M. (Material Pair B)

($\sigma_t = N/h$, $\sigma_b = 6M/h^2$)

	h_2/h_1=10.		h_2/h_1=1.		h_2/h_1=0.1	
$\frac{L}{h_1}$	$\frac{k_t}{\sigma_t \sqrt{L}}$	$\frac{k_b}{\sigma_b \sqrt{L}}$	$\frac{k_t}{\sigma_t \sqrt{L}}$	$\frac{k_b}{\sigma_b \sqrt{L}}$	$\frac{k_t}{\sigma_t \sqrt{L}}$	$\frac{k_b}{\sigma_b \sqrt{L}}$
0.001	1.100	1.100	1.100	1.100	1.100	1.100
0.1	1.060	1.003	1.120	1.050	1.192	1.004
0.2	1.000	0.984	1.164	1.016	1.298	1.021
0.3	1.031	0.985	1.248	1.016	1.545	1.077
0.4	1.036	0.988	1.355	1.028	1.904	1.178
0.5	1.054	0.993	1.492	1.055	2.436	1.344
0.6	1.073	1.000	1.664	1.097	3.254	1.609
0.7	1.094	1.007	1.881	1.157	4.591	2.046
0.8	1.117	1.016	2.160	1.243	6.949	2.803
0.9	1.143	1.027	2.538	1.368	11.342	4.126

Table 4.6 Stress Intensity Factor in a two-layer strip containing an edge crack under membrane loading N and bending moment M. (Material Pair C)

($\sigma_t = N/h$, $\sigma_b = 6M/h^2$)

	$h_2/h_1 = 1.$		$h_2/h_1 = 5.$	
$\frac{L}{h_1}$	$\frac{k_t}{\sigma_t \sqrt{L}}$	$\frac{k_b}{\sigma_b \sqrt{L}}$	$\frac{k_t}{\sigma_t \sqrt{L}}$	$\frac{k_b}{\sigma_b \sqrt{L}}$
0.001	1.121	1.121	1.121	1.121
0.1	1.140	1.062	1.103	1.078
0.2	1.200	1.039	1.143	1.092
0.3	1.293	1.038	1.169	1.093
0.4	1.417	1.056	1.201	1.098
0.5	1.578	1.090	1.240	1.109
0.6	1.782	1.143	1.287	1.126
0.7	2.046	1.219	1.345	1.150
0.8	2.398	1.330	1.418	1.186
0.9	2.915	1.506	1.521	1.245

Table 4.7 Stress Intensity Factor in a two-layer strip containing an edge crack under membrane loading N and bending moment M. (Material Pair D)

($\sigma_t = N/h$, $\sigma_b = 6M/h^2$)

	$h_2/h_1=5.$		$h_2/h_1=1.$		$h_2/h_1=0.2$	
$\frac{L}{h_1}$	$\frac{k_t}{\sigma_t\sqrt{L}}$	$\frac{k_b}{\sigma_b\sqrt{L}}$	$\frac{k_t}{\sigma_t\sqrt{L}}$	$\frac{k_b}{\sigma_b\sqrt{L}}$	$\frac{k_t}{\sigma_t\sqrt{L}}$	$\frac{k_b}{\sigma_b\sqrt{L}}$
0.001	1.120	1.120	1.120	1.120	1.120	1.120
0.1	1.119	1.074	1.132	1.070	1.161	1.052
0.2	1.114	1.072	1.171	1.044	1.278	1.045
0.3	1.113	1.049	1.234	1.036	1.464	1.081
0.4	1.113	1.027	1.319	1.043	1.734	1.158
0.5	1.114	1.007	1.426	1.062	2.119	1.284
0.6	1.114	0.987	1.556	1.091	2.677	1.480
0.7	1.112	0.967	1.709	1.130	3.522	1.785
0.8	1.109	0.944	1.882	1.174	4.874	2.277
0.9	1.104	0.914	2.058	1.212	7.147	3.093

Table 4.8 Stress Intensity Factor in a two-layer strip containing an edge crack under membrane loading N and bending moment M. (Material Pair E)

($\sigma_t = N/h$, $\sigma_b = 6M/h^2$)

	h_2/h_1=5.		h_2/h_1=1.		h_2/h_1=0.2	
$\frac{L}{h_1}$	$\frac{k_t}{\sigma_t \sqrt{L}}$	$\frac{k_b}{\sigma_b \sqrt{L}}$	$\frac{k_t}{\sigma_t \sqrt{L}}$	$\frac{k_b}{\sigma_b \sqrt{L}}$	$\frac{k_t}{\sigma_t \sqrt{L}}$	$\frac{k_b}{\sigma_b \sqrt{L}}$
0.001	1.120	1.120	1.120	1.120	1.120	1.120
0.1	1.101	1.078	1.139	1.063	1.167	1.045
0.2	1.138	1.090	1.196	1.040	1.300	1.039
0.3	1.161	1.088	1.284	1.038	1.515	1.079
0.4	1.188	1.087	1.403	1.055	1.827	1.163
0.5	1.222	1.095	1.556	1.088	2.277	1.298
0.6	1.263	1.107	1.750	1.139	2.940	1.508
0.7	1.312	1.125	2.000	1.212	3.958	1.834
0.8	1.374	1.152	2.328	1.316	5.618	2.357
0.9	1.459	1.198	2.802	1.480	8.581	3.256

Table 4.9 The coefficients C_{tk} and C_{bk} for the shape functions $g_t(\epsilon)$ and $g_b(\epsilon)$. (Material Pair I)

k	C_{tk}	C_{bk}
1	1.121	1.121
2	6.520	-1.887
3	-12.39	18.014
4	89.06	-87.38
5	-188.61	241.91
6	207.39	-391.94
7	-32.05	168.01

Table 4.10 The coefficients C_{tk} and C_{bk} for the shape functions $g_t(\epsilon)$ and $g_b(\epsilon)$. (Material Pair A, $h_2/h_1=1.$)

k	C_{tk}	C_{bk}
1	1.103	1.107
2	6.172	-1.278
3	-13.434	6.195
4	90.976	-7.717
5	-196.82	5.208

Table 4.11 The coefficients C_{tk} and C_{bk} for the shape functions $g_t(\epsilon)$ and $g_b(\epsilon)$. (Material Pair B)

	h_2/h_1=10.		h_2/h_1=1.		h_2/h_1=0.1	
k	C_{tk}	C_{bk}	C_{tk}	C_b	C_{tk}	C_{bk}
1	1.019	1.033	1.101	1.102	1.107	1.102
2	17.083	-2.537	6.637	-1.499	5.837	-2.159
3	24.226	19.186	-9.789	8.323	-4.321	16.133
4			64.081	-17.56	50.836	-53.66
5			-22.357	20.85	-116.98	108.80
6					180.96	-112.50
7					-87.04	52.913

Table 4.12 The coefficients C_{tk} and C_{bk} for the shape functions $g_t(\epsilon)$ and $g_b(\epsilon)$. (Material Pair C)

	h_2/h_1=5.		h_2/h_1=1.	
k	C_{tk}	C_{bk}	C_{tk}	C_{bk}
1	1.09	1.110	1.121	1.121
2	0.528	-0.901	7.786	-1.672
3	15.81	8.284	-12.31	10.71
4	-5.67	23.269	78.050	-26.47
5			43.543	33.67

Table 4.13 The coefficients C_{tk} and C_{bk} for the shape functions $g_t(\varepsilon)$ and $g_b(\varepsilon)$. (Material Pair D)

	h_2/h_1=5.		h_2/h_1=1.		h_2/h_1=0.2	
k	C_{tk}	C_{bk}	C_{tk}	C_{bk}	C_{tk}	C_{bk}
1	1.120	1.116	1.12	1.120	1.12	1.12
2	-0.333	-1.732	5.25	-1.189	5.83	-1.36
3	4.849	9.058	-8.925	4.565	-9.20	7.81
4	-22.62	-42.95	66.168	-2.533	76.80	-20.42
5			-183.23	-1.605	-203.60	45.04
6					321.69	-53.50
7					-181.34	31.81

Table 4.14 The coefficients C_{tk} and C_{bk} for the shape functions $g_t(\varepsilon)$ and $g_b(\varepsilon)$. (Material Pair E)

	h_2/h_1=5.		h_2/h_1=1.		h_2/h_1=0.2	
k	C_{tk}	C_{bk}	C_{tk}	C_{bk}	C_{tk}	C_{bk}
1	1.11	1.11	1.12	1.121	1.12	1.12
2	0.487	-1.091	7.37	-1.622	6.64	-1.61
3	7.227	8.513	-10.52	10.10	-9.47	10.63
4	32.19	13.05	66.22	-24.12	80.09	-34.84
5			41.11	30.25	-185.27	83.77
6					256.77	-103.51
7					-108.72	56.83

Table 4.15 Normalized stress intensity factor at the center of a semi-elliptical surface crack in a two-layer plate subjected to tension. In 15a the normalization factor k_{ot}^{∞} is calculated from the corresponding crack depth $L=L_0$. The results in 15b are normalized with respect to $k_{0t} = \sigma_t\sqrt{h_1}$ $\sigma_t = N/h$.

(Material Pair A, $h_2/h_1=1.$)

Table 4.15 a

$k_t(L_0)/k_{ot}^{\infty}$

L_0/h_1	0.3	0.6	0.9
a/h			
6.	0.955	0.821	0.637
4.	0.936	0.768	0.563
2.	0.892	0.663	0.442
1.	0.829	0.546	0.333
0.5	0.736	0.419	0.255
0.25	0.607	0.299	0.179

Table 4.15 b

$k_t(L_0)/k_{0t}$

L_0/h_1	0.3	0.6	0.9
a/h			
6.	0.647	1.019	1.345
4.	0.643	0.995	1.189
2.	0.604	0.823	0.929
1.	0.562	0.678	0.703
0.5	0.499	0.550	0.538
0.25	0.411	0.371	0.378

Table 4.16 Normalized stress intensity factor at the center of a semi-elliptical surface crack in a two-layer plate subjected to bending. In 16a the normalization factor k_{ob}^{∞} is calculated from the corresponding crack depth $L=L_0$. The results in 16b are normalized with respect to $k_{0b} = \sigma_b\sqrt{h_1}$, $\sigma_b=6M/h^2$.

(Material Pair A, $h_2/h_1=1.$)

Table 4.16 a

$k_b(L_0)/k_{ob}^{\infty}$

L_0/h_1	0.3	0.6	0.9
a/h			
6.	0.954	0.806	0.591
4.	0.934	0.747	0.506
2.	0.888	0.631	0.365
1.	0.821	0.500	0.238
0.5	0.723	0.358	0.130
0.25	0.586	0.223	0.050

Table 4.16 b

$k_b(L_0)/k_{0b}$

L_0/h_1	0.3	0.6	0.9
a/h			
6.	0.540	0.695	0.727
4.	0.512	0.645	0.622
2.	0.486	0.544	0.449
1.	0.450	0.431	0.293
0.5	0.396	0.309	0.160
0.25	0.321	0.192	0.061

Table 4.17 Normalized stress intensity factor at the center of a semi-elliptical surface crack in a two-layer plate subjected to tension. In 17 the normalization factor k_{ot}^{∞} is calculated from the corresponding crack depth $L=L_0$. The results in 17b are normalized with respect to $k_{0t} = \sigma_t\sqrt{h_1}$ $\sigma_t = N/h$.

(Material Pair B, $h_2/h_1=1.$)

Table 4.17 a

$k_t(L_0)/k_{ot}^{\infty}$

L_0/h_1	0.3	0.6	0.9
a/h			
6.	0.961	0.840	0.648
4.	0.944	0.790	0.575
2.	0.904	0.688	0.451
1.	0.843	0.568	0.337
0.5	0.751	0.437	0.241
0.25	0.586	0.312	0.169

Table 4.17 b

$k_t(L_0)/k_{0t}$

L_0/h_1	0.3	0.6	0.9
a/h			
6.	0.657	1.083	1.560
4.	0.645	1.018	1.384
2.	0.618	0.887	1.086
1.	0.576	0.732	0.811
0.5	0.513	0.563	0.580
0.25	0.400	0.402	0.407

Table 4.18 Normalized stress intensity factor at the center of a semi-elliptical surface crack in a two-layer plate subjected to bending. In 18a the normalization factor k_{ob}^{∞} is calculated from the corresponding crack depth $L=L_0$. The results in 18b are normalized with respect to $k_{0b} = \sigma_b\sqrt{h_1}$, $\sigma_b=6M/h^2$.

(Material Pair B, $h_2/h_1=1.$)

Table 4.18 a

$k_b(L_0)/k_{ob}^{\infty}$

L_0/h_1	0.3	0.6	0.9
a/h			
6.	0.960	0.824	0.601
4.	0.942	0.768	0.515
2.	0.899	0.653	0.369
1.	0.835	0.518	0.234
0.5	0.738	0.368	0.121
0.25	0.601	0.225	0.038

Table 4.18 b

$k_b(L_0)/k_{0b}$

L_0/h_1	0.3	0.6	0.9
a/h			
6.	0.543	0.711	0.780
4.	0.533	0.663	0.668
2.	0.509	0.563	0.479
1.	0.472	0.447	0.304
0.5	0.418	0.318	0.157
0.25	0.340	0.194	0.049

Table 4.19 Normalized stress intensity factor at the center of a semi-elliptical surface crack in a two-layer plate subjected to tension. In 19a the normalization factor k_{ot}^{∞} is calculated from the corresponding crack depth $L=L_0$. The results in 19b are normalized with respect to $k_{0t} = \sigma_t\sqrt{h_1}$ $\sigma_t = N/h$.

(Material Pair B, $h_2/h_1=10.$)

Table 4.19 a

$k_t(L_0)/k_{ot}^{\infty}$

L_0/h_1	0.3	0.6	0.9
a/h			
6.	0.996	0.988	0.968
4.	0.995	0.984	0.956
2.	0.993	0.973	0.928
1.	0.990	0.957	0.885
0.5	0.984	0.927	0.813
0.25	0.971	0.872	0.691

Table 4.19 b

$k_t(L_0)/k_{0t}$

L_0/h_1	0.3	0.6	0.9
a/h			
6.	0.562	0.821	1.049
4.	0.562	0.817	1.037
2.	0.560	0.778	1.006
1.	0.559	0.775	0.960
0.5	0.555	0.770	0.882
0.25	0.548	0.724	0.749

Table 4.20 Normalized stress intensity factor at the center of a semi-elliptical surface crack in a two-layer plate subjected to bending. In 20a the normalization factor k_{ob}^{∞} is calculated from the corresponding crack depth $L=L_0$. The results in 20b are normalized with respect to $k_{0b} = \sigma_b\sqrt{h_1}$, $\sigma_b=6M/h^2$.

(Material Pair B, $h_2/h_1=10.$)

Table 4.20 a

$k_b(L_0)/k_{ob}^{\infty}$

L_0/h_1	0.3	0.6	0.9
a/h			
6.	0.996	0.992	0.981
4.	0.996	0.989	0.974
2.	0.994	0.981	0.955
1.	0.991	0.969	0.924
0.5	0.986	0.946	0.872
0.25	0.975	0.905	0.794

Table 4.20 b

$k_b(L_0)/k_{0b}$

L_0/h_1	0.3	0.6	0.9
a/h			
6.	0.537	0.768	0.956
4.	0.537	0.766	0.949
2.	0.536	0.759	0.930
1.	0.535	0.756	0.900
0.5	0.532	0.756	0.850
0.25	0.526	0.701	0.774

Table 4.21 Normalized stress intensity factor at the center of a semi-elliptical surface crack in a two-layer plate subjected to tension. In 21a the normalization factor k_{ot}^{∞} is calculated from the corresponding crack depth $L=L_0$. The results in 21b are normalized with respect to $k_{0t} = \sigma_t\sqrt{h_1}$ $\sigma_t = N/h$.

(Material Pair B, $h_2/h_1=0.1$)

Table 4.21 a

$k_t(L_0)/k_{ot}^{\infty}$

L_0/h_1	0.3	0.6	0.9
a/h			
6.	0.862	0.503	0.137
4.	0.817	0.430	0.112
2.	0.722	0.320	0.078
1.	0.609	0.231	0.054
0.5	0.477	0.163	0.037

Table 4.21 b

$k_t(L_0)/k_{0t}$

L_0/h_1	0.3	0.6	0.9
a/h			
6.	0.729	1.268	1.474
4.	0.691	1.084	1.205
2.	0.611	0.807	0.839
1.	0.508	0.557	0.581
0.5	0.385	0.386	0.398

Table 4.22 Normalized stress intensity factor at the center of a semi-elliptical surface crack in a two-layer plate subjected to bending. In 22a the normalization factor k_{ob}^{∞} is calculated from the corresponding crack depth $L=L_0$. The results in 22b are normalized with respect to $k_{0b} = \sigma_b\sqrt{h_1}$, $\sigma_b=6M/h^2$.

(Material Pair B, $h_2/h_1=0.1$)

Table 4.22 a

$k_b(L_0)/k_{ob}^{\infty}$

L_0/h_1	0.3	0.6	0.9
a/h			
6.	0.852	0.432	0.034
4.	0.802	0.345	0.007
2.	0.699	0.215	-0.024
1.	0.573	0.111	-0.041
0.5	0.428	0.033	-0.043

Table 4.22 b

$k_b(L_0)/k_{0b}$

L_0/h_1	0.3	0.6	0.9
a/h			
6.	0.503	0.538	0.133
4.	0.473	0.430	0.027
2.	0.412	0.268	-0.094
1.	0.338	0.138	-0.160
0.5	0.252	0.041	-0.168

Table 4.23 Normalized stress intensity factor at the center of a semi-elliptical surface crack in a two-layer plate subjected to tension. In 23 the normalization factor k_{ot}^{∞} is calculated from the corresponding crack depth $L=L_0$. The results in 23b are normalized with respect to $k_{0t} = \sigma_t\sqrt{h_1}$ $\sigma_t = N/h$.

(Material Pair C, $h_2/h_1=1.$)

Table 4.23 a

$k_t(L_0)/k_{ot}^{\infty}$

L_0/h_1	0.3	0.6	0.9
a/h			
6.	0.972	0.897	0.747
4.	0.960	0.857	0.674
2.	0.931	0.767	0.538
1.	0.887	0.653	0.404
0.5	0.818	0.520	0.281

Table 4.23 b

$k_t(L_0)/k_{0t}$

L_0/h_1	0.3	0.6	0.9
a/h			
6.	0.688	1.238	2.065
4.	0.680	1.183	1.863
2.	0.459	1.058	1.487
1.	0.433	0.901	1.117
0.5	0.393	0.717	0.777

Table 4.24 Normalized stress intensity factor at the center of a semi-elliptical surface crack in a two-layer plate subjected to bending. In 24a the normalization factor k_{ob}^{∞} is calculated from the corresponding crack depth $L=L_0$. The results in 24b are normalized with respect to $k_{0b} = \sigma_b\sqrt{h_1}$, $\sigma_b=6M/h^2$.

(Material Pair C, $h_2/h_1=1.$)

Table 4.24 a

$k_b(L_0)/k_{ob}^{\infty}$

L_0/h_1	0.3	0.6	0.9
a/h			
6.	0.974	0.900	0.739
4.	0.964	0.861	0.663
2.	0.938	0.775	0.523
1.	0.899	0.669	0.390
0.5	0.843	0.549	0.273

Table 4.24 b

$k_b(L_0)/k_{0b}$

L_0/h_1	0.3	0.6	0.9
a/h			
6.	0.554	0.796	1.056
4.	0.548	0.762	0.974
2.	0.533	0.686	0.747
1.	0.511	0.592	0.557
0.5	0.479	0.486	0.390

Table 4.25 Normalized stress intensity factor at the center of a semi-elliptical surface crack in a two-layer plate subjected to tension. In 25a the normalization factor k_{ot}^{∞} is calculated from the corresponding crack depth $L=L_0$. The results in 25b are normalized with respect to $k_{0t} = \sigma_t\sqrt{h_1}$ $\sigma_t = N/h$.

(Material Pair C, $h_2/h_1=5.$)

Table 4.25 a

$k_t(L_0)/k_{ot}^{\infty}$

L_0/h_1	0.3	0.6	0.9
a/h			
6.	1.003	0.995	0.979
4.	1.001	0.991	0.968
2.	0.998	0.979	0.940
1.	0.994	0.961	0.900
0.5	0.986	0.932	0.840
0.25	0.972	0.883	0.750

Table 4.25 b

$k_t(L_0)/k_{0t}$

L_0/h_1	0.3	0.6	0.9
a/h			
6.	0.642	0.992	1.412
4.	0.641	0.988	1.397
2.	0.639	0.976	1.356
1.	0.636	0.958	1.299
0.5	0.631	0.929	1.212
0.25	0.622	0.880	1.082

Table 4.26 Normalized stress intensity factor at the center of a semi-elliptical surface crack in a two-layer plate subjected to bending. In 26a the normalization factor k_{ob}^{∞} is calculated from the corresponding crack depth $L=L_0$. The results in 26b are normalized with respect to $k_{0b} = \sigma_b\sqrt{h_1}$, $\sigma_b=6M/h^2$.

(Material Pair C, $h_2/h_1=5.$)

Table 4.26 a

$k_b(L_0)/k_{ob}^{\infty}$

L_0/h_1	0.3	0.6	0.9
a/h			
6.	1.003	0.996	0.979
4.	1.002	0.991	0.967
2.	0.999	0.978	0.938
1.	0.994	0.960	0.896
0.5	0.986	0.930	0.834
0.25	0.972	0.879	0.740

Table 4.26 b

$k_b(L_0)/k_{0b}$

L_0/h_1	0.3	0.6	0.9
a/h			
6.	0.600	0.869	1.156
4.	0.600	0.864	1.142
2.	0.598	0.853	1.108
1.	0.595	0.837	1.058
0.5	0.590	0.811	0.985
0.25	0.582	0.767	0.874

Table 4.27 Normalized stress intensity factor at the center of a semi-elliptical surface crack in a two-layer plate subjected to tension. In 27a the normalization factor k_{ot}^{∞} is calculated from the corresponding crack depth $L=L_0$. The results in 27b are normalized with respect to $k_{0t} = \sigma_t\sqrt{h_1}$ $\sigma_t = N/h$.

(Material Pair D, $h_2/h_1=1.$)

Table 4.27 a

$k_t(L_0)/k_{ot}^{\infty}$

L_0/h_1	0.3	0.6	0.9
a/h			
6.	0.959	0.856	0.707
4.	0.942	0.804	0.627
2.	0.899	0.693	0.483
1.	0.836	0.563	0.348
0.5	0.747	0.424	0.262

Table 4.27 b

$k_t(L_0)/k_{0t}$

L_0/h_1	0.3	0.6	0.9
a/h			
6.	0.648	1.032	1.380
4.	0.637	0.969	1.224
2.	0.608	0.835	0.943
1.	0.565	0.675	0.679
0.5	0.505	0.511	0.512

Table 4.28 Normalized stress intensity factor at the center of a semi-elliptical surface crack in a two-layer plate subjected to bending. In 28a the normalization factor k_{ob}^{∞} is calculated from the corresponding crack depth $L=L_0$. The results in 28b are normalized with respect to $k_{0b} = \sigma_b\sqrt{h_1}$, $\sigma_b=6M/h^2$.

(Material Pair D, $h_2/h_1=1.$)

Table 4.28 a

$k_b(L_0)/k_{ob}^{\infty}$

L_0/h_1	0.3	0.6	0.9
a/h			
6.	0.962	0.863	0.706
4.	0.946	0.813	0.624
2.	0.909	0.709	0.481
1.	0.855	0.591	0.353
0.5	0.782	0.468	0.246

Table 4.28 b

$k_b(L_0)/k_{0b}$

L_0/h_1	0.3	0.6	0.9
a/h			
6.	0.552	0.729	0.812
4.	0.537	0.687	0.717
2.	0.516	0.599	0.553
1.	0.485	0.499	0.406
0.5	0.444	0.395	0.283

Table 4.29 Normalized stress intensity factor at the center of a semi-elliptical surface crack in a two-layer plate subjected to tension. In 29a the normalization factor k_{ot}^{∞} is calculated from the corresponding crack depth $L=L_0$. The results in 29b are normalized with respect to $k_{0t} = \sigma_t\sqrt{h_1}$ $\sigma_t = N/h$.

(Material Pair D, $h_2/h_1=5.$)

Table 4.29 a

$k_t(L_0)/k_{ot}^{\infty}$

L_0/h_1	0.3	0.6	0.9
a/h			
6.	0.993	0.981	0.965
4.	0.991	0.974	0.950
2.	0.986	0.954	0.913
1.	0.977	0.926	0.862
0.5	0.944	0.883	0.791
0.25	0.940	0.815	0.689

Table 4.29 b

$k_t(L_0)/k_{0t}$

L_0/h_1	0.3	0.6	0.9
a/h			
6.	0.605	0.847	1.001
4.	0.604	0.840	0.995
2.	0.601	0.802	0.956
1.	0.596	0.799	0.903
0.5	0.575	0.718	0.828
0.25	0.573	0.703	0.722

Table 4.30 Normalized stress intensity factor at the center of a semi-elliptical surface crack in a two-layer plate subjected to bending. In 30a the normalization factor k_{ob}^{∞} is calculated from the corresponding crack depth $L=L_0$. The results in 30b are normalized with respect to $k_{0b} = \sigma_b\sqrt{h_1}$, $\sigma_b=6M/h^2$.

(Material Pair D, $h_2/h_1=5.$)

Table 4.30 a

$k_b(L_0)/k_{ob}^{\infty}$

L_0/h_1	0.3	0.6	0.9
a/h			
6.	0.993	0.981	0.964
4.	0.991	0.973	0.949
2.	0.985	0.954	0.911
1.	0.977	0.925	0.858
0.5	0.964	0.882	0.784
0.25	0.939	0.813	0.677

Table 4.30 b

$k_b(L_0)/k_{0b}$

L_0/h_1	0.3	0.6	0.9
a/h			
6.	0.571	0.750	0.836
4.	0.569	0.744	0.823
2.	0.566	0.729	0.816
1.	0.561	0.707	0.744
0.5	0.554	0.674	0.680
0.25	0.539	0.622	0.587

Table 4.31 Normalized stress intensity factor at the center of a semi-elliptical surface crack in a two-layer plate subjected to tension. In 31a the normalization factor k_{ot}^{∞} is calculated from the corresponding crack depth $L=L_0$. The results in 31b are normalized with respect to $k_{0t} = \sigma_t\sqrt{h_1}$ $\sigma_t = N/h$.

(Material Pair D, $h_2/h_1=0.2$)

Table 4.31 a

$k_t(L_0)/k_{ot}^{\infty}$

L_0/h_1	0.3	0.6	0.9
a/h			
6.	0.918	0.662	0.278
4.	0.886	0.587	0.226
2.	0.811	0.459	0.160
1.	0.718	0.348	0.114
0.5	0.606	0.256	0.081
0.25	0.470	0.183	0.057

Table 4.31 b

$k_t(L_0)/k_{0t}$

L_0/h_1	0.3	0.6	0.9
a/h			
6.	0.736	1.373	1.885
4.	0.710	1.217	1.532
2.	0.650	0.952	1.108
1.	0.576	0.722	0.773
0.5	0.486	0.531	0.549
0.25	0.377	0.379	0.386

C-3

Table 4.32 Normalized stress intensity factor at the center of a semi-elliptical surface crack in a two-layer plate subjected to bending. In 32a the normalization factor k_{ob}^{∞} is calculated from the corresponding crack depth $L=L_0$. The results in 32b are normalized with respect to $k_{0b} = \sigma_b\sqrt{h_1}$, $\sigma_b=6M/h^2$.

(Material Pair D, $h_2/h_1=0.2$)

Table 4.32 a

$k_b(L_0)/k_{ob}^{\infty}$

L_0/h_1	0.3	0.6	0.9
a/h			
6.	0.913	0.621	0.195
4.	0.878	0.543	0.136
2.	0.796	0.384	0.061
1.	0.694	0.254	0.013
0.5	0.572	0.147	-0.018
0.25	0.430	0.064	-0.033

Table 4.32 b

$k_b(L_0)/k_{0b}$

L_0/h_1	0.3	0.6	0.9
a/h			
6.	0.541	0.712	0.572
4.	0.520	0.622	0.399
2.	0.471	0.440	0.179
1.	0.411	0.291	0.038
0.5	0.339	0.169	-0.053
0.25	0.255	0.073	-0.097

Table 4.33 Normalized stress intensity factor at the center of a semi-elliptical surface crack in a two-layer plate subjected to tension. In 33a the normalization factor k_{ot}^{∞} is calculated from the corresponding crack depth $L=L_0$. The results in 33b are normalized with respect to $k_{0t} = \sigma_t\sqrt{h_1}$ $\sigma_t = N/h$.

(Material Pair E, $h_2/h_1=1.$)

Table 4.33 a

$k_t(L_0)/k_{ot}^{\infty}$

L_0/h_1	0.3	0.6	0.9
a/h			
6.	0.971	0.890	0.734
4.	0.958	0.850	0.660
2.	0.927	0.754	0.523
1.	0.880	0.638	0.390
0.5	0.809	0.504	0.270

Table 4.33 b

$k_t(L_0)/k_{0t}$

L_0/h_1	0.3	0.6	0.9
a/h			
6.	0.683	1.206	1.951
4.	0.674	1.152	1.754
2.	0.652	1.022	1.390
1.	0.619	0.865	1.037
0.5	0.569	0.683	0.718

Table 4.34 Normalized stress intensity factor at the center of a semi-elliptical surface crack in a two-layer plate subjected to bending. In 34a the normalization factor k_{ob}^{∞} is calculated from the corresponding crack depth $L=L_0$. The results in 34b are normalized with respect to $k_{0b} = \sigma_b\sqrt{h_1}$, $\sigma_b=6M/h^2$.

(Material Pair E, $h_2/h_1=1.$)

Table 4.34 a

$k_b(L_0)/k_{ob}^{\infty}$

L_0/h_1	0.3	0.6	0.9
a/h			
6.	0.973	0.893	0.725
4.	0.961	0.852	0.647
2.	0.933	0.762	0.506
1.	0.893	0.654	0.374
0.5	0.834	0.533	0.260

Table 4.34 b

$k_b(L_0)/k_{0b}$

L_0/h_1	0.3	0.6	0.9
a/h			
6.	0.553	0.788	1.018
4.	0.546	0.752	0.908
2.	0.530	0.672	0.710
1.	0.508	0.577	0.525
0.5	0.474	0.470	0.365

Table 4.35 Normalized stress intensity factor at the center of a semi-elliptical surface crack in a two-layer plate subjected to tension. In 35a the normalization factor k_{ot}^{∞} is calculated from the corresponding crack depth $L=L_0$. The results in 35b are normalized with respect to $k_{0t} = \sigma_t\sqrt{h_1}$ $\sigma_t = N/h$.

(Material Pair E, $h_2/h_1=5.$)

Table 4.35 a

$k_t(L_0)/k_{ot}^{\infty}$

L_0/h_1	0.3	0.6	0.9
a/h			
6.	1.003	0.995	0.979
4.	1.001	0.990	0.967
2.	0.998	0.977	0.938
1.	0.993	0.958	0.896
0.5	0.985	0.927	0.836
0.25	0.969	0.876	0.744

Table 4.35 b

$k_t(L_0)/k_{0t}$

L_0/h_1	0.3	0.6	0.9
a/h			
6.	0.638	0.973	1.355
4.	0.637	0.969	1.338
2.	0.635	0.956	1.298
1.	0.631	0.937	1.240
0.5	0.626	0.907	1.157
0.25	0.616	0.857	1.029

Table 4.36 Normalized stress intensity factor at the center of a semi-elliptical surface crack in a two-layer plate subjected to bending. In 36a the normalization factor k_{ob}^{∞} is calculated from the corresponding crack depth $L=L_0$. The results in 36b are normalized with respect to $k_{0b} = \sigma_b\sqrt{h_1}$, $\sigma_b=6M/h^2$.

(Material Pair E, $h_2/h_1=5.$)

Table 4.36 a

$k_b(L_0)/k_{ob}^{\infty}$

L_0/h_1	0.3	0.6	0.9
a/h			
6.	1.002	0.996	0.979
4.	1.001	0.990	0.966
2.	0.998	0.977	0.936
1.	0.993	0.957	0.892
0.5	0.984	0.925	0.828
0.25	0.969	0.872	0.732

Table 4.36 b

$k_b(L_0)/k_{0b}$

L_0/h_1	0.3	0.6	0.9
a/h			
6.	0.597	0.854	1.113
4.	0.597	0.849	1.098
2.	0.595	0.838	1.064
1.	0.592	0.821	1.014
0.5	0.586	0.793	0.932
0.25	0.577	0.748	0.832

Table 4.37 Normalized stress intensity factor at the center of a semi-elliptical surface crack in a two-layer plate subjected to tension. In 37a the normalization factor k_{ot}^{∞} is calculated from the corresponding crack depth $L=L_0$. The results in 37b are normalized with respect to $k_{0t} = \sigma_t\sqrt{h_1}$ $\sigma_t = N/h$.

(Material Pair E, $h_2/h_1=0.2$)

Table 4.37 a

$k_t(L_0)/k_{ot}^{\infty}$

L_0/h_1	0.3	0.6	0.9
a/h			
6.	0.934	0.693	0.280
4.	0.907	0.619	0.228
2.	0.841	0.489	0.159
1.	0.756	0.372	0.111
0.5	0.651	0.270	0.076
0.25	0.523	0.178	0.052

Table 4.37 b

$k_t(L_0)/k_{0t}$

L_0/h_1	0.3	0.6	0.9
a/h			
6.	0.775	1.578	2.280
4.	0.753	1.410	1.856
2.	0.698	1.114	1.294
1.	0.627	0.847	0.904
0.5	0.540	0.615	0.619
0.25	0.274	0.405	0.423

Table 4.38 Normalized stress intensity factor at the center of a semi-elliptical surface crack in a two-layer plate subjected to bending. In 38a the normalization factor k_{ob}^{∞} is calculated from the corresponding crack depth $L=L_0$. The results in 38b are normalized with respect to $k_{0b} = \sigma_b\sqrt{h_1}$, $\sigma_b=6M/h^2$.

(Material Pair E, $h_2/h_1=0.2$)

Table 4.38 a

$k_b(L_0)/k_{ob}^{\infty}$

L_0/h_1	0.3	0.6	0.9
a/h			
6.	0.930	0.652	0.184
4.	0.901	0.566	0.123
2.	0.828	0.413	0.045
1.	0.734	0.274	-0.005
0.5	0.618	0.157	-0.035
0.25	0.476	0.065	-0.049

Table 4.38b

$k_b(L_0)/k_{0b}$

L_0/h_1	0.3	0.6	0.9
a/h			
6.	0.550	0.762	0.568
4.	0.532	0.661	0.380
2.	0.489	0.482	0.139
1.	0.434	0.320	-0.015
0.5	0.365	0.183	-0.108
0.25	0.281	0.076	-0.151

Table 4.39 a and b Normalized stress intensity factor at the crack front for a semi-elliptical (a), or rectangular (b) surface crack in a two-layer plate subjected to tension. (Material Pair B, $h_2/h_1=1.$)

Semi-elliptical surface crack

a.1 a/h=1. $k_b(y)/k_{ot}^{\infty}$

L_0/h_1	0.3	0.6	0.9
y/a			
0.	0.843	0.568	0.337
0.1	0.838	0.566	0.336
0.2	0.827	0.559	0.333
0.3	0.814	0.553	0.328
0.4	0.803	0.547	0.324
0.5	0.793	0.542	0.320
0.6	0.774	0.532	0.314
0.7	0.732	0.512	0.304
0.8	0.667	0.483	0.292
0.9	0.616	0.463	0.284

a.2) a/h=2.

L_0/h_1	0.3	0.6	0.9
y/a			
0.	0.904	0.688	0.451
0.1	0.899	0.684	0.449
0.2	0.885	0.675	0.443
0.3	0.869	0.664	0.436
0.4	0.854	0.653	0.429
0.5	0.839	0.643	0.421
0.6	0.814	0.625	0.411
0.7	0.762	0.591	0.392
0.8	0.683	0.540	0.365
0.9	0.616	0.498	0.345

Table 4.39b continued

Rectangular surface crack

b.1 a/h=1. $k_b(y)/k_{ot}^{\infty}$

L_0/h_1	0.3	0.6	0.9
y/a			
0.	0.891	0.627	0.376
0.1	0.886	0.622	0.373
0.2	0.875	0.610	0.364
0.3	0.866	0.598	0.355
0.4	0.863	0.589	0.348
0.5	0.862	0.581	0.342
0.6	0.850	0.561	0.329
0.7	0.814	0.518	0.301
0.8	0.752	0.453	0.261
0.9	0.662	0.380	0.222

b.2) a/h=2.

L_0/h_1	0.3	0.6	0.9
y/a			
0.	0.944	0.752	0.508
0.1	0.937	0.747	0.504
0.2	0.921	0.735	0.494
0.3	0.910	0.724	0.483
0.4	0.913	0.717	0.475
0.5	0.923	0.712	0.468
0.6	0.923	0.695	0.452
0.7	0.891	0.653	0.416
0.8	0.837	0.586	0.363
0.9	0.786	0.502	0.306

Table 4.40 a and b Normalized stress intensity factor at the crack front for a semi-elliptical (a), or a rectangular (b) surface crack in a two-layer plate subjected to bending. (Material Pair B, $h_2/h_1=1.$)

Semi-elliptical surface crack

a.1 a/h=1. $k_b(y)/k_{ob}^{\infty}$

L_0/h_1	0.3	0.6	0.9
y/a			
0.	0.835	0.518	0.234
0.1	0.831	0.516	0.235
0.2	0.821	0.515	0.237
0.3	0.812	0.514	0.243
0.4	0.809	0.521	0.253
0.5	0.808	0.532	0.267
0.6	0.801	0.542	0.283
0.7	0.771	0.544	0.299
0.8	0.717	0.545	0.318
0.9	0.685	0.557	0.351

a.2) a/h=2.

L_0/h_1	0.3	0.6	0.9
y/a			
0.	0.899	0.653	0.369
0.1	0.894	0.650	0.368
0.2	0.883	0.645	0.368
0.3	0.871	0.642	0.371
0.4	0.863	0.644	0.380
0.5	0.859	0.650	0.394
0.6	0.845	0.652	0.408
0.7	0.806	0.643	0.415
0.8	0.738	0.616	0.420
0.9	0.689	0.611	0.442

Table 4.40b continued

Rectangular surface crack

b.1) a/h=1. $k_b(y)/k_{ob}^{\infty}$

L_0/h_1	0.3	0.6	0.9
y/a			
0.	0.876	0.563	0.258
0.1	0.874	0.563	0.257
0.2	0.870	0.562	0.257
0.3	0.863	0.556	0.254
0.4	0.857	0.540	0.241
0.5	0.848	0.515	0.222
0.6	0.831	0.485	0.199
0.7	0.799	0.450	0.179
0.8	0.745	0.398	0.151
0.9	0.635	0.289	0.086

b.2) a/h=2.

L_0/h_1	0.3	0.6	0.9
y/a			
0.	0.933	0.705	0.409
0.1	0.928	0.704	0.410
0.2	0.918	0.704	0.408
0.3	0.911	0.699	0.405
0.4	0.910	0.686	0.391
0.5	0.914	0.664	0.367
0.6	0.909	0.637	0.339
0.7	0.883	0.604	0.312
0.8	0.837	0.550	0.273
0.9	0.767	0.428	0.181

Table 4.41 a and b Normalized stress intensity factor at the crack front for a semi-elliptical (a), or rectangular (b) surface crack in a two-layer plate subjected to tension. (Material Pair C, $h_2/h_1=1.$)

Semi-elliptical surface crack

a.1 a/h=1. $k_b(y)/k_{ot}^{\infty}$

L_0/h_1	0.3	0.6	0.9
y/a			
0.	0.887	0.653	0.404
0.1	0.885	0.652	0.403
0.2	0.881	0.650	0.401
0.3	0.871	0.643	0.396
0.4	0.852	0.632	0.388
0.5	0.826	0.614	0.377
0.6	0.792	0.593	0.365
0.7	0.754	0.571	0.353
0.8	0.704	0.542	0.341
0.9	0.603	0.481	0.315

a.2) a/h=2.

L_0/h_1	0.3	0.6	0.9
y/a			
0.	0.932	0.767	0.538
0.1	0.930	0.765	0.537
0.2	0.924	0.760	0.532
0.3	0.911	0.748	0.522
0.4	0.889	0.729	0.507
0.5	0.857	0.701	0.486
0.6	0.818	0.667	0.463
0.7	0.773	0.629	0.438
0.8	0.714	0.580	0.408
0.9	0.600	0.492	0.354

Table 4.41b continued

Rectangular surface crack

a.1 a/h=1. $k_b(y)/k_{ot}^{\infty}$

L_0/h_1	0.3	0.6	0.9
y/a			
0.	0.930	0.722	0.459
0.1	0.927	0.721	0.457
0.2	0.921	0.717	0.453
0.3	0.915	0.709	0.446
0.4	0.913	0.697	0.434
0.5	0.912	0.680	0.418
0.6	0.904	0.656	0.396
0.7	0.880	0.618	0.395
0.8	0.839	0.558	0.319
0.9	0.757	0.445	0.245

a.2) a/h=2.

L_0/h_1	0.3	0.6	0.9
y/a			
0.	0.977	0.833	0.615
0.1	0.968	0.832	0.613
0.2	0.949	0.827	0.608
0.3	0.936	0.820	0.599
0.4	0.942	0.812	0.587
0.5	0.959	0.800	0.570
0.6	0.964	0.781	0.546
0.7	0.933	0.750	0.511
0.8	0.885	0.696	0.457
0.9	0.865	0.591	0.364

Table 4.42 a and b Normalized stress intensity factor at the crack front for a semi-elliptical (a), or a rectangular (b) surface crack in a two-layer plate subjected to bending. (Material Pair B, $h_2/h_1=1.$)

Semi-elliptical surface crack

a.1 a/h=1. $k_b(y)/k_{ob}^{\infty}$

L_0/h_1	0.3	0.6	0.9
y/a			
0.	0.899	0.669	0.390
0.1	0.899	0.670	0.391
0.2	0.897	0.672	0.395
0.3	0.891	0.672	0.399
0.4	0.879	0.670	0.403
0.5	0.859	0.664	0.407
0.6	0.834	0.657	0.411
0.7	0.806	0.652	0.420
0.8	0.767	0.643	0.431
0.9	0.673	0.597	0.427

a.2) a/h=2.

L_0/h_1	0.3	0.6	0.9
y/a			
0.	0.938	0.775	0.523
0.1	0.937	0.775	0.524
0.2	0.934	0.774	0.526
0.3	0.926	0.770	0.527
0.4	0.911	0.762	0.526
0.5	0.887	0.748	0.522
0.6	0.857	0.731	0.517
0.7	0.823	0.713	0.514
0.8	0.777	0.687	0.510
0.9	0.672	0.615	0.478

Table 4.42b continued

Rectangular surface crack

b.1) a/h=1. $k_b(y)/k_{ob}^{\infty}$

L_0/h_1	0.3	0.6	0.9
y/a			
0.	0.947	0.730	0.436
0.1	0.939	0.728	0.434
0.2	0.923	0.722	0.430
0.3	0.911	0.714	0.423
0.4	0.915	0.705	0.413
0.5	0.927	0.693	0.398
0.6	0.928	0.672	0.377
0.7	0.897	0.636	0.348
0.8	0.844	0.579	0.305
0.9	0.798	0.480	0.236

b.2) a/h=2.

L_0/h_1	0.3	0.6	0.9
y/a			
0.	0.990	0.838	0.592
0.1	0.977	0.835	0.591
0.2	0.947	0.826	0.586
0.3	0.928	0.818	0.577
0.4	0.938	0.812	0.565
0.5	0.969	0.806	0.549
0.6	0.982	0.791	0.526
0.7	0.941	0.757	0.491
0.8	0.878	0.703	0.439
0.9	0.890	0.616	0.351

Table 4.43 a and b Normalized stress intensity factor at the crack front for a semi-elliptical (a), or rectangular (b) surface crack in a two-layer plate subjected to tension. (Material Pair B, $h_2/h_1=0.1$)

Semi-elliptical surface crack

a.1 a/h=1. $k_b(y)/k_{ot}^{\infty}$

L_0/h_1	0.3	0.6	0.9
y/a			
0.	0.609	0.231	0.055
0.1	0.606	0.231	0.055
0.2	0.600	0.230	0.055
0.3	0.593	0.228	0.055
0.4	0.587	0.226	0.054
0.5	0.582	0.224	0.054
0.6	0.573	0.219	0.052
0.7	0.553	0.213	0.049
0.8	0.524	0.207	0.049
0.9	0.500	0.196	0.048

a.2) a/h=2.

L_0/h_1	0.3	0.6	0.9
y/a			
0.	0.722	0.321	0.078
0.1	0.718	0.319	0.078
0.2	0.709	0.317	0.078
0.3	0.697	0.314	0.078
0.4	0.688	0.310	0.078
0.5	0.678	0.307	0.078
0.6	0.661	0.300	0.078
0.7	0.626	0.289	0.077
0.8	0.575	0.275	0.074
0.9	0.529	0.262	0.070

Table 4.43b continued

Rectangular surface crack

b.1 a/h=1. $k_b(y)/k_{ot}^{\infty}$

L_0/h_1	0.3	0.6	0.9
y/a			
0.	0.669	0.257	0.065
0.1	0.664	0.255	0.065
0.2	0.653	0.250	0.064
0.3	0.641	0.244	0.063
0.4	0.632	0.239	0.062
0.5	0.622	0.235	0.059
0.6	0.601	0.226	0.057
0.7	0.558	0.207	0.053
0.8	0.492	0.181	0.047
0.9	0.410	0.155	0.038

b.2) a/h=2.

L_0/h_1	0.3	0.6	0.9
y/a			
0.	0.783	0.362	0.092
0.1	0.779	0.359	0.091
0.2	0.768	0.351	0.090
0.3	0.758	0.343	0.088
0.4	0.752	0.337	0.086
0.5	0.746	0.331	0.084
0.6	0.731	0.318	0.089
0.7	0.691	0.292	0.074
0.8	0.626	0.254	0.065
0.9	0.538	0.215	0.053

Table 4.44 a and b Normalized stress intensity factor at the crack front for a semi-elliptical (a), or a rectangular (b) surface crack in a two-layer plate subjected to bending. (Material Pair B, $h_2/h_1=0.1$)

Semi-elliptical surface crack

a.1 a/h=1. $k_b(y)/k_{ob}^{\infty}$

L_0/h_1	0.3	0.6	0.9
y/a			
0.	0.573	0.111	-0.040
0.1	0.572	0.112	-0.040
0.2	0.572	0.116	-0.037
0.3	0.570	0.123	-0.032
0.4	0.573	0.134	-0.024
0.5	0.575	0.148	-0.014
0.6	0.576	0.167	-0.002
0.7	0.576	0.187	0.012
0.8	0.577	0.214	0.028
0.9	0.577	0.245	0.048

a.2) a/h=2.

L_0/h_1	0.3	0.6	0.9
y/a			
0.	0.698	0.215	-0.024
0.1	0.696	0.216	-0.023
0.2	0.693	0.219	-0.019
0.3	0.692	0.225	-0.012
0.4	0.691	0.237	-0.001
0.5	0.690	0.254	0.012
0.6	0.673	0.272	0.028
0.7	0.654	0.290	0.044
0.8	0.640	0.310	0.061
0.9	0.619	0.338	0.084

Table 4.44b continued

Rectangular surface crack

b.1) a/h=1. $k_b(y)/k_{ob}^{\infty}$

L_0/h_1	0.3	0.6	0.9
y/a			
0.	0.622	0.123	-0.045
0.1	0.622	0.123	-0.045
0.2	0.620	0.122	-0.045
0.3	0.613	0.120	-0.046
0.4	0.599	0.112	-0.046
0.5	0.576	0.099	-0.046
0.6	0.546	0.084	-0.045
0.7	0.510	0.071	-0.044
0.8	0.454	0.055	-0.044
0.9	0.343	0.016	-0.042

b.2) a/h=2.

L_0/h_1	0.3	0.6	0.9
y/a			
0.	0.750	0.241	-0.024
0.1	0.749	0.240	-0.024
0.2	0.748	0.239	-0.024
0.3	0.743	0.236	-0.025
0.4	0.731	0.227	-0.027
0.5	0.713	0.201	-0.031
0.6	0.689	0.187	-0.034
0.7	0.657	0.168	-0.037
0.8	0.603	0.142	-0.039
0.9	0.484	0.079	-0.043

Table 4.45 a and b Normalized stress intensity factor at the crack front for a semi-elliptical surface crack in a two-layer plate subjected to tension (a), bending (b).

(Material Pair B, $h_2/h_1=10$)

a.1) a/h=1. $k_b(y)/k_{ot}^{\infty}$

L_0/h_1	0.3	0.6	0.9
y/a			
0.	0.989	0.967	0.885
0.1	0.988	0.955	0.884
0.2	0.983	0.950	0.880
0.3	0.971	0.939	0.873
0.4	0.951	0.920	0.859
0.5	0.921	0.894	0.839
0.6	0.883	0.858	0.812
0.7	0.837	0.815	0.777
0.8	0.774	0.755	0.727
0.9	0.652	0.640	0.625

a.2) a/h=2.

L_0/h_1	0.3	0.6	0.9
y/a			
0.	0.993	0.973	0.928
0.1	0.991	0.972	0.927
0.2	0.986	0.965	0.921
0.3	0.974	0.953	0.910
0.4	0.953	0.933	0.891
0.5	0.923	0.904	0.865
0.6	0.885	0.866	0.830
0.7	0.838	0.819	0.786
0.8	0.775	0.756	0.726
0.9	0.651	0.636	0.614

Table 4.45b continued

b.1) a/h=1. $k_b(y)/k_{ob}^{\infty}$

L_0/h_1	0.3	0.6	0.9
y/a			
0.	0.991	0.969	0.924
0.1	0.990	0.967	0.923
0.2	0.985	0.963	0.919
0.3	0.975	0.954	0.911
0.4	0.957	0.938	0.898
0.5	0.929	0.913	0.878
0.6	0.894	0.882	0.852
0.7	0.852	0.844	0.819
0.8	0.794	0.791	0.773
0.9	0.675	0.681	0.675

b.2) a/h=2.

L_0/h_1	0.3	0.6	0.9
y/a			
0.	0.994	0.981	0.955
0.1	0.993	0.980	0.953
0.2	0.988	0.975	0.948
0.3	0.977	0.965	0.938
0.4	0.959	0.947	0.922
0.5	0.931	0.922	0.898
0.6	0.896	0.888	0.866
0.7	0.853	0.848	0.828
0.8	0.794	0.791	0.775
0.9	0.675	0.678	0.669

Table 4.46 a and b Normalized stress intensity factor at the crack front for a semi-elliptical surface crack in a two-layer plate subjected to tension (a), bending (b).

(Material Pair C, $h_2/h_1=5$)

a.1) a/h=1. $k_t(y)/k_{ot}^{\infty}$

L_0/h_1	0.3	0.6	0.9
y/a			
0.	0.994	0.961	0.900
0.1	0.989	0.956	0.899
0.2	0.975	0.941	0.884
0.3	0.958	0.922	0.864
0.4	0.940	0.902	0.842
0.5	0.919	0.880	0.817
0.6	0.886	0.846	0.780
0.7	0.829	0.786	0.720
0.8	0.746	0.698	0.635
0.9	0.646	0.611	0.554

a.2) a/h=2.

L_0/h_1	0.3	0.6	0.9
y/a			
0.	0.998	0.979	0.940
0.1	0.993	0.973	0.937
0.2	0.980	0.958	0.920
0.3	0.962	0.937	0.897
0.4	0.944	0.916	0.871
0.5	0.922	0.892	0.842
0.6	0.888	0.855	0.801
0.7	0.830	0.792	0.733
0.8	0.747	0.701	0.640
0.9	0.645	0.609	0.552

Table 4.46b continued

b.1) a/h=1. $k_b(y)/k_{ob}^{\infty}$

L_0/h_1	0.3	0.6	0.9
y/a			
0.	0.994	0.960	0.896
0.1	0.989	0.956	0.892
0.2	0.976	0.942	0.882
0.3	0.961	0.925	0.865
0.4	0.945	0.910	0.851
0.5	0.927	0.895	0.835
0.6	0.898	0.868	0.809
0.7	0.844	0.815	0.759
0.8	0.766	0.734	0.682
0.9	0.670	0.657	0.616

b.2) a/h=2.

L_0/h_1	0.3	0.6	0.9
y/a			
0.	0.999	0.978	0.938
0.1	0.994	0.973	0.930
0.2	0.981	0.959	0.921
0.3	0.965	0.941	0.901
0.4	0.949	0.925	0.883
0.5	0.931	0.907	0.863
0.6	0.900	0.878	0.831
0.7	0.846	0.822	0.774
0.8	0.767	0.738	0.689
0.9	0.670	0.656	0.615

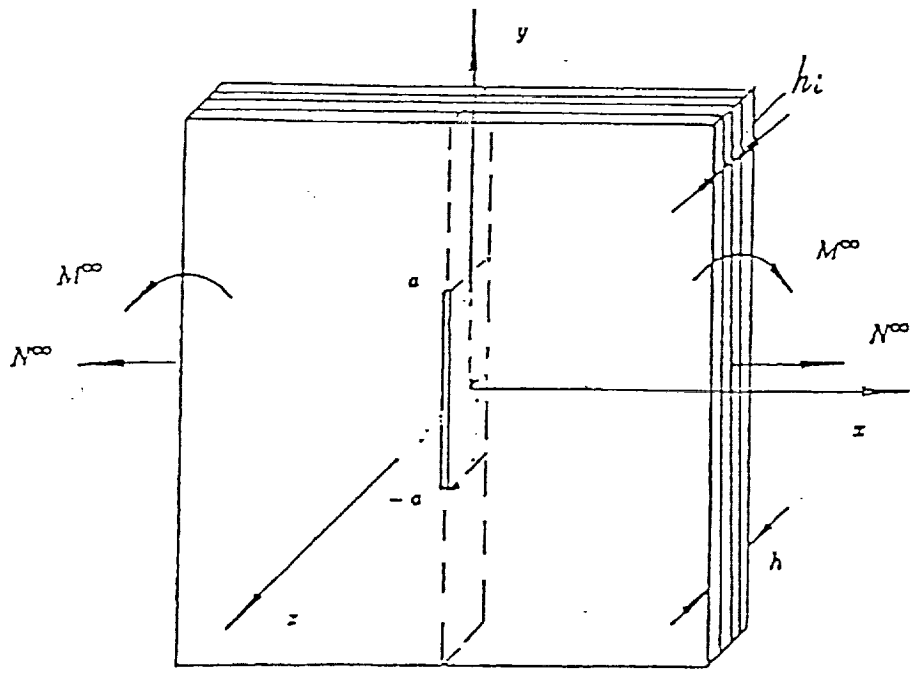

Figure 2.1 Geometry and the loading of the plate with a through crack.

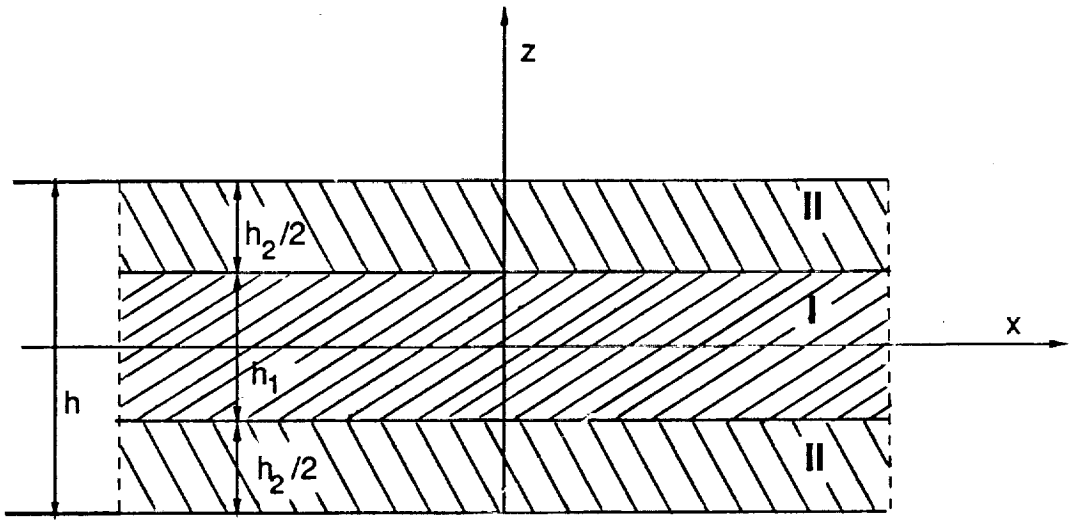

Figure 2.2 (a) Geometry and notations of the three-layer symmetric laminated plate.

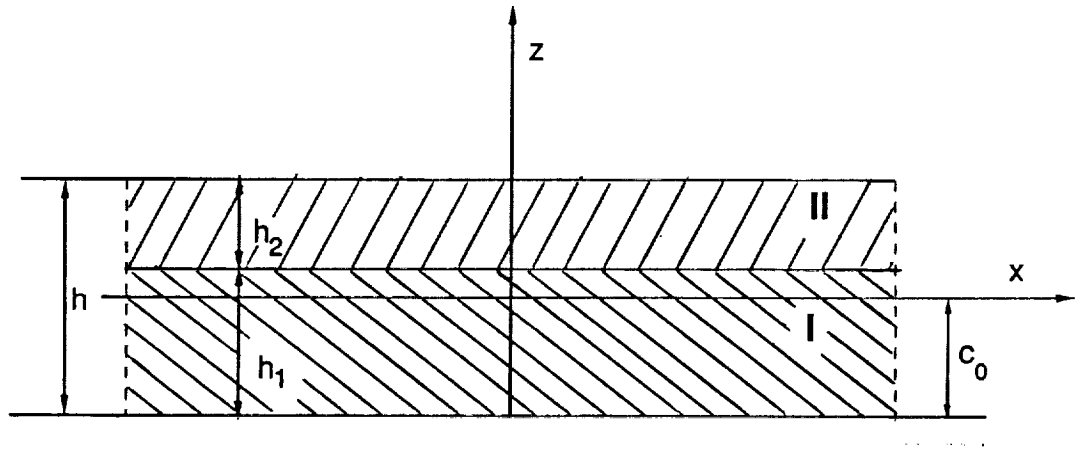

Figure 2.2 (b) Geometry and notations of the two-layer laminated plate.

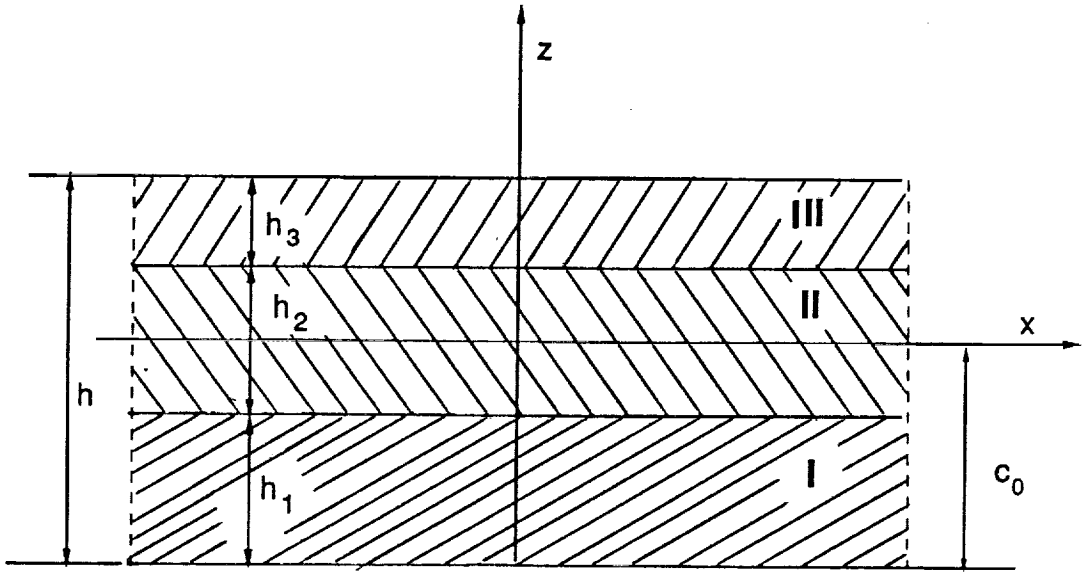

Figure 2.2 (c) Geometry and notations of the three-layer unsymmetric laminated plate.

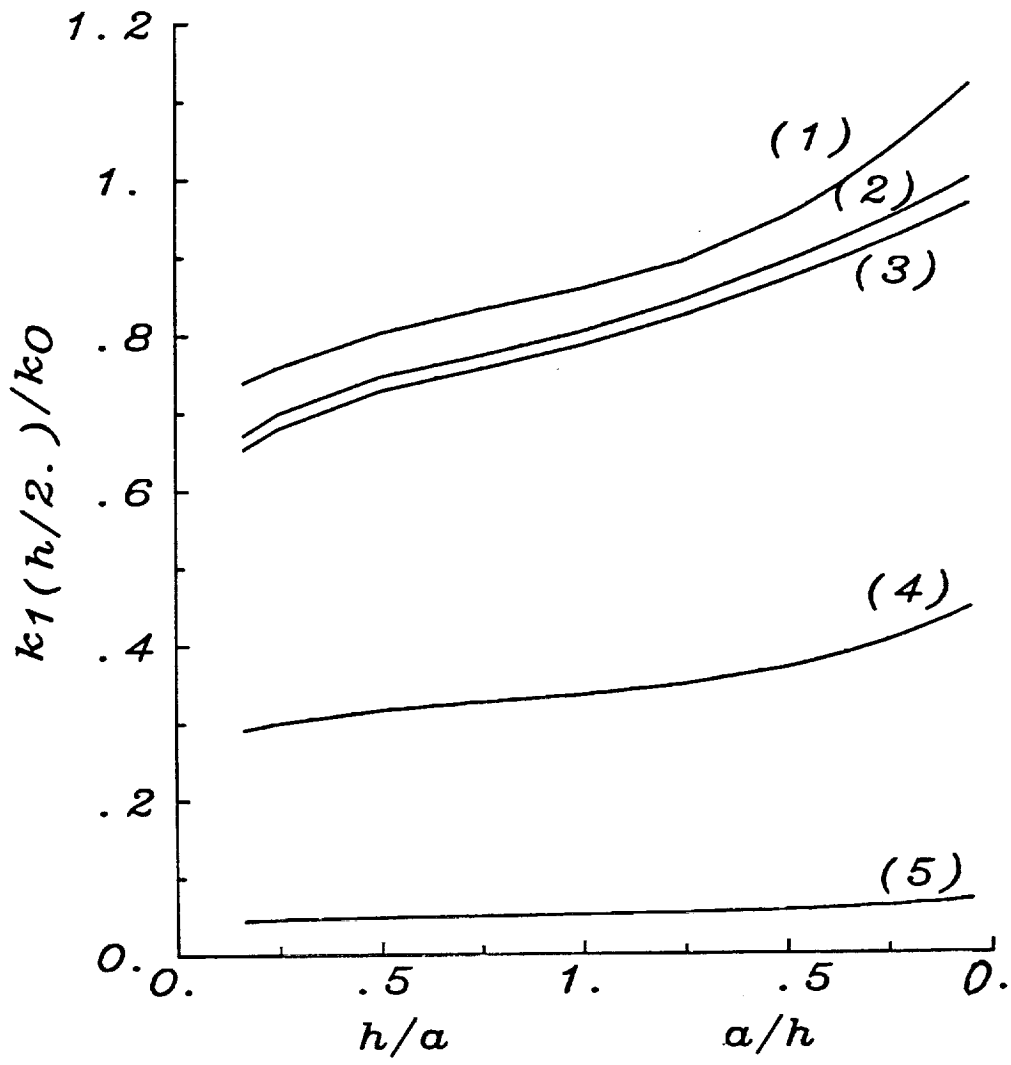

	(1)	(2)	(3)	(4)	(5)
Material II	E_2=390.	Mat.A	Mat.B	E_2=3.9	E_2=0.39

Figure 2.3 Normalized stress intensity factor in a 3-symmetrically-layered plate containing a through crack of length 2a. (see Figure 2.2 a)
(Material I is fixed as Material A and Material II is Material A, Material B, or isotropic materials with $\nu_2 \equiv 0.3$ and E_2 = 390., 3.9, 0.39 (GPA) respectively)
($k_0 = \sigma_b \sqrt{a}$, $\sigma_b = 6\, M^{\infty}/h^2$, $h_1 = h_2 = h/2.$)

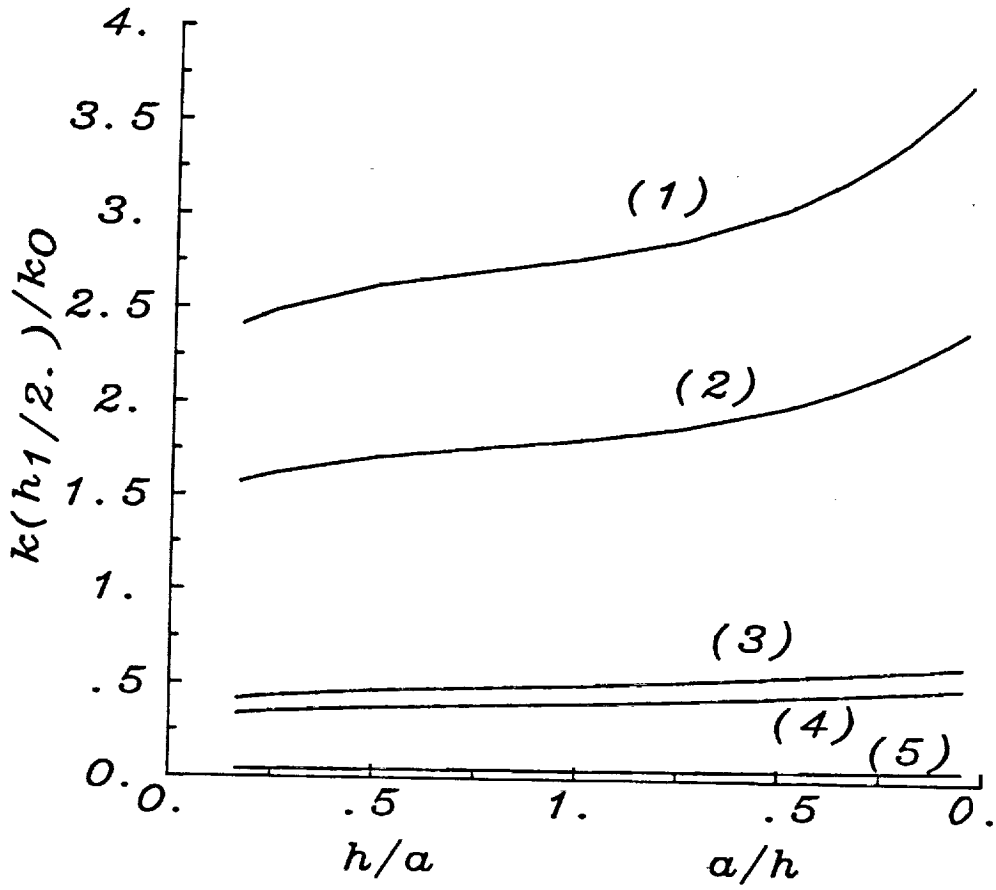

	(1)	(2)	(3)	(4)	(5)
Material II	E_2=0.39	E_2=3.9	Mat.B	Mat.A	E_2=390.

Figure 2.4 Normalized stress intensity factor in a 3-symmetrically-layered plate containing a through crack of length 2a. (see Figure 2.2 a)
(Material I is fixed as Material A and Material II is Material A, Material B, or isotropic materials with $\nu_2 \equiv 0.3$ and E_2 = 390., 3.9, 0.39 (GPA) respectively)
($k_0 = \sigma_b \sqrt{a}$, $\sigma_b = 6\, M^{\infty}/h^2$, $h_1 = h_2 = h/2.$)

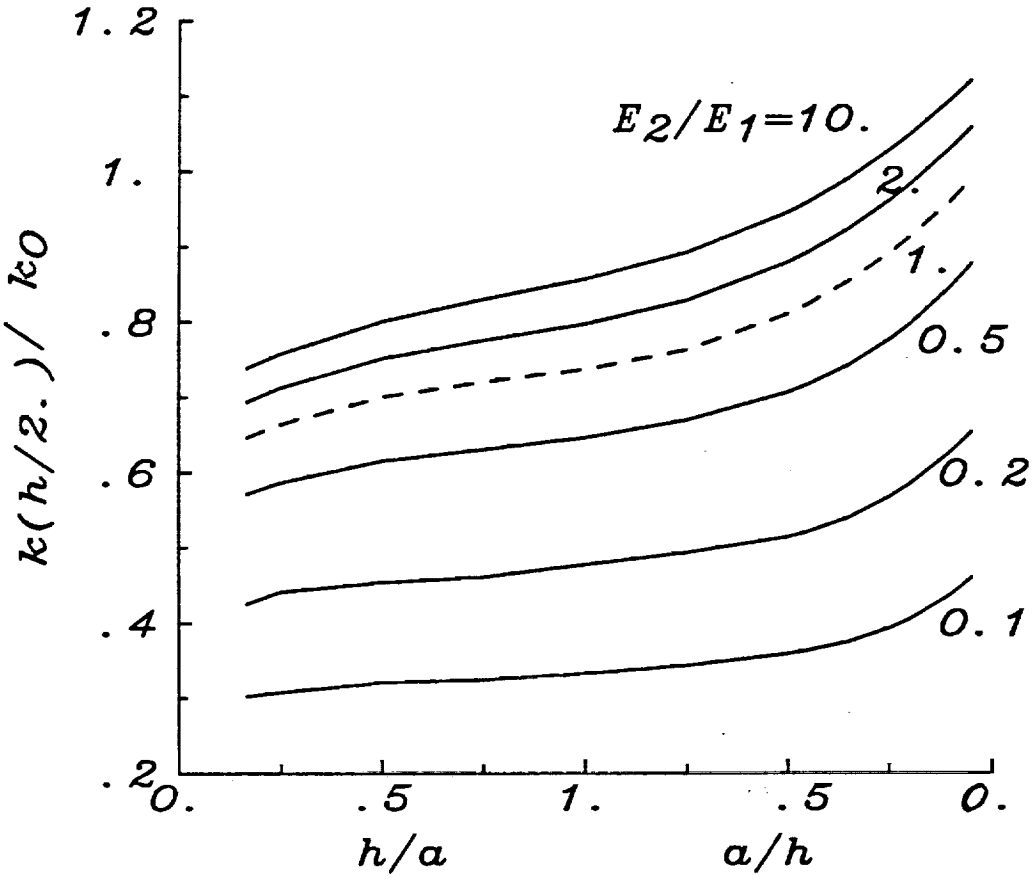

Figure 2.5 Normalized stress intensity factor in a 3-symmetrically-layered plate containing a through crack of length 2a. (see Figure 2.2 a)
(both Material I and Material II are isotropic materials with $\nu_1 = \nu_2 = 0.3$ and different E_2/E_1 ratios)
($k_0 = \sigma_b \sqrt{a}$, $\sigma_b = 6\, M^{\infty}/h^2$, $h_1 = h_2 = h/2.$)

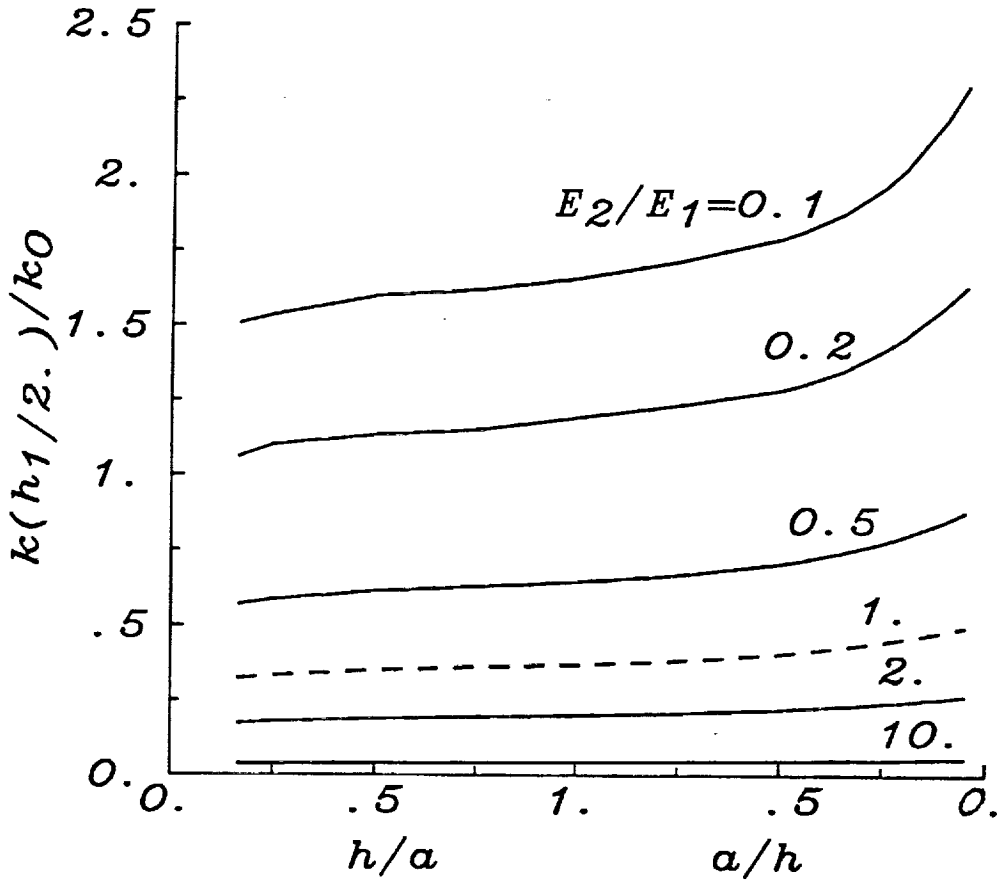

Figure 2.6 Normalized stress intensity factor in a 3-symmetrically-layered plate containing a through crack of length 2a. (see Figure 2.2 a)
(both Material I and Material II are isotropic materials with $\nu_1 = \nu_2 = 0.3$ and different E_2/E_1 ratios)
($k_0 = \sigma_b \sqrt{a}$, $\sigma_b = 6\, M^{\infty}/h^2$, $h_1 = h_2 = h/2.$)

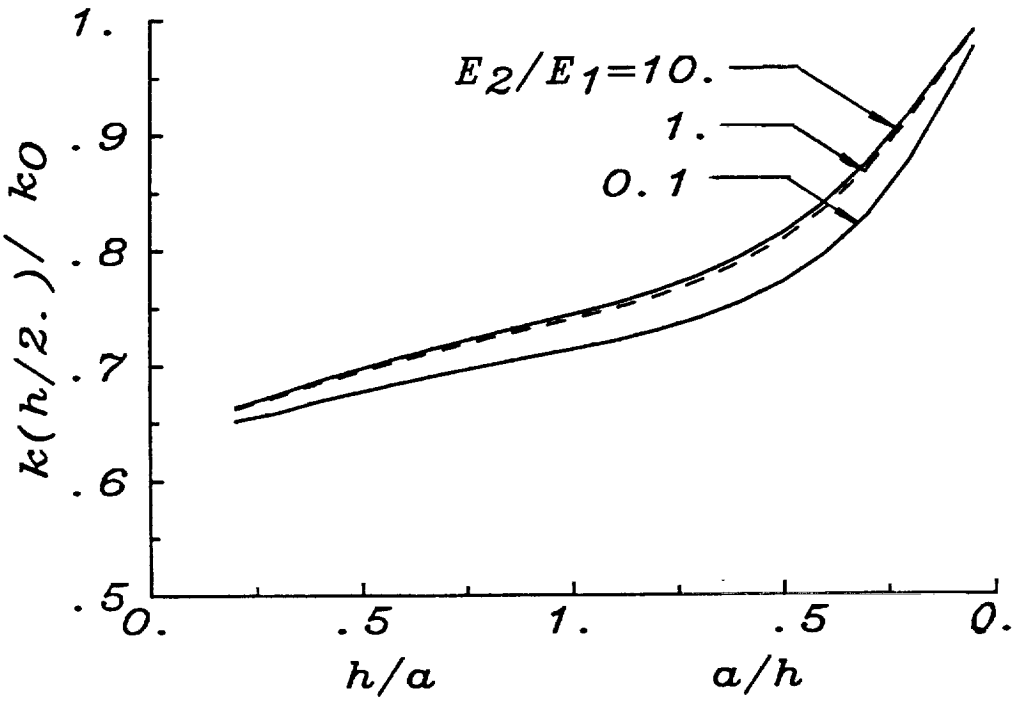

Figure 2.7 Normalized stress intensity factor in a 3-symmetrically-layered plate containing a through crack of length 2a. (see Figure 2.2 a)
(both Material I and Material II are isotropic materials with $\nu_1 = \nu_2 = 0.3$ and different E_2/E_1 ratios)
($k_0 = \sigma_b \sqrt{a}$, $\sigma_b = 6\, M^{\infty}/h^2$, $h_1/h_2 = 0.1$)

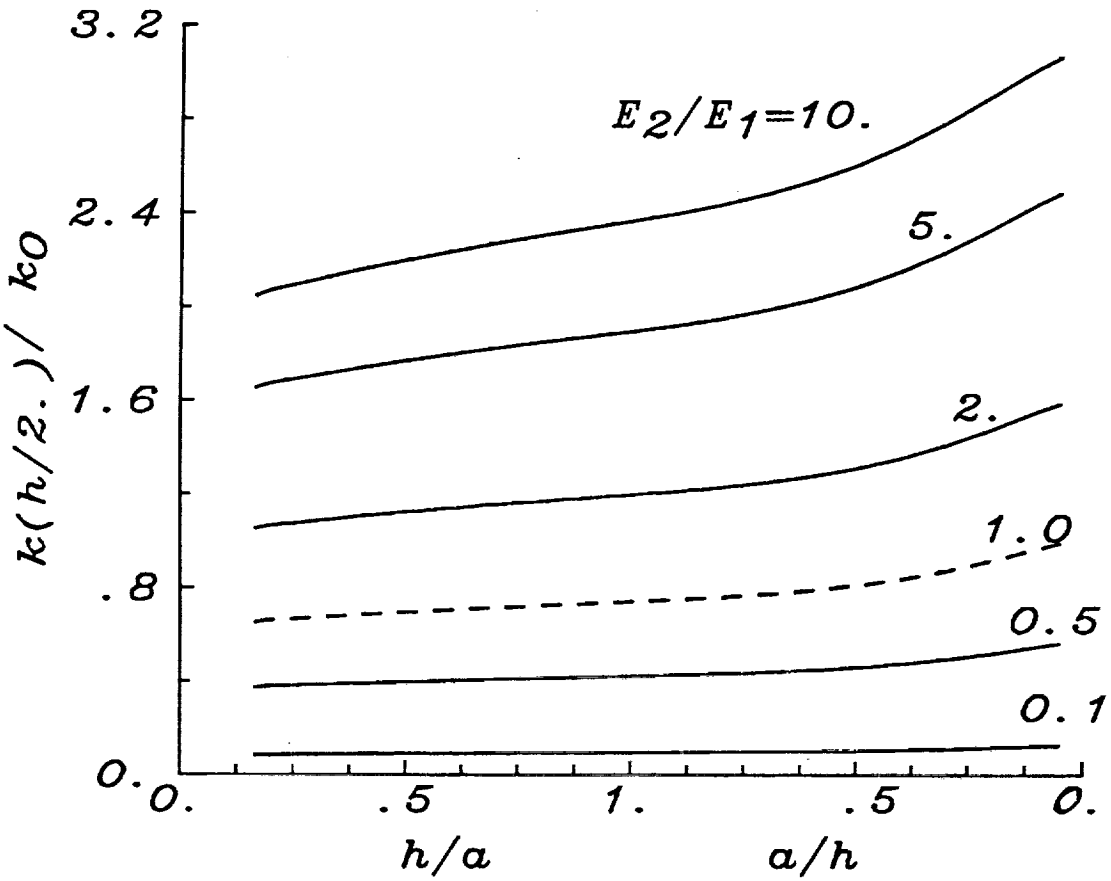

Figure 2.8 Normalized stress intensity factor in a 3-symmetrically-layered plate containing a through crack of length 2a. (see Figure 2.2 a)
(both Material I and Material II are isotropic materials with $\nu_1 = \nu_2 = 0.3$ and different E_2/E_1 ratios)
($k_0 = \sigma_b \sqrt{a}$, $\sigma_b = 6\, M^{\infty}/h^2$, $h_1/h_2 = 10$)

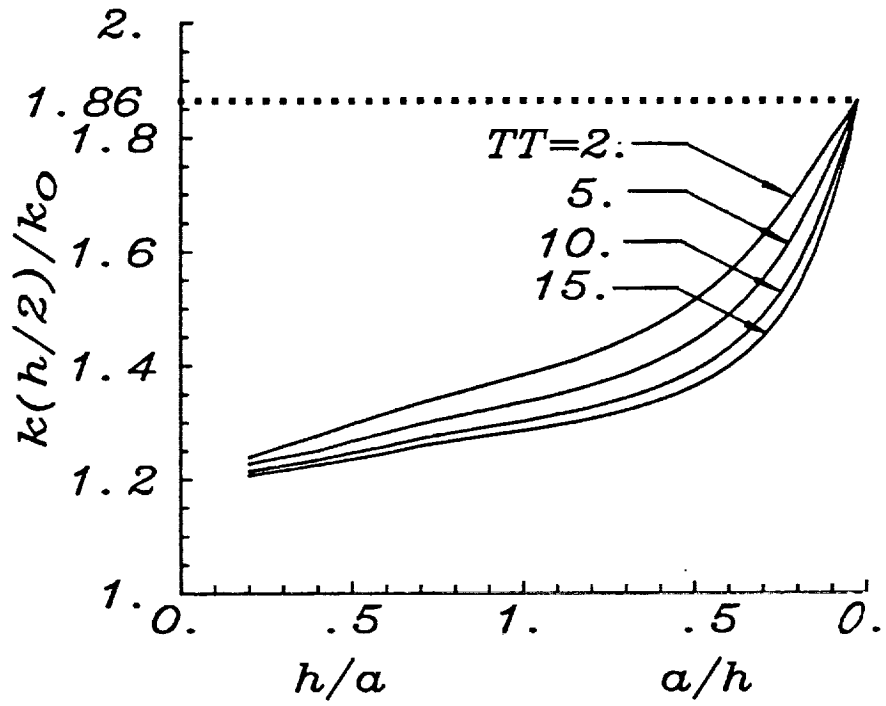

Figure 2.9 Normalized stress intensity factor in a 3-symmetrically-layered "honeycomb structure" plate containing a through crack of length 2a.
(Material II is isotropic material and being fixed ,

for Material I $TT = \frac{G_{xz}}{G_{xy}} = \frac{G_{yz}}{G_{xy}}$)

($k_0 = \sigma_b \sqrt{a}$, $\sigma_b = 6\, M^{\infty}/h^2$, $h_1/h_2 = 5$, $E_2/E_1 = 5$)

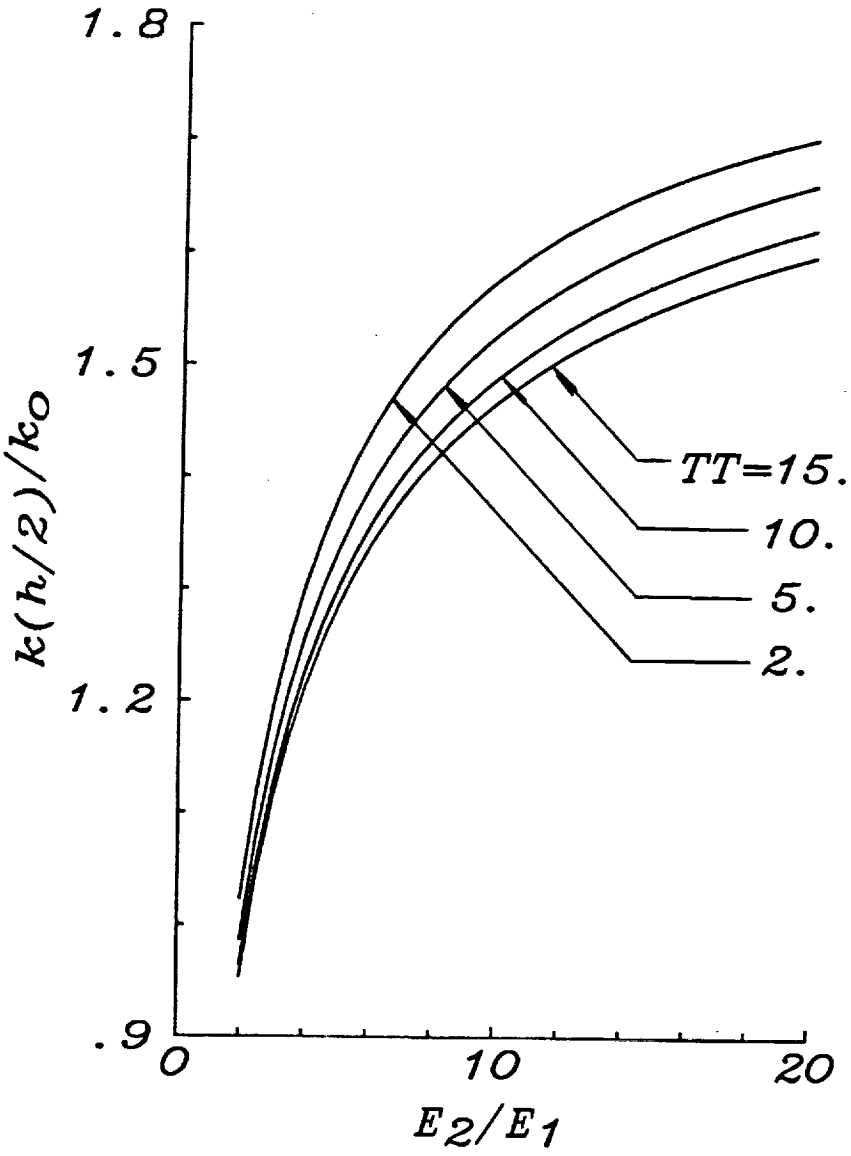

Figure 2.10 Normalized stress intensity factor in a 3-symmetrically-layered "honeycomb structure" plate containing a through crack of length 2a. (Material II is isotropic material and being fixed ,

for Material I $TT = \frac{G_{xz}}{G_{xy}} = \frac{G_{yz}}{G_{xy}}$)

($k_0 = \sigma_b \sqrt{a}$, $\sigma_b = 6\, M^{\infty}/h^2$, $h_1/h_2 = 5$, $a/h = 1$)

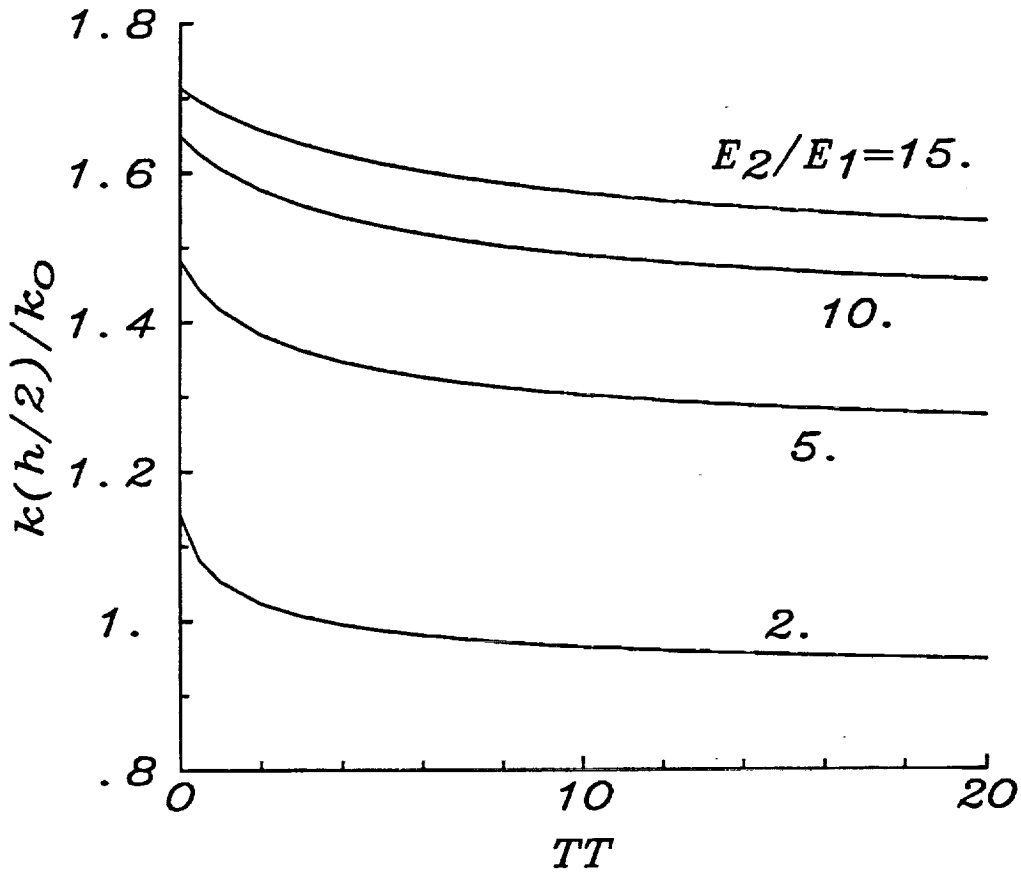

Figure 2.11 Normalized stress intensity factor in a 3-symmetrically-layered "honeycomb structure" plate containing a through crack of length 2a. (Material II is isotropic material and being fixed ,

for Material I $TT = \frac{G_{xz}}{G_{xy}} = \frac{G_{yz}}{G_{xy}}$)

($k_0 = \sigma_b \sqrt{a}$, $\sigma_b = 6\, M^{\infty}/h^2$, $h_1/h_2 = 5$, $a/h = 1$)

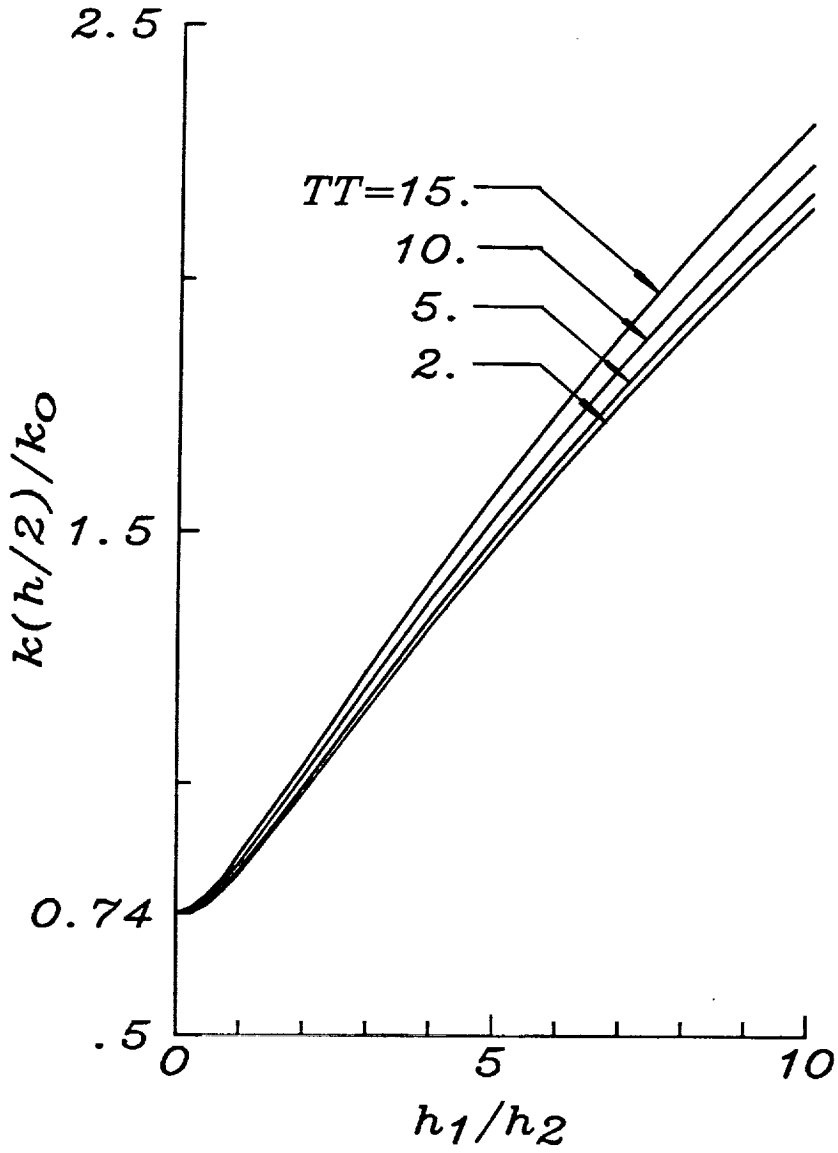

Figure 2.12 Normalized stress intensity factor in a 3-symmetrically-layered "honeycomb structure" plate containing a through crack of length 2a. (Material II is isotropic material and being fixed ,

for Material I $TT = \frac{G_{xz}}{G_{xy}} = \frac{G_{yz}}{G_{xy}}$)

($k_0 = \sigma_b \sqrt{a}$, $\sigma_b = 6\, M^{\infty}/h^2$, $E_2/E_1 = 10$, $a/h = 1$)

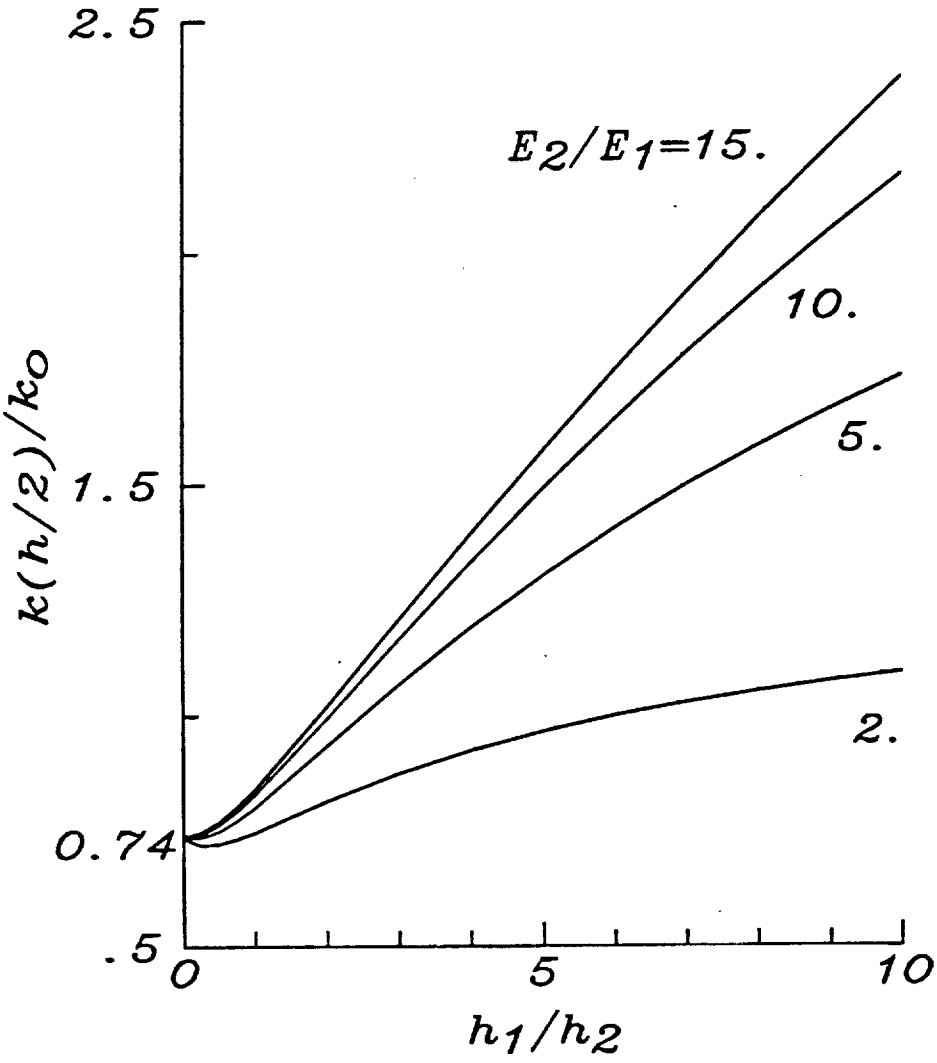

Figure 2.13 Normalized stress intensity factor in a 3-symmetrically-layered "honeycomb structure" plate containing a through crack of length 2a.
(Material II is isotropic material and being fixed ,

for Material I $TT = \frac{G_{xz}}{G_{xy}} = \frac{G_{yz}}{G_{xy}}$)

($k_0 = \sigma_b \sqrt{a}$, $\sigma_b = 6\, M^{\infty}/h^2$, TT = 10, a/h = 1)

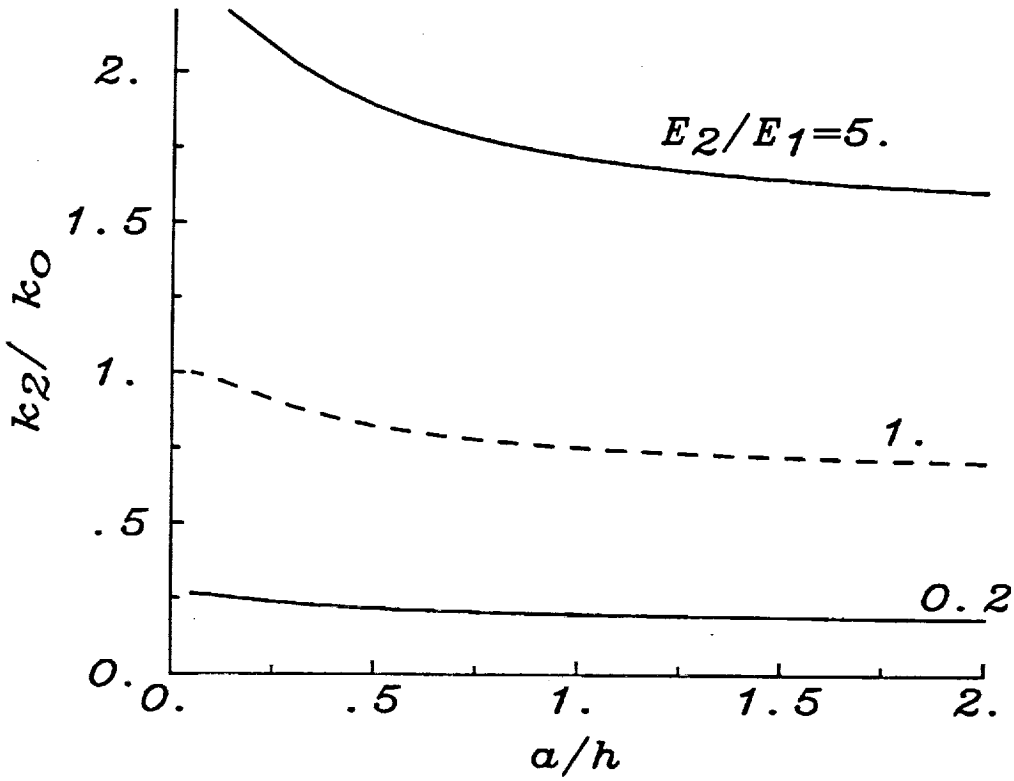

Figure 2.14 Normalized stress intensity factor in a two - layer isotropic plate containing a through crack of length 2a under bending. (see Figure 2.2 b)
(both Material I and Material II are isotropic materials with $\nu_1 = \nu_2 = 0.3$ and different E_2/E_1 ratios)
($k_2 = k(h\text{-}c_0)$, $k_0 = \sigma_b \sqrt{a}$, $\sigma_b = 6\, M^{\infty}/h^2$, $h_2/h_1 = 0.1$)

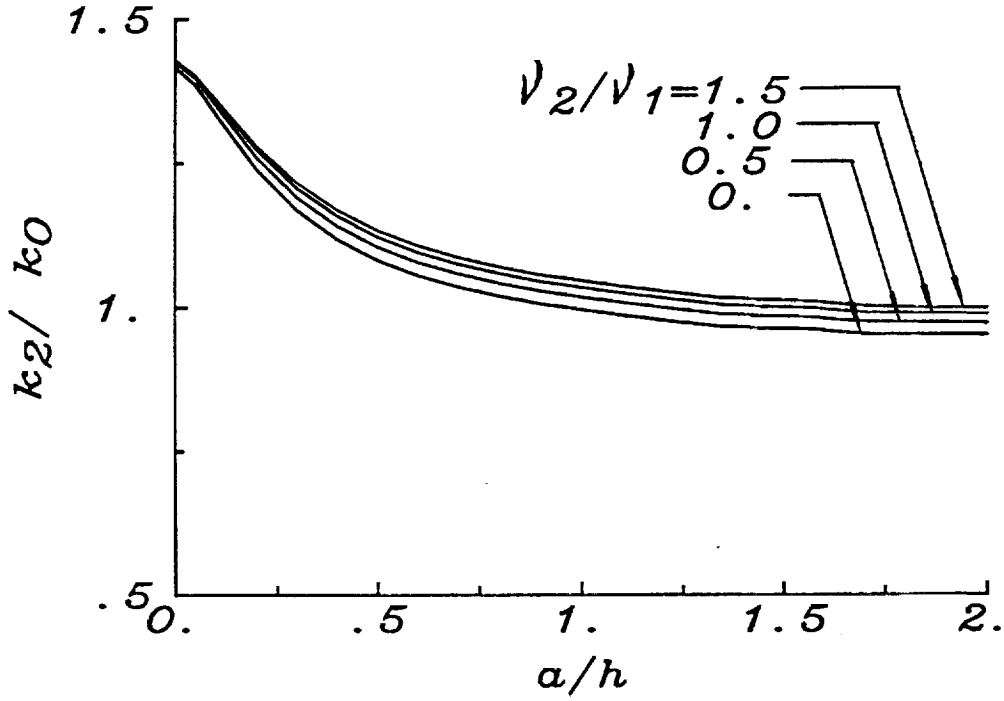

Figure 2.15 Normalized stress intensity factor in a two - layer isotropic plate containing a through crack of length 2a under bending. (see Figure 2.2 b)
(both Material I and Material II are isotropic materials with ν_1 = 0.3 and different ν_2/ν_1 ratios)
($k_2 = k(h\text{-}c_0)$, $k_0 = \sigma_b \sqrt{a}$, $\sigma_b = 6\, M^{\infty}/h^2$, $h_2/h_1 = 1$)

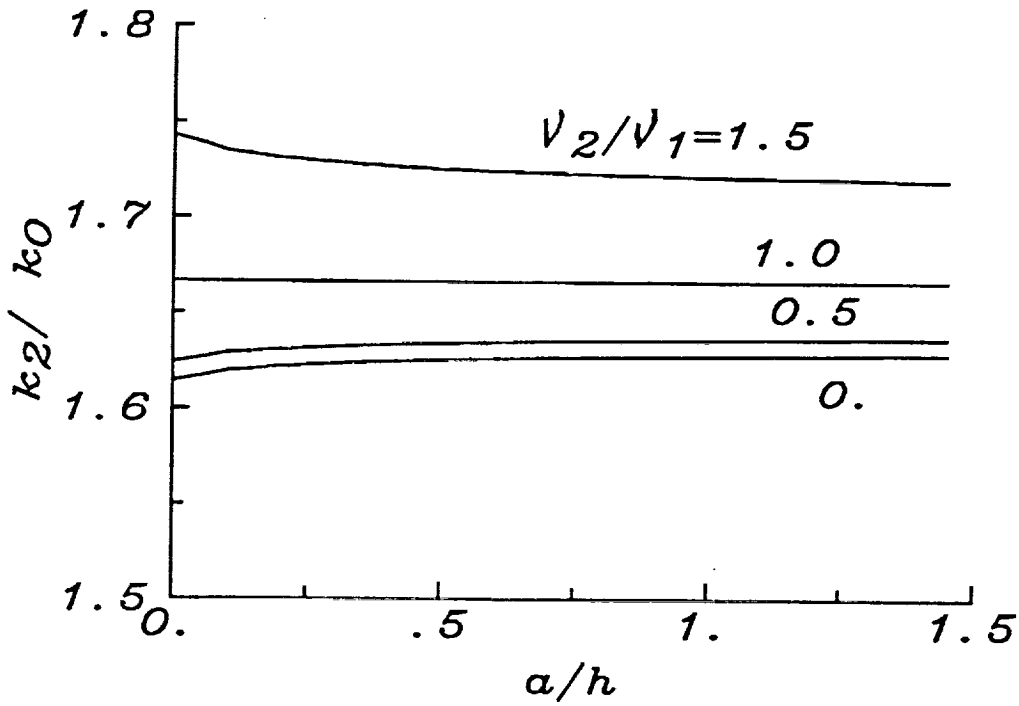

Figure 2.16 Normalized stress intensity factor in a two - layer isotropic plate containing a through crack of length 2a under tension. (see Figure 2.2 b)
(both Material I and Material II are isotropic materials
with $\nu_1 = 0.3$ and different ν_2/ν_1 ratios)
($k_2 = k(h\text{-}c_0)$, $k_0 = \sigma_t \sqrt{a}$, $\sigma_t = N^{\infty}/h$, $h_2/h_1 = 1$)

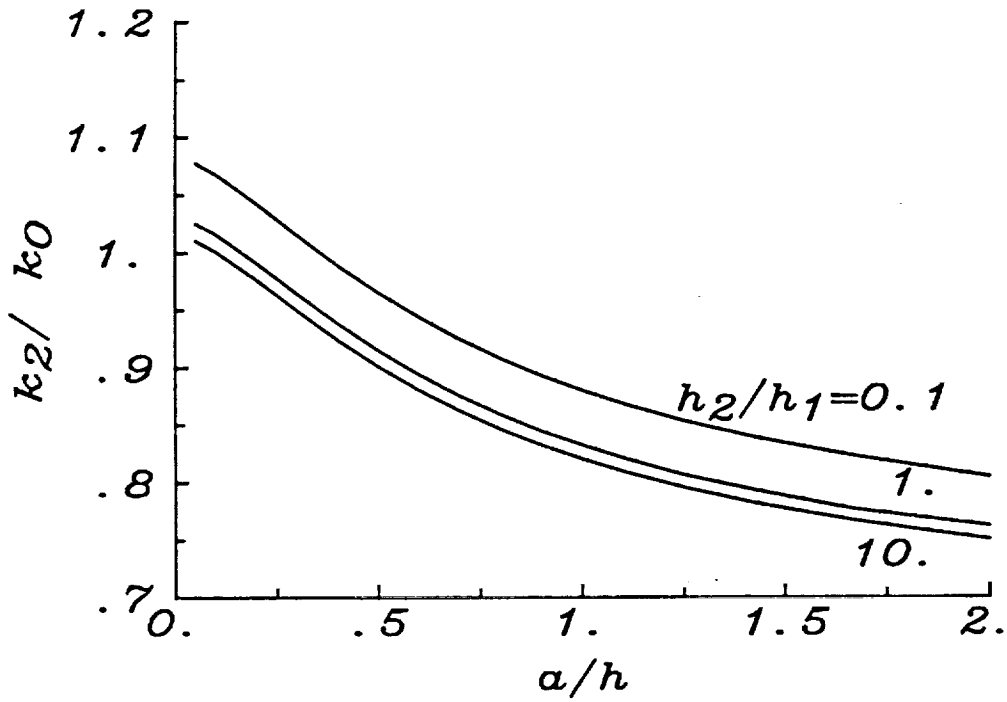

Figure 2.17 Normalized stress intensity factor in a two - layer orthotropic plate containing a through crack of length 2a under bending. (see Figure 2.2 b)
(both Material I and Material II are orthotropic materials
with Material I being Material B and Material II being Material A)
($k_2 = k(h\text{-}c_0)$, $k_0 = \sigma_b \sqrt{a}$, $\sigma_b = 6\, M^{\infty}/h^2$)

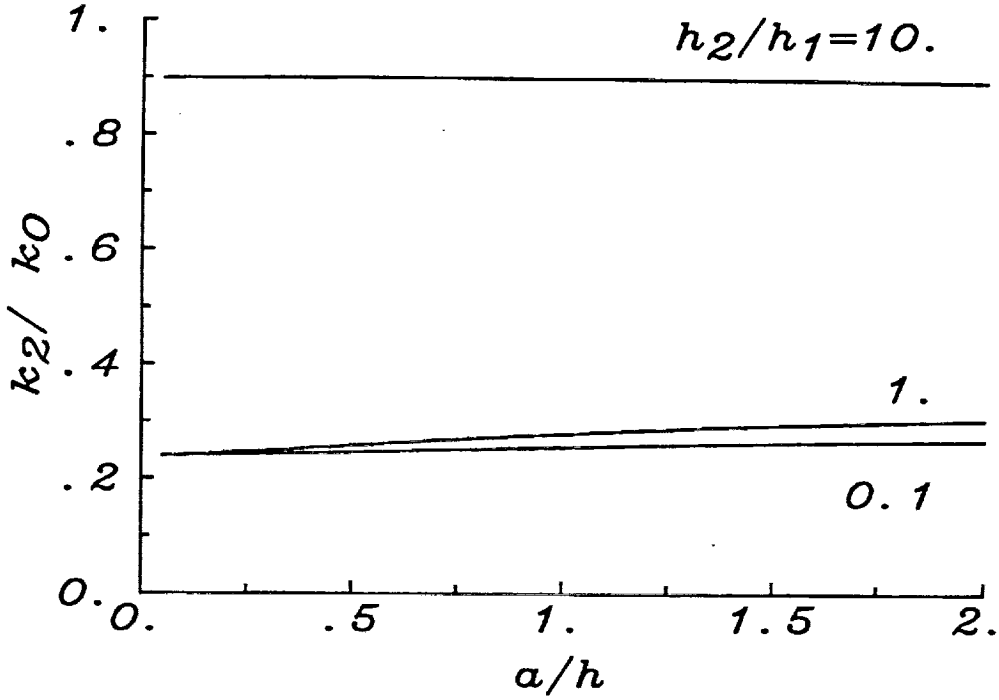

Figure 2.18 Normalized stress intensity factor in a two - layer orthotropic plate containing a through crack of length 2a under tension. (see Figure 2.2 b)
(both Material I and Material II are orthotropic materials
with Material I being Material C and Material II being Material D)
($k_2 = k(h\text{-}c_0)$, $k_0 = \sigma_t \sqrt{a}$, $\sigma_t = N^{\infty}/h$)

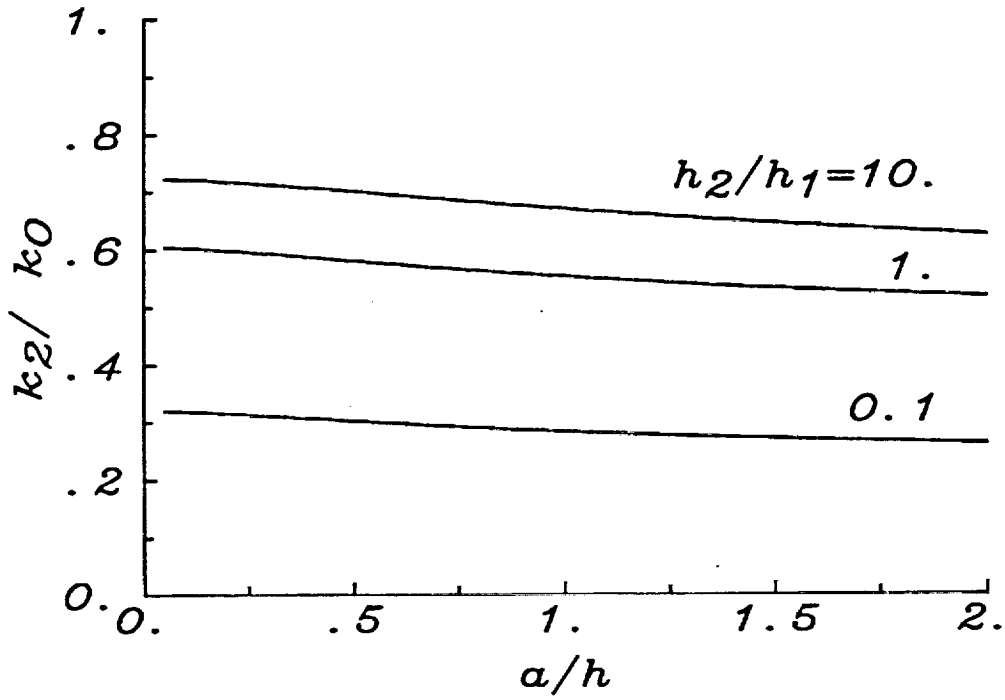

Figure 2.19 Normalized stress intensity factor in a two - layer orthotropic plate containing a through crack of length 2a under bending. (see Figure 2.2 b)
(both Material I and Material II are orthotropic materials
with Material I being Material C and Material II being Material D)
($k_2 = k(h\text{-}c_0)$, $k_0 = \sigma_b \sqrt{a}$, $\sigma_b = 6\, M^{\infty}/h^2$)

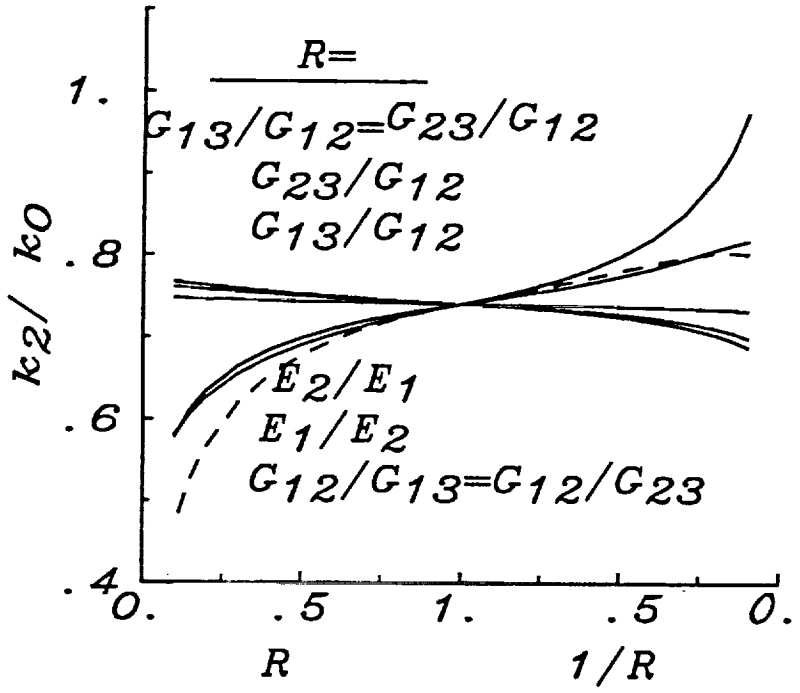

Figure 2.20 The effect of individual material constants on the normalized stress intensity factor in a two - layer plate containing a through crack of length 2a under bending moment M^{∞}. (see Figure 2.2 b)
(Material I is isotropic materials and it is fixed; Material II is assumed to be "isotropic" expect one constant varies)
($k_2 = k(h\text{-}c_0)$, $k_0 = \sigma_b \sqrt{a}$, $\sigma_b = 6\, M^{\infty}/h^2$)
($a/h = 1$, $h_1/h_2 = 1$)

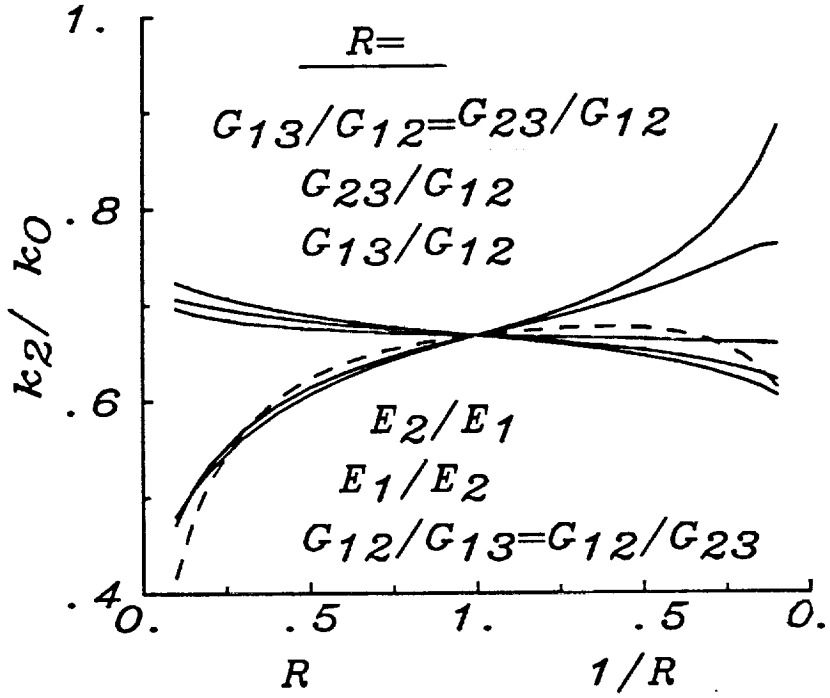

Figure 2.21 The effect of individual material constants on the normalized stress intensity factor in a two - layer plate containing a through crack of length 2a under bending moment M^{∞}. (see Figure 2.2 b)
(Material I is Material D, an orthotropic material, Material II is assumed to be "isotropic", with E = 40.41 (GPA), expect one constant varies)
($k_2 = k(h\text{-}c_0)$, $k_0 = \sigma_b \sqrt{a}$, $\sigma_b = 6\, M^{\infty}/h^2$)
($a/h = 1$, $h_2/h_1 = 1$)

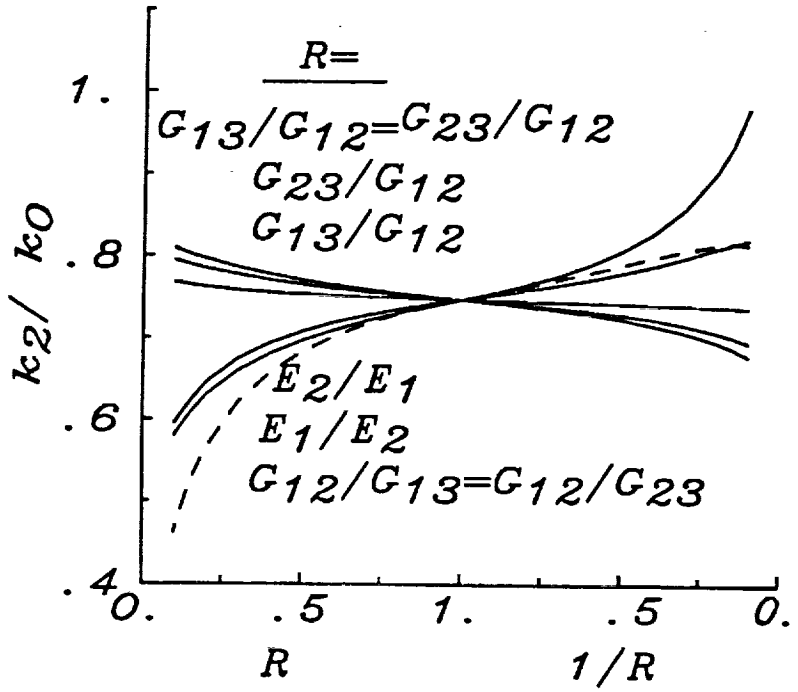

Figure 2.22 The effect of individual material constants on the normalized stress intensity factor in a two - layer plate containing a through crack of length 2a under bending moment M^{∞}. (see Figure 2.2 b) (Material I is Material A, an orthotropic material, Material II is assumed to be "isotropic", with E = 39.0 (GPA), expect one constant varies)

($k_2 = k(h\text{-}c_0)$, $k_0 = \sigma_b \sqrt{a}$, $\sigma_b = 6\, M^{\infty}/h^2$)

($a/h = 1$, $h_2/h_1 = 1$)

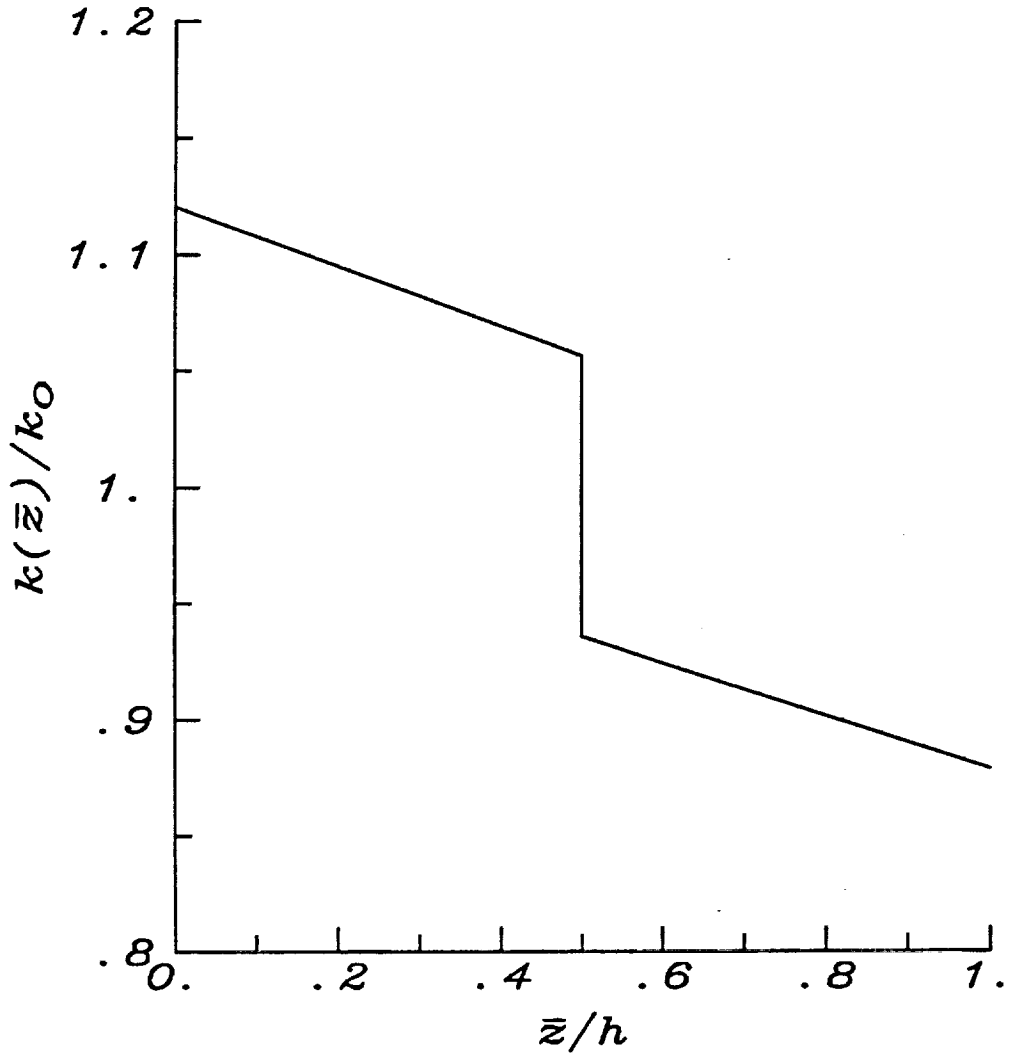

Figure 2.23 Normalized stress intensity factor distribution in a two - layer orthotropic plate containing a through crack of length 2a under tension. (see Figure 2.2 b)
(both Material I and Material II are orthotropic materials
with Material I being Material A and Material II being Material B)
($\bar{z} = z + c_0$, $k_0 = \sigma_t \sqrt{a}$, $\sigma_t = N^{\infty}/h$)
($a/h = 1$, $h_2/h_1 = 1$)

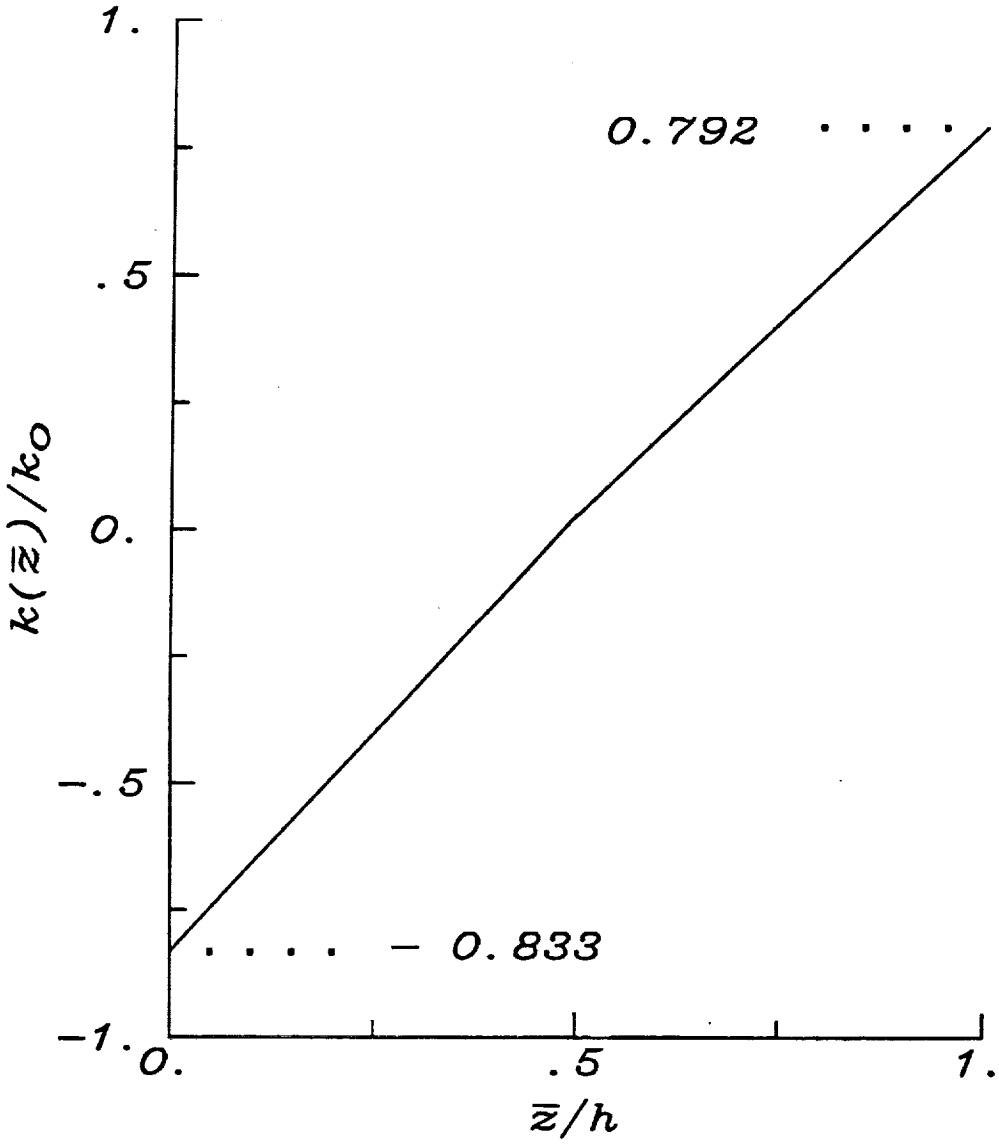

Figure 2.24 Normalized stress intensity factor distribution in a two - layer orthotropic plate containing a through crack of length 2a under bending. (see Figure 2.2 b)
(both Material I and Material II are orthotropic materials
with Material I being Material A and Material II being Material B)
($\bar{z} = z + c_0$, $k_0 = \sigma_b \sqrt{a}$, $\sigma_b = 6\, M^{\infty}/h^2$)
($a/h = 1$, $h_2/h_1 = 1$)

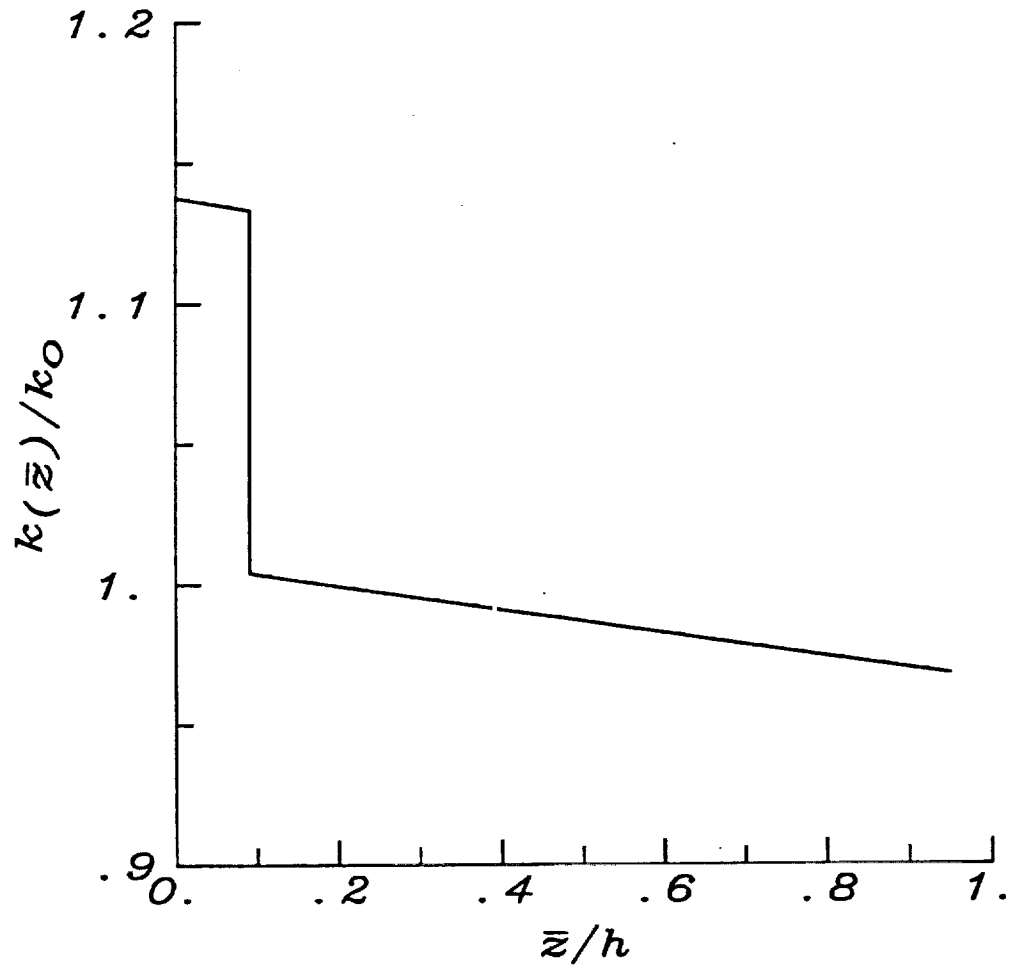

Figure 2.25 Normalized stress intensity factor distribution in a two - layer orthotropic plate containing a through crack of length 2a under tension. (see Figure 2.2 b)
(both Material I and Material II are orthotropic materials
with Material I being Material A and Material II being Material B)
($\bar{z} = z + c_0$, $k_0 = \sigma_t \sqrt{a}$, $\sigma_t = N^{\infty}/h$)
($a/h = 1$, $h_2/h_1 = 10$)

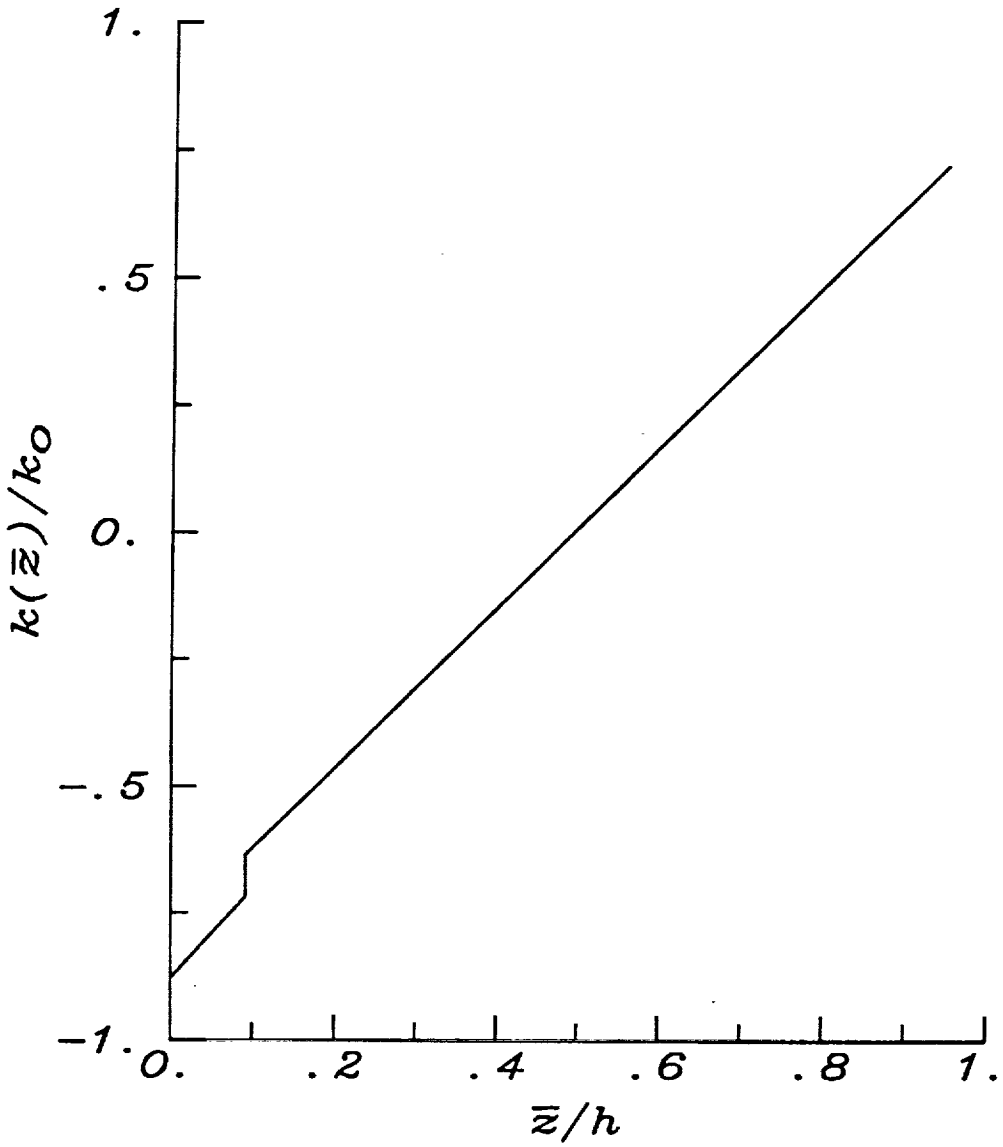

Figure 2.26 Normalized stress intensity factor distribution in a two - layer orthotropic plate containing a through crack of length 2a under bending. (see Figure 2.2 b)
(both Material I and Material II are orthotropic materials
with Material I being Material A and Material II being Material B)
($\bar{z} = z + c_0$, $k_0 = \sigma_b \sqrt{a}$, $\sigma_b = 6\ M^{\infty}/h^2$)
($a/h = 1$, $h_2/h_1 = 10$)

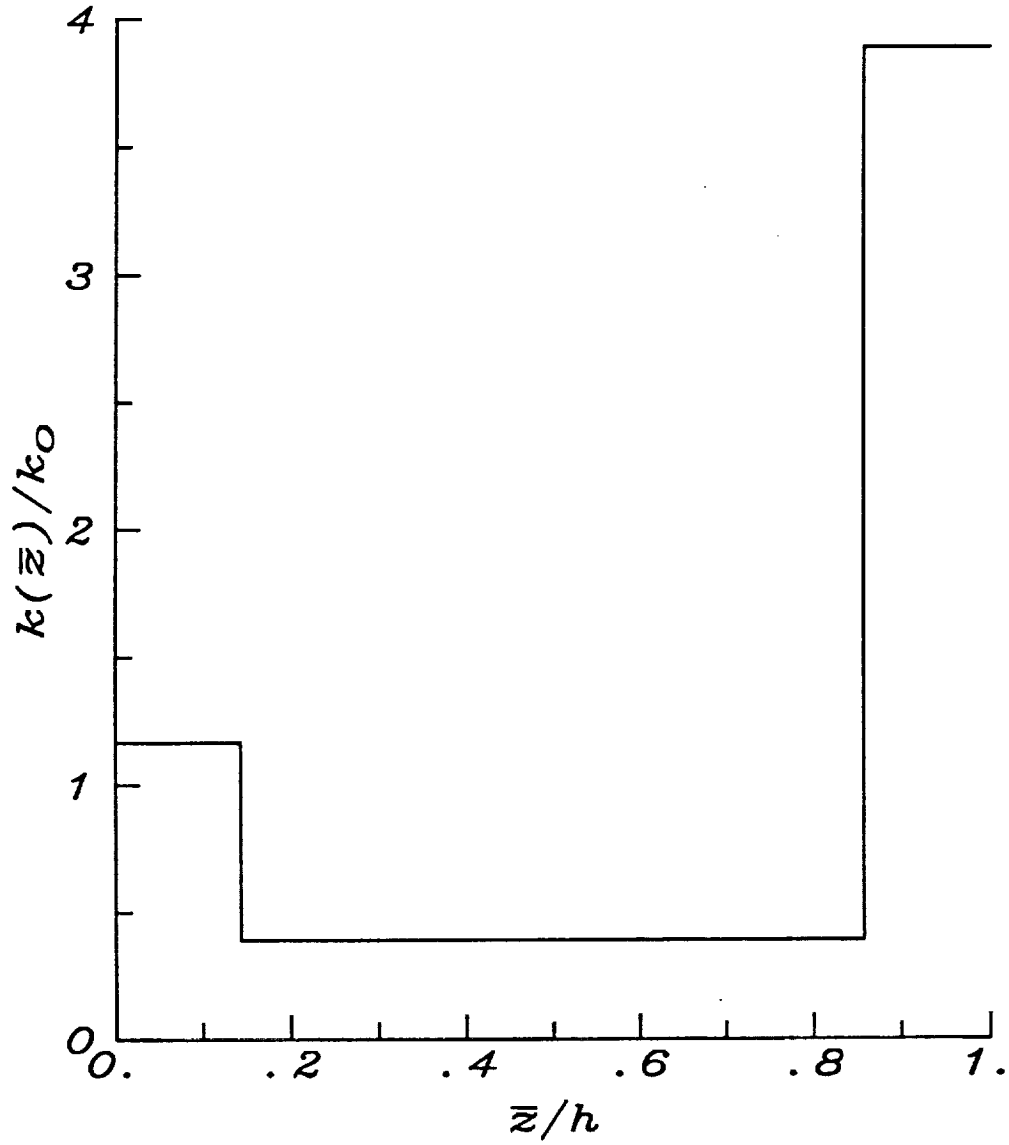

Figure 2.27 Normalized stress intensity factor distribution in a 3-unsymmetrically -layered plate containing a through crack under tension. (see Figure 2.2 c)

(Materials I and III are isotropic, with $\nu_1 = \nu_3 = 0.3$,

and $E_1/E_2 = 3.0$, $E_3/E_2 = 10.$;

Material II is "as if" isotropic, with E_2 and $\nu_2 = 0.3$,

and $G_{xz} = G_{yz} = 3\,G_{xy}$)

($\bar{z} = z + c_0$, $k_0 = \sigma_t \sqrt{a}$, $\sigma_t = N^{\infty}/h$)

($a/h = 0.5$, $h_3/h_2 = 0.2$, $h_1/h_2 = 0.2$)

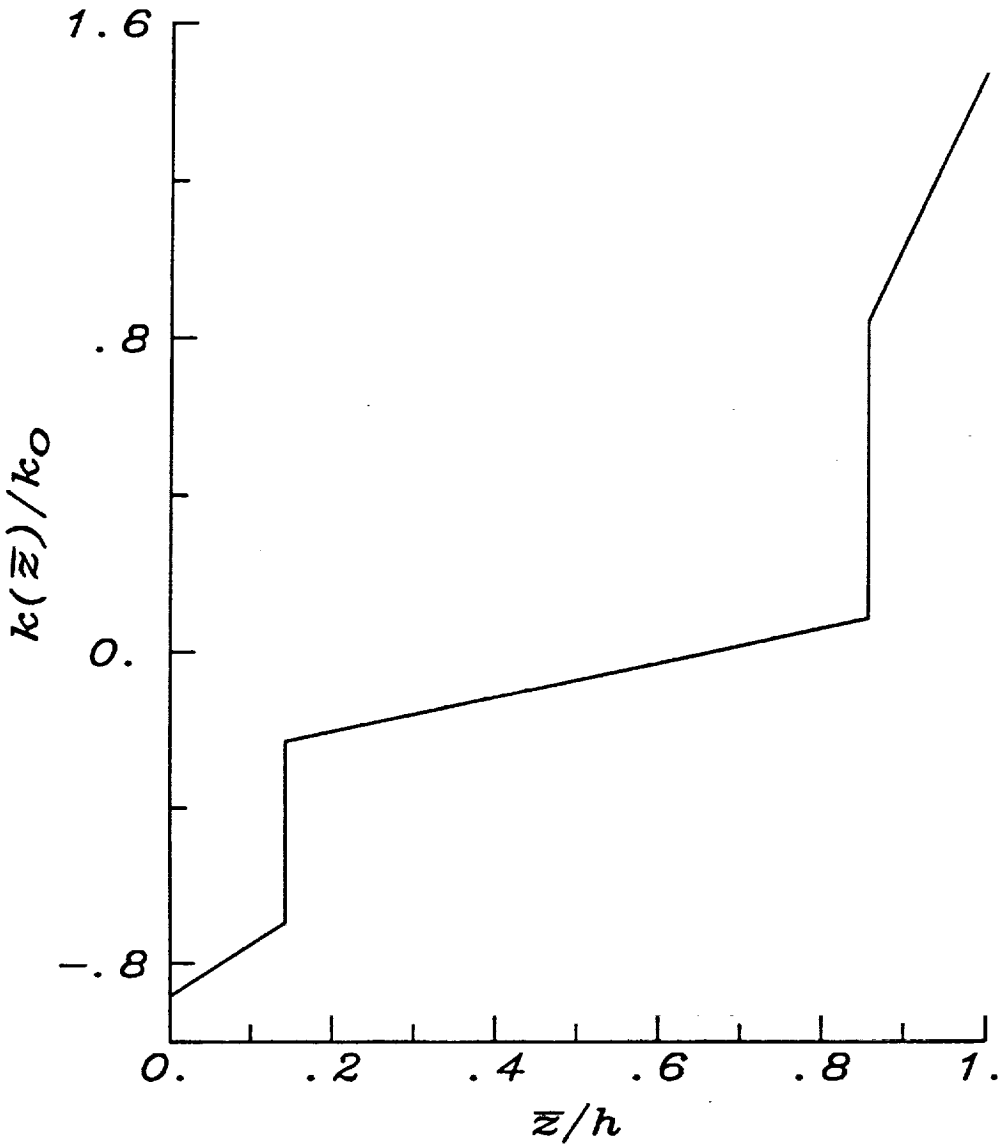

Figure 2.28 Normalized stress intensity factor distribution in a 3-unsymmetrically -layered plate containing a through crack under bending. (see Figure 2.2 c)

(Materials I and III are isotropic, with $\nu_1 = \nu_3 = 0.3$,

and $E_1 / E_2 = 3.0$, $E_3 / E_2 = 10.$;

Material II is "as if" isotropic, with E_2 and $\nu_2 = 0.3$,

and $G_{xz} = G_{yz} = 3\ G_{xy}$)

($\bar{z} = z + c_0$, $k_0 = \sigma_b \sqrt{a}$, $\sigma_b = 6\ M^{\infty}/h^2$)

($a/h = 0.5$, $h_3/h_2 = 0.2$, $h_1/h_2 = 0.2$)

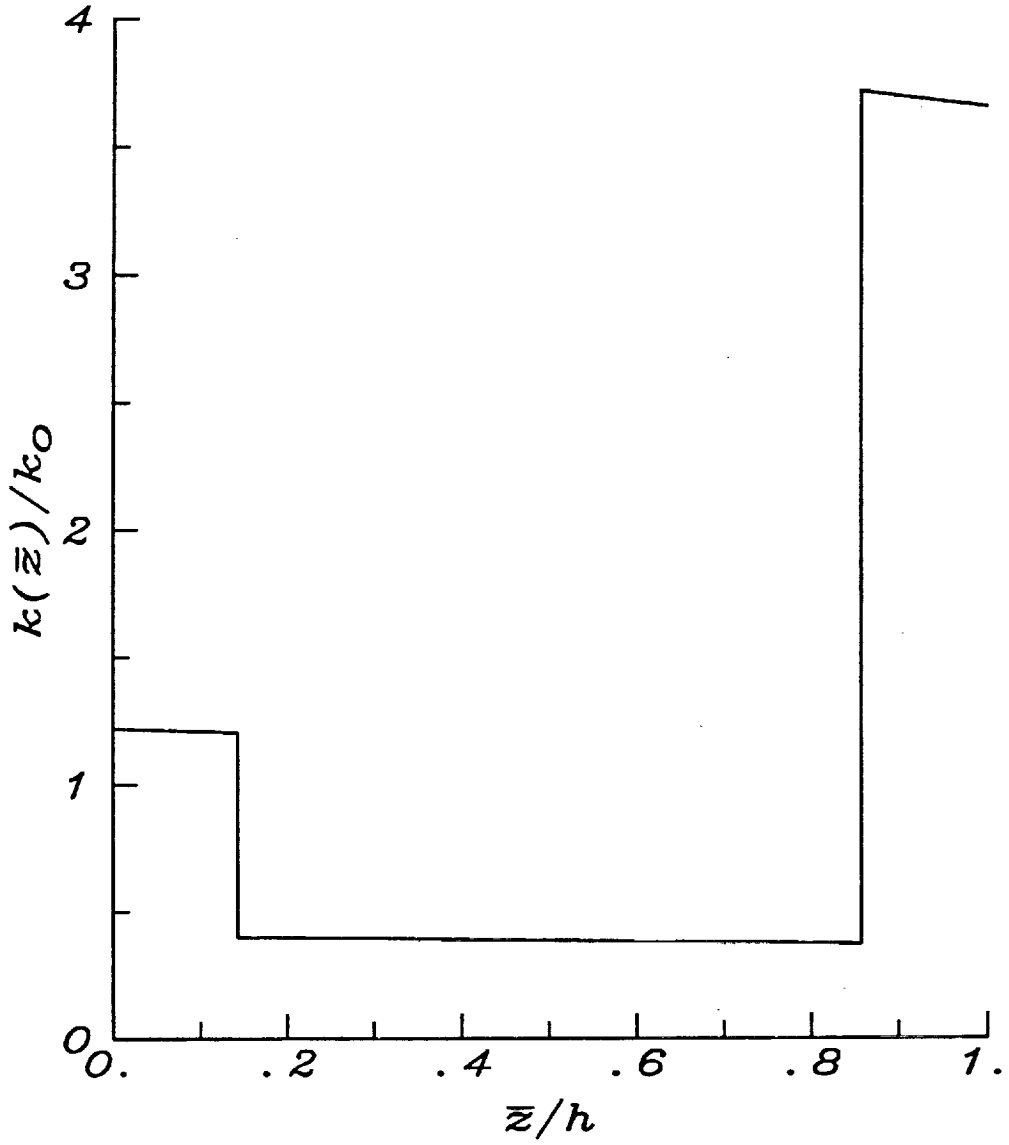

Figure 2.29 Normalized stress intensity factor distribution in a 3-unsymmetrically -layered plate containing a through crack under tension. (see Figure 2.2 c)

(Materials I and III are isotropic, with $\nu_1 = 0.5$ and $\nu_3 = 0.2$,

and $E_1 / E_2 = 3.0$, $E_3 / E_2 = 10.$;

Material II is "as if" isotropic, with E_2 and $\nu_2 = 0.$,

and $G_{xz} = G_{yz} = 3\ G_{xy}$)

($\bar{z} = z + c_0$, $k_0 = \sigma_t \sqrt{a}$, $\sigma_t = N^{\infty}/h$)

($a/h = 0.5$, $h_3/h_2 = 0.2$, $h_1/h_2 = 0.2$)

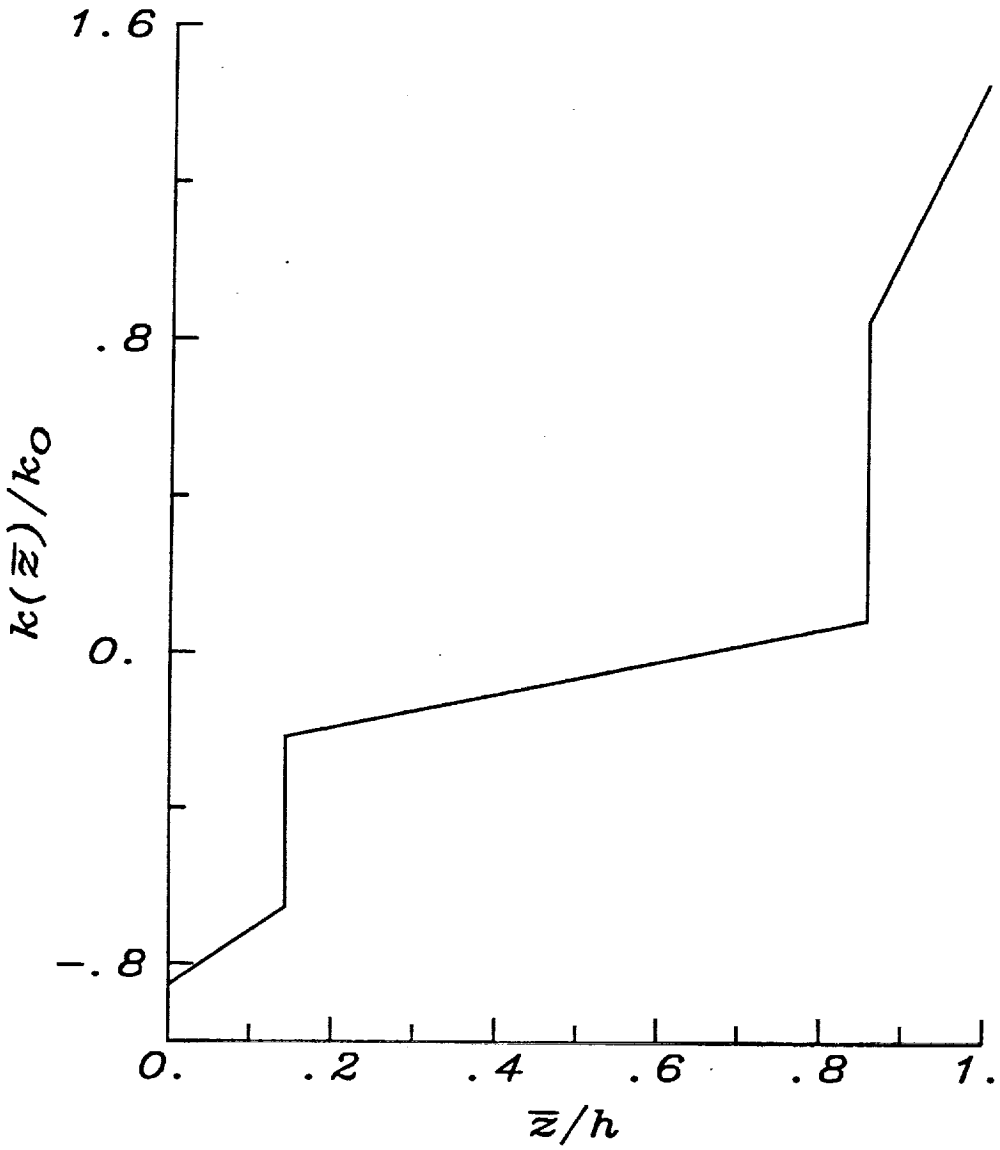

Figure 2.30 Normalized stress intensity factor distribution in a 3-unsymmetrically -layered plate containing a through crack under bending. (see Figure 2.2 c)
(Materials I and III are isotropic, with $\nu_1 = 0.5$ and $\nu_3 = 0.2$,
and $E_1 / E_2 = 3.0$, $E_3 / E_2 = 10.$;
Material II is "as if" isotropic, with E_2 and $\nu_2 = 0.$,
and $G_{xz} = G_{yz} = 3\ G_{xy}$)
($\bar{z} = z + c_0$, $k_0 = \sigma_b \sqrt{a}$, $\sigma_b = 6\ M^{\infty}/h^2$)

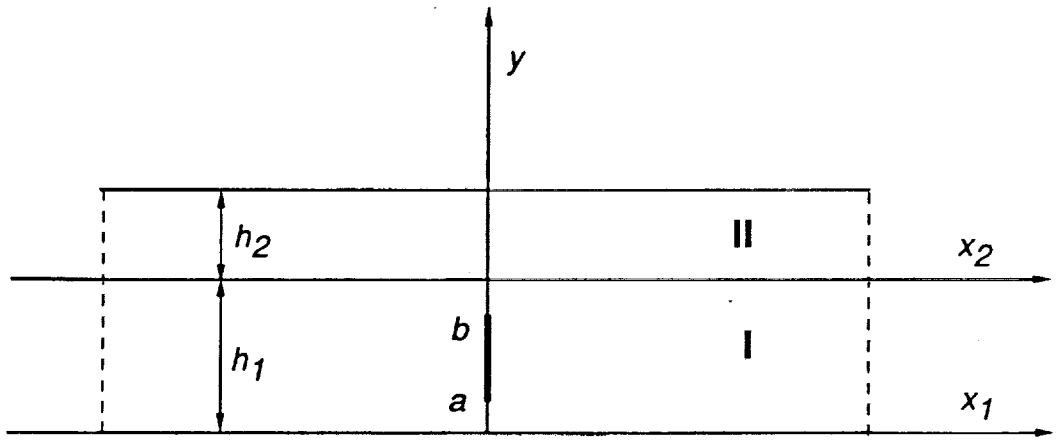

Figure 3.1 Geometry and notation of the crack problem.

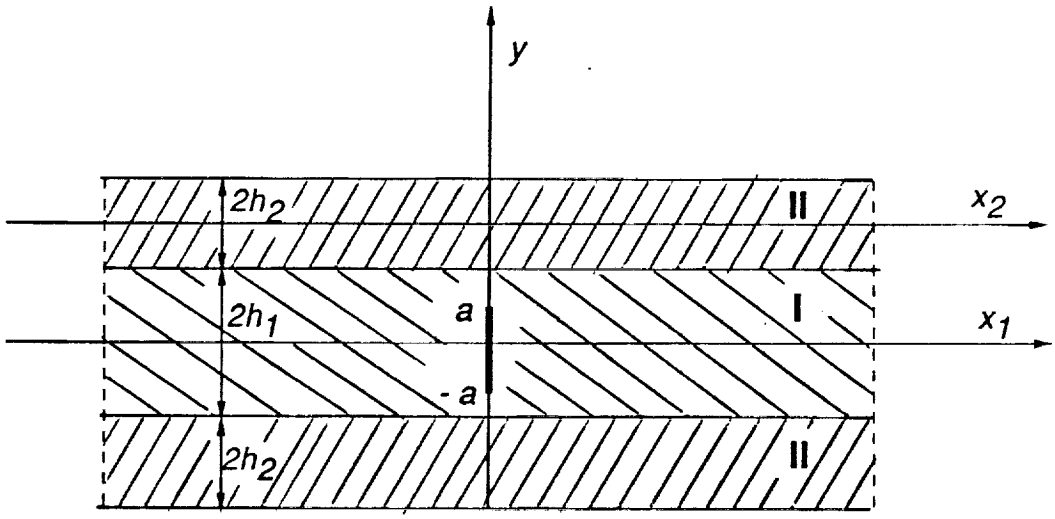

Figure 3.2 Geometry and notation of the corresponding symmetric crack problem.

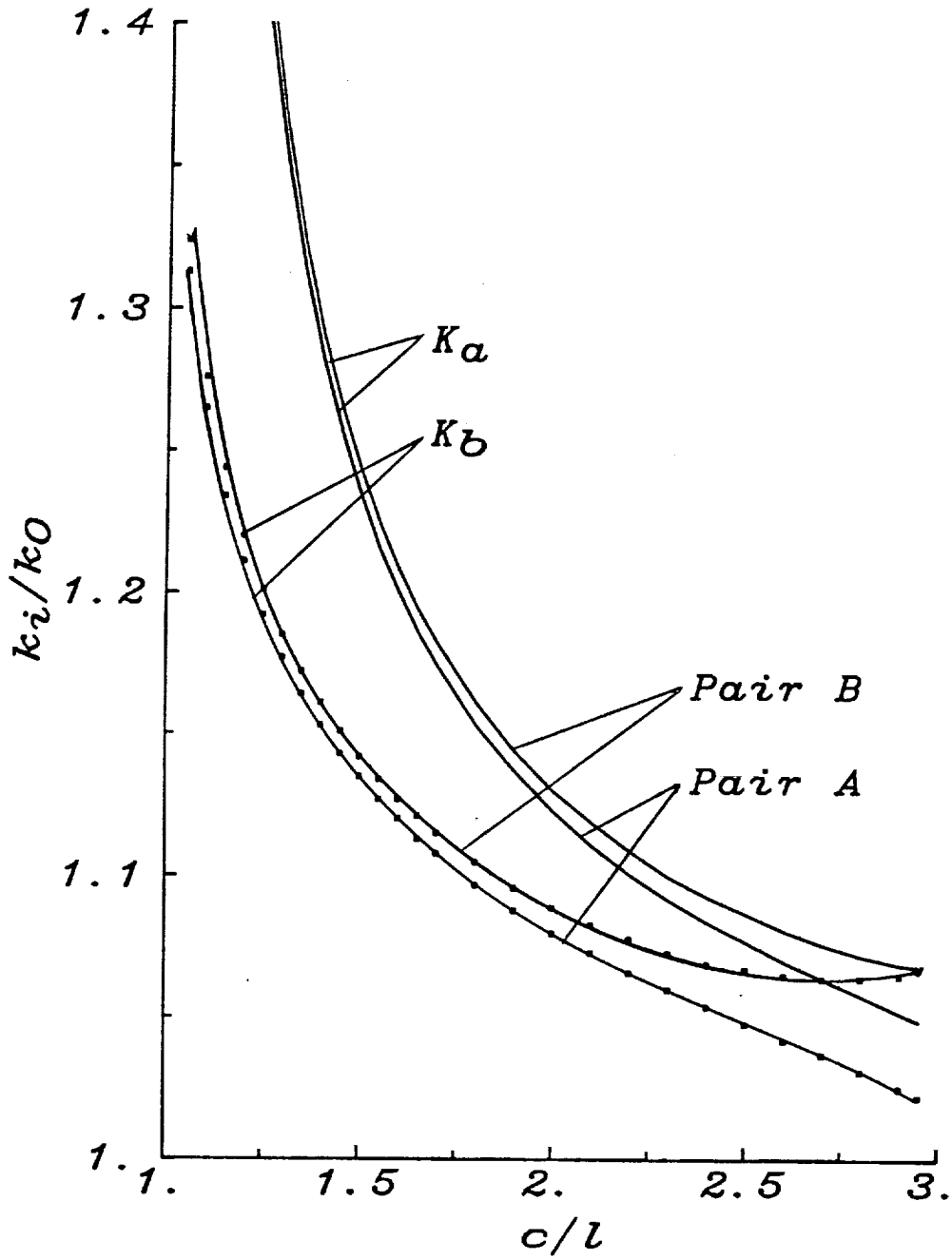

Figure 3.3 Stress intensity factors in two-orthotropic bonded layers containing an embedded crack under constant pressure p_1. ($k_0=p_1\sqrt{l}$)

($h_1=h_2$, $c=\frac{b+a}{2}$, $l=\frac{b-a}{2}=h_1/4.$, see Figure 3.1)

(for Pair A: $\mu_2^*/\mu_1^*=1.149$, $\beta=0.481$)

(for Pair B: $\mu_2^*/\mu_1^*=0.871$, $\beta=0.520$)

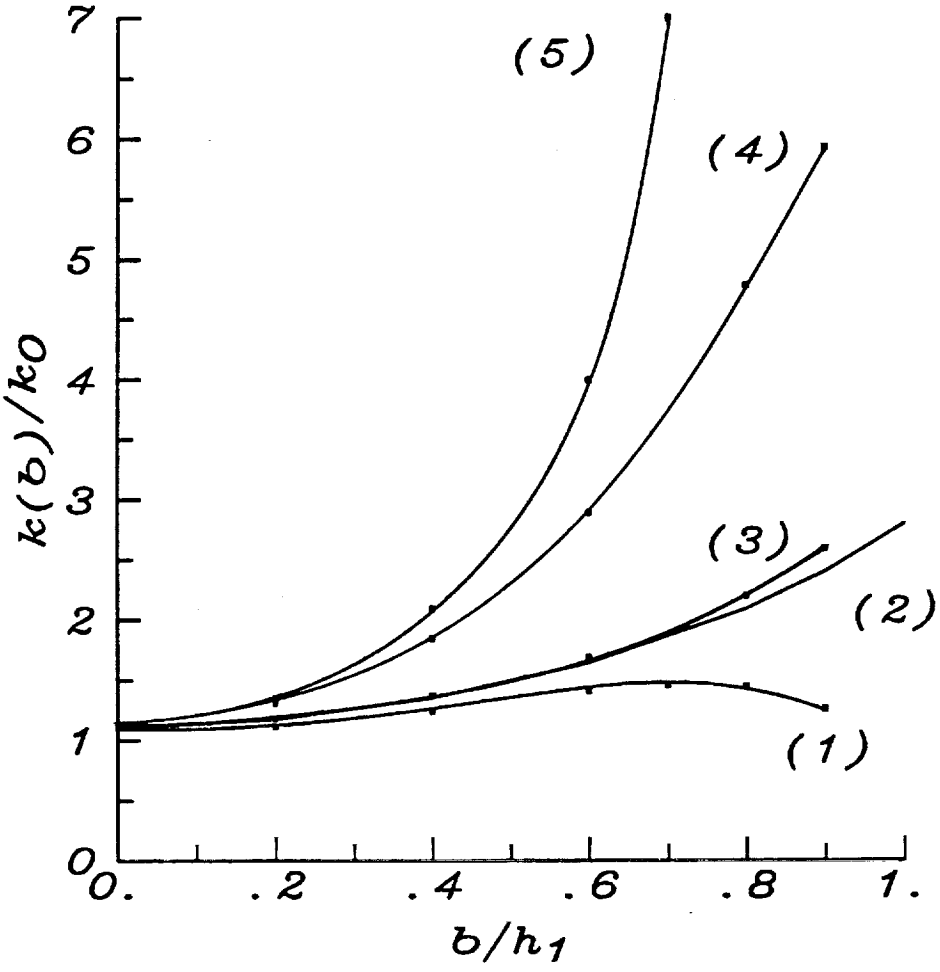

	(1)	(2)	(3)	(4)	(5)
μ_2^*/μ_1^*	8.88	1.	0.871	0.046	0.

Figure 3.4 Stress intensity factors in two-orthotropic bonded layers with a pressured edge crack for different ratio of μ_2^*/μ_1^*. ($k_0=p_1\sqrt{b}$, $h_1=h_2=h/2.$)
(Material I is material 1 and $\mu_1^*=12.078$)

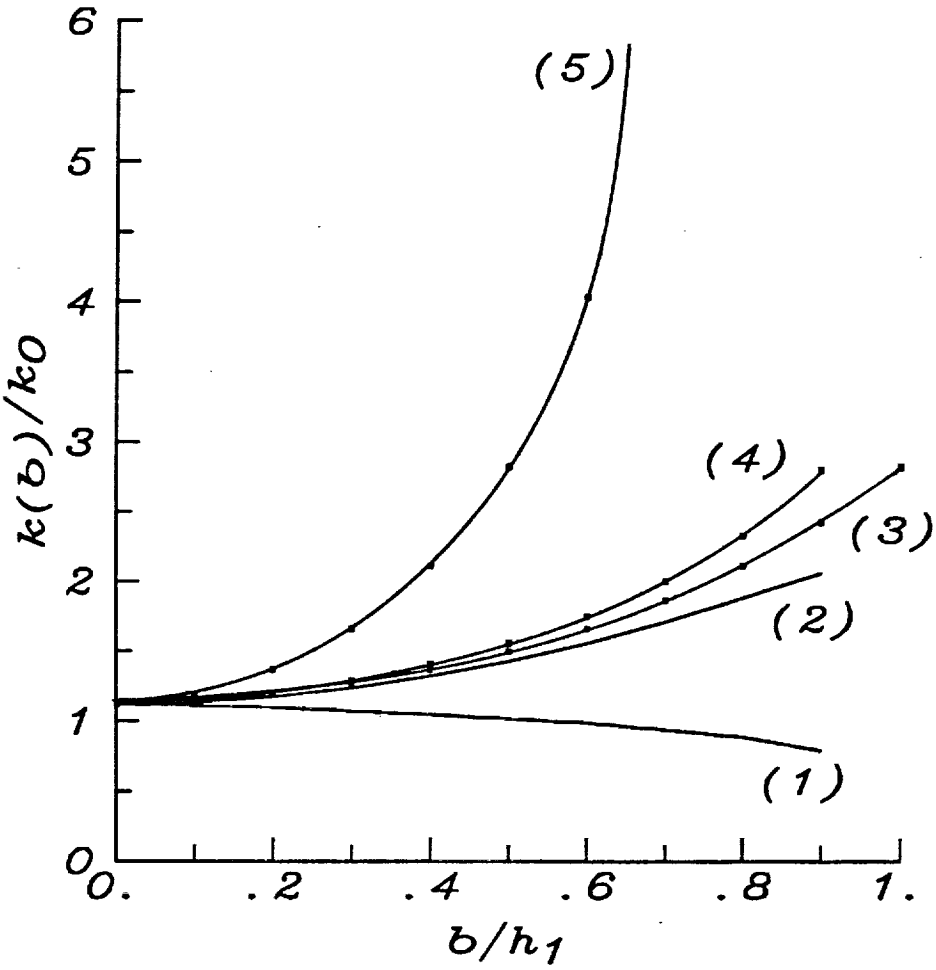

	(1)	(2)	(3)	(4)	(5)
E_2/E_1	40.	1.45	1.	0.69	0.

Figure 3.5 Stress intensity factors in two-isotropic bonded layers with a pressured edge crack for different ratio of E_2/E_1. ($\nu_2=\nu_1=0.3$)
($k_0=p_1\sqrt{b}$, $h_1=h_2=h/2.$)

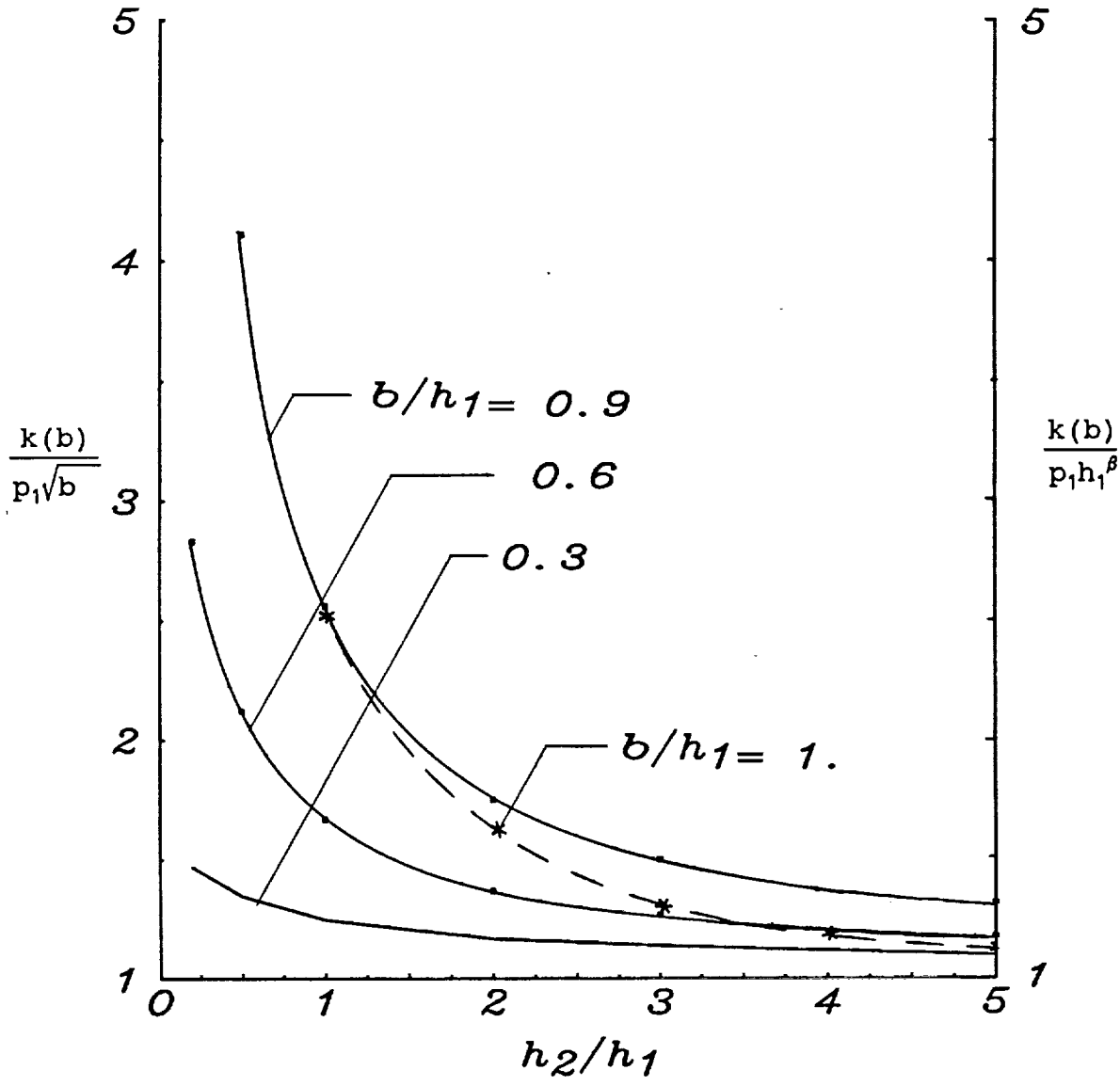

Figure 3.6 The effect of thickness ratio on the stress intensity factor in two-orthotropic bonded layers with a pressured edge crack. (Material Pair B, β=0.520)

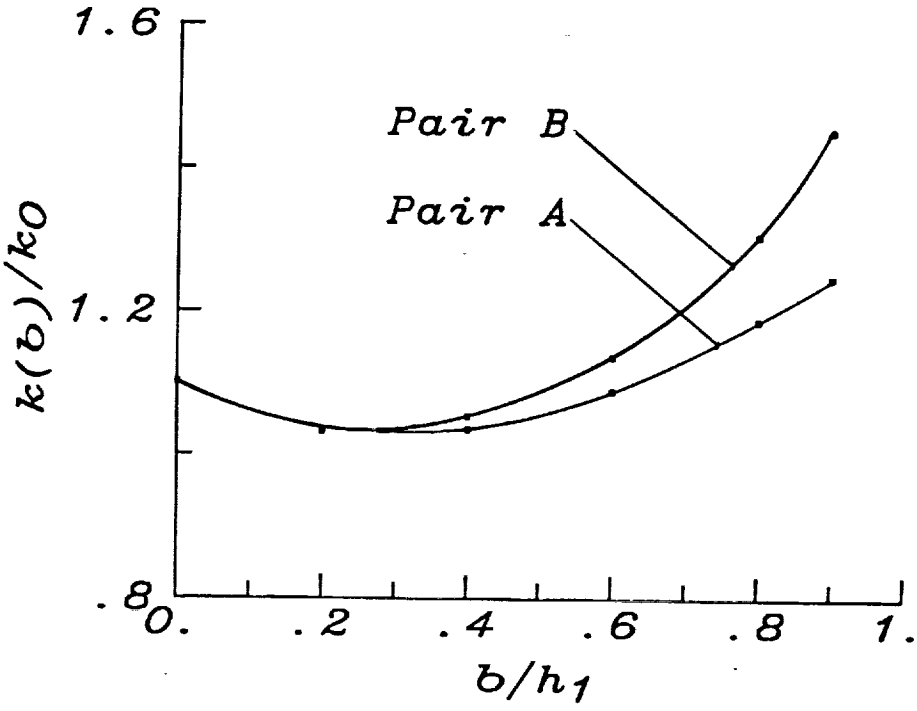

Figure 3.7 Stress intensity factor in two-orthotropic bonded layers containing an edge crack and subjected to uniform bending away from the crack region.

($k_0 = p_b\sqrt{b}$, Eq. 3.116)

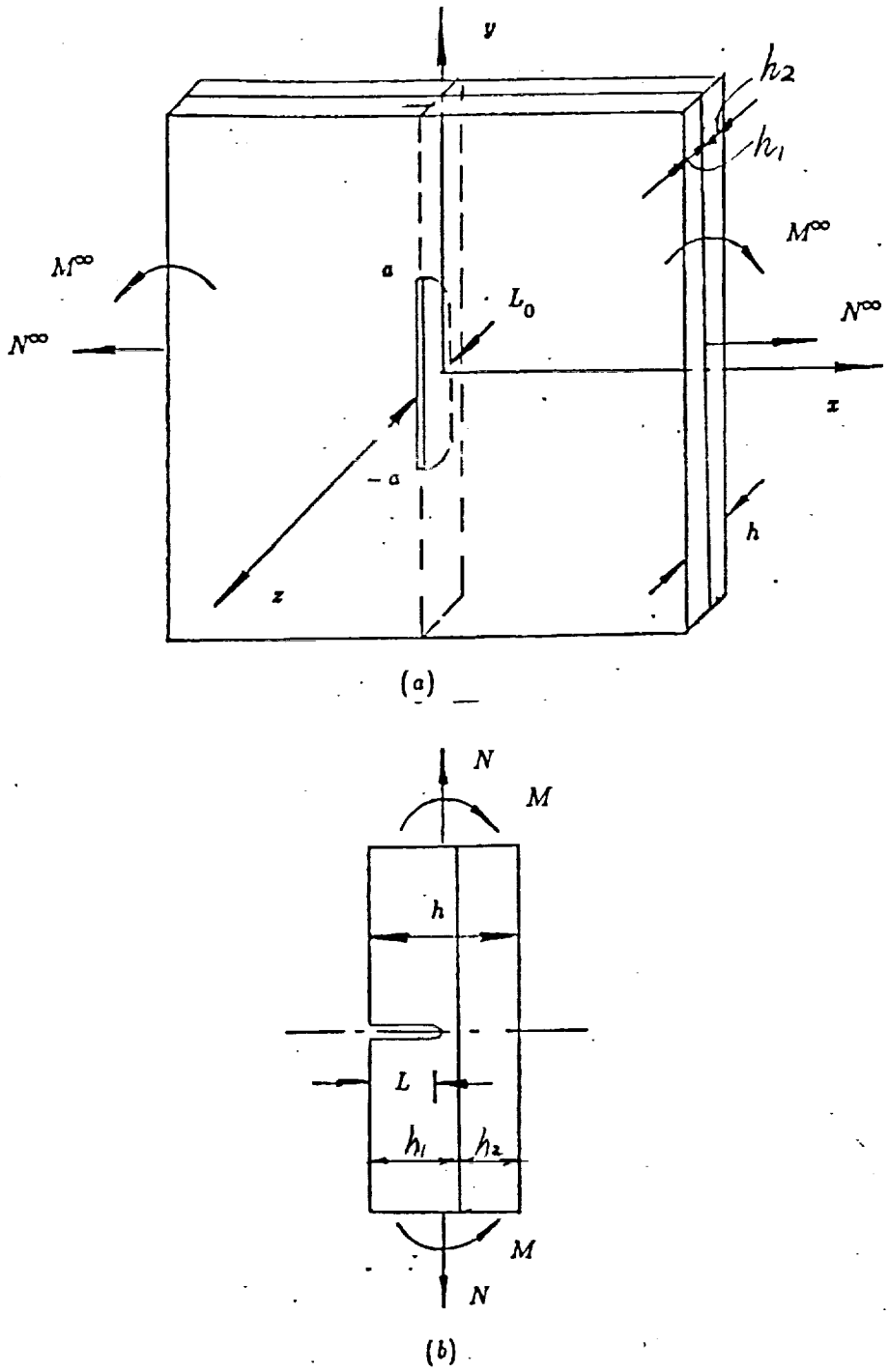

Figure 4.1 Geometry and Loading of the layered plate with a part-through surface crack.

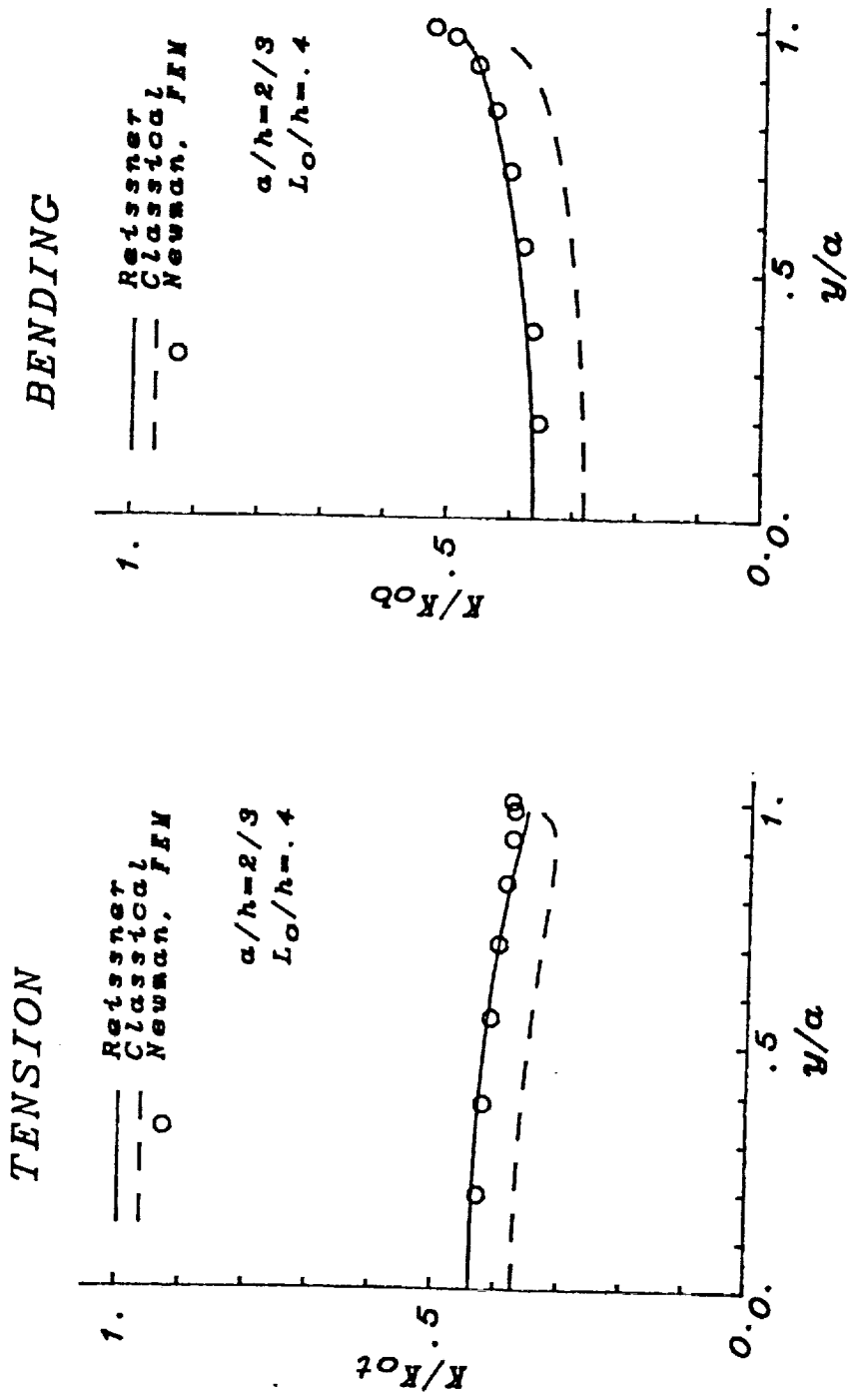

Figure 4.2 Comparison of the stress intensity factors obtained from the finite element solution [21], the classical plate theory and the Reissner theory, ν=0.3, a/h=(2/3).

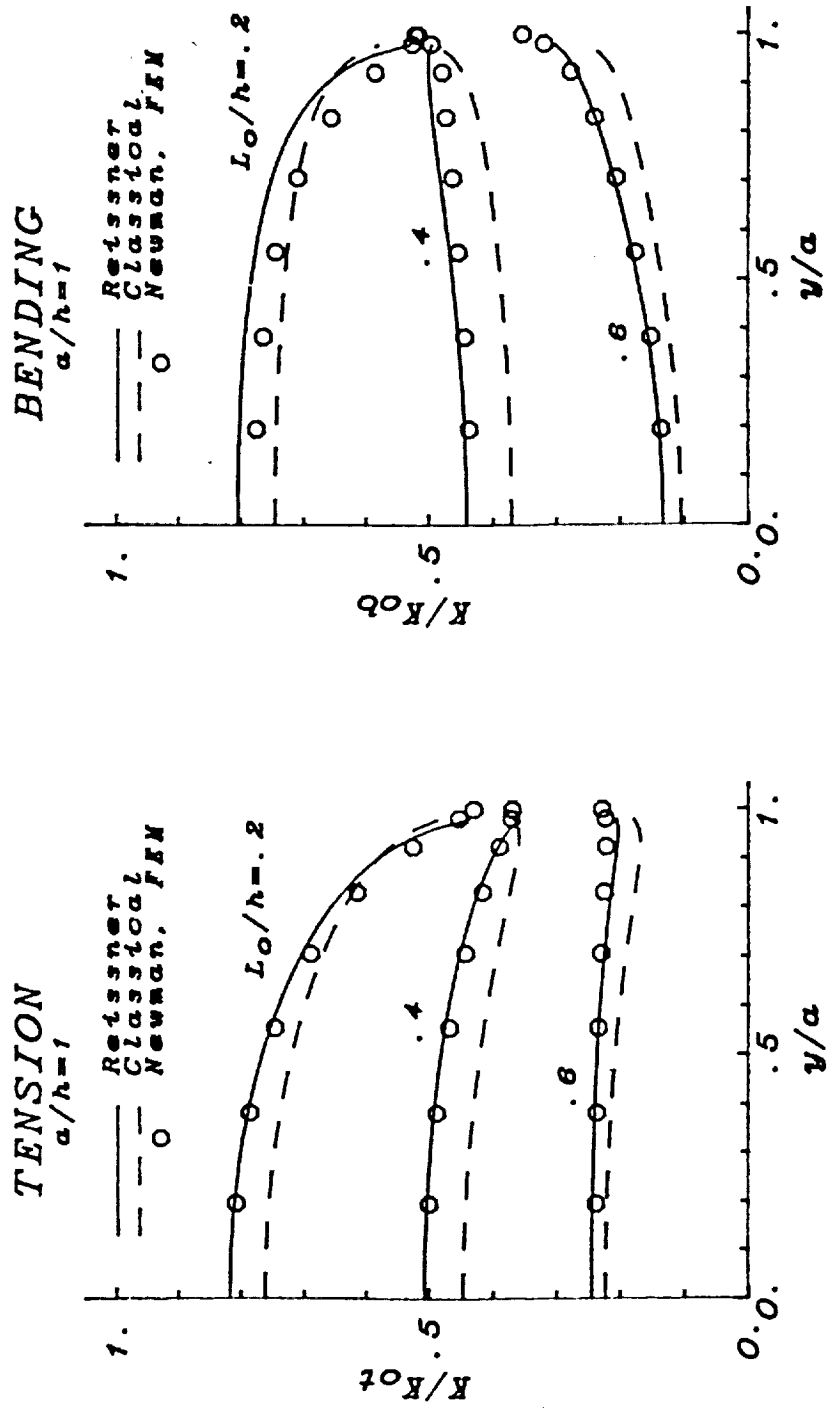

Figure 4.3 Comparison of the stress intensity factors obtained from the finite element solution [21], the classical plate theory and the Reissner theory, ν=0.3, a/h=1.

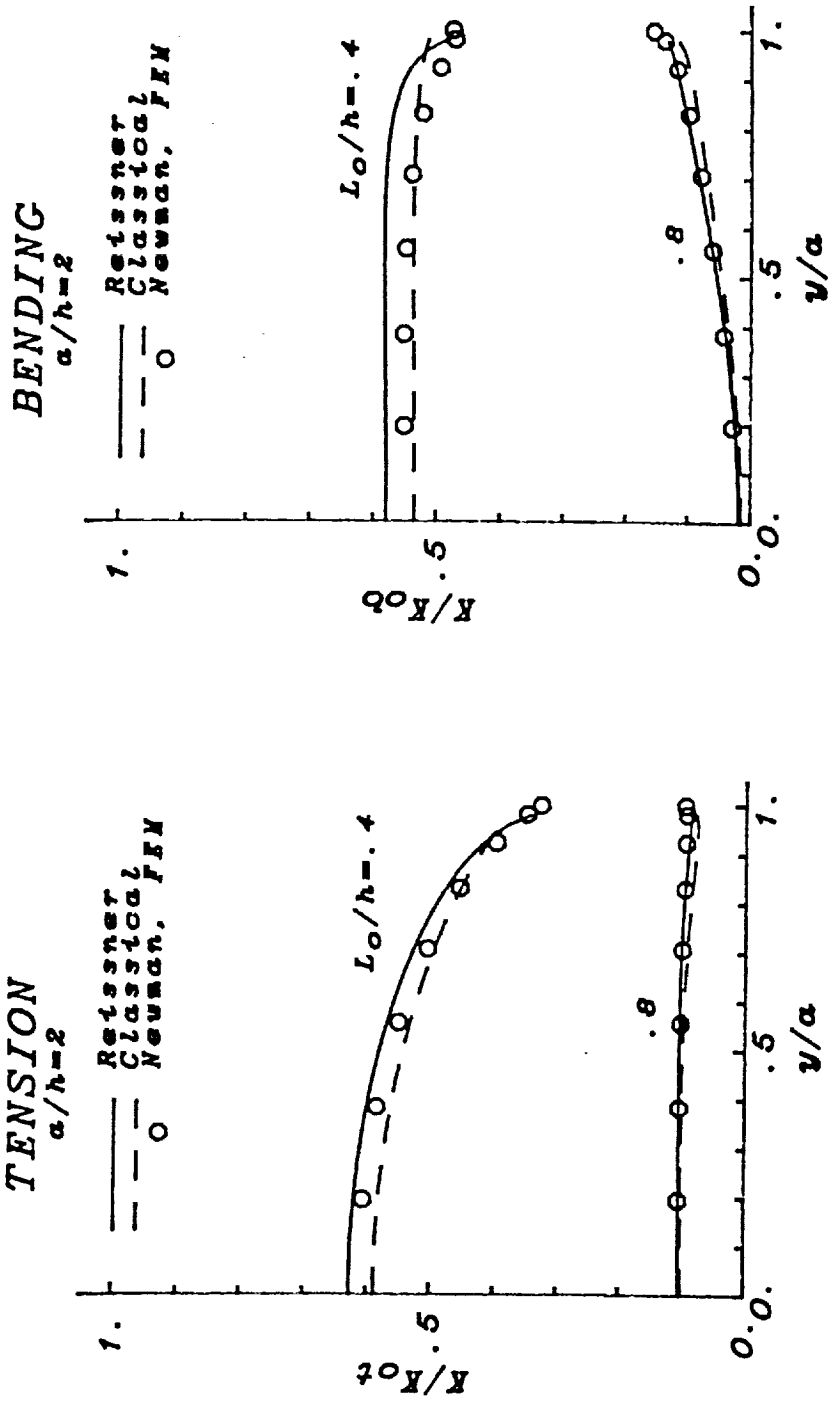

Figure 4.4 Comparison of the stress intensity factors obtained from the finite element solution [21], the classical plate theory and the Reissner theory, ν=0.3, a/h=2.

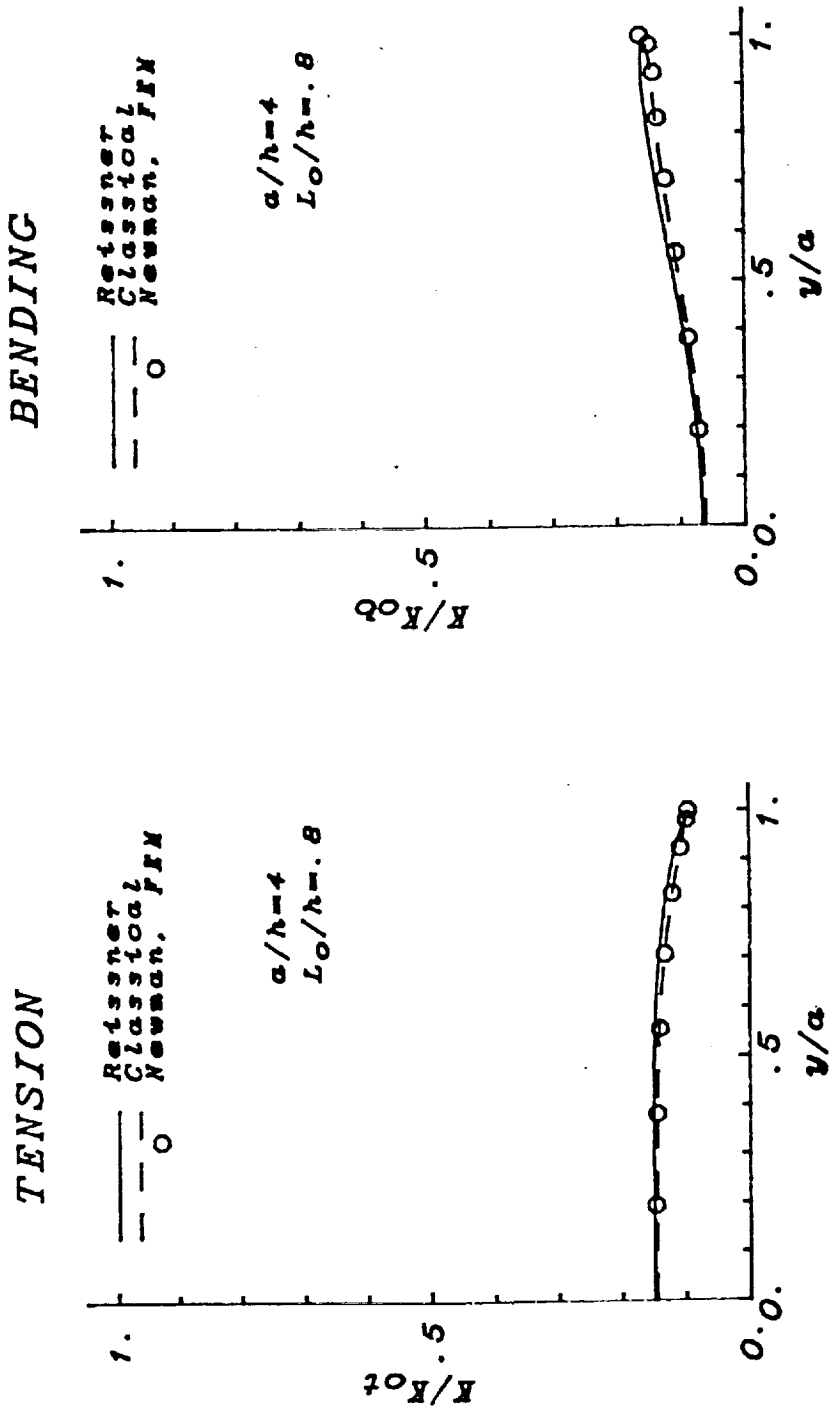

Figure 4.5 Comparison of the stress intensity factors obtained from the finite element solution [21], the classical plate theory and the Reissner theory, ν=0.3, a/h=4.

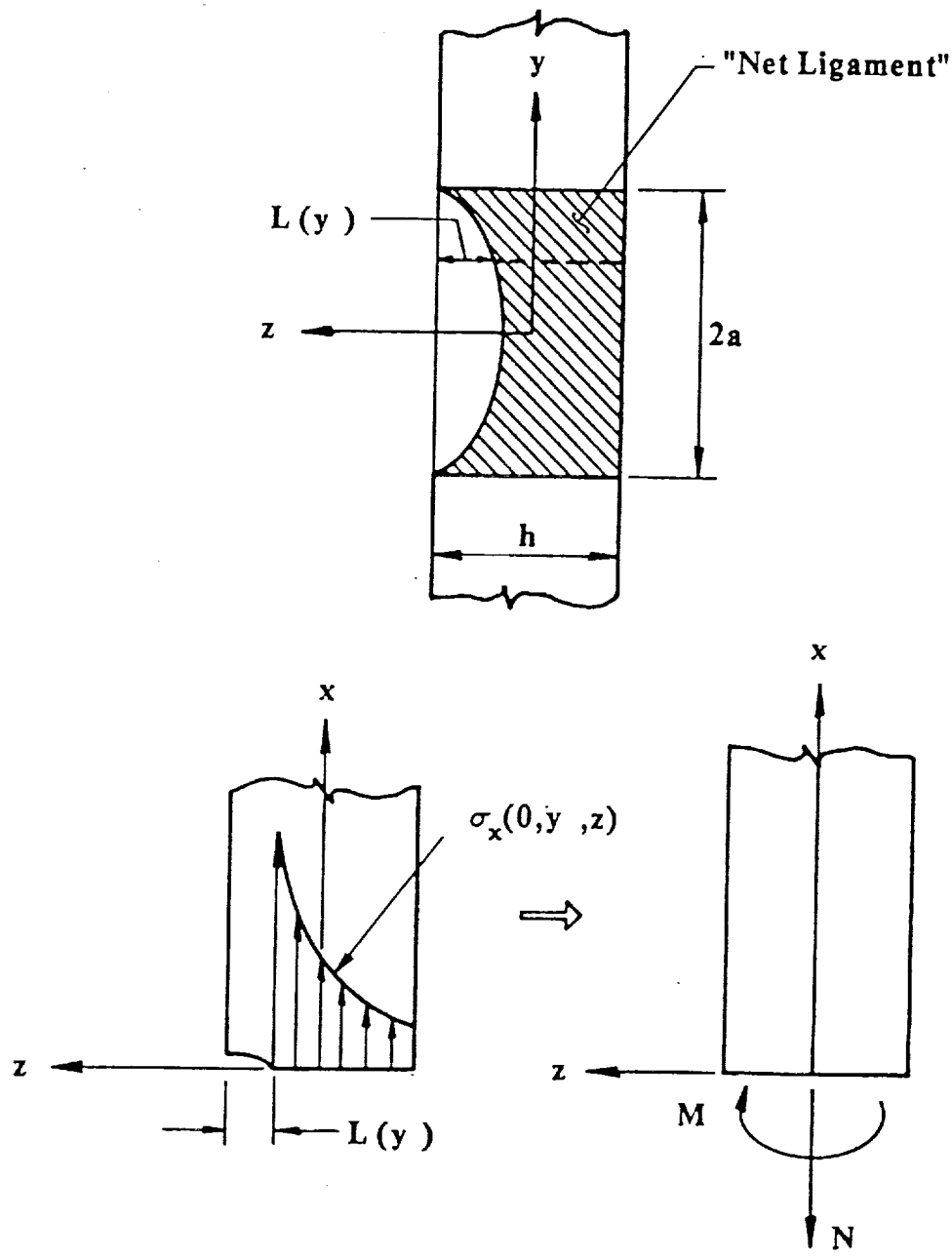

Figure 4.6 Representation of the two-dimensional stress state in the net ligament with stress resultants.

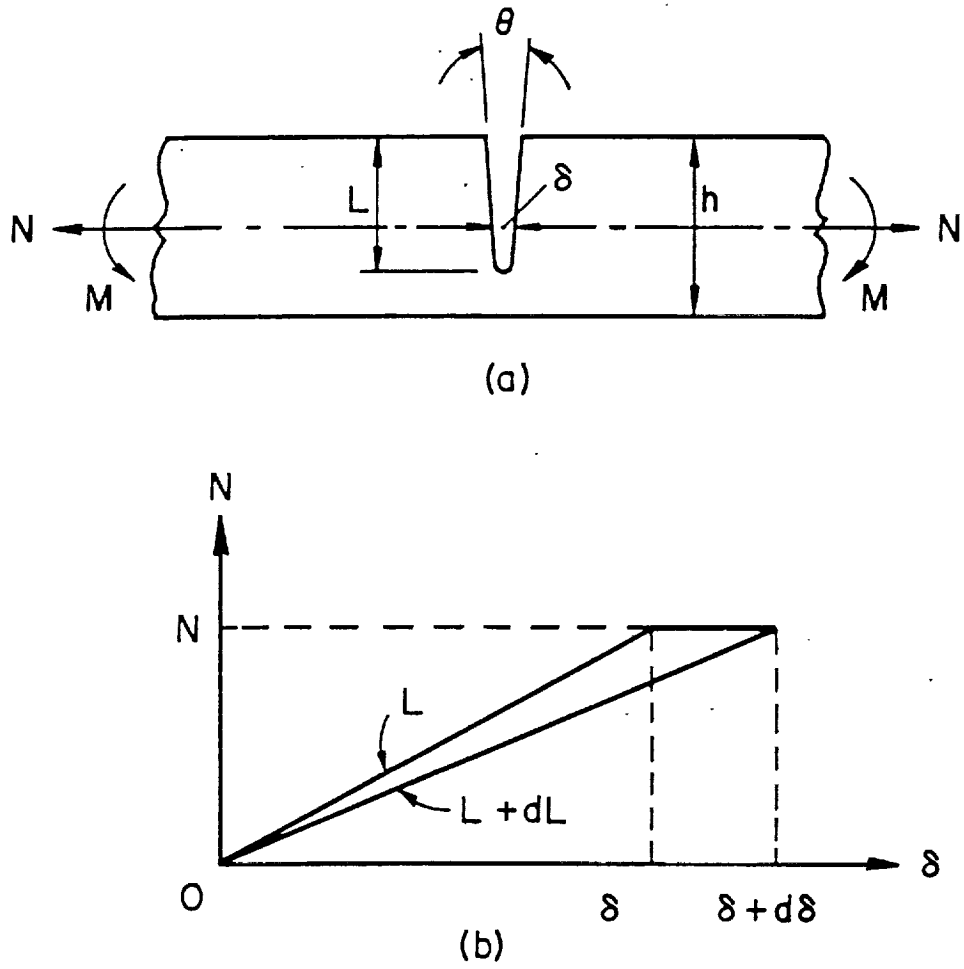

Figure 4.7 Notation for the related plane strain problem.

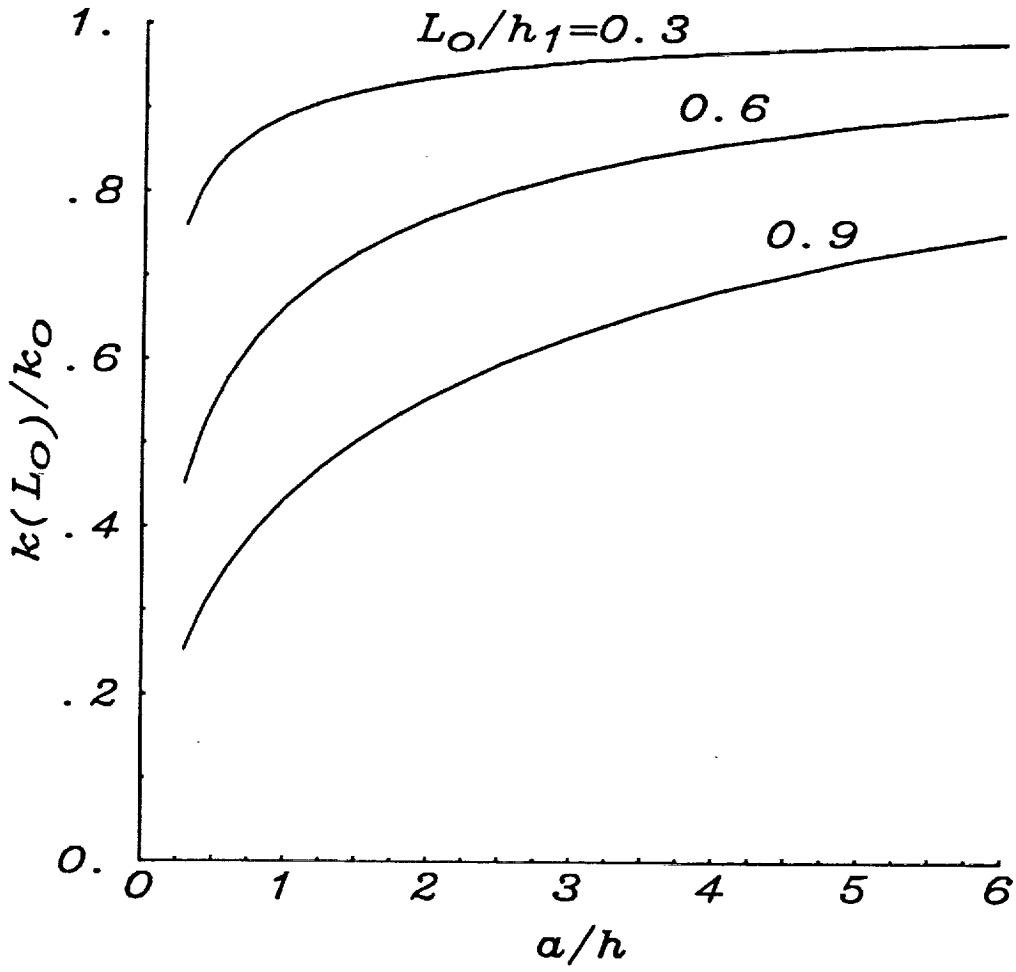

Figure 4.8 Normalized stress intensity factor at the maximum penetration point of a semi-elliptic surface crack in an isotropic plate subjected to tension. The normalization factor $k_0 = k_{ot}^{\infty}$ is the corresponding value for an edge-cracked strip under plane strain conditions with the same crack depth $L=L_0$.

(Material Pair I, $h_1=h_2=h/2$.)

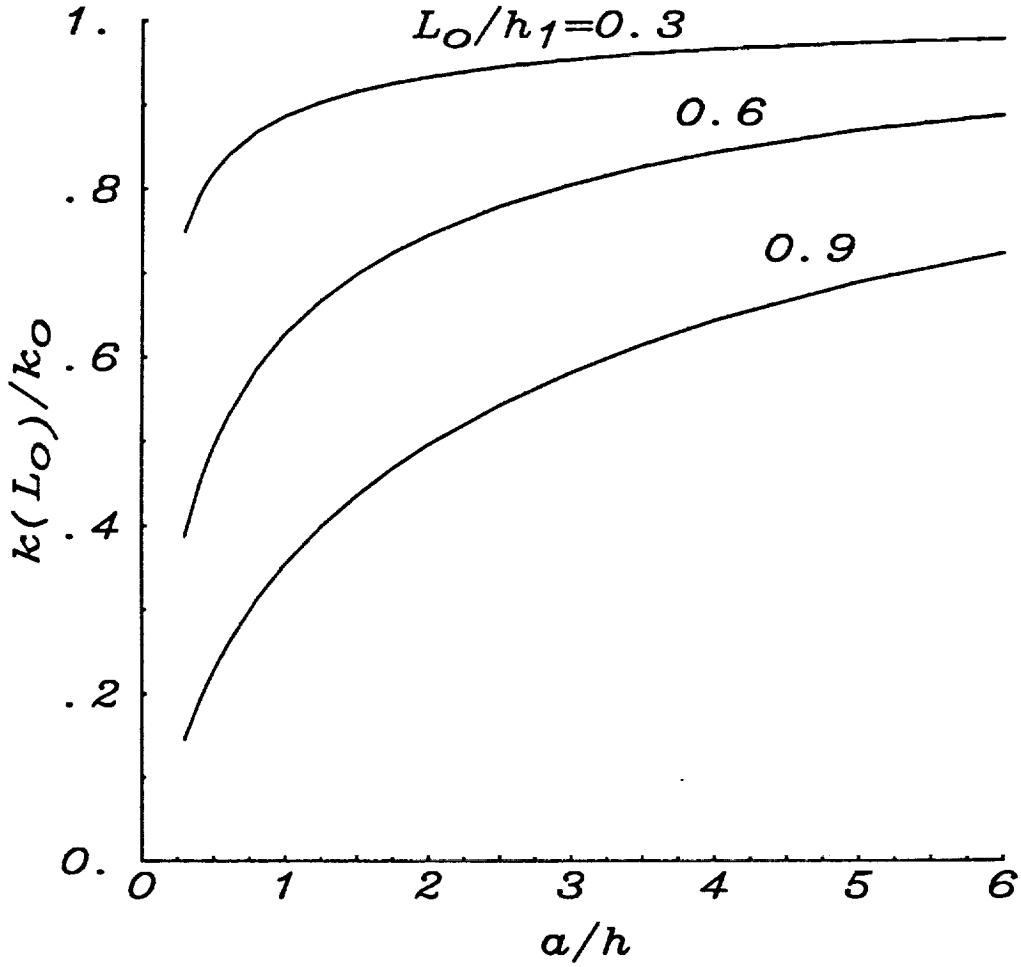

Figure 4.9 Normalized stress intensity factor at the maximum penetration point of a semi-elliptic surface crack in an isotropic plate subjected to bending. The normalization factor $k_0 = k_{ob}^{\infty}$ is the corresponding value for an edge-cracked strip under plane strain conditions with the same crack depth $L=L_0$.

(Material Pair I, $h_1=h_2=h/2.$)

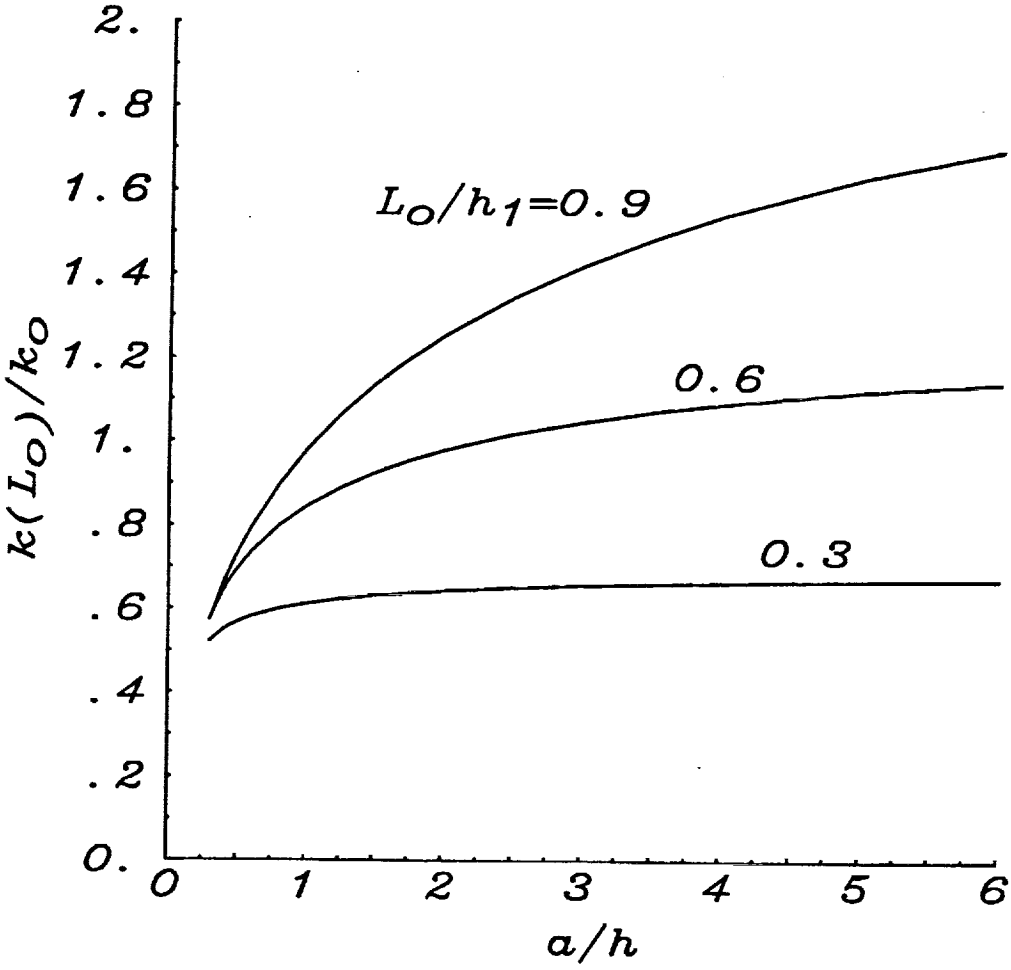

Figure 4.10 Normalized stress intensity factor at the maximum penetration point of a semi-elliptic surface crack in an isotropic plate subjected to tension.
($k_0 = \sigma_t\sqrt{h_1}$, σ_t=N/h, Material Pair I, $h_1=h_2=h/2.$)

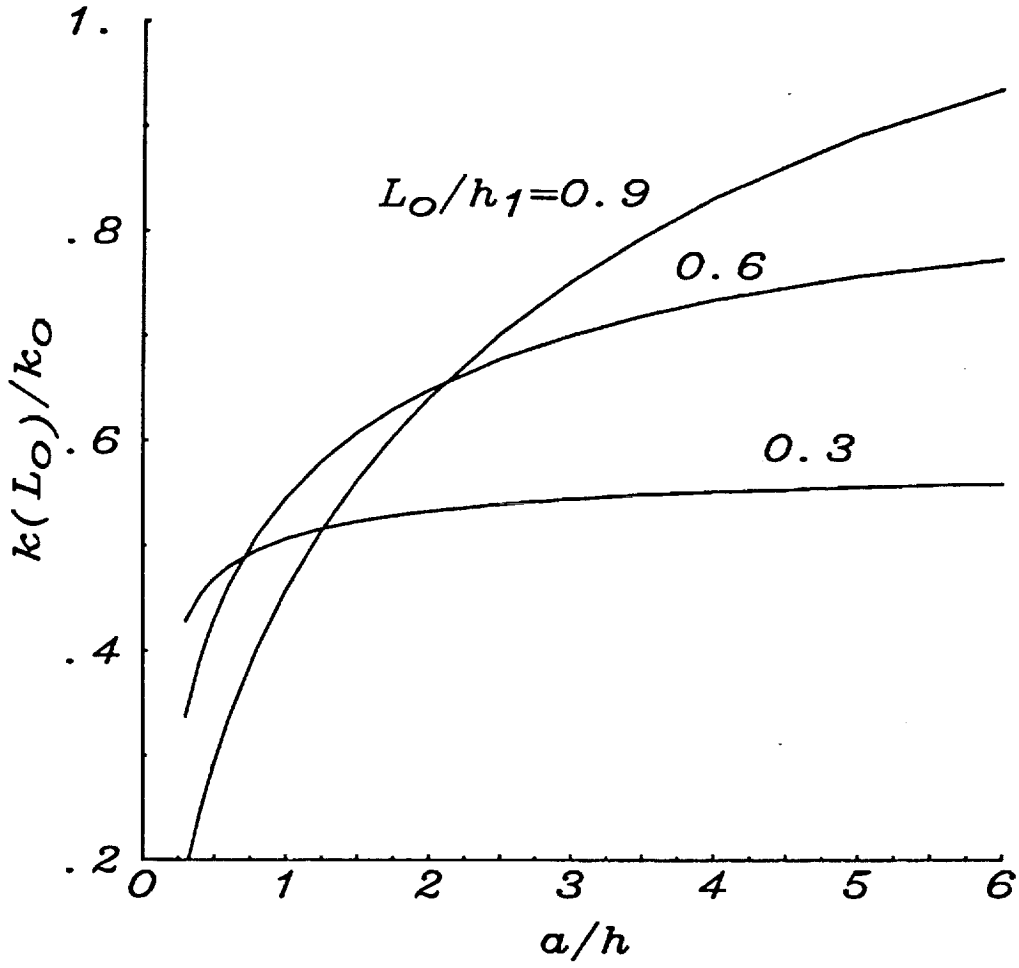

Figure 4.11 Normalized stress intensity factor at the maximum penetration point of a semi-elliptic surface crack in a plate subjected to bending.

($k_0 = \sigma_b\sqrt{h_1}$, $\sigma_b = 6M/h^2$, Material Pair I, $h_1 = h_2 = h/2$.)

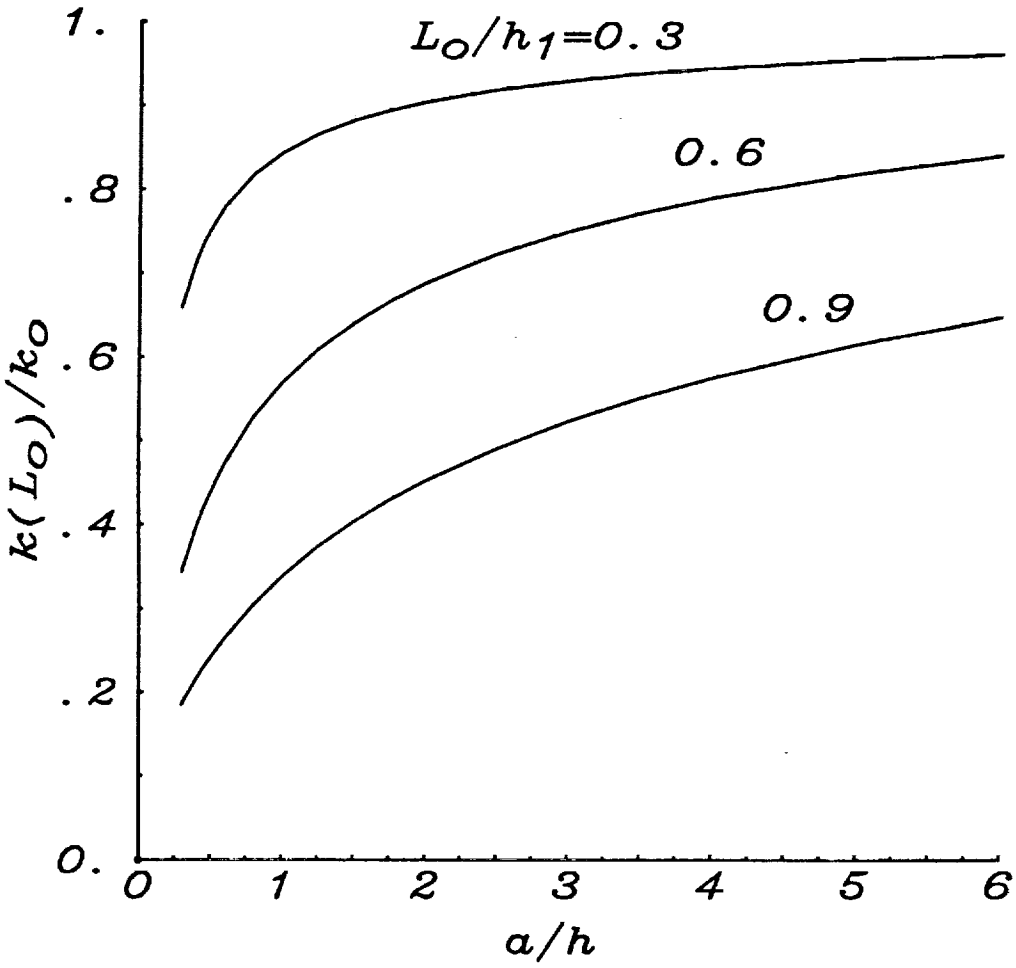

Figure 4.12 Normalized stress intensity factor at the maximum penetration point of a semi-elliptic surface crack in a two-layer plate subject to tension. The normalization factor $k_0 = k_{ot}^{\infty}$ is the corresponding value for an edge-cracked strip under plane strain conditions with the same crack depth $L=L_0$.

(Material Pair B, $h_1=h_2=h/2$.)

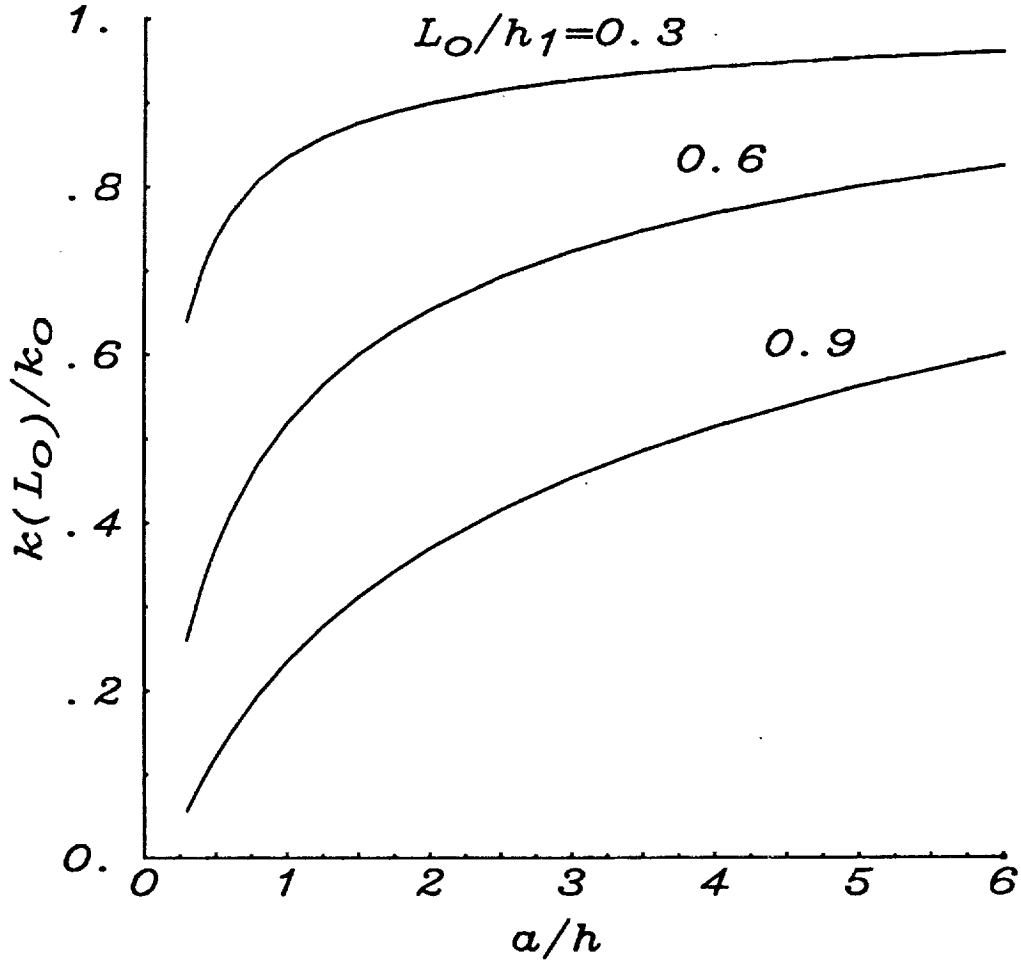

Figure 4.13 Normalized stress intensity factor at the maximum penetration point of a semi-elliptic surface crack in a two-layer plate subject to bending. The normalization factor $k_0=k^{\infty}_{ob}$ is the corresponding value for an edge-cracked strip under plane strain conditions with the same crack depth $L=L_0$.

(Material Pair B, $h_1=h_2=h/2$.)

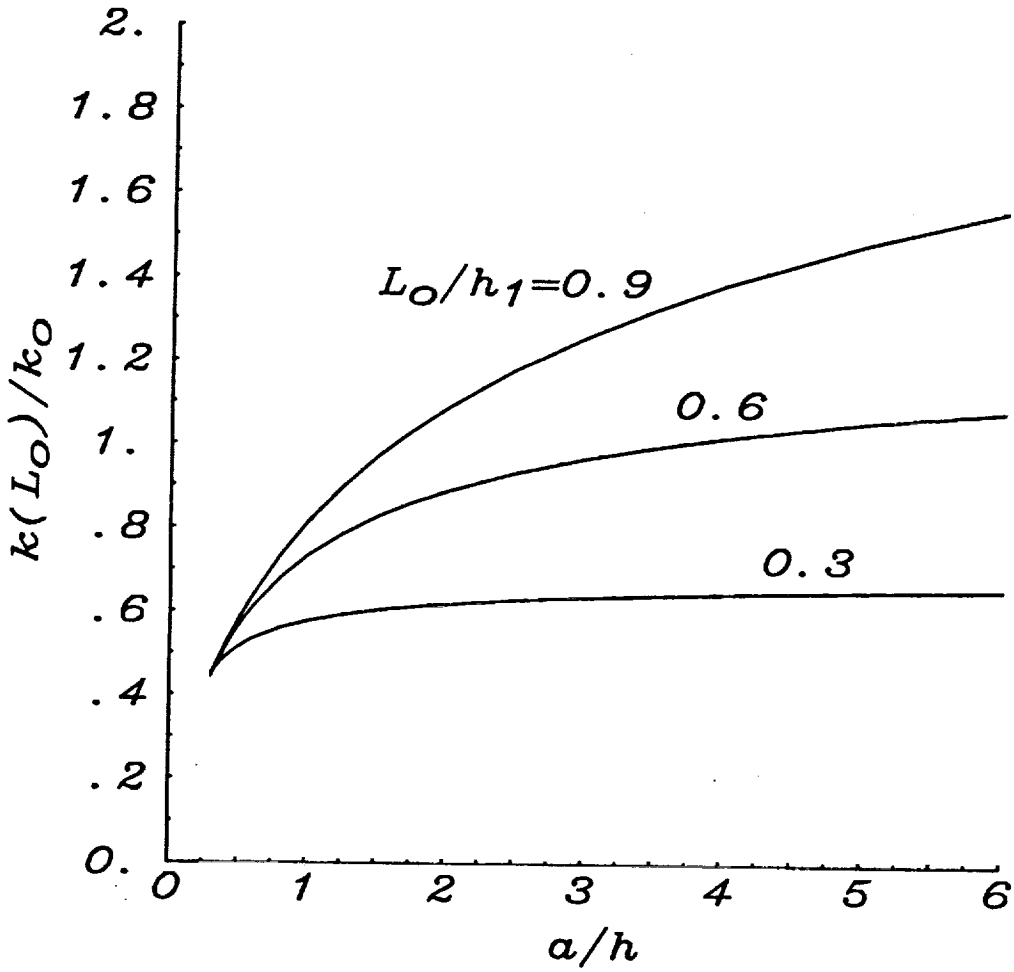

Figure 4.14 Normalized stress intensity factor at the maximum penetration point of a semi-elliptic surface crack in a two-layer plate subjected to tension.
($k_0 = \sigma_t\sqrt{h_1}$, σ_t=N/h, Material Pair B, $h_1=h_2=h/2$.)

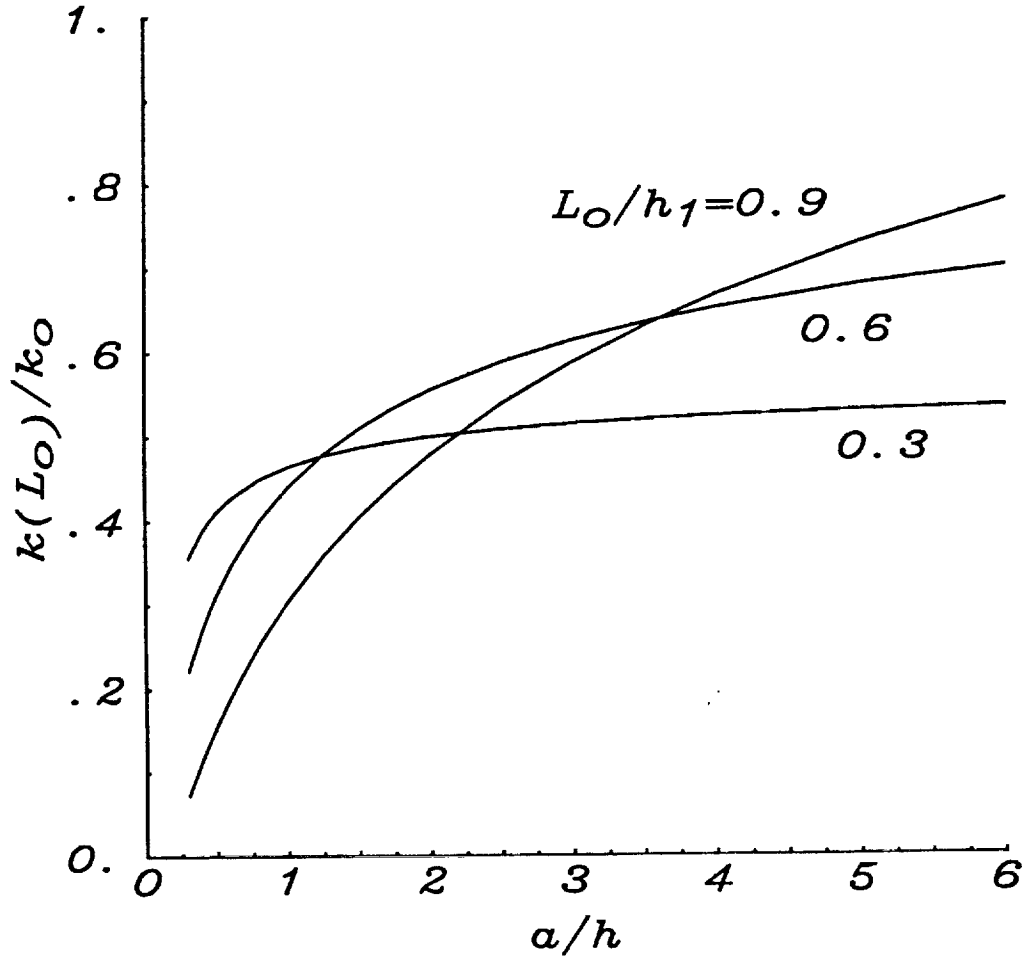

Figure 4.15 Normalized stress intensity factor at the maximum penetration point of a semi-elliptic surface crack in a plate subjected to bending.

($k_0 = \sigma_b L_0$, $\sigma_b = 6M/h^2$, Material Pair B, $h_1 = h_2 = h/2$.)

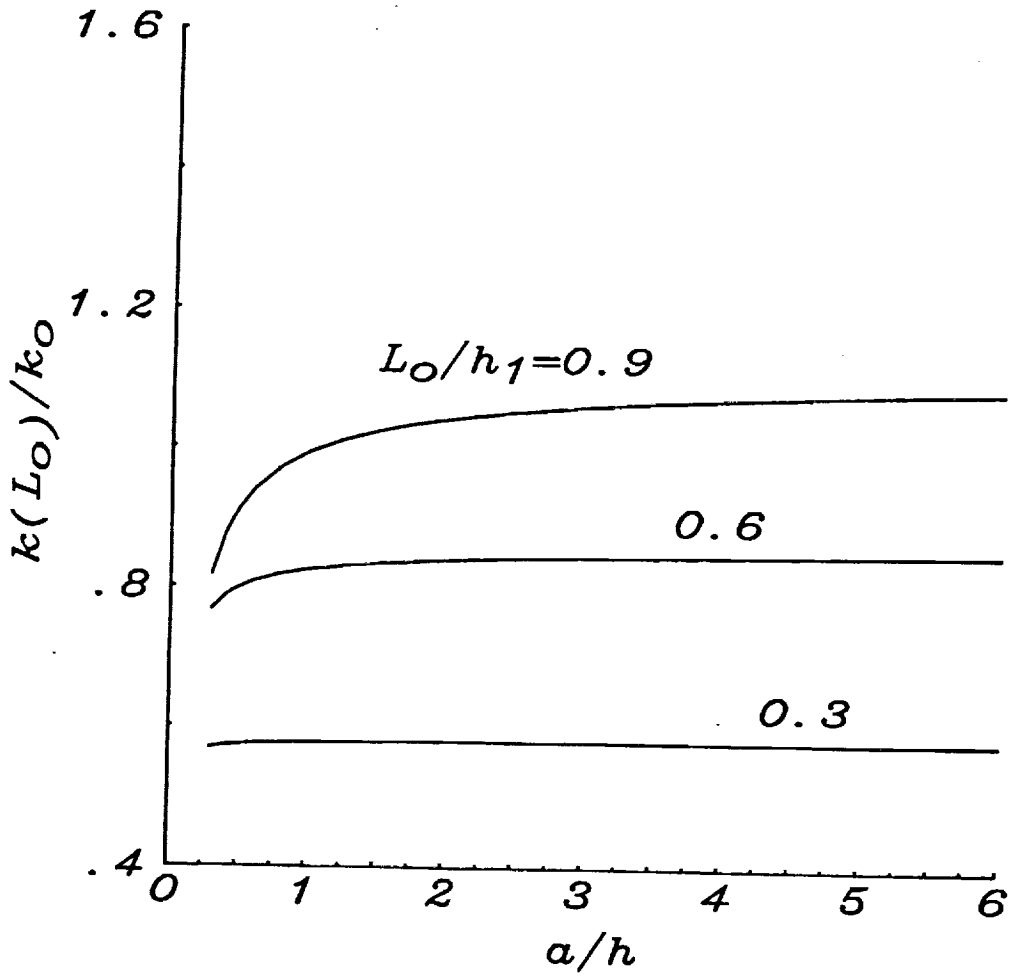

Figure 4.16 Normalized stress intensity factor at the maximum penetration point of a semi-elliptic surface crack in a two-layer plate subjected to tension.
($k_0 = \sigma_t\sqrt{h_1}$, σ_t=N/h, Material Pair B, h_2/h_1=10.)

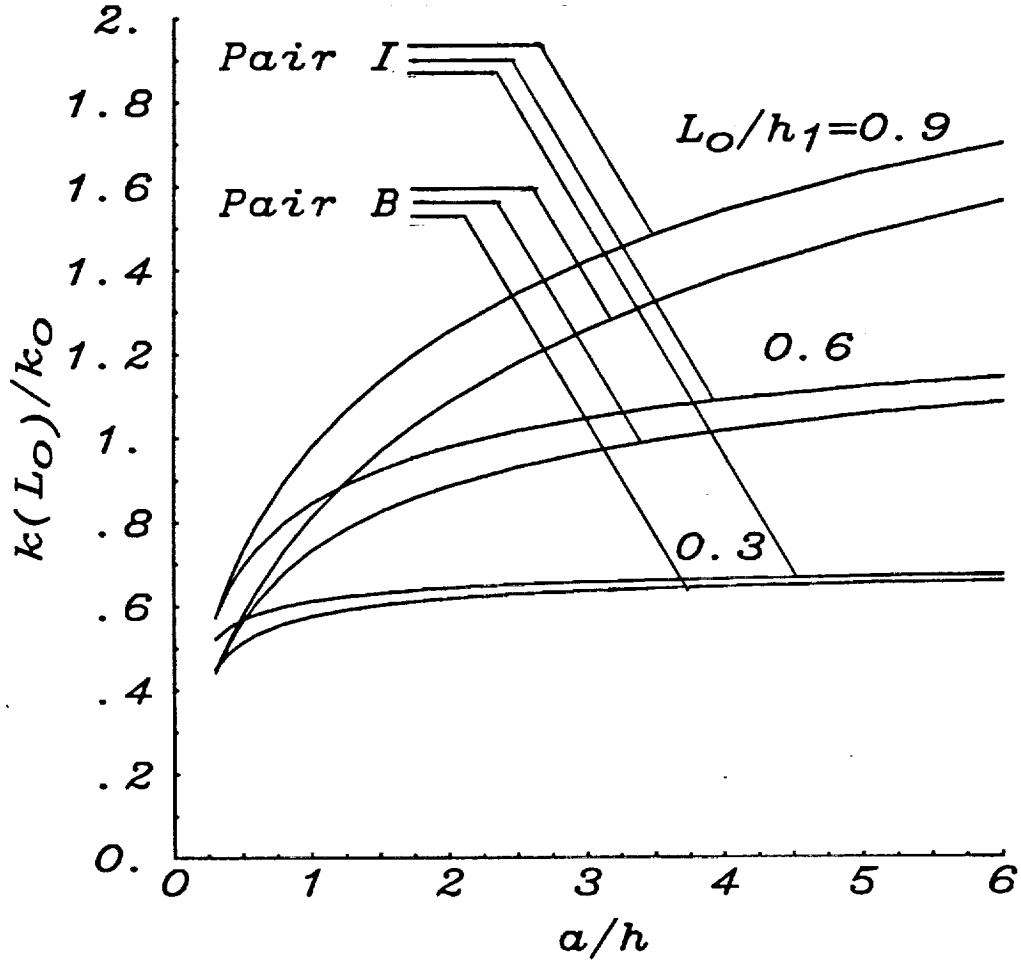

Figure 4.17 Comparison of normalized stress intensity factor at the maximum penetration point of a semi-elliptic surface crack in a two-layer plate subjected to tension for Material Pair I and Material Pair B.

($k_0 = \sigma_t\sqrt{h_1}$, $\sigma_t = N/h$, $h_1 = h_2 = h/2$.)

References

1. S. G. Lekhnitskii, "Anisotropic Plates", translated from the second Russian edition by S. W. Tais and T. Cheron, Gordon and Breach, 1968.
2. Erdogan, F. "Crack problems in cylindrical and spherical shells", in Plates and Shells with Cracks, Sih, G.C., ed., Noordhoff Int, Publ., Leyyden,1977.
3. Yahsi,O.S. and Erdogan, F. "A cylindrical shell with an arbitrarily oriented crack", Int. J. Solids Structures, Vol. 19, pp955-972, 1983.
4. Reissner, E. "The effect of transverse shear deformation on the bending of elastic plates", J. Appl. Mech, Vol. 12, No.l, ppA69-77, 1945.
5. Reissner, E. "On bending of elastic plates" Q. Appl. Math, Vol. 5, pp. 55-68, 1947.
6. Basset, A. B. :"On the extension and flexure of cylindrical and spherical thin elastic shells." Phil. Trans. Royal Soc., ser. A, Vol. 181, No. 6, pp 433-480, 1980.
7. Hildebrand, F. B. ; Reissner, E. ; and Thomas, G. B. :"Notes on the foundations of the theory of small displacements of orthotropic shells." NACA Technical Note No. 1833, March 1949.
8. Mindlin, R. D. :"Influence of Rotatory inertia and shear on flexural motions of isotropic, elastic plates." J. Appl. Mech, Vol. 18, pp. 31-38, 1951.
9. Yang, P. C. , Norris, C. H. and Stavsky, Y. ,"Elastic Wave Propagation in Heterogeneous plates," Int. J. Solids and structures, Vol. 12, pp 665-684, 1966.
10. Lo, K. H. ; Christensen, R. M. ; and Wu, E. M. :"A higher-order theory of plate deformation, Part 1: Homogeneous plates." J. Appl. Mech. , Vol. 44, pp 663-668, 1977.
11. Reddy, J. N. :"A simple higher-order theory for laminated composite plates." J. Appl. Mech. Vol. 51, pp 745-752, 1984.
12. Levinson, M. :"An accurate simple theory of the statics and dynamics of elastic plates." Mechanics Research Communications, Vol. 7, pp 343-350, 1980.
13. Mindlin, R. D. ; Schachnow, A. and Deresiewicz, H., "Flexural Vibrations of Rectangular Plates," J. of Applied Mechanics, Vol. 23, No. 3, Trans, ASME, Vol. 78, Sept. 1956, pp 430-436.

14. Uflyand, Ya. S., "The Propagation of waves in the transverse vibrations of bars and plates, " Akademiya Nauk SSSR, Prikladnaya metematika i Mekhanika, Vol. 12, 1948, pp 287-300.
15. Timoshenko, S. and Woinowsky-Krieger, S. "Theory of plates and shell", McGraw-Hill, New York, 1959.
16. Reissner, E., and Stavsky, Y., "Bending and Stretching of certain Types of Heterogeneous Aelotropic Elastic Plates," J. Appl. Mech., Vol. 28, No. 3, pp 402-408, 1961.
17. Stavsky, Y. , "Bending and stretching of Laminated Aeolotropic plates," Proc. Amer. Soc. of Civil Eng., Vol. 87, EM 6, pp 31-56, 1961.
18. Whitney, J. M. and Pagano, N. J., "Shear Deformation in heterogeneous anisotropic plates," J. Appl. Mech., pp 1031-1036, 1970.
19. Erdogan, F. :"Mixed boundary value problems," Mechanics Today, S. Nemat -Nasser, ed. Vol. 4, 1978, pp 1-86.
20. Kaya, A. C. and F. Erdogan :"On the solution of integral equations with strongly singular kernels," Quarterly of Applied Methematics, Vol. 45, 1987, pp 105-122.
21. Joseph, P. and Erdogan, F. :"Plate and shells containing a surface crack under general loading conditions", NASA report, Grant NAG-1-713, 1987.
22. Wu, B. and Erdogan, F :"The surface and through crack problem in orthotropic plate ", Int. J. Solid Structures, Vol. 25, 1989, pp 167-188.
23. T. S. Cook and F. Erdogan ,"Stress in bonded materials with a crack perpendicular to the interface ", Int. J. Eng. Science, Vol. 10, pp. 677-697, 1972.
24 F. Erdogan and V. Biricikoglu, "Two Bonded half planes with a crack going through the interfaces", Int. J. Eng. Science, Vol. 11, pp. 745-766, 1973.
25. D. B. Bogy, "The plane elastostatic solution for a symmetrically loaded crack in a strip composite ", Int. J. Eng. Science, Vol. 11, pp 985-996, 1973.
26. G. D. Gupta, "A layered composite with a broken laminates ", Int. J. Solids structures, Vol. 9, pp 1141-1154, 1973.
27. F. Delale and F. Erdogan, "Bonded orthotropic strips with cracks ", Int. J. of fracture, Vol. 15, pp 343-364, 1979.
28. M. R. Gecit and F. Erdogan, "The effect of adhesive layers on the fracture of laminated strctures ", J. of Eng. Materials and Technology, Trans. ASME, Vol. 100, pp 2-9, 1978.

29. Ming-Che Lu and F. Erdogan, "Stress intensity factors in two bonded elastic layer containing cracks perpendicular to and on the interface - I analysis", Eng. Fracture Mechanics, Vol. 18, pp 491-506, 1983.
30. Ming-Che Lu and F. Erdogan, "Stress intensity factors in two bonded elastic layer containing cracks perpendicular to and on the interface - II Solution and Results", Eng. Fracture Mechanics, Vol. 18, pp 501-528, 1983.
31. N. I. Muskhelishvili, Singular Integral Equations, P. Noordhoff, Gnoningen, The Netherlands, 1953.
32. F. Erdogan, "Complex Function Technique", Continuum Physis, Vol. II, A. C. Eringen, ed., Academic Press, pp. 523-603, 1975.
33. F. Erdogan, "Mixed Boundary-Value Problems in Mechanics", Mechanics Today, Vol. 4, S. Nemat-Nasser, ed., pergamon press, Oxford, pp. 1-85, 1978.
34. A. C. Kaya, "Stress Intensity Factor in an orthotropic strip under general loading conditions", Master Thesis, Lehigh University, 1978.
35. A. C. Kaya and F. Erdogan, "On the solution of Integral Equations with a Generalized Canchy Kernel", Quarterly of Applied Math., Vol. Xlv, pp 455-469, 1987.
36. G. C. Sih and H. Liebowitz, "Mathematical Theories of Brittle Fracture", Fracture An Advanced Treatise, H. Liebowitz, ed., Vol. 2, Academic Press, 1968.
37. Newman, J.C.,Jr. and Raju, I.S., "Analysis of Surface Cracks in Finite Plates Under Tension or Bending Loads", NASA Technical Paper 1578, 1979.
38. Raju, I.S. and Newman, J.C.,Jr., "Stress Intensity Factors for Internal and External Surface Cracks in Cylindrical Vessels", J. Pressure Vessel Technology, Vol.104, 1982, pp.293-298.
39. Shah, R.C. and Kobayashi, A.S., "On the Surface Flaw Problem", The surface Crack: Physical problems and Computational Solutions, Swedlow, J.L., ed., ASME New York,1972, pp.79-124.
40. Smith,F.W. and Sorensen, D.R., "The Semi-Elliptical Surface Crack - A Solution by the Alternating Method", International Journal of Fracture Mechanics, Vol. 12,1976, pp47-57.
41. Heliot, J., Labbens, R.C. and Pellisier-tanon, A., "Semi-Elliptical Cracks in a Cylinder Subjected to Stress Gradients", Fracture Mechanics, ASTM,STP 677, 1979, pp341-364.

42. Nishioka,T. and Atluri,S.N., "Analytical Solution for Embedded Elliptical Cracks, and Finite Element Alternating Method for Elliptical Surface Cracks, Subjected to Arbitrary Loadings", Engineering Fracture Mechanics, Vol. 17, 1982, pp247-268.

43. Mattheck,C., Morawietz, P. and Munz, D., "Stress Intensity Factor at the Surface and at the deepest Point of a Semi-Elliptical Surface Crack in Plates Under Stress Gradients", Int. J. of Fracture Mechanics, Vol.22, 1985, pp.201-212.

44. Isida, M., Noguchi, H. and Yoshida,T., "Tension and Bending of Finite Thickness Plates With a Semi-Elliptical Surface Crack", Int. J. of Fracture Mechanics, Vol. 26,1984,pp.157-188.

45 Newman, J.C., Jr., "A Review and Assessment of the Stress-Intensity Factors for Surface Cracks", NASA Technical Memorandum 78805, 1978.

46. Scott, P.M. and Thorpe, T.W. , "A Critical Review of Crack Tip Stress Intensity Factors For Semi-Elliptical Cracks", Fatigue of Engineering Materials and Structures, Vol. 4, 1981, pp.101-114.

47. Rice, J.R. and Levy, N., "The Part-Through Surface Crack in an Elastic Plate", ASME J. of Applied Mechanics, Vol. 39., 1972, pp.185-194.

48. Rice, J.R., "The Line Spring Model for Surface Flaws", The Surface Crack: Physical Problems and Computational Solutions, Swedlow, J.L., ed., ASME New York, 1972, pp. 171-186.

49. Delale, F. and Erdogan, F., "Line-spring Model for Surface Cracks in a Reissner Plate", Int. J. of Engineering Science, Vol. 19, 1981, pp. 1331-1340.

50. Irwin, G.R., "Analysis of Stresses and Strains Near the End of a Crack Transversing a Plate", ASME J. of Applied Mechanics, Vol. 24, 1957, pp.361-364.

51. Irwin, G.R., "Fracture Mechanics", Structural Mechanics, Goodier, J.N. and Hoff, N.J., eds., Pergamon Press, New York, 1960, pp.557-591.

52. Nicholas, M.G. and Mortimer, D.A., "Ceramic/Metal Joining for Structural Applications", Materials Science and Technology, Vol.1, 1985, pp.659-665.

53. Wittmer, M. , Boer, C.R., and Gudmundson, P., "Mechanical Properties of Liquid-Phase-Bonded Copper-Ceramic Substrates", J. Am. Ceram. Soc., Vol.65, 1982, pp149-153.

Appendix I

Expressions $\overline{\mu}$ and λ

A. The general Hookes' law for an orthotropic plate can be expressed as follows:

$$\epsilon_x = \frac{1}{E_x}\sigma_x - \frac{\nu_{xy}}{E_x}\sigma_y - \frac{\nu_{xz}}{E_x}\sigma_z$$

$$= c_{11}\sigma_x + c_{12}\sigma_y + c_{13}\sigma_z ,$$

$$\epsilon_y = \frac{-\nu_{yx}}{E_y}\sigma_x + \frac{1}{E_y}\sigma_y - \frac{\nu_{yz}}{E_y}\sigma_z$$

$$= c_{21}\sigma_x + c_{22}\sigma_y + c_{23}\sigma_z ,$$

$$\epsilon_z = \frac{-\nu_{zx}}{E_z}\sigma_x - \frac{-\nu_{zy}}{E_z}\sigma_y + \frac{1}{E_z}\sigma_z$$

$$= c_{31}\sigma_x + c_{32}\sigma_y + c_{33}\sigma_z ,$$

$$\gamma_{yz} = c_{44}\sigma_{yz}, \qquad \gamma_{zx} = c_{55}\sigma_{zx}, \qquad \gamma_{xy} = c_{66}\sigma_{xy}.$$

B. When a crack is located in the position as shown in Fig. 2.1 it can be shown that

$$\tilde{\mu} = \frac{1}{2} \left(\frac{d_{11} d_{22}}{2} \right)^{-1/2} \left[\left(\frac{d_{11}}{d_{22}} \right)^{1/2} + \frac{2 d_{12} + d_{66}}{2 d_{22}} \right]^{-1/2},$$

where

$$d_{11} = c_{11}, \qquad d_{22} = c_{22},$$

$$d_{12} = c_{12}, \qquad d_{66} = c_{66},$$

for general plane stress ,

$$d_{11} = \frac{c_{11} c_{33} - c_{13}^2}{c_{33}},$$

$$d_{22} = \frac{c_{22} c_{33} - c_{23}^2}{c_{33}},$$

$$d_{12} = \frac{c_{12} c_{33} - c_{13} c_{23}}{c_{33}},$$

$$d_{66} = c_{66},$$

for plane strain.

C. When a crack is located in the position as shown in Fig. 4.1(b) it can be shown that

$$\lambda = \left(\frac{e_{11}\, e_{33}}{2} \right)^{1/2} \left[\left(\frac{e_{11}}{e_{33}} \right)^{1/2} + \frac{2\, e_{13} + e_{55}}{2\, e_{33}} \right]^{1/2},$$

where

$$e_{11} = \frac{c_{11}\, c_{22} - c_{12}^{\,2}}{c_{22}},$$

$$e_{33} = \frac{c_{33}\, c_{22} - c_{23}^{\,2}}{c_{22}},$$

$$e_{13} = \frac{c_{13}\, c_{22} - c_{12} c_{32}}{c_{22}},$$

$$e_{55} = c_{55},$$

for plane strain.

Appendix II

Expressions Used in Subsections 3.2 and 3.3

A. See (3.8) and (3.43) for expressions λ_i ($i = 1, 14$), and

$$\lambda_{15} = \lambda_3 \lambda_{14}, \qquad \lambda_{16} = \lambda_4 \lambda_{13} .$$

B. See (3.2), (3.9), (3.11) and (3.14) for expressions β_i ($i = 1, 8$).

C. Expressions ρ_i ($i = 1, 8$):

$$\rho_1 = \beta_7, \qquad \rho_2 = \beta_8, \qquad \rho_3 = \lambda_5, \qquad \rho_4 = \lambda_6,$$

$$\rho_5 = \lambda_9, \qquad \rho_6 = \lambda_{10}, \qquad \rho_7 = \lambda_1, \qquad \rho_8 = \lambda_2 .$$

D. Expressions B_i ($i = 1, 11$):

$$B_1 = \lambda_{14}/2, \qquad B_2 = \lambda_{13}/2, \qquad B_3 = -\frac{1}{2}\beta_9 \lambda_{14},$$

$$B_4 = -\frac{1}{2}\beta_{10} \lambda_{13}, \quad B_5 = -\frac{1}{2\beta_{11}} \lambda_7 \lambda_{14}, \quad B_6 = -\frac{1}{2\beta_{12}} \lambda_8 \lambda_{13},$$

$$B_7 = \frac{1}{2\beta_{11}} \lambda_{12} \lambda_{13}, \quad B_8 = -\frac{1}{2\beta_{12}} \lambda_{12} \lambda_{13}, \quad B_9 = \lambda_{14} \lambda_3,$$

$$B_{10} = \lambda_4 \lambda_{13}, \qquad B_{11} = -\frac{B_9 + B_{10}}{2} .$$